

# First record of the flat-skulled woolly bat *Kerivoula depressa* and the Indochinese woolly bat *K. dongduongana* (Chiroptera, Vespertilionidae) in China

Xiaoling Liang<sup>1</sup>, Huixian Xie<sup>1</sup>, Yannan Li<sup>1</sup>,  
Zhenglangyi Huang<sup>1</sup>, Song Li<sup>2</sup>, Yi Wu<sup>1</sup>, Wenhua Yu<sup>1</sup>

**1** Key Laboratory of Conservation and Application in Biodiversity of South China, School of Life Sciences, Guangzhou University, Guangzhou 510006, China **2** Kunming Natural History Museum of Zoology, Kunming Institute of Zoology, Chinese Academy of Sciences, Kunming 650223, China

Corresponding authors: Yi Wu ([wuyi@gzhu.edu.cn](mailto:wuyi@gzhu.edu.cn)); Wenhua Yu ([wenhua\\_yu@gzhu.edu.cn](mailto:wenhua_yu@gzhu.edu.cn))

Academic editor: W. Bogdanowicz | Received 30 April 2022 | Accepted 19 December 2022 | Published 22 February 2023

<https://zoobank.org/D6FFAFDE-5310-4BA1-AD68-8FE762189718>

**Citation:** Liang X, Xie H, Li Y, Huang Z, Li S, Wu Y, Yu W (2023) First record of the flat-skulled woolly bat *Kerivoula depressa* and the Indochinese woolly bat *K. dongduongana* (Chiroptera, Vespertilionidae) in China. ZooKeys 1149: 1–15. <https://doi.org/10.3897/zookeys.1149.85821>

## Abstract

Recent studies have revealed that the *Kerivoula depressa* complex should be divided into two species, *K. depressa* distributed mainly in Myanmar, Vietnam, Laos and Cambodia, and *K. dongduongana* found only in the Annamite Mountains of Vietnam, Laos and Cambodia. In November 2018 and April 2019, 24 woolly bats were collected by two-band harp traps in Xishuangbanna, Yunnan, China. Based on morphological, morphometric, and phylogenetic (*COI*, *Cytb*, and *RAG2* gene sequences) analyses, these bats were identified as *K. depressa* and *K. dongduongana*, representing two new species records for the country. Including the new records, six *Kerivoula* species have been recorded in China, namely *K. depressa*, *K. dongduongana*, *K. furva*, *K. kachinensis*, *K. picta* and *K. titania*. To facilitate their identification and biological research in the future, we have provided an up-to-date key to all *Kerivoula* species occurring in China.

## Keywords

*COI*, *Cytb*, *Kerivoula dongduongana*, morphology, morphometric analyses, new records, phylogenetic inferences, *RAG2*, Yunnan

## Introduction

The genus *Kerivoula* (Gray, 1842) contains 27 species in the Indomalaya-Australasia and Afrotropic ecozones (Wilson and Mittermeier 2019). Among these, *Kerivoula hardwickii* (sensu stricto) (Horsfield 1824), the most widespread species of the genus has long been treated as a species complex, with up to six recognized subspecies (Ellerman and Morrison-Scott 1951; Hill 1965; Corbet and Hill 1992). Because of the lack of comparative material, Corbet and Hill (1992), Sinha (1999), and Simmons (2005) did not acknowledge any subspecies of *K. hardwickii*. Subsequently, Bates et al. (2007) divided the species into two morphological types, *K. hardwickii* (with domed skull) and *K. depressa* (Miller, 1906) (with flattened skull). However, molecular phylogenies indicate that the taxonomy and systematics of the *K. hardwickii* complex are still ambiguous because of the occurrence of multiple divergent lineages (Francis et al. 2007, 2010; Khan et al. 2010; Douangboubpha et al. 2016; Nguyen et al. 2016). Recent genetic analyses revealed that *K. depressa* can be divided into two distinct clades (Kuo et al. 2017). Tu et al. (2018) described *K. depressa* and *K. dongduongana* (Tu et al. 2018) based on phylogenetic analyses using *COI*, *Cytb*, and *RAG2* sequences from newly obtained specimens and those from previous studies across the Indo-China Peninsula and the Philippines (Hoofer et al. 2003; Stadelmann et al. 2004; Francis et al. 2010; Khan et al. 2010; Wu et al. 2012; Kruskop 2013; Kuo et al. 2014; Kuo et al. 2017). Currently, the *K. hardwickii* complex contains five species: *K. hardwickii* (sensu stricto), *K. kachinensis* (Bates et al., 2004), *K. furva* (Kuo et al., 2017), *K. depressa*, and *K. dongduongana* (Kuo et al. 2017; Tu et al. 2018).

In China, four species of woolly bats from the genus *Kerivoula* have been recorded, including *K. picta* (Pallas, 1767), *K. furva*, *K. kachinensis*, and *K. titania* (Bates et al., 2014) (Wu et al. 2012; Kuo et al. 2017; Tu et al. 2018; Yu et al. 2018; Wilson and Mittermeier 2019; Yu et al. 2022). In November 2018 and April 2019, a series of chiropteran surveys were conducted in the southwestern region of Yunnan Province, and 24 *Kerivoula* individuals were sampled. Based on morphology, morphometric analyses, and phylogenetic inferences using *COI*, *Cytb*, and *RAG2* sequences, they were identified as *K. depressa* and *K. dongduongana*, which represent two new records of *Kerivoula* in China. In this paper, we provided details about these findings, new distribution information and an up-to-date key to identify all *Kerivoula* species occurring in China.

## Materials and methods

### Specimen sampling and morphological measurements and analyses

In November 2018 and April 2019, 24 *Kerivoula* bats were collected using two-band harp traps during field surveys in Xishuangbanna Tropical Botanical Garden, Yunnan, China (21°57'17"N, 101°15'26"E and 21°30'58"N, 101°30'38"E). All field survey

and sample collection protocols complied with the current laws of Yunnan Province, China. We followed the guidelines of the American Society of Mammalogists (Sikes 2016) for the care and use of animals. All voucher specimens were determined to be adults based on the degree of epiphyseal-diaphyseal fusion (Brunet-Rossinni and Wilkinson 2009). The specimens were preserved in 75% ethanol and deposited at the School of Life Sciences, Guangzhou University, China.

External and skull measurements were taken with a digital caliper to the nearest 0.01 mm following Bates and Harrison (1997) and Bates et al. (2004). Body mass was measured with an electronic scale. Twenty-four adult specimens were examined using six external and eight craniodental measurements following Tu et al. (2018) and Yu et al. (2018), and further morphometric analyses were performed using 20 specimens (Table 1). We conducted a principal component analysis (PCA) and discriminant analysis of principal components (DAPC) of craniodental measurements using the R Core Team (2013) and R add-in packages: psych (Revelle 2013), ade4 (Dray et al. 2007), adegenet (Jombart 2008), FactoMineR (Le et al. 2008), and ggplot2 (Wickham 2016).

## Phylogenetic inference

We followed the DNA extraction, amplification, and sequencing procedures according to Yu et al. (2022). Three gene sequences from all 24 voucher *Kerivoula* specimens were obtained (GenBank accession numbers: *COI*: OM716930–OM716952; *Cytb*: OM735691–OM735714; *RAG2*: OM735715–OM735736). These sequences were compared with 87 *COI*, 38 *Cytb*, and 28 *RAG2* sequences of the subfamily Kerivoulinae from NCBI nucleotide databases and with the three outgroup species, including *Myotis muricola* (Gray, 1846), *Harpiocephalus harpia* (Temminck, 1840), and *Murina cyclotis* (Dobson, 1872) (Hooper et al. 2003; Khan et al. 2010; Ruedi et al. 2012). Newly generated and downloaded sequences are detailed in Appendix 1. The final matrices of *COI*, *Cytb*, and *RAG2* contained 110 taxa and 734 bp, 62 taxa and 1220 bp, and 50 taxa and 1267 bp, respectively. We inferred phylogenetic relationships using both Bayesian and maximum likelihood (ML) approaches. Sequences were aligned with MUSCLE (Edgar 2004). Bayesian analyses were performed using MrBayes v.3.2.7 (Ronquist et al. 2012), and the best-fitting models of sequence evolution were selected by MrModeltest v.2.4 (Nylander 2004) using the Akaike information criterion (GTR+I+G for *COI*, HKY+I+G for *Cytb*, HKY+G for *RAG2*). Four independent Markov chains were run, and 10,000,000 Metropolis-coupled Markov Chain Monte Carlo generations with sampling every 1000 generations were set. The first 25% samples were discarded. ML analyses were performed in IQ-TREE (Minh et al. 2020) with the best model setting in ModelFinder (Kalyaanamoorthy et al. 2017) using Bayesian information criterion (TPM2+F+I+G4 for *COI* and *Cytb*, HKY+F+R2 for *RAG2*).

**Table 1.** External and craniodental measurements (mm) and body mass (g) of studied *Kerivoula* species, and variable loadings on principal components (PCs) and contribution of original variables in discriminant functions (DFs).

Characters	<i>Kerivoula depressa</i>			<i>Kerivoula dongluogangana</i>					
	Yunnan, China (This study)	Vietnam and Cambodia Tu et al. 2018	Yunnan, China (This study)	Yunnan, China (This study)	Vietnam and Cambodia Tu et al. 2018	PC1	PC2	DF1	DF2
	Mean ± SD (n) (Range)	Mean ± SD (n) (Range)	Mean ± SD (n) (Range)	Mean ± SD (n) (Range)	Mean ± SD (n) (Range)				
MASS	3.53±0.49 (12) (3.00–4.50)	–	4.05±0.25 (12) (3.50–4.40)	–	4.50 (1)	–	–	–	–
HB	36.88±2.31 (12) (32.99–39.74)	–	38.43±2.84 (12) (34.40–42.75)	–	–	–	–	–	–
TL	39.13±1.35 (12) (36.68–41.49)	–	39.97±1.90 (12) (37.20–44.50)	–	38.00 (1)	–	–	–	–
E	11.55±0.91 (12) (9.96–13.15)	–	12.05±0.89 (12) (10.83–14.04)	–	–	–	–	–	–
HF	6.98±0.65 (12) (6.09–7.83)	–	7.57±0.48 (12) (7.00–8.43)	–	–	–	–	–	–
FA	30.75±1.08 (12) (28.82–32.29)	32.08±0.15 (4) (32.00–32.30)	34.02±0.94 (12) (32.56–35.86)	–	32.00±1.73 (3) (30.00–33.00)	–	–	–	–
TIB	15.95±0.44 (12) (15.38–16.61)	–	16.37±0.58 (11) (15.70–17.44)	–	18.00 (1)	–	–	–	–
GTL	13.75±0.17 (10) (13.57–14.08)	13.65±0.27 (5) (13.34–13.98)	14.28±0.30 (10) (13.71–14.59)	–	13.51±0.38 (7) (12.70–13.79)	0.98	–0.14	0.21	0.01
CCL	12.14±0.17 (10) (11.88–12.43)	12.51±0.23 (5) (12.17–12.75)	12.79±0.31 (10) (12.34–13.43)	–	12.43±0.36 (7) (11.68–12.76)	0.95	–0.24	0.41	0.13
M <sup>3</sup> –M <sup>3</sup>	4.90±0.16 (10) (4.70–5.16)	5.09±0.16 (5) (4.84–5.24)	5.12±0.14 (10) (4.92–5.37)	–	4.99±0.17 (7) (4.70–5.15)	0.97	–0.02	0.04	0.01
ZB	7.95±0.18 (10) (7.71–8.35)	8.22±0.21 (5) (7.89–8.45)	8.29±0.35 (10) (7.63–8.67)	–	8.18±0.24 (7) (7.72–8.49)	0.98	–0.10	0.05	–
GBB	6.99±0.11 (10) (6.85–7.15)	7.12±0.05 (5) (7.06–7.19)	6.99±0.11 (10) (6.85–7.15)	–	7.14±0.20 (7) (6.73–7.31)	–	–	–	–
BH	4.91±0.10 (10) (4.74–5.06)	4.97±0.16 (5) (4.86–5.25)	4.47±0.29 (10) (3.98–4.97)	–	4.81±0.20 (7) (4.57–5.13)	0.60	0.80	0.29	0.75
C <sup>1</sup> –M <sup>3</sup>	5.11±0.09 (10) (4.94–5.22)	5.37±0.13 (5) (5.17–5.49)	5.23±0.14 (10) (5.00–5.50)	–	5.25±0.13 (7) (5.06–5.45)	0.97	0.07	–	0.04
ML	9.17±0.28 (10) (8.61–9.56)	9.52±0.21 (5) (9.17–9.75)	9.46±0.29 (10) (8.97–9.88)	–	9.42±0.26 (7) (9.00–9.78)	0.98	–	0.02	0.06
C <sub>1</sub> –M <sub>3</sub>	5.47±0.14 (10) (5.26–5.65)	5.71±0.15 (5) (5.48–5.86)	5.40±0.22 (10) (4.92–5.71)	–	5.46±0.15 (7) (5.29–5.76)	0.96	–0.07	0.02	–

## Results

### Morphological examination

*Kerivoula depressa* is a moderate-sized species with a forearm (FA) length of  $30.75 \pm 1.08$  mm. Ears are small and rounded, and the posterior margin of the pinnae has a deep, smoothly concave emargination just below the apex. Overall pelage color is buff brown to dark brown. The lower part of ventral hair is dark brown, whereas its tip is light brownish yellow. Dorsal fur is of black base but with dark brown tip (Fig. 1A–C). The domed skull is small, with the greatest length of  $13.75 \pm 0.17$  mm. The mid-portion of the braincase exceeds the frontal region in height. Its lateral profile is flattened from the rostrum to the forehead. A sagittal crest is not evident, and the lambdoid crests are relatively weak. The dental formula is I 2/3, C 1/1, P 3/3, M 3/3. The second upper incisor ( $I^2$ ) is about half of the first upper incisor ( $I^1$ ) in height, and the latter is one half the height of the upper canine. The third upper premolar ( $P^3$ ) is distinctly higher than the anterior two. The third upper molar ( $M^3$ ) is degenerated. The crown area of the first and second lower molars is approximately equal and slightly larger than the last molar ( $M_3$ ).

*Kerivoula dongduongana*, with FA of  $34.02 \pm 0.94$  mm, is slightly larger than *K. depressa*. Its ears are rounded with a tiny, smooth depression near the tip. *Kerivoula dongduongana* is obviously yellower than *K. depressa* in pelage coloration (Fig. 1D–F).



**Figure 1.** Photographs of *K. depressa* (A–C voucher GZHU 19202, male) and *K. dongduongana* (D–F voucher GZHU 19198, female) representing their lateral view (A, D), ventral pelage (B, E) and dorsal pelage (C, F).

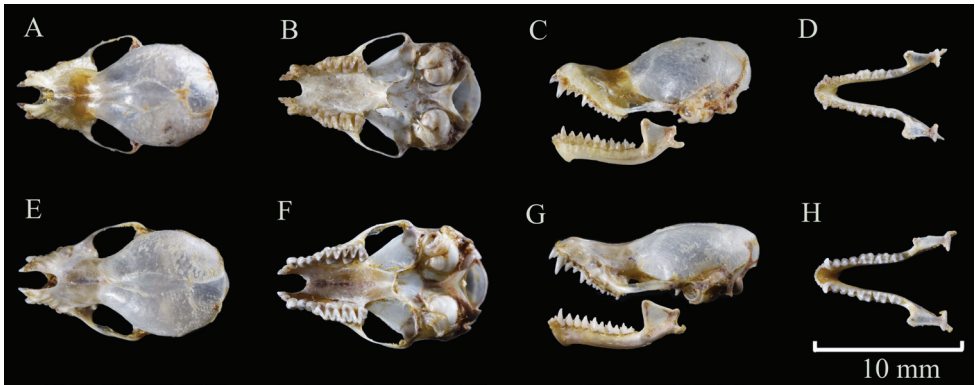


**Figure 2.** Skull morphology of *K. depressa* (A–D voucher GZHU 19222, female) and *K. dongduongana* (E–H voucher GZHU 19308, female). Scale bar: 10 mm.

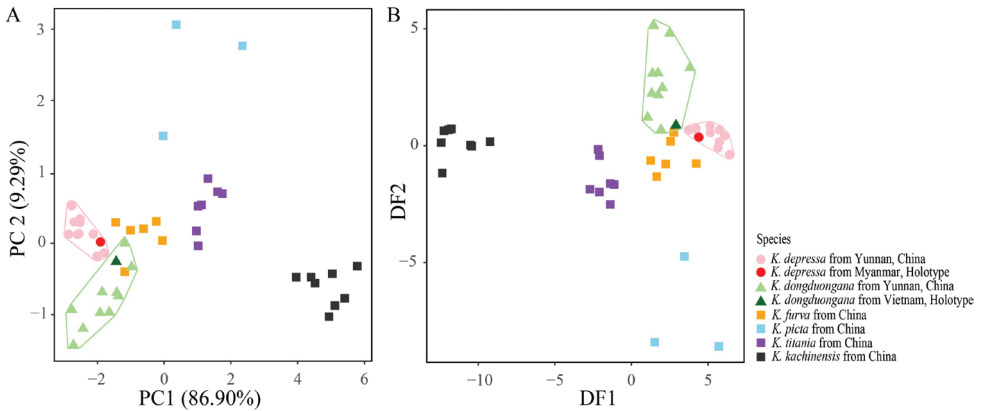


**Figure 3.** Two-dimensional PCA and DAPC plots of *Kerivoula* species based on nine craniodental measurements **A** PCA plots for *K. depressa*, *K. dongduongana*, *K. furva*, *K. kachinensis*, *K. picta*, and *K. tania* showing projections of individual specimens and variable loadings on the first two principal components **B** projections of 46 specimens and variable loadings on two discriminant functions obtained from external and craniodental measurements.

The ventral pelage is golden brown, and the base and middle portions are medium brown with golden-brown tips. The dorsal pelage is dark brown with golden-brown tips. Craniodental features are similar to *K. depressa*, but *K. dongduongana* is characterized by a flatter and longer skull (Fig. 2C, G; Table 1).

### Multivariate comparison analysis

PCA based on eight craniodental measurements revealed 96.2% of the total variance from the first two principal components (PCs) (86.9% and 9.3% for PC1 and PC2, respectively) in the scatter plot of the six morphological groups (Fig. 3A). For PC1,

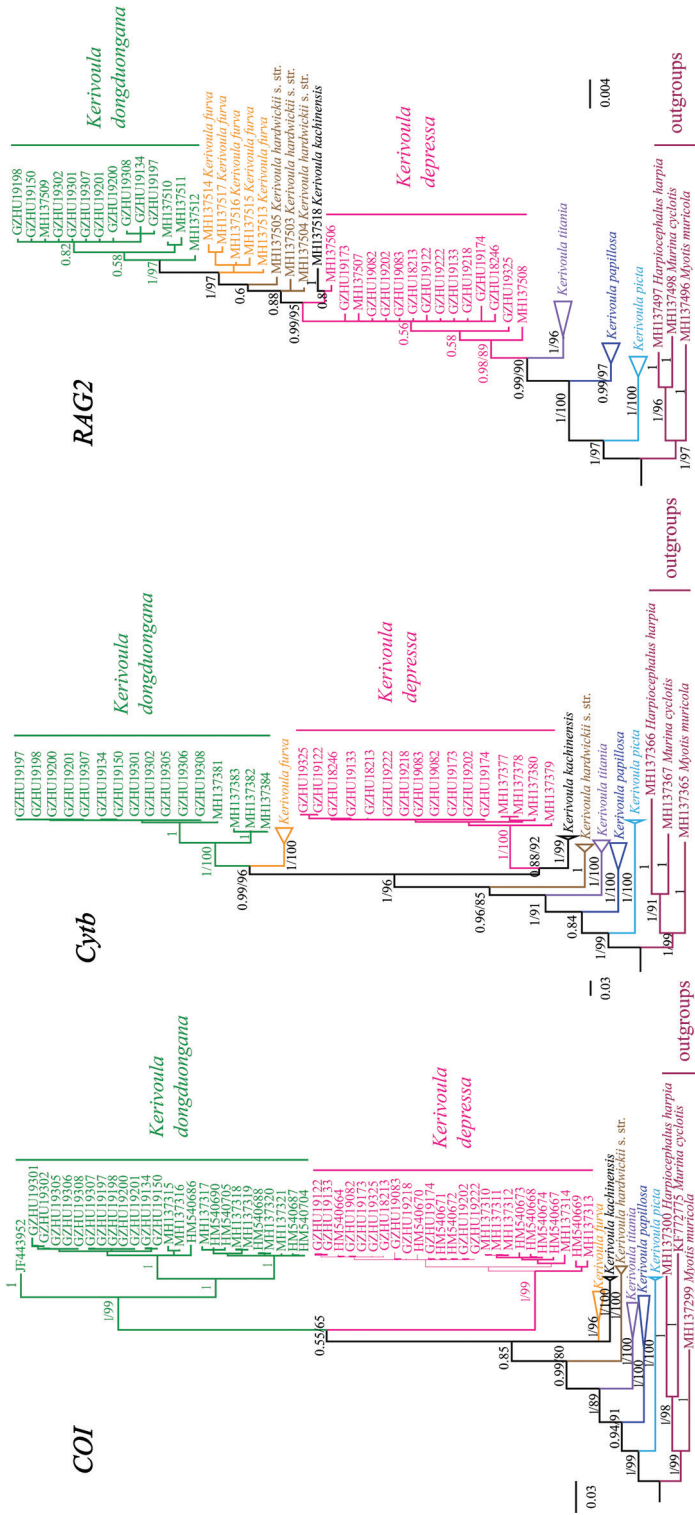


**Figure 4.** Bayesian and ML trees from analysis of *COI*, *Cytb*, and *RAG2* sequences for the *K. hardwickii* complex. Values on the branches indicate posterior probabilities and bootstrap values, respectively. The terminals *K. picta*, *K. hardwickii* (sensu stricto), *K. kachinensis*, and *K. furva* each include multiple samples (see Appendix 1).

all measurements had positive loadings (Table 1), reflecting the skull size. Larger bats were characterized by higher PC1 scores; thus, specimens of *K. kachinensis* clustered to the right compared with those of other taxa (Fig. 3A). For PC2, all measurements had low loadings except for the braincase height (BH) (Table 1). Therefore, based on PC2, *K. picta* and *K. titania*, which had a larger BH, were clustered to the top of the plot, whereas *K. dongduongana* and *K. kachinensis* were assigned to the bottom (Fig. 3). For DAPC, we entered the first two PCs from the PCA results and obtained two discriminant functions (DFs) to distinguish among studied *Kerivoula* specimens. PCA and DAPC scatter plots showed that *K. depressa* and *K. dongduongana* specimens formed distinct and separated clusters (pale pink and green triangles in Fig. 3), although some scatter values overlapped with those from *K. furva*. Meanwhile, *K. picta*, *K. titania*, and *K. kachinensis* clustered into three distinguishable groups (Fig. 3).

### Phylogenetic relationships of *Kerivoula*

Bayesian and ML trees using *COI*, *Cytb*, and *RAG2* matrices highly supported monophyly of the genus *Kerivoula* (Fig. 4) [posterior probabilities (PP)/bootstrap values (BS), 1/99 for *COI* and *Cytb*, 1/97 for *RAG2*] and revealed a similar well-supported topology. *Kerivoula picta* and *K. papillosa* occurred outside of the clade uniting all other examined species within *Kerivoula*. All inferences clustered our sequences with *K. depressa* (PP = 1 in *COI/Cytb*; BS: 99 for *COI*, 100 for *Cytb*) and *K. dongduongana* (PP = 1 in *COI/Cytb/RAG2*; BS: 99 for *COI*, 100 for *Cytb*, 97 for *RAG2*), thus verifying our morphological species identification results (Fig. 4). However, interspecific relationships of *K. depressa*, *K. dongduongana*, *K. kachinensis*, *K. furva*, and *K. hardwickii* (*sensu stricto*) remain ambiguous and could not be resolved herein.

### Discussion

The major interspecific phylogenetic relationships of our analyses are comparable with those reported by Kuo et al. (2017) and Tu et al. (2018). Our studies similarly confirmed the monophyly of *K. depressa* and *K. dongduongana*. However, the topology of the phylogenetic tree based on the *RAG2* gene remains unresolved and needs further study. Finally, combining the results of external and craniodental examination and multivariate analyses, 24 specimens were determined as *K. depressa* and *K. dongduongana* (Table 1).

Our discovery of *K. depressa* and *K. dongduongana* in China indicates that six species of *Kerivoula* live in China. According to morphological analyses, *K. picta* is easily distinguished by its unique pelage color pattern and skull shape (Wilson and Mittermeier 2019), whereas *K. kachinensis* is the largest species with a distinctly flattened skull (Bates et al. 2004; Tu et al. 2018; Yu et al. 2022). As for the remaining four similar-sized species, *K. titania* has a distinctly longer tibia and higher braincase than the others (Kuo et al. 2017; Tu et al. 2018). In pelage coloration, *K. furva* has the darkest fur color, varying from black brown to black gray, whereas *K. depressa* and *K. dongduongana* are pale brown.

Among the four species, *K. dongduongana* has the shortest BH (Kuo et al. 2017; Tu et al. 2018). A key to the *Kerivoula* species occurring in China is provided in Appendix 2.

Until recently, *Kerivoula* species were considered forest-dependent (Wilson and Mittermeier 2019). They are known in the south of China across Yunnan to Taiwan, and from Hainan to Chongqing. It is worth noting that five of the “Chinese” *Kerivoula* species are found in the southwest region of Yunnan Province, which is often treated as a biodiversity hotspot near Myanmar, Laos, and Vietnam. Its unique terrain, vegetation, and environmental conditions, including a low latitude, warm and tropical forest, and humid micro-climate, appear suitable for inhabitation and colonization (Kruskop 2013; Wilson and Mittermeier 2019; Qian et al. 2020). The high diversity of woolly bats in tropical forest areas may indicate the origin in their diversification progress.

Based on a comparison of the recorded *Kerivoula* diversity from the bordering countries of Myanmar (five species), Laos (seven species), and Vietnam (eight species) (Wilson and Mittermeier 2019), we suggest that there is still a risk of underestimating the diversity of *Kerivoula* in China. More surveys should therefore be conducted, especially on the border/unexplored region and using effective sampling tools such as multi-bank harp traps.

## Acknowledgements

The authors thank National Nature Reserve Administration of Xishuangbanna Dai Autonomous Prefecture for their guides and help during the field survey. We also thank Ruichang Quan from Xishuangbanna Tropical Botanical Garden, Chinese Academy of Sciences, for the assistance in the field survey. This study was financially supported by the National Sciences Foundation of China (31970394, 32192421), The Special Foundation for National Science and Technology Basic Research Program of China [2021FY100303].

## References

- Bates PJJ, Harrison DL (1997) Bats of the Indian Subcontinent. Harrison Zoological Museum, Sevenoaks, Kent, 212–215.
- Bates PJJ, Struebig MJ, Rossiter SJ, Kingston T, Oo SSL, Mya KM (2004) A New Species of *Kerivoula* (Chiroptera: Vespertilionidae) from Myanmar (Burma). *Acta Chiropterologica* 6(2): 219–226. <https://doi.org/10.3161/001.006.0203>
- Bates PJJ, Struebig MJ, Hayes BD, Furey NM, Mya KM, Thong VD, Tien PD, Son NT, Harrison DL, Francis CM, Csorba G (2007) A new species of *Kerivoula* (Chiroptera: Vespertilionidae) from Southeast Asia. *Acta Chiropterologica* 9(2): 323–337. [https://doi.org/10.3161/1733-5329\(2007\)9\[323:ANSOKC\]2.0.CO;2](https://doi.org/10.3161/1733-5329(2007)9[323:ANSOKC]2.0.CO;2)
- Brunet-Rossinni AK, Wilkinson GS (2009) Methods for age estimation and the study of senescence in bats. In: Kunz TH, Parsons S (Eds) *Ecological & behavioral methods for the study of bats*. The Johns Hopkins University Press, Baltimore, 315–325.
- Corbet GB, Hill JE (1992) *The Mammals of Indomalayan Region: a Systematic Review*. Oxford University Press, Oxford, 488 pp.

- Douangboubpha B, Bumrungsri S, Satasook C, Wanna W, Soisook P, Bates PJJ (2016) Morphology, genetics and echolocation calls of the genus *Kerivoula* (Chiroptera: Vespertilionidae: Kerivoulinae) in Thailand. *Mammalia* 80(1): 21–47. <https://doi.org/10.1515/mammalia-2014-0004>
- Dray S, Dufour AB, Chessel D (2007) The ade4 Package– II. Two-table and K-table Methods. 7: 6–6.
- Edgar RC (2004) MUSCLE: Multiple sequence alignment with high accuracy and high throughput. *Nucleic Acids Research* 32(5): 1792–1797. <https://doi.org/10.1093/nar/gkh340>
- Ellerman JR, Morrison-Scott TC (1951) Check list of Palaearctic and Indian mammals 1758 to 1946. British Museum, Natural History, London, 810 pp.
- Francis CM, Kingston T, Zubaid A (2007) A new species of *Kerivoula* (Chiroptera: Vespertilionidae) from peninsular Malaysia. *Acta Chiropterologica* 9(1): 1–12. [https://doi.org/10.3161/1733-5329\(2007\)9\[1:ANSOKC\]2.0.CO;2](https://doi.org/10.3161/1733-5329(2007)9[1:ANSOKC]2.0.CO;2)
- Francis CM, Borisenko AV, Ivanova NV, Eger JL, Lim BK, Guillén-Servent A, Kruskop SV, Mackie I, Hebert PDN (2010) The Role of DNA Barcodes in Understanding and Conservation of Mammal Diversity in Southeast Asia. *PLoS ONE* 5: e12575. <https://doi.org/10.1371/journal.pone.0012575>
- Gray JE (1842) Descriptions of some new Genera and fifty unrecorded Species of Mammalia. *Annals & Magazine of Natural History* 10(65): 255–267. <https://doi.org/10.1080/03745484209445232>
- Hill JE (1965) Asiatic bats of the genera *Kerivoula* and *Phoniscus* (Vespertilionidae), with a note on *Kerivoula aerosa* Tomes. *Mammalia* 29(4): 524–556. <https://doi.org/10.1515/mamm.1965.29.4.524>
- Hoofer SR, Reeder SA, Hansen EW, Van Den Bussche RA (2003) Molecular phylogenetics and taxonomic review of Noctilionoid and Vespertilionoid bats (Chiroptera: Yangochiroptera). *Journal of Mammalogy* 84(3): 809–821. <https://doi.org/10.1644/BWG-034>
- Horsfield T (1824) Zoological researches in Java, and the neighbouring islands. Printed for Kingsbury, Parbury and Allen, London. <https://doi.org/10.5962/bhl.title.44848>
- Jombart T (2008) adegenet: A R package for the multivariate analysis of genetic markers. *Bioinformatics* 24(11): 1403–1405. <https://doi.org/10.1093/bioinformatics/btn129>
- Kalyaanamoorthy S, Minh BQ, Wong TKF, von Haeseler A, Jermiin LS (2017) ModelFinder: Fast model selection for accurate phylogenetic estimates. *Nature Methods* 14(6): 587–589. <https://doi.org/10.1038/nmeth.4285>
- Khan FAA, Solari S, Swier VJ, Larsen PA, Abdullah MT, Baker RJ (2010) Systematics of Malaysian woolly bats (Vespertilionidae: *Kerivoula*) inferred from mitochondrial, nuclear, karyotypic, and morphological data. *Journal of Mammalogy* 91(5): 1058–1072. <https://doi.org/10.1644/09-MAMM-A-361.1>
- Kruskop SV (2013) Bats of Vietnam: Checklist and an Identification Manual (2<sup>nd</sup> edn.). *Tovarishchestvo nauchnykh izdaniï KMK, Moscow*, 154–160.
- Kuo HC, Chen SF, Fang YP, Flanders J, Rossiter SJ (2014) Comparative range wide phylogeography of four endemic Taiwanese bat species. *Molecular Ecology* 23(14): 3566–3586. <https://doi.org/10.1111/mec.12838>
- Kuo HC, Soisook P, Ho YY, Csorba G, Wang CN, Rossiter SJ (2017) A Taxonomic Revision of the *Kerivoula hardwickii* Complex (Chiroptera: Vespertilionidae) with the Description

- of a New Species. *Acta Chiropterologica* 19(1): 19–19. <https://doi.org/10.3161/15081109ACC2017.19.1.002>
- Le S, Josse J, Husson F (2008) FactoMineR: An R Package for Multivariate Analysis. *Journal of Statistical Software* 25(1): 1–18. <https://doi.org/10.18637/jss.v025.i01>
- Minh BQ, Schmidt HA, Chernomor O, Schrempf D, Woodhams MD, von Haeseler A, Lanfear R (2020) IQ-TREE 2: New Models and Efficient Methods for Phylogenetic Inference in the Genomic Era. *Molecular Biology and Evolution* 37: 1530–1534. <https://doi.org/10.1093/molbev/msaa015>
- Nguyen ST, Motokawa M, Oshida T, Endo H (2016) A morphological analysis of the skull size and shape of Kerivoulineae (Chiroptera: Vespertilionidae) from Vietnam. *The Journal of Veterinary Medical Science* 78(2): 187–198. <https://doi.org/10.1292/jvms.15-0270>
- Nylander JAA (2004) MrModeltest v2. Program distributed by the author. Evolutionary Biology Centre, Uppsala University.
- Qian LS, Chen JH, Deng T, Sun H (2020) Plant diversity in Yunnan: Current status and future directions. *Plant Diversity* 42(4): 281–291. <https://doi.org/10.1016/j.pld.2020.07.006>
- R Core Team (2013) R: A language and environment for statistical computing. R Foundation for Statistical Computing, Vienna. <http://www.R-project.org/>
- Revelle W (2013) Psych: Procedures for psychological, psychometric, and personality Research, 1. R Package Version 1.0–95.
- Ronquist F, Teslenko M, van der Mark P, Ayres DL, Darling A, Höhna S, Larget B, Liu L, Suchard MA, Huelsenbeck JP (2012) MrBayes 3.2: Efficient Bayesian phylogenetic inference and model choice across a large model space. *Systematic Biology* 61(3): 539–542. <https://doi.org/10.1093/sysbio/sys029>
- Ruedi M, Biswas J, Csorba G (2012) Bats from the wet: two new species of tube-nosed bats (Chiroptera: Vespertilionidae) from Meghalaya, India. *Revue Suisse de Zoologie* 119(1): 111–135. <https://doi.org/10.5962/bhl.part.150145>
- Sikes RS (2016) the Animal Care Use Committee of the American Society of Mammalogists Guidelines of the American Society of Mammalogists for the use of wild mammals in research and education. *Journal of Mammalogy* 97: 663–688. <https://doi.org/10.1093/jmammal/gyw078>
- Simmons NB (2005) Order Chiroptera. In: Wilson DE, Reeder DM (Eds) *Mammal Species of the World: a Taxonomic and Geographic Reference* (3<sup>rd</sup> ed.). Johns Hopkins University Press, London, 312–529.
- Sinha YR (1999) Records of the zoological survey of India: contribution to the knowledge of bats (Mammalia: Chiroptera) from North East Hills, India. *Zoological Survey of India, Calcutta*, 52 pp.
- Stadelmann B, Jacobs DS, Schoeman C, Ruedi M (2004) Phylogeny of African *Myotis* Bats (Chiroptera, Vespertilionidae) Inferred from Cytochrome b Sequences. *Acta Chiropterologica* 6(2): 177–192. <https://doi.org/10.3161/001.006.0201>
- Tu VT, Hassanin A, Furey NM, Son NT, Csorba G (2018) Four species in one: multigene analyses reveal phylogenetic patterns within Hardwicke's woolly bat, *Kerivoula hardwickii*-complex (Chiroptera, Vespertilionidae) in Asia. *Hystrix, the Italian Journal of Mammalogy* 29(1): 111–121. <https://doi.org/10.4404/hystrix-00017-2017>
- Wickham H (2016) *ggplot2: Elegant Graphics for Data Analysis*. Springer-Verlag New York. ISBN 978-3-319-24277-4. <https://ggplot2.tidyverse.org>

- Wilson DE, Mittermeier RA (2019) Handbook of the Mammals of the World (Vol. 9). Bats. Lynx Edicions, Barcelona, 894–900.
- Wu Y, Li YC, Lin LK, Harada M, Chen Z, Motokawa M (2012) New Records of *Kerivoula titania* (Chiroptera: Vespertilionidae) from Hainan Island and Taiwan. *Mammal Study* 37(1): 69–72. <https://doi.org/10.3106/041.037.0109>
- Yu WH, Li F, Csorba G, Xu ZX, Wang XY, Guo WJ, Li YC, Wu Y (2018) A revision of *Kerivoula hardwickii* and occurrence of *K. furva* (Chiroptera: Vespertilionidae) in China. *Zootaxa* 4461(1): 45–45. <https://doi.org/10.11646/zootaxa.4461.1.2>
- Yu W, Lin C, Huang Z, Liu S, Wang Q, Quan R, Li S, Wu Y (2022) Discovery of *Kerivoula kachinensis* and a validity of *K. titania* (Chiroptera: Vespertilionidae) in China. *Mammalia* 86(3): 303–308. <https://doi.org/10.1515/mammalia-2021-0102>

## Appendix I

**Table A1.** Sample used in molecular analyses, with GenBank accession numbers for *COI*, *Cytb* and *RAG2* genes provided. Newly generated sequences in this study are shown in bold.

Taxon	Voucher	GenBank accession numbers			Location	Reference	
		<i>COI</i>	<i>Cytb</i>	<i>RAG2</i>			
<i>Kerivoula depressa</i>	GZHU 18213	<b>OM716942</b>	<b>OM735703</b>	<b>OM735730</b>	Yunnan, China	This study	
	GZHU 18246	–	<b>OM735713</b>	<b>OM735736</b>	Yunnan, China	This study	
	GZHU 19082	<b>OM716943</b>	<b>OM735707</b>	<b>OM735727</b>	Yunnan, China	This study	
	GZHU 19083	<b>OM716948</b>	<b>OM735704</b>	<b>OM735729</b>	Yunnan, China	This study	
	GZHU 19122	<b>OM716946</b>	<b>OM735712</b>	<b>OM735731</b>	Yunnan, China	This study	
	GZHU 19133	<b>OM716947</b>	<b>OM735714</b>	<b>OM735734</b>	Yunnan, China	This study	
	GZHU 19173	<b>OM716944</b>	<b>OM735708</b>	<b>OM735732</b>	Yunnan, China	This study	
	GZHU 19174	<b>OM716949</b>	<b>OM735710</b>	<b>OM735725</b>	Yunnan, China	This study	
	GZHU 19202	<b>OM716950</b>	<b>OM735709</b>	<b>OM735728</b>	Yunnan, China	This study	
	GZHU 19218	<b>OM716952</b>	<b>OM735705</b>	<b>OM735735</b>	Yunnan, China	This study	
	GZHU 19222	<b>OM716951</b>	<b>OM735706</b>	<b>OM735733</b>	Yunnan, China	This study	
	GZHU 19325	<b>OM716945</b>	<b>OM735711</b>	<b>OM735726</b>	Yunnan, China	This study	
	<i>Kerivoula dongduongana</i>	GZHU 19134	<b>OM716941</b>	<b>OM735697</b>	<b>OM735715</b>	Yunnan, China	This study
		GZHU 19150	<b>OM716940</b>	<b>OM735696</b>	<b>OM735720</b>	Yunnan, China	This study
		GZHU 19197	<b>OM716936</b>	<b>OM735691</b>	<b>OM735717</b>	Yunnan, China	This study
		GZHU 19198	<b>OM716937</b>	<b>OM735692</b>	<b>OM735721</b>	Yunnan, China	This study
GZHU 19200		<b>OM716938</b>	<b>OM735693</b>	<b>OM735722</b>	Yunnan, China	This study	
GZHU 19201		<b>OM716939</b>	<b>OM735694</b>	<b>OM735724</b>	Yunnan, China	This study	
GZHU 19301		<b>OM716930</b>	<b>OM735698</b>	<b>OM735718</b>	Yunnan, China	This study	
GZHU 19302		<b>OM716931</b>	<b>OM735699</b>	<b>OM735719</b>	Yunnan, China	This study	
GZHU 19305		<b>OM716932</b>	<b>OM735700</b>	–	Yunnan, China	This study	
GZHU 19306		<b>OM716933</b>	<b>OM735701</b>	–	Yunnan, China	This study	
GZHU 19307	<b>OM716935</b>	<b>OM735695</b>	<b>OM735723</b>	Yunnan, China	This study		
GZHU 19308	<b>OM716934</b>	<b>OM735702</b>	<b>OM735716</b>	Yunnan, China	This study		
<i>Murina cyclotis</i>	VN11-1199	KF772775	MH137367	MH137498	Viet Nam	Tu et al. 2018	
<i>Harpiocephalus harpia</i>	VN11-1288	MH137300	MH137366	MH137497	Viet Nam	Tu et al. 2018	
<i>Myotis muricola</i>	VN11-1186	MH137299	MH137365	MH137496	Viet Nam	Tu et al. 2018	
<i>Kerivoula picta</i>	VN11-1565	MH137303	–	–	Cambodia	Tu et al. 2018	
	VN11-1576	MH137304	MH137370	MH137501	Cambodia	Tu et al. 2018	
	VN11-1577	MH137305	MH137371	MH137502	Cambodia	Tu et al. 2018	
<i>Kerivoula papillosa</i>	20467	MH137301	MH137368	MH137499	Thailand	Tu et al. 2018	
	21719	MH137302	MH137369	MH137500	Cambodia	Tu et al. 2018	

Taxon	Voucher	GenBank accession numbers			Location	Reference	
		<i>COI</i>	<i>Cytb</i>	<i>RAG2</i>			
<i>K. dongduongana</i>	ROM 110828	JF443952	–	–	Vietnam	Tu et al. 2018	
	CPV10-295	MH137318	–	–	Cambodia	Tu et al. 2018	
	CPV10-297	MH137319	MH137382	MH137510	Cambodia	Tu et al. 2018	
<i>K. dongduongana</i>	ROM MAM 111278	HM540688	–	–	Viet Nam	Francis et al. 2010	
	VN11-1158	MH137320	MH137383	MH137511	Vietnam	Tu et al. 2018	
	VN11-1178	MH137321	MH137384	MH137512	Vietnam	Tu et al. 2018	
	ROM MAM 111298	HM540687	–	–	Viet Nam	Francis et al. 2010	
	ROM MAM 111277	HM540704	–	–	Viet Nam	Francis et al. 2010	
	CPV10-292	MH137317	–	–	Cambodia	Tu et al. 2018	
	ROM MAM 110605	HM540690	–	–	Laos	Francis et al. 2010	
	ROM MAM 110604	HM540705	–	–	Laos	Francis et al. 2010	
	23028	MH137315	–	–	Viet Nam	Tu et al. 2018	
	23036	MH137316	MH137381	MH137509	Viet Nam	Tu et al. 2018	
<i>Kerivoula titania</i>	PSUZC-MM2011.48	KY034089	–	–	Thailand	Soisook et al. 2016	
	PSUZC-MM2011.15	KY034108	–	–	Thailand	Soisook et al. 2016	
	VN11-0945	MH137361	–	–	Viet Nam	Tu et al. 2018	
	VN11-0013	MH137349	–	–	Viet Nam	Tu et al. 2018	
	23034	MH137340	MH137396	–	Viet Nam	Tu et al. 2018	
	VN11-0010	MH137346	–	–	Viet Nam	Tu et al. 2018	
	VN11-0025	MH137352	–	–	Viet Nam	Tu et al. 2018	
	VN11-0026	MH137353	–	–	Viet Nam	Tu et al. 2018	
	VN11-0027	MH137354	–	–	Viet Nam	Tu et al. 2018	
	VN11-0030	MH137355	–	–	Viet Nam	Tu et al. 2018	
	<i>K. titania</i>	VN11-0031	MH137356	–	–	Viet Nam	Tu et al. 2018
		VN11-0944	MH137360	–	–	Viet Nam	Tu et al. 2018
		VN11-1832	MH137364	MH137402	–	Viet Nam	Tu et al. 2018
CPV10-415		MH137343	–	–	Cambodia	Tu et al. 2018	
CPV10-363		MH137341	MH137398	MH137520	Cambodia	Tu et al. 2018	
CPV10-399		MH137342	MH137399	MH137521	Cambodia	Tu et al. 2018	
VN11-1188		MH137362	MH137401	MH137523	Viet Nam	Tu et al. 2018	
VN11-1193		MH137363	–	–	Viet Nam	Tu et al. 2018	
21942		MH137339	MH137395	MH137519	Viet Nam	Tu et al. 2018	
VN11-0002		MH137344	–	–	Viet Nam	Tu et al. 2018	
VN11-0009		MH137345	–	–	Viet Nam	Tu et al. 2018	
VN11-0011		MH137347	–	–	Viet Nam	Tu et al. 2018	
VN11-0012		MH137348	MH137400	MH137522	Viet Nam	Tu et al. 2018	
VN11-0014		MH137350	–	–	Viet Nam	Tu et al. 2018	
VN11-0018		MH137351	–	–	Viet Nam	Tu et al. 2018	
VN11-0035		MH137357	–	–	Viet Nam	Tu et al. 2018	
VN11-0040		MH137358	–	–	Viet Nam	Tu et al. 2018	
VN11-0044	MH137359	–	–	Viet Nam	Tu et al. 2018		
<i>Kerivoula hardwickii</i> s. str.	23041	–	MH137397	–	Vietnam	Tu et al. 2018	
	21746	MH137306	MH137373	MH137503	Indonesia	Tu et al. 2018	
	VN11-1623	MH137309	MH137376	MH137505	Cambodia	Tu et al. 2018	
	VN11-1593	MH137307	MH137374	MH137504	Cambodia	Tu et al. 2018	
	VN11-1622	MH137308	MH137375	–	Cambodia	Tu et al. 2018	
<i>K. depressa</i>	17348	–	MH137372	–	Indonesia	Tu et al. 2018	
	ROM MAM 118429	HM540670	–	–	Laos	Francis et al. 2010	
	AGS980322-65	HM540664	–	–	Laos	Francis et al. 2010	
	ROM MAM 118186	HM540671	–	–	Laos	Francis et al. 2010	
	ROM MAM 118026	HM540672	–	–	Laos	Francis et al. 2010	
	ROM MAM 107721	HM540669	–	–	Viet Nam	Francis et al. 2010	
	VN11-1554	MH137313	MH137379	MH137506	Cambodia	Tu et al. 2018	
	VN11-1835	MH137314	MH137380	–	Vietnam	Tu et al. 2018	
	ROM MAM 117982	HM540673	–	–	Laos	Francis et al. 2010	
	ROM MAM 110602	HM540667	–	–	Laos	Francis et al. 2010	
	ROM MAM 117971	HM540668	–	–	Laos	Francis et al. 2010	
	ROM MAM 110585	HM540674	–	–	Laos	Francis et al. 2010	
	CPV10-291	MH137310	MH137377	MH137507	Cambodia	Tu et al. 2018	

Taxon	Voucher	GenBank accession numbers			Location	Reference
		<i>COI</i>	<i>Cytb</i>	<i>RAG2</i>		
<i>K. depressa</i>	CPV10-293	MH137311	–	–	Cambodia	Tu et al. 2018
	CPV10-409	MH137312	MH137378	MH137508	Cambodia	Tu et al. 2018
<i>Kerivoula kachinensis</i>	MAM 107718	HM540736	–	–	Viet Nam	Francis et al. 2010
	VN11-1831	MH137338	MH137394	–	Viet Nam	Tu et al. 2018
	VN11-0940	MH137337	MH137393	–	Viet Nam	Tu et al. 2018
	CPV10-416	MH137336	MH137392	MH137518	Cambodia	Tu et al. 2018
	ZMMU S-184667	GU684767	–	–	Viet Nam	Tu et al. 2018
<i>Kerivoula furva</i>	EDB 25747	HM540734	–	–	Laos	Francis et al. 2010
	16481	MH137335	MH137391	MH137513	Nepal	Tu et al. 2018
	VN11-0050	MH137330	–	–	Viet Nam	Tu et al. 2018
	VN11-0004	MH137324	MH137387	MH137515	Viet Nam	Tu et al. 2018
	VN11-0045	MH137325	–	–	Viet Nam	Tu et al. 2018
	VN11-0046	MH137326	–	–	Viet Nam	Tu et al. 2018
	VN11-0047	MH137327	–	–	Viet Nam	Tu et al. 2018
	VN11-0048	MH137328	–	–	Viet Nam	Tu et al. 2018
	VN11-0049	MH137329	–	–	Viet Nam	Tu et al. 2018
	VN11-0943	MH137333	MH137389	MH137516	Viet Nam	Tu et al. 2018
	VN11-0937	MH137331	MH137388	–	Viet Nam	Tu et al. 2018
	VN11-0942	MH137332	–	–	Viet Nam	Tu et al. 2018
	23024	MH137322	–	–	Viet Nam	Tu et al. 2018
	23025	MH137323	MH137385	MH137514	Viet Nam	Tu et al. 2018
	VN11-1361	MH137334	MH137390	MH137517	Viet Nam	Tu et al. 2018
2005-670	–	MH137386	–	Nepal	Tu et al. 2018	

## Appendix 2

### A key to the *Kerivoula* species occurring in China (both in English and Chinese)

- 1 Pelage color relatively bright. Fur orange. Wing membranes dark brown with reddish brown markings / 体色鲜艳,体毛橙黄色;翼膜深棕色,具红褐色斑块 .... *Kerivoula picta* / 彩蝠
- Pelage color duller. Fur dark gray, brown, or blackish gray / 体色较暗淡,体毛暗灰色、棕色或黑灰色 ..... **2**
- 2 Size larger, forearm length more than 40 mm. Greatest length of skull more than 16 mm, greatest breadth of braincase more than 8 mm / 体型较大,前臂长超过 40 mm; 颅全长大于 16 mm, 脑颅宽大于 8 mm ..... *Kerivoula kachinensis* / 克钦彩蝠
- Size smaller, forearm length less than 40 mm. Greatest length of skull less than 16 mm, greatest breadth of braincase less than 8 mm / 体型较小,前臂长不及 40 mm; 颅全长小于 16 mm, 脑颅宽小于 8 mm ..... **3**
- 3 Tibia length usually more than 18.5 mm. Greatest length of skull 14.5–16.0 mm, braincase height usually more than 5.3 mm / 胫骨长常大于 18.5 mm; 颅全长 14.5–16 mm, 颅高常大于 5.3 mm..... *Kerivoula titania* / 泰坦尼亚彩蝠
- Tibia length less than or equal to 18.5 mm. Greatest length of skull less than 14.5 mm, braincase height usually less than 5.3 mm / 胫骨长小于或等于 18.5 mm; 颅全长小于 14.5 mm, 颅高不及 5.3 mm..... **4**

- 4 Greatest width across the outer edges of the third upper molars more than 5.3 mm, greatest length of mandible more than 9.8 mm. Dorsal pelage dark brown to blackish gray, broadly uniform in colour from bases to tips / 第三上臼齿宽大于5.3 mm, 下颌长大于9.8 mm; 背毛深棕色到黑灰色, 毛基到毛尖颜色大致相同 ..... *Kerivoula furva* / 暗褐彩蝠
- Greatest width across the outer edges of the third upper molars less than 5.3 mm, greatest length of mandible less than 9.8 mm. Dorsal pelage buff brown to dark brown, its base and tip significantly different / 第三上臼齿宽小于5.3 mm, 下颌长小于9.8 mm; 背毛浅棕色到深棕色, 毛基与毛尖颜色明显不同 ..... 5
- 5 Braincase slightly flattened, braincase height more than 4.7 mm, more than 1/3 of greatest length of skull. Dorsal pelage buff brown to dark brown, ventral pelage dark brown / 脑颅略为扁平, 颅高大于4.7 mm, 超过颅全长1/3; 背毛浅棕色到深棕色, 腹毛深棕色 ..... *Kerivoula depressa* / 平颅彩蝠
- Braincase flatter, braincase height usually less than 4.7 mm, less than 1/3 of greatest length of skull. Dorsal pelage dark brown to golden brown, ventral pelage golden brown / 脑颅更扁平, 颅高多小于4.7 mm, 不及颅全长1/3; 背毛深棕色到金棕色, 腹毛金棕色 ..... *Kerivoula dongduongana* / 印支彩蝠



# Diet composition and interspecific niche of Taohongling Sika deer (*Cervus nippon kopschi*) and its sympatric Reeve's muntjac (*Muntiacus reevesi*) and Chinese hare (*Lepus sinensis*) in winter (Animalia, Mammalia)

Dandan Wang<sup>1</sup>, Xiaolong Hu<sup>2</sup>, Minling Li<sup>1</sup>, Jie Liu<sup>1</sup>, Ming Tang<sup>1</sup>,  
Wuhua Liu<sup>3</sup>, Jianwen Zhan<sup>3</sup>, Yongtao Xu<sup>1</sup>, Weiwei Zhang<sup>1</sup>

**1** College of Forestry, Wildlife Conservation Research Center, Jiangxi Agricultural University, Nanchang, Jiangxi, China **2** College of Animal Science and Technology, Jiangxi Agricultural University, Nanchang, Jiangxi, China **3** Taohongling Sika Deer National Nature Reserve, Pengze, Jiangxi, China

Corresponding authors: Yongtao Xu (ytxu666@jxau.edu.cn); Weiwei Zhang (zhangweiwei\_nefu@163.com)

Academic editor: Pavel Stoev | Received 2 November 2022 | Accepted 30 December 2022 | Published 22 February 2023

<https://zoobank.org/4FA6DE60-0F7A-4694-86E0-767A77F431A8>

**Citation:** Wang D, Hu X, Li M, Liu J, Tang M, Liu W, Zhan J, Xu Y, Zhang W (2023) Diet composition and interspecific niche of Taohongling Sika deer (*Cervus nippon kopschi*) and its sympatric Reeve's muntjac (*Muntiacus reevesi*) and Chinese hare (*Lepus sinensis*) in winter (Animalia, Mammalia). ZooKeys 1149: 17–36. <https://doi.org/10.3897/zookeys.1149.96936>

## Abstract

Species co-existence depends on how organisms utilize their environment and resources. Little is known about the winter diet composition and sympatric co-existence of South China sika deer and its companion species in Taohongling. In this study, high-throughput sequencing and metabarcoding trnL were used to study the diet composition and interspecific relationship including sika deer, Reeve's muntjac, and Chinese hare. Our results show that 203 genera in 90 families are contained in the diet of sika deer, 203 genera in 95 families for Reeve's muntjac, and 163 genera in 75 families for Chinese hare. Sika deer fed on *Rubus chingii*, *Loropetalum chinense*, and *Eurya japonica* in winter, accounting for 75.30%; Reeve's muntjac consumed mainly *R. chingii*, *E. japonica*, and *Euonymus grandiflorus*, accounting for 68.80%, and Chinese hare mainly fed on *R. chingii*, *Smilax china*, and *Rbus chinensis*, accounting for 41.98%. The Shannon index showed no significant difference between groups ( $p > 0.05$ ). The NMDS analysis found considerable overlap among three species. Sika deer and Reeve's muntjac consumed similar forage plants but varied greatly in Chinese hare, which occupied the widest choice in winter, resulting in higher diet breadth and increased dietary divergence, thereby reducing competition and facilitating coexistence. The diet niche

overlap index among them, as represented by Pianka's index, ranging from 0.62 between sika deer and Chinese hare to 0.83 between sika deer and Reeve's muntjac, which indicated a more similar niche and potential competition in closely related species. Our findings provide a new diet perspective of three herbivores, leading to a more comprehensive understanding of resource partitioning and species coexistence.

### Keywords

Diet composition, niche breadth, niche overlap, sympatry, winter

## Introduction

Sika deer (*Cervus nippon* Temminck, 1838), also known as the spotted deer, is a species native to much of East Asia and a national first-class protected wild animal in China (Yao et al. 2010). Its conservation status is Endangered globally and Endangered in China (Wang and Song 2013). Most wild sika deer populations in China have disappeared due to heavy hunting pressure that has existed for a very long period (Zhang et al. 2011a), and populations have also become gradually more isolated. South China sika deer (*Cervus nippon kopschi* Swinhoe, 1873) are mainly distributed in the Taohongling Sika deer National Nature Reserve (hereafter, TNNR) in northeastern Jiangxi Province, southern Anhui Province, and a part of northwestern Zhejiang Province. Statistics have previously shown that the population of sika deer in TNNR is 365 individuals (Gao et al. 2009; Jiang et al. 2012) which inhabit the hilly area at 300–500 m elevation (Wang 2018). Reeve's muntjac and Chinese hare are the main companion species of sika deer, and they have co-existed in the TNNR for numerous generations. Infrared-camera detection has been used to determine that the relative abundance of the Reeve's muntjac was 0.4160, which is significantly higher than that of the sika deer population (0.0411), and the relative abundance of the Chinese hare was 0.0138. Furthermore, the spatial distribution of both sika deer and Reeve's muntjac is primarily concentrated in the core area (Zhou 2019). Nowadays, little is known about the diets and sympatric co-existence of these three herbivores, particularly in winter when their food resources are scarcer.

Diet analysis is one of the core contents of studying the habitat requirements of animals (Liu 2009; Hoenig et al. 2022). Food not only provides the necessary energy and nutrients for life activities but also reflects the trophic niche of the species in the biome (Lu et al. 2020). Therefore, diet analysis can serve to understand a species' access to resources and habitat distribution to facilitate population conservation and recovery of endangered species. The study of diet mainly includes stomach contents analysis, indirect utilization methods, direct tracking observation, microscopic fecal analysis, and DNA metabarcoding analysis (Monro 1982; Zheng and Bao 2004; Lu et al. 2020). Stomach contents analysis is more accurate for identifying food resources but collecting stomach contents requires sacrificing animals (Fujii et al. 2019). Utilization methods and tracking observations are difficult to observe and may be influenced by subjective factors (Gong et al. 2022). Fecal microscopic analysis can be quantitative

(Zhang et al. 2011b) but requires accurate identification of taxa from partially digested plant fragments and likely over-emphasizes less digestible components of the diet (Holechek 1982). For the endangered species, it is necessary to prioritize noninvasive sampling. Diet research must adopt proven selection methods based on actual needs and conditions.

High-throughput sequencing (HTS) has the advantages of high throughput, a large amount of data, high sensitivity, and fine classification (Pompanon et al. 2012; Deagle et al. 2019). Compared with conventional methods of diet research, the metabarcoding method based on high-throughput sequencing can improve the deficiencies of the traditional methods that do not fully reflect consumers' diet information (Ma et al. 2021; Tabassum et al. 2022). The present technique has achieved remarkable results in diet research on filter-feeding shellfish (Kasim and Mukai 2009), small herbivores, fish, etc. (Soininen et al. 2009; Lin et al. 2018; Li et al. 2021), and this can identify species of lower taxonomic orders.

Food resources are the medium that connects the natural environment and often influence the distribution and survival of species. Species coexistence theory suggests that niche overlap and potential competition will inevitably occur when closely related species with similar ecological needs share the same area, which requires them to obtain more resources to survive by expanding the niche scale (Schaller 2000; Palmer and Truscott 2003). We predict that the three species in this study have been sympatric and have evolved together for numerous generations in the TNNR. Natural selection may have led to a separation in forage use (niche differentiation) among them (Pascual-Rico et al. 2020). Fitness may be reduced by competition; i.e., sika deer may increase their niche breadth, particularly in winter when food resources are scarcer (Schoener 1971). We explore the diet composition and dietary overlap of Taohongling Sika deer, Reeve's muntjac, and Chinese hare and assess the extent of potential dietary competition among these species to enhance our understanding of mechanisms underlying their coexistence. Research into the diet of sika deer and its sympatric herbivores can clarify food items and explore the interspecific competition and coexistence, which is of great significance to the population conservation of sika deer and biodiversity monitoring.

## Methods

### Study area

This study was conducted in the TNNR, the area where South China sika deer is distributed. The TNNR is located on the south bank of the middle and lower reaches of the Yangtze River, Pengze, Jiangxi Province, China. The total area of TNNR is 12,500 hm<sup>2</sup>, the core area is 2,670 hm<sup>2</sup>, the experimental area is 1,830 hm<sup>2</sup>, and the buffer zone is 8,000 hm<sup>2</sup>. The TNNR mainly consists of low mountains and hills (Wang et al. 2021). The TNNR lies in a climatic zone transitional from tropical to middle subtropical and has transitional climate characteristics that are warm, with a

humid monsoon, and four distinct seasons. The frost-free period is up to 247 days with little snow cover (Zhou 2019). The vegetation type is mainly composed of mixed evergreen–deciduous broad-leaved forest, coniferous forest, mixed coniferous–broad-leaved forest, broad-leaved forest, and bamboo (Zhou 2019). From December 2020 to February 2021, 90 fecal samples were collected from sika deer, Reeve’s muntjac, and Chinese hare in the TNNR and stored at  $-80^{\circ}\text{C}$ . Sampling sites mainly focused on Nursery bases (MP), Fir forests (SS), NieJiashan (NJS), XianLingAn (XLA), WuGuiShi (WGS), and Bamboo Garden (ZY) (Fig. 1).

## DNA extraction and PCR amplification

In our study, to minimize possible bias caused by variation in individual digestibility, five fecal pellets were randomly taken from each fecal sample and mixed to form a single composite sample. Total DNA was extracted using the DNA extraction kit (TIANGEN, Beijing) following the liquid nitrogen grinding method. The final DNA concentration and purification were determined by NanoDrop 2000 UV-vis spectrophotometer (Thermo Scientific, Wilmington, USA), and DNA quality was checked by 1% agarose gel electrophoresis. The P6 loop region of the *trnL(UAA)* intron region was amplified with universal primers g (5'-GGGCAATC CTGAGCCAA-3') and h (5'-CCATTGAGTCTCTGCACCTATC-3') by thermocycler PCR system (Gene Amp 9700, ABI, USA). PCR amplifications were carried out in a total volume of 25  $\mu\text{l}$

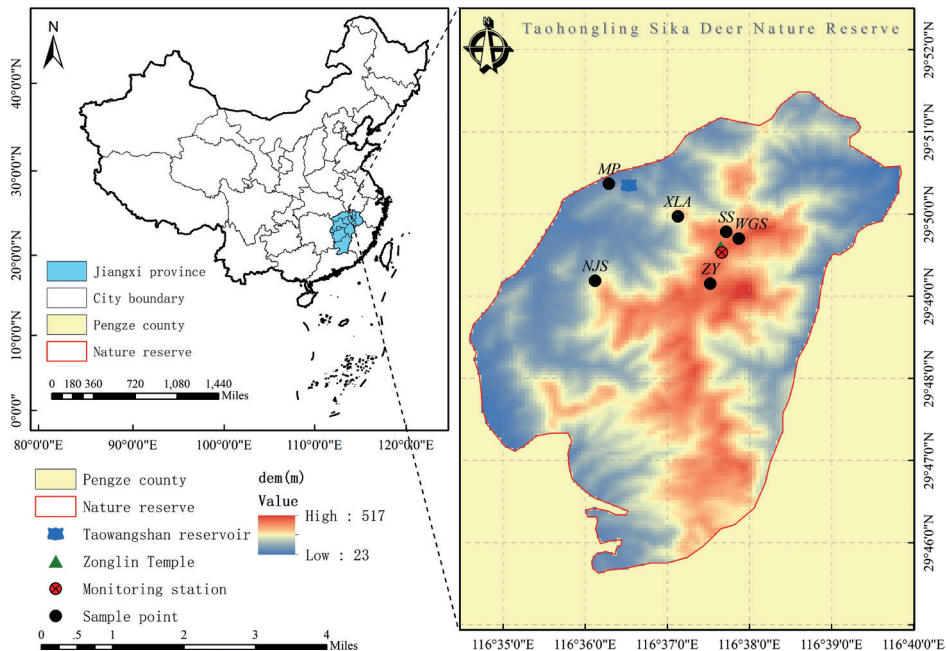


**Figure 1.** Fecal samples sites of three sympatric species at Taohongling Sika Deer Nature Reserve (MP: Nursery bases; SS: Fir forests; NJS: NieJiashan; XLA: XianLingAn; WGS: WuGuiShi; ZY: Bamboo Garden).

containing 12.5  $\mu\text{l}$  PCR mix (Tiangen, Beijing, China), 1  $\mu\text{l}$  DNA, 1  $\mu\text{l}$  of each primer, and 9.5  $\mu\text{l}$   $\text{H}_2\text{O}$ . The reaction conditions were as follows: denaturation at 95 °C for 3 min followed by 35 cycles at 95 °C for 30 sec, 56 °C for 30 sec, and 72 °C for 45 sec, with a final 10 min at 72 °C and storage at 4 °C for 10 h. The PCR products were detected by Agarose gel electrophoresis and sequenced by Shanghai Personal Biotechnology Co., Ltd.

## Illumina MiSeq sequencing and bioinformatics analysis

Purified amplicons were pooled in equimolar and paired end sequenced ( $2 \times 300$ ) on an Illumina MiSeq platform (Illumina, San Diego, USA) according to the standard protocols. The analysis was conducted by following the tutorial of QIIME2 docs along with customized program scripts (<https://docs.qiime2.org/2019.1/>). Briefly, raw FASTQ files were demultiplexed using the QIIME2 v. 2019.4 demux plugin based on their unique barcodes (Caporaso et al. 2010). Demultiplexed sequences from each sample were quality filtered and trimmed, denoised, and merged, and then the chimeric sequences were identified and removed using the QIIME2 dada2 plugin to obtain the feature table of operational taxonomic units (OTUs). The QIIME2 feature-classifier plugin was then used to align OTUs sequences to the National Center for Biotechnology Information (NCBI) database to generate the taxonomy table. Diversity metrics were calculated using the core-diversity plugin within QIIME2. Feature level alpha diversity indices, such as observed OTUs, Chao1 richness estimator, and Goods coverage index were calculated to estimate the diet diversity within an individual sample. A difference significance test was performed by R v. 4.1.3. Beta diversity distance measurements using Bray–Curtis were performed to investigate the structural variation of fecal plant communities across samples and then visualized via principal coordinate analysis (PCoA) and nonmetric multi-dimensional scaling (NMDS) (Vázquez-Baeza et al. 2013). Venn diagram analysis was performed to explore the common and special OTUs types among the three herbivores.

## Data statistics

Formulas of forage plants diversity and niche analysis were conducted as follows:

The Shannon–Wiener diversity index ( $H'$ ) was calculated to explore diet diversity (Shannon 1948), according to the following formula:

$$H' = -\sum_{i=1}^n P_i \ln P_i \quad (1)$$

Where  $P_i$  is the proportion of food item  $i$  out of all foods, and  $n$  is the total number of food items.

Pielou evenness index (Pielou 1969), according to the following formula:

$$J' = H' / H_{\max} \quad (2)$$

$$H_{\max} = \ln n \quad (3)$$

Where  $n$  is the number of plant species in the fecal sample, and the number of plant species is represented by the number of plant OTUs types.

The Levin index (Smith 1982) was applied to standardize the trophic niche measure, and the formula was as follows:

$$B = 1/\sum_{i=1}^s p_i^2 \quad (4)$$

The niche overlap index was obtained using the Pianka index (Pianka 1973; Hou et al. 2021), and the formula was as follows:

$$Q_{jk} = \frac{\sum_{i=1}^s P_{ij} P_{ik}}{\sqrt{\sum_{i=1}^s P_{ij}^2 \sum_{i=1}^s P_{ik}^2}} \quad (5)$$

Where  $Q_{jk}$  is Pianka's niche overlap index between species  $j$  and species  $k$ ;  $P_{ij}$  is the proportion of resource  $i$  out of all resources used by species  $j$ , and  $P_{ik}$  is the proportion of resource  $i$  out of all resources used by species  $k$ . The values range from 0 (no food item in common) to 1 (complete overlap in resource use).

## Results

### OTUs analysis

After processing the raw reads, a total of 11,411,958 counts were obtained from 90 fecal samples. The mean OTUs length was 67.96 bp with a range from 32 bp to 189 bp. Venn diagram showed that the OTUs in the overlap were commonly shared, and those in the nonoverlapping parts were special OTUs. In total, 764 OTUs, 833 OTUs, and 843 OTUs were obtained from sika deer, Reeve's muntjac, and Chinese hare samples, respectively. The number of OTUs among the three herbivore groups was 373, and the specific OTUs in sika deer, Reeve's muntjac, and Chinese hare were 391, 449, and 470, respectively (Fig. 2).

Based on OTUs sequences alignment in the NCBI database, the diets of sika deer, Reeve's muntjac, and Chinese hare includes 203 genera in 90 families, 203 genera in 95 families, and 163 genera in 75 families, respectively (Editorial Committee of FRPS 2004; Jiang 2009; see Suppl. material 1). The three species consumed common and specific forage plants but varied greatly in their use of the available forages. On the whole, the 10 most abundant families in the diet of sika deer include Rosaceae (36.94%), Hamamelidaceae (25.75%), Pentaphragacaceae (13.41%), Theaceae (3.89%), Celastraceae (3.01%), Poaceae (2.98%), Ericaceae (2.43%), Moraceae (2.09%), Cupressaceae (1.68%), and Cannabaceae (1.16%). For the Reeve's muntjac, the 10 most abundant families include Rosaceae (52.41%), Pentagliaceae (11.01%), Celastraceae (6.12%), Poaceae (4.52%), Cannabaceae (3.27%), Moraceae (2.64%), Sabiaceae (2.14%), Asteraceae (2.10%), Oleaceae (1.50%), and Smilacaceae (1.26%), and the 10 most abundant families in the Chinese hare consist of Rosaceae (16.35%),

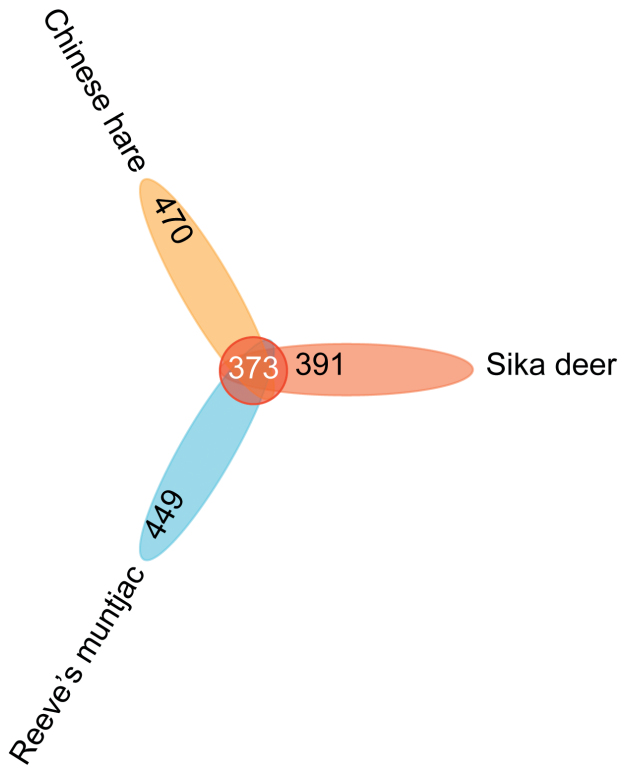


**Figure 2.** Venn analysis of OTUs in three herbivores of Taohongling nature reserve.

Poaceae (16.33%), Smilacaceae (15.58%), Anacardiaceae (10.71%), Fabaceae (9.74%), Asteraceae (6.77%), Rubiaceae (5.56%), and Cupressaceae (4.49%).

The dominant genera foraged by sika deer were *Rubus* (36.49%) and *Loropetalum* (25.52%), followed by *Eurya* (13.41%), *Camellia* (3.89%), *Euonymus* (2.94%), *Phyllostachys* (2.46%), *Maclura* (1.88%), *Cunninghamia* (1.67%), *Rhododendron* (1.45%), and *Celtis* (0.99%), and others (9.30%). For Reeve's muntjac the diet was strongly dominated by *Rubus* (51.77%), other genera high abundance were *Eurya* (11.01%), *Euonymus* (6.11%), *Celtis* (3.21%), *Arrhenatherum* (3.02%), *Sabia* (2.14%), *Maclura* (1.67%), *Ligustrum* (1.49%), *Phyllostachys* (1.31%), and *Smilax* (1.26%). Chinese hare consumed almost equal proportions of *Rubus* (15.81%) and *Smilax* (15.58%), followed by *Rhus* (10.64%), *Campylotropis* (9.52%), *Bidens* (5.37%), *Hedyotis* (5.02%), *Cunninghamia* (4.47%), *Eleusine* (3.57%), *Digitaria* (3.09%) and *Miscanthus* (2.55%). To sum up, these three herbivores all mostly feed on *Rubus* in winter. The species composition heatmap was drawn from the species and sample levels. The 20 genera with the highest abundance were selected based on species annotation information for 90 samples of the three species. The clustering results show the differences in the relative abundances of sika deer, Chinese hare, and Reeve's muntjac (Fig. 3).

High-throughput sequencing can be used to detect the diet on species levels in most samples combined with a background survey of TNNR, except for OTUs that

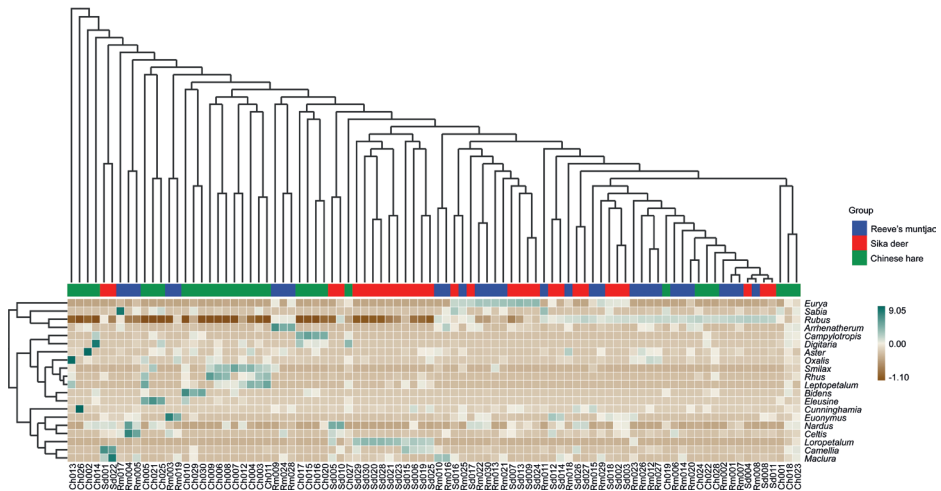


**Figure 3.** Species composition heat map at the genus level. (Ch: Chinese hare; Sd: Sika deer; Rm: Reeve's muntjac).

were undetectable. Sika deer food items included *Rubus chingii*, *Loropetalum chinense*, *Eurya japonica*, *Camellia japonica*, *Euonymus grandiflorus*, etc. The forage plants of Reeve's muntjac consisted of *Rubus chingii*, *Eurya japonica*, *Euonymus grandiflorus*, *Arrhenatherum elatius*, *Celtis sinensis*, etc. The diet of Chinese hares mainly focused on *Rubus chingii*, *Smilax china*, *Rhus chinensis*, *Campylotropis* sp., *Hedyotis diffusa*, etc. The detailed top 30 forage species in three species are shown in Table 1.

### Diet diversity and interspecific niche analysis

Alpha diversity reflects the abundance and diversity of species communities. The Chao1 and Observed species indices showed the highest community richness was Reeve's muntjac (Chao1 index; Reeve's muntjac = 242.46, Sika deer = 236.52, Chinese hare = 192.03, on average). The Shannon and Simpson indices showed the highest community diversity was Chinese hare (Shannon index; Chinese hare = 2.36, Reeve's muntjac = 2.21, Sika deer = 1.82, on average), with no significant differences ( $P > 0.05$ ). The goods coverage of 0.998 indicated that an average of 99% of the species were annotated (Fig. 4a; Table 2). Rarefaction curves describe the increase in species diversity as the sample size increases. It is crucial to point out that the characterization of species diversity was considered very reliable since the depth of rarefaction applied (35,000) was found to be sufficiently satisfactory (e.g., rarefaction curves had already reached a plateau at ~35,000 sequences in all samples) (Fig. 4b). The rank abundance curve reflects the richness and evenness of species in the sample through the flatness. The evenness of community composition of sika deer and Reeve's muntjac was higher, while the lowest of Chinese hare (Fig. 4c).

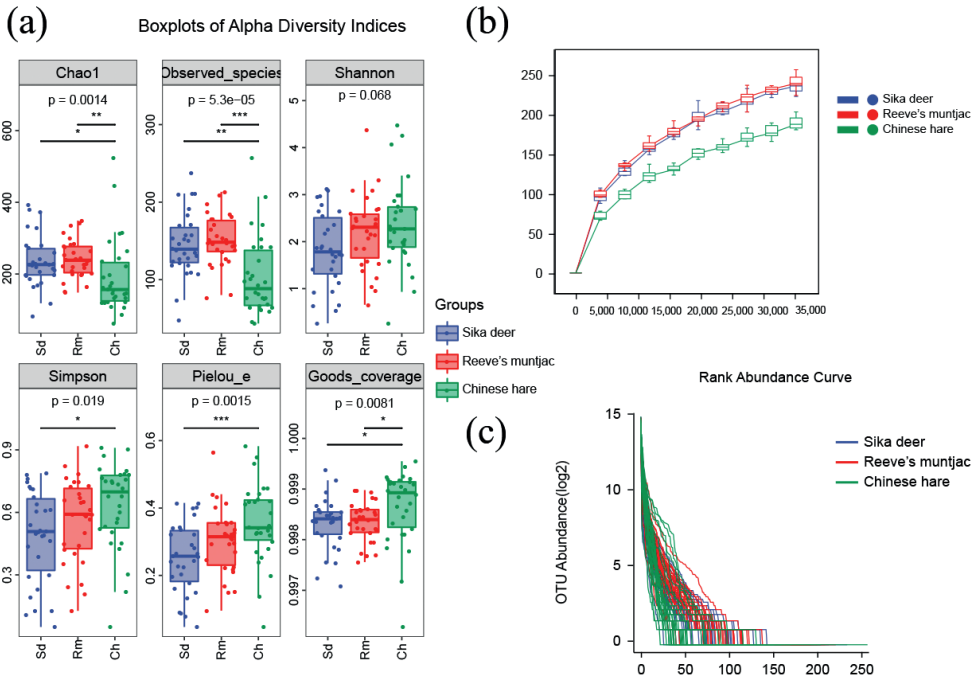
We assessed the beta diversity using the Bray–Curtis distance. When the distance between the samples was smaller, the species-composition structure was more similar,

Table 1. Winter diet of sika deer, Reeve's muntjac, and Chinese hare in Taohongling nature reserve. "+" = present in Jiangxi; "-" = not or uncertain present in Jiangxi.

Number	Sika deer			Reeve's muntjac			Chinese hare					
	Species	Genus	Distribution	Percentage of abundance	Species	Genus	Distribution	Percentage of abundance	Species	Genus	Distribution	Percentage of abundance
1	<i>Rubus chingii</i>	<i>Rubus</i>	+	36.42%	<i>Rubus chingii</i>	<i>Rubus</i>	+	51.69%	<i>Rubus chingii</i>	<i>Rubus</i>	+	15.78%
2	<i>Loropetalum chinense</i>	<i>Loropetalum</i>	+	25.48%	<i>Eurya japonica</i>	<i>Eurya</i>	+	11.01%	<i>Smilax china</i>	<i>Smilax</i>	+	15.56%
3	<i>Eurya japonica</i>	<i>Eurya</i>	+	13.41%	<i>Euonymus grandiflorus</i>	<i>Euonymus</i>	+	6.10%	<i>Rubus chinensis</i>	<i>Rubus</i>	+	10.64%
4	<i>Camellia japonica</i>	<i>Camellia</i>	+	3.88%	<i>Arnhematherum elatius</i>	<i>Arnhematherum</i>	+	3.02%	<i>Campylotropis</i> sp.	<i>Campylotropis</i>	-	9.40%
5	<i>Euonymus grandiflorus</i>	<i>Euonymus</i>	+	2.94%	<i>Celtis sinensis</i>	<i>Celtis</i>	+	2.57%	<i>Bidens</i> sp.	<i>Bidens</i>	-	5.37%
6	<i>Phyllonathys edulis</i>	<i>Phyllonathys</i>	+	2.46%	<i>Sabia swinhoei</i>	<i>Sabia</i>	+	2.14%	<i>Hedyotis diffusa</i>	<i>Hedyotis</i>	+	5.02%
7	<i>Maclura tricuspidata</i>	<i>Maclura</i>	+	1.88%	<i>Maclura tricuspidata</i>	<i>Maclura</i>	+	1.66%	<i>Gunninghamia lanceolata</i>	<i>Gunninghamia</i>	+	4.47%
8	<i>Gunninghamia lanceolata</i>	<i>Gunninghamia</i>	+	1.67%	<i>Ligustrum lucidum</i>	<i>Ligustrum</i>	+	1.48%	<i>Elaeagnus indica</i>	<i>Elaeagnis</i>	+	3.57%
9	<i>Rhododendron mucronatum</i>	<i>Rhododendron</i>	+	1.45%	<i>Phyllonathys edulis</i>	<i>Phyllonathys</i>	+	1.31%	<i>Digataria</i> sp.	<i>Digataria</i>	-	2.79%
10	<i>Vaccinium vitis-idaea</i>	<i>Vaccinium</i>	+	0.77%	<i>Smilax china</i>	<i>Smilax</i>	+	1.26%	<i>Miscanthus sinensis</i>	<i>Miscanthus</i>	+	2.55%
11	<i>Celtis sinensis</i>	<i>Celtis</i>	+	0.78%	<i>Gunninghamia lanceolata</i>	<i>Gunninghamia</i>	+	1.21%	<i>Oxalis corniculata</i>	<i>Oxalis</i>	+	2.31%
12	<i>Ilex cornuta</i>	<i>Ilex</i>	+	0.59%	<i>Nyssa</i> sp.	<i>Nyssa</i>	-	1.16%	<i>Setaria viridis</i>	<i>Setaria</i>	+	1.56%
13	<i>Sabia swinhoei</i>	<i>Sabia</i>	+	0.48%	<i>Aster</i> sp.	<i>Aster</i>	-	1.08%	<i>Panicum bisulcatum</i>	<i>Panicum</i>	+	1.49%
14	<i>Coccoloba orbiculatus</i>	<i>Coccoloba</i>	+	0.37%	<i>Loropetalum chinense</i>	<i>Loropetalum</i>	+	0.83%	<i>Pinus masoniana</i>	<i>Pinus</i>	+	1.46%
15	<i>Lysimachia congestiflora</i>	<i>Lysimachia</i>	+	0.32%	<i>Lysimachia congestiflora</i>	<i>Lysimachia</i>	+	0.81%	<i>Aster</i> sp.	<i>Aster</i>	-	1.18%
16	<i>Saxifraga stolonifera</i>	<i>Saxifraga</i>	+	0.30%	<i>Oxalis corniculata</i>	<i>Oxalis</i>	+	0.79%	<i>Scade cereale</i>	<i>Scade</i>	+	1.16%
17	<i>Arnhematherum elatius</i>	<i>Arnhematherum</i>	+	0.27%	<i>Ilex cornuta</i>	<i>Ilex</i>	+	0.67%	<i>Polygogon fugax</i>	<i>Polygogon</i>	+	1.00%
18	<i>Ehretia acuminata</i>	<i>Ehretia</i>	+	0.27%	<i>Celtis</i> sp.	<i>Celtis</i>	-	0.64%	<i>Phyllonathys edulis</i>	<i>Phyllonathys</i>	+	0.96%
19	<i>Nyssa</i> sp.	<i>Nyssa</i>	-	0.22%	<i>Cirsium arvense</i>	<i>Cirsium</i>	+	0.62%	<i>Sabia swinhoei</i>	<i>Sabia</i>	+	0.96%
20	<i>Hedyotis diffusa</i>	<i>Hedyotis</i>	+	0.21%	<i>Broussonetia papyrifera</i>	<i>Broussonetia</i>	+	0.59%	<i>Eurya japonica</i>	<i>Eurya</i>	+	0.73%
21	<i>Rubus chinensis</i>	<i>Rubus</i>	+	0.22%	<i>Saxifraga stolonifera</i>	<i>Saxifraga</i>	+	0.44%	<i>Mallotus japonicus</i>	<i>Mallotus</i>	+	0.59%
22	<i>Celtis</i> sp.	<i>Celtis</i>	-	0.20%	<i>Rhododendron mucronatum</i>	<i>Rhododendron</i>	+	0.40%	<i>Liquidambar formosana</i>	<i>Liquidambar</i>	+	0.55%
23	<i>Corylopsis multiflora</i>	<i>Corylopsis</i>	+	0.20%	<i>Mallotus japonicus</i>	<i>Mallotus</i>	+	0.37%	<i>Nicotiana tabacum</i>	<i>Nicotiana</i>	+	0.55%
24	<i>Polygogon fugax</i>	<i>Polygogon</i>	+	0.19%	<i>Tetradium</i>	<i>Tetradium</i>	+	0.32%	<i>Loropetalum chinense</i>	<i>Loropetalum</i>	+	0.49%
25	<i>Abelia schumannii</i>	<i>Abelia</i>	+	0.18%	<i>Gallium aparine</i>	<i>Gallium</i>	+	0.32%	<i>Prunus sibirica</i>	<i>Prunus</i>	-	0.46%
26	<i>Broussonetia papyrifera</i>	<i>Broussonetia</i>	+	0.15%	<i>Coreopsis tinctoria</i>	<i>Coreopsis</i>	+	0.29%	<i>Arnhematherum elatius</i>	<i>Arnhematherum</i>	+	0.39%
27	<i>Vaccinium ovalifolium</i>	<i>Vaccinium</i>	-	0.15%	<i>Leptodermis</i> sp.	<i>Leptodermis</i>	-	0.25%	<i>Ilex cornuta</i>	<i>Ilex</i>	+	0.38%
28	<i>Pinus masoniana</i>	<i>Pinus</i>	+	0.14%	<i>Iryanthes bosmanii</i>	<i>Iryanthes</i>	-	0.25%	<i>Sargentodoxa caneta</i>	<i>Sargentodoxa</i>	+	0.32%
29	<i>Pteroceltis tatarinowii</i>	<i>Pteroceltis</i>	+	0.14%	<i>Morus yunnanensis</i>	<i>Morus</i>	+	0.24%	<i>Rhododendron mucronatum</i>	<i>Rhododendron</i>	+	0.29%
30	<i>Oxalis corniculata</i>	<i>Oxalis</i>	+	0.12%	<i>Acorus gramineus</i>	<i>Acorus</i>	+	0.24%	<i>Microstegium vimineum</i>	<i>Microstegium</i>	+	0.28%
31	Others			4.14%	Others			6.24%	Others			7.74%

Table 2. Alpha diversity index among three sympatric species including sika deer, Reeve's muntjac, and Chinese hare.

Sample ID	Sika deer					Reeve's muntjac					Chinese hare							
	Chao1	Goods_coverage	Observed_species	Pielou_e	Shannon	Simpson	Chao1	Goods_coverage	Observed_species	Pielou_e	Shannon	Simpson	Chao1	Goods_coverage	Observed_species	Pielou_e	Shannon	Simpson
001	280.705	0.998038	170.2	0.40159	2.97535	0.760442	221.216	0.998458	147.5	0.169581	1.22164	0.254821	234.755	0.998217	141.9	0.384791	2.75059	0.766172
002	229.404	0.998361	154.1	0.257889	1.87412	0.511389	223.198	0.998492	144.1	0.22161	1.58889	0.400989	144.924	0.998847	93.3	0.348889	2.28297	0.717446
003	226.705	0.998481	131.2	0.265175	1.86516	0.504481	148.447	0.998978	76.4	0.152733	0.955071	0.242638	122.406	0.999139	66.2	0.442545	2.67587	0.781497
004	83.0718	0.999378	47.5	0.04717	0.262596	0.050021	199.96	0.997608	139	0.4334	3.08469	0.822047	190.257	0.999583	97.2	0.342704	2.26105	0.678976
005	260.610	0.998344	140.5	0.41492	2.95988	0.745168	343.206	0.998601	213.2	0.565935	4.37752	0.917577	132.754	0.999174	64.7	0.442643	2.66008	0.786546
006	197.435	0.998546	118.2	0.265982	1.83103	0.542388	265.68	0.998131	178.1	0.247444	1.84993	0.420895	244.217	0.998111	141.9	0.27918	1.99433	0.632656
007	231.011	0.998546	109.6	0.321788	2.17979	0.606797	198.505	0.998824	126.7	0.148754	1.03889	0.208596	109.736	0.999253	59.4	0.34015	2.00346	0.532667
008	186.477	0.998679	128.3	0.132388	0.926968	0.19294	173.466	0.998816	119.8	0.095464	0.658982	0.127527	223.278	0.998833	109.7	0.32719	2.21691	0.679038
009	176.872	0.998759	121.7	0.227483	1.57562	0.515318	201.798	0.998665	123.3	0.357705	2.48433	0.745497	147.016	0.999049	62.2	0.32465	1.9334	0.602632
010	226.03	0.998381	138.1	0.243521	1.73098	0.492527	284.977	0.998421	170.6	0.336498	2.49463	0.590127	145.945	0.998992	82.5	0.320825	2.04777	0.75727
011	224.427	0.998378	150.5	0.177627	1.28473	0.291992	230.017	0.998401	151.9	0.307556	2.22853	0.589744	199.096	0.998449	125.3	0.333101	2.32102	0.750859
012	280.773	0.997847	183.2	0.340063	2.55598	0.716689	244.458	0.998393	151.8	0.297168	2.15298	0.502685	290.705	0.998009	142.6	0.418089	2.99021	0.757656
013	220.095	0.998438	135.6	0.242773	1.71921	0.485882	239.338	0.99831	135.8	0.292677	2.0731	0.64653	264.841	0.9981	152.8	0.411819	2.9874	0.809688
014	328.541	0.997802	209.9	0.343807	2.65167	0.673406	217.883	0.998549	146.6	0.32392	2.33042	0.568292	138.488	0.999117	76.9	0.42012	2.63072	0.749443
015	381.036	0.997089	237.8	0.336105	2.65258	0.723663	150.282	0.998963	80.2	0.218794	1.38847	0.43972	132.877	0.999191	76.6	0.198498	1.2422	0.305309
016	334.337	0.997563	191.8	0.413	3.13158	0.781254	277.335	0.997947	181.3	0.440708	3.30546	0.785065	120.473	0.999199	68.5	0.32578	1.9862	0.504604
017	207.833	0.998586	107.7	0.282636	1.90708	0.611331	348.937	0.997558	209	0.401727	3.09589	0.765458	87.2741	0.999438	43.5	0.3264	1.77444	0.551934
018	393.986	0.997237	210.8	0.292397	2.257	0.609557	274.614	0.998214	178.1	0.318902	2.38396	0.58144	445.677	0.997171	207.1	0.583434	4.48816	0.909631
019	233.482	0.998353	158.1	0.323043	2.35938	0.639344	260.417	0.998234	165	0.310687	2.28763	0.651905	167.976	0.998648	98.6	0.239998	1.58907	0.424112
020	170.192	0.998677	118.9	0.07857	0.541529	0.109537	210.012	0.9986	148.8	0.21039	1.51822	0.361145	155.937	0.998963	75.2	0.299848	1.86801	0.523298
021	198.276	0.998529	127.2	0.162252	1.134	0.299678	237.626	0.998549	147.7	0.32251	2.32356	0.61479	107.632	0.999233	60.8	0.419374	2.48264	0.744613
022	373.107	0.997535	211.1	0.400956	3.09591	0.787719	281.474	0.998185	143.1	0.355952	2.54866	0.668624	121.692	0.999142	64.6	0.25249	1.51731	0.452847
023	242.856	0.998137	145.9	0.195825	1.40746	0.387288	253.578	0.998359	153.8	0.294375	2.13846	0.59175	524.096	0.996277	257.2	0.531387	4.2544	0.873609
024	194.829	0.998489	123.5	0.202812	1.40898	0.463457	226.685	0.998458	137.9	0.414342	2.94376	0.747215	162.056	0.99889	105.8	0.138661	0.932367	0.218141
025	228.774	0.998424	157.8	0.381325	2.78406	0.712446	316.573	0.997734	187.1	0.357447	2.69716	0.728621	157.534	0.999094	76.6	0.459812	2.87668	0.781035
026	165.272	0.998938	108.6	0.256367	1.73316	0.499269	200.122	0.998572	119.8	0.269879	1.86281	0.449013	62.196	0.999548	45.3	0.047218	0.259645	0.051564
027	118.54	0.999171	73.7	0.150522	0.933483	0.232503	165.642	0.998935	115.2	0.224842	1.54008	0.352465	316.768	0.997776	171.4	0.550003	4.08039	0.905171
028	216.523	0.998398	133.9	0.089286	0.630779	0.129084	241.525	0.998131	156.7	0.35582	2.59425	0.723594	176.083	0.998725	101.4	0.270131	1.80004	0.452913
029	274.14	0.998097	171.2	0.226096	1.67727	0.435829	300.379	0.997947	184.8	0.326165	2.45546	0.660694	313.133	0.997844	172.6	0.458045	3.40363	0.799484
030	210.264	0.998441	152.1	0.089529	0.64893	0.128594	336.477	0.997683	197.7	0.353038	2.69256	0.689019	121.149	0.999105	81.2	0.424873	2.69476	0.734457
Average	236.520	0.998321	145.6	0.252097	1.82321	0.488000	242.461	0.998353	151.0	0.304205	2.21037	0.561616	192.032	0.998654	104.1	0.355422	2.36686	0.635203



**Figure 4.** **a** box-plot of the alpha diversity index. In each panel, the abscissa is the group, and the ordinate is the value of the corresponding alpha diversity index **b** sample rare fraction curves **c** rank abundance curve. The abscissa is the sequence number of OTUs arranged according to the Abundance size. The ordinate is the abundance value of each OTU in this grouping by Log2 log transformation (Ch: Chinese hare; Sd: Sika deer; Rm: Reeve's muntjac).

and the PCoA diagram and NMDS analysis revealed the similarity of the composition of the diet between sika deer and Reeve's muntjac (Fig. 5a, b), which was consistent with our expected results. In addition, a hierarchical clustering heat map was convenient for the intuitive identification of the species present in corresponding samples; *Rubus* had the highest abundance among the three species. The tree plot indicated that there was much similar distance in the samples between sika deer and Reeve's muntjac but less similar with Chinese hare (Fig. 5c).

The intergroup difference analysis shows the difference between the intragroup and intergroup sample distances. Compared with Reeve's muntjac, the intragroup distance of Reeve's muntjac was smaller than the intergroup distance of sika deer and Chinese hare (Fig. 6a). While compared with sika deer, the intragroup distance of sika deer was slightly higher than the intergroup distance of Reeve's muntjac (Fig. 6b). With different species composition, the difference between the intragroup should be smaller than the intergroup. In comparison with the NMDS, this phenomenon was speculated to be the fact that the diet composition of Reeve's muntjac was much similar to those of sika deer, and the Reeve's muntjac has more forage plant diversity.

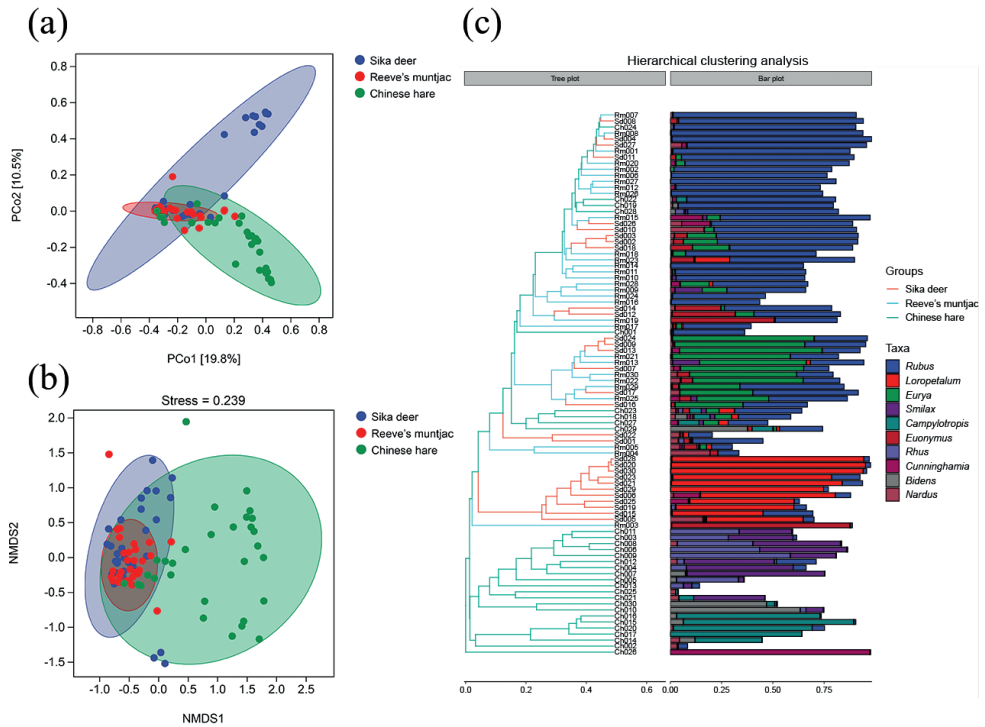


**Figure 5.** **a** PCoA analysis chart, in which each point represents a sample **b** NMDS analysis chart. Diagram analysis with 95% confidence ellipse **c** hierarchical clustering diagram. Analysis of the hierarchical clustering tree diagram and the stacked bar diagram of the top 10 genera in abundance (Ch: Chinese hare; Sd: Sika deer; Rm: Reeve's muntjac).

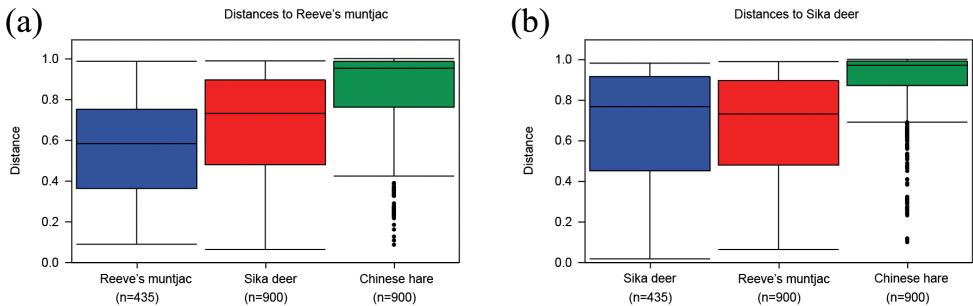


**Figure 6.** Intergroup difference analysis **a** shows the boxplots of the distances between samples in the sika deer group and the distances between samples in this group and samples in other groups **b** shows the boxplots of the distances between samples in Reeve's muntjac group and the distances between samples in this group and samples in other groups.

By analyzing the niches of the three sympatric herbivorous animals, we found that the highest niche breadth was Chinese hare (~7.78), followed by sika deer (~4.53) and Reeve's muntjac (~3.44). The niche overlap index between sika deer and Reeve's muntjac

**Table 3.** The dietary niche overlap and Observed niche overlap index among the three sympatric species.

	Dietary niche breadth	Interspecific comparison	Observed niche overlap index
Sika deer	4.53	Sika deer vs Reeve's muntjac	0.83
Reeve's muntjac	3.44	Sika deer vs Chinese hare	0.62
Chinese hare	7.78	Reeve's muntjac vs Chinese hare	0.69
–	–	Sika deer vs Reeve's muntjac vs Chinese hare	0.68

was 0.83, sika deer and Chinese hare was 0.62, and Reeve's muntjac and Chinese hare was 0.69. The overlap index ranges from 0 to 1, where 0 indicates that the food ranges do not overlap at all, and 1 indicates that the food ranges overlap entirely. Our results suggested that Reeve's muntjac and sika deer have the highest diet overlap (Table 3).

## Discussion

### The food composition of the three herbivorous animals

Quantitative analysis is of great significance for the families, genera, and species of the herbivores' diet. Liu (2012) investigated the diet of wild northeast sika deer in winter and found the sika deer feed on 35 plant species belonging to 25 genera in 17 families. Liu (2020) showed that 131 plants, including nine herbs, 31 shrubs, and eight trees, were foraged by South China sika deer in the Tianmu Mountains. One hundred and thirty-nine food items were identified in the feces of sika deer in our study. Comparative analysis shows that the metabarcoding method based on high-throughput sequencing provides more detailed forage plant information.

Yao et al. (2010) found that the sika deer in TNNR mainly eat *Homonoia riparia*, *Fallopia multiflora*, *Lespedeza bicolor*, *Pueraria montana*, and *Vicia faba*, and other species, and then especially fed on young leaves and shoots (Li et al. 2014). Compared with our study, the dominant forages in the feces of sika deer were *Rubus chingii*, *Loropetalum chinense*, *Eurya japonica*, *Camellia japonica*, *Euonymus grandiflorus*, and *Phyllostachys edulis* in winter; these are all Chinese medicinal herbs, which ensure the prevention of various diseases throughout the life cycle of sika deer (Yao et al. 2010; Ye 2015). The differences may be attributed to geographical and seasonal differences. The vegetation condition varied according to the different regions, which means that diverse forage plants are available for the sika deer.

In seasons when plant resources are scarce, sika deer will choose to eat non-favorable plants or the available food resources at the moment. Studies on Japanese sika deer showed that they mainly choose their favorite deciduous species from summer to autumn, such as *Cornus controversa*, and *Quercus* sp., but from early winter to spring, non-favored herbaceous and tree species, such as *Juncus decipiens* and *Cryptomeria japonica*, will be foraged (Nakahama et al. 2020). Therefore, sika deer have a diverse diet and feed on various plants in different seasons (Yao et al. 2010; Wang et al. 2019). In the TNNR, oaks included *Quercus acutissima*, *Q. aliena*, *Q. chenii*, *Q. fabri*, and *Q. serrata* (Jiang 2009). Significantly, oak leaves, which are rich in tannins and toxic to

most mammals, including cattle (Doce et al. 2009), are conversely found to increase the reproductive rate and fawn survival rate of sika deer in captive breeding by some farmers (Xing et al. 2022). Oak leaves are essential for maintaining healthy sika deer in wild and farmed populations. However, we found a lower abundance in *Quercus* for three herbivorous mammals' diets. We speculated this might be related to deciduous *Quercus* in winter or the gestation period of female sika deer, even though some studies claimed that tannins were not toxic to sika deer because of their rumen microbes and fermentation processes (Li et al. 2013). There are differences in the forage plants of South China sika deer in different seasons and regions.

In our study, we identified most of the forage species; however, some of the forage species that we identified were not previously known from Jiangxi Province. It may be difficult to identify all forage plants using a single gene fragment, and continuous succession of plant communities caused by invasive species adds a level of complication to this. Therefore, it is necessary to add auxiliary barcodes as well as strengthen the overall investigation of potential food resources in the reserve. The construction of a database of plant species barcodes for the Taohongling Sika Deer Reserve would provide a reference and source of sequence alignments. Such a database would allow for a more accurate determination of the diets of herbivores and allow for better comparisons of the diets of sympatric herbivores.

## Interspecific niches

Competition theory indicates that the greater the overlap of resources between species, the greater the competition coefficient because of the widespread use of niche overlap to estimate competition for resources (Colwell and Futuyma 1971). Tibetan red deer have a similar diet to sympatric ungulates, which inevitably leads to interspecific conflicts in food use (Lu et al. 2020). However, spatial-temporal variations in dietary consumption of the two dominant rodent species on Mount Kilimanjaro, Tanzania, have been found to serve as a mechanism of resource partitioning that enable these species to coexist with a niche overlap (Mulungu et al. 2011; Thomas et al. 2022); this contradicts the key assumption of competition theory. Thus, we cannot limit the research on interspecific competition in sympatric species to trophic ecological niches, and spatial-temporal dimensions should also be considered. For sika deer in the TNNR, we do not know the exact reasons for spatial variations in dietary overlaps with its two sympatric herbivores. We suggest that a cautious approach is required to interpret the high dietary overlaps and their implications for competitive interactions among the three studied herbivores in the TNNR. As pointed out by others (Belovsky 1986; Jenkins and Wright 1988; Gordon and Illius 1989), high dietary overlaps may not necessarily imply competition (Andersen et al. 2017) and may simply indicate that the food item is sufficient, permitting sympatric species to share resources. In the TNNR there are increasing populations of sympatric wild boar and Reeve's muntjac. Sika deer face competition stress in space and food resources, especially when food is scarce in winter (Li et al. 2014). Thus, even when the determinants of competition mechanisms are uncertain, competition does exist and its important role among species cannot be denied.

Competition among sympatric species is mostly expressed as a compensatory mechanism in ecological niches when species are similar in one dimension, they differ on another. Food resources, habitat, and temporal partitioning are the most common dimension partitioned (Bagchi et al. 2003). For example, high dietary overlap among the species may result in niche differentiation (Reitz and Trumble 2002; Yin et al. 2007; Cao et al. 2009); large herbivores are forced to expand their food range to avoid competition during periods of food scarcity (Noor et al. 2013). In northeastern China, red deer tend to increase their browsing intensity to maintain their high food intake, but sika deer meet their relatively constant food intake and potential nutritional requirements by increasing their bite diameter in winter. This reflects the short-term foraging strategies by sharing similar foods with the sympatric ungulates (Zhong et al. 2020). Currently, we do not know the competition mechanism of sika deer and further studies are needed to determine the coexistence mechanism with its sympatric species.

In our study, we found the niche breadth of the sika deer was higher than the Reeve's muntjac. Optimal forage theory suggests that preference and palatability will be selected for the animals in abundant food periods. While in a period of scarce food resources, feeding generalization will occur by selecting different forage plants (Belovsky 1978). It remains to be studied whether the higher dietary niche breadth of sika deer results from the physiological characteristics of digesting a wide range of foods or to avoid competition. Moreover, the niche breadth of Chinese hare was larger than sika deer and Reeve's muntjac. We speculate that Chinese hare, as opportunistic feeders, have a broader range of forage plants but consume less due to their smaller body size. The diet composition of Chinese hares includes trees, shrubs, and herbs, but this may be due to a passive and random proximity foraging strategy or even the indirect ingestion from the process of grinding teeth.

## Conclusions

The South China sika deer is the most endangered among the three remaining subspecies of sika deer in China. In our study, sika deer and Reeve's muntjac showed a higher overlapping index of niche. Reeve's muntjac may affect the survival of the sika deer due to the shortage of food resources in winter. We speculated that potential competition probably occurs in two cervid species. In addition, the growth of the secondary vegetation has accelerated in the reserve, and the decline of suitable habitats is a serious threat to the growth of the sika deer population. It is urgent to strengthen habitat management, improve habitat quality, and study forage plants. It is also necessary to provide food for sika deer and other wildlife through artificial planting during food shortages and dry seasons. Further studies need to establish local DNA databases to identify the forage plants and introduce the auxiliary barcoding to solve accurate species-level diet composition. Overall, our study determined the diet composition and interspecific niches of South China sika deer and its sympatric Reeve's muntjac and Chinese hare. These results should be helpful to facilitate habitat improvements and artificial planting, monitor forage resources, and conserve biodiversity, and manage the reserve.

## Acknowledgements

This research was supported by the Science and Technology Program of the Jiangxi Provincial Department of Education (GJJ180225) and the National Natural Science Foundation of China (31960118). We are grateful to Xiaohong Liu, Yongjiang Chen, and Yulu Chen of Taohongling Sika Deer National Nature Reserve for their help in sample collection, and Dr Hao Zang for the help with the R analysis.

## References

- Andersen GE, Johnson CN, Barmuta LA, Jones ME (2017) Dietary partitioning of Australia's two marsupial hypercarnivores, the Tasmanian devil and the spotted-tailed quoll, across their shared distributional range. *PLoS ONE* 12(11): e0188529. <https://doi.org/10.1371/journal.pone.0188529>
- Bagchi S, Goyal SP, Sankar K (2003) Niche relationships of an ungulate assemblage in a dry tropical forest. *Journal of Mammalogy* 84(3): 981–988. <https://doi.org/10.1644/BBa-024>
- Belovsky GE (1978) Diet optimization in a generalist herbivore: The moose. *Theoretical Population Biology* 14(1): 105–134. [https://doi.org/10.1016/0040-5809\(78\)90007-2](https://doi.org/10.1016/0040-5809(78)90007-2)
- Belovsky GE (1986) Generalist herbivore foraging and its role in competitive interactions. *American Zoologist* 26(1): 51–69. <https://doi.org/10.1093/icb/26.1.51>
- Cao YF, Zhang TZ, Lian XM, Cui QH, Deng DD, Su JP (2009) Diet overlap among selected ungulates in Kekexili region, Qinghai province. *Sichuan Journal of Zoology* 28: 49–54. [In Chinese]
- Caporaso JG, Kuczynski J, Stombaugh J, Bittinger K, Bushman FD, Costello EK, Fierer N, Peña AG, Goodrich JK, Gordon JI, Huttley GA, Kelley ST, Knights D, Koenig JE, Ley RE, Lozupone CA, McDonald D, Muegge BD, Pirrung M, Reeder J, Sevinsky JR, Turnbaugh PJ, Walters WA, Widmann J, Yatsunencko T, Zaneveld J, Knight R (2010) QIIME allows analysis of high-throughput community sequencing data. *Nature Methods* 7(5): 335–336. <https://doi.org/10.1038/nmeth.f.303>
- Colwell RK, Futuyama DJ (1971) On the measurement of niche breadth and overlap. *Ecology* 52(4): 567–576. <https://doi.org/10.2307/1934144>
- Deagle BE, Thomas AC, McInnes JC, Clarke LJ, Vesterinen EJ, Clare EL, Kartzinel TR, Eveson JP (2019) Counting with DNA in metabarcoding studies: How should we convert sequence reads to dietary data? *Molecular Ecology* 28(2): 391–406. <https://doi.org/10.1111/mec.14734>
- Doce RR, Hervás G, Belenguer A, Toral PG, Giráldez FJ, Frutos P (2009) Effect of the administration of young oak (*Quercus pyrenaica*) leaves to cattle on ruminal fermentation. *Animal Feed Science and Technology* 150(1–2): 75–85. <https://doi.org/10.1016/j.anifeedsci.2008.08.005>
- Editorial Committee of FRPS (2004) *Flora Reipublicae Popularis Sinicae (FRPS) (Vol. 1)*. Science Press, Beijing. [In Chinese]
- Fujii T, Ueno K, Minami M (2019) Identification of food plants in the diet of Japanese ptarmigan (*Lagopus mutus japonicus*) in the Japan's Northern Japan Alps using DNA Barcoding. *Wildlife and Human Society* 6(2): 13–18. [https://doi.org/10.20798/awhswhs.6.2\\_13](https://doi.org/10.20798/awhswhs.6.2_13)

- Gao YM, Yu B, Wang JQ, Wu WG, Gao B (2009) Habitat characteristics used by sika deer at Taohongling Natural Reserve. *Jiangxi Science* 27(6): 877–878. [+891] <https://doi.org/10.13990/j.issn1001-3679.2009.06.012>
- Gong S, Zhang P, Luan X, Bao H, Jiang GS (2022) Application and comparison of Fecal microscopic analysis and DNA metabarcoding technology for dietary analysis of wild boar. *Chinese Journal of Wildlife* 43: 1–9. <https://doi.org/10.12375/ysdwx.20220308>
- Gordon I, Illius AW (1989) Resource partitioning by ungulates on the Isle of Rhum. *Oecologia* 79(3): 383–389. <https://doi.org/10.1007/BF00384318>
- Hoenig BD, Snider AM, Forsman AM, Hobson KA, Latta SC, Miller ET, Polito MJ, Powell LL, Rogers SL, Sherry TW, Toews DPL, Welch AJ, Taylor SS, Porter BA (2022) Current methods and future directions in avian diet analysis. *Ornithology* 139(1): ukab077. <https://doi.org/10.1093/ornithology/ukab077>
- Holechek JL (1982) Sample preparation techniques for microhistological analysis. *Journal of Range Management Archives* 35(2): 267–268. <https://doi.org/10.2307/3898409>
- Hou J, Li L, Wang YF, Wang WJ, Zhan HY, Dai NH, Lu P (2021) Influences of submerged plant collapse on diet composition, breadth, and overlap among four crane species at Poyang Lake, China. *Frontiers in Zoology* 18(24): 1–17. <https://doi.org/10.1186/s12983-021-00411-2>
- Jenkins KJ, Wright RG (1988) Resource partitioning and competition among cervids in the northern Rocky Mountains. *Journal of Applied Ecology* 25(1): 11–24. <https://doi.org/10.2307/2403606>
- Jiang ZG (2009) Study on the Biodiversity of Taohongling Sika Deer National Nature Reserve in Jiangxi. Tsinghua University Press, Beijing. [In Chinese]
- Jiang ZG, Xu XR, Liu WH, Li CL, Li CW, Lu XL, Xiao JP, Li YK, Tang SH, Ping XG, Li F, Luo ZH, Fang HX, Yu B, Zang JH, Chen QJ, Gao YM, Wu JD, Wu WG, Wang LB, Wu YF, Zu HB, Wang C, Dai J, Ying X, Wang JQ, Liu Z, Chen J, Li LL, Chen DQ, Zhang XW, Cui SP, Li J, Yuan FK, Zhang BB, Zhu JH, Gao HZ, Li HB, Chen YL, Chen YJ, Lin ZH, Wang Y, Zhang C, Zhou QH (2012) Population status of South China sika deer in Taohongling National Nature Reserve. *Chinese Journal of Wildlife* 33(6): 305–308. [+332] <https://doi.org/10.19711/j.cnki.issn2310-1490.2012.06.001>
- Kasim M, Mukai H (2009) Food sources of the oyster (*Crassostrea gigas*) and the clam (*Ruditapes philippinarum*) in the Akkeshi-ko estuary. *Plankton & Benthos Research* 4(3): 104–114. <https://doi.org/10.3800/pbr.4.104>
- Li ZP, Liu HL, Li GY, Bao K, Wang KY, Xu C, Feng Y, Yang YF, Wright ADG (2013) Molecular diversity of rumen bacterial communities from tannin-rich and fiber-rich forage fed domestic sika deer (*Cervus nippon*) in China. *BMC Microbiology* 13(1): e151. <https://doi.org/10.1186/1471-2180-13-151>
- Li J, Li YK, Liao LJ, Xie GY, Yuan FK (2014) Habitat assessment of sika deer (*Cervus nippon*) in the Taohongling National Nature Reserve, Jiangxi Province, China. *Acta Ecologica Sinica* 34(5): 1274–1283. <https://doi.org/10.5846/stxb201305171102>
- Li FX, Du MR, Gao YP, Wang JW, Zhang YT, Zhang ZX, Jiang ZJ (2021) Analysis of food sources of *Crassostrea gigas* using high-throughput sequencing techniques. *Yuye Kexue Jinzhan* 42(5): 86–96. <https://doi.org/10.19663/j.issn2095-9869.20200404001>
- Lin XZ, Hu SM, Liu S, Huang H (2018) Comparison between traditional sequencing and high throughput sequencing on the dietary analysis of juvenile fish. *Chinese Journal of Applied Ecology* 29(9): 3093–3101. <https://doi.org/10.13287/j.1001-9332.201809.005>

- Liu XP (2009) Feeding habits and Food niche overlap of three Canids in Eastern Inner Mongolia. Master's thesis, Qufu Normal University, Shandong, China. [In Chinese]
- Liu WS (2012) Winter Diet Composition and Non-invasive Health Assessment of Feral Sika Deer. PhD thesis, Northeast Forestry University, Heilongjiang, China. [In Chinese]
- Liu Z (2020) Sika Deer's Feeding Habits Biochemical Analysis and Community Composition of Large and Medium-sized Mammals and Birds in Tianmu Mountains. Master's thesis, China Jiliang University, Zhejiang, China. [In Chinese]
- Lu ZH, Zhang WQ, Liu H, Zhang HM, Li YR (2020) Comparison on feeding habits of *Cervus wallichii* and sympatric ungulates and domestic animals in green grass period. Chinese Journal of Applied Ecology 31(2): 651–658. <https://doi.org/10.13287/j.1001-9332.202002.002>
- Ma J, Li KZ, Qiu DJ, Tan YH, Huang LM, Zhang JB (2021) Dietary analysis of *Flaccisagitta enflata* based on high-throughput sequencing technology in Daya Bay. Ecologic Science 40(2): 9–17. <https://doi.org/10.14108/j.cnki.1008-8873.2021.02.002>
- Monro RH (1982) An appraisal of some techniques used to investigate the feeding ecology of large herbivores with reference to a study on impala in the northern Transvaal. African Journal of Ecology 20(2): 71–80. <https://doi.org/10.1111/j.1365-2028.1982.tb00277.x>
- Mulungu LS, Mahlaba TA, Massawe AW, Kennis J, Crauwels D, Eiseb S, Monadjem A, Makundi RH, Katakweba AAS, Leirs H, Belmain SR (2011) Dietary differences of the multimammate mouse, *Mastomys natalensis* (Smith, 1834), across different habitats and seasons in Tanzania and Swaziland. Wildlife Research 3(8): 640–646. <https://doi.org/10.1071/WR11028>
- Nakahama N, Furuta T, Ando H, Setsuko S, Takayanagi A, Isagi Y (2020) DNA meta-barcoding revealed that sika deer foraging strategies vary with season in a forest with degraded understory vegetation. Forest Ecology and Management 484: e118637. <https://doi.org/10.1016/j.foreco.2020.118637>
- Noor A, Habib B, Kumar S (2013) Habitat selection and niche segregation between chital and nilgai in Keoladeo National Park, India. European Journal Zoological Research 2: 1–9.
- Palmer SCE, Truscott AM (2003) Seasonal habitat use and browsing by deer in Caledonian pine-woods. Forest Ecology and Management 174(1–3): 149–166. [https://doi.org/10.1016/S0378-1127\(02\)00032-4](https://doi.org/10.1016/S0378-1127(02)00032-4)
- Pascual-Rico R, Sánchez-Zapata JA, Navarro J, Eguía S, Anadón JD, Botella F (2020) Ecological niche overlap between co-occurring native and exotic ungulates: Insights for a conservation conflict. Biological Invasions 22(8): 2497–2508. <https://doi.org/10.1007/s10530-020-02265-x>
- Pianka ER (1973) The structure of lizard communities. Annual Review of Ecology and Systematics 4(1): 53–74. <https://doi.org/10.1146/annurev.es.04.110173.000413>
- Pielou EC (1969) An Introduction to Mathematical Ecology. Wiley-Interscience, New York. <https://doi.org/10.1111/j.1558-5646.1970.tb01782.x>
- Pompanon F, Deagle BE, Symondson WOC, Brown DS, Jarman SN, Taberlet P (2012) Who is eating what: Diet assessment using next generation sequencing. Molecular Ecology 21(8): 1931–1950. <https://doi.org/10.1111/j.1365-294X.2011.05403.x>
- Reitz SR, Trumble JT (2002) Competitive displacement among insects and arachnids. Annual Review of Entomology 47(1): 435–465. <https://doi.org/10.1146/annurev.ento.47.091201.145227>

- Schaller GB (2000) Wildlife of the Tibetan Steppe. University of Chicago Press, Chicago. [https://doi.org/10.1644/1545-1542\(2000\)081<0908>2.3.CO;2](https://doi.org/10.1644/1545-1542(2000)081<0908>2.3.CO;2)
- Schoener TW (1971) Theory of feeding strategies. *Annual Review of Ecology and Systematics* 2(1): 369–404. <https://doi.org/10.1146/annurev.es.02.110171.002101>
- Shannon CE (1948) A mathematical theory of communication. *The Bell Technical Journal* 27(3): 379–423. <https://doi.org/10.1002/j.1538-7305.1948.tb01338.x>
- Smith EP (1982) Niche breadth, resource availability, and inference. *Ecology* 63(6): e1675. <https://doi.org/10.2307/1940109>
- Soininen EM, Valentini A, Coissac E, Miquel C, Gielly L, Brochmann C, Brysting AK, Sonstebo JH, Lms RA, Yoccoz NG, Taberlet P (2009) Analysing diet of small herbivores: The efficiency of DNA barcoding coupled with high-throughput pyrosequencing for deciphering the composition of complex plant mixtures. *Frontiers in Zoology* 6(1): 1–16. <https://doi.org/10.1186/1742-9994-6-16>
- Tabassum N, Lee JH, Lee SR, Kim JU, Park H, Kim HW, Kim JH (2022) Molecular diet analysis of Adélie penguins (*Pygoscelis adeliae*) in the Ross Sea using fecal DNA. *Biology* 11(2): e182. <https://doi.org/10.3390/biology11020182>
- Thomas SM, Soka GE, Mulungu LS, Makonda FBS (2022) Spatial-temporal variations in dietary consumption of two dominant rodent species (*Rhabdomys dilectus* and *Lophuromys acquirilus*) on Mount Kilimanjaro, Tanzania. *Diversity* 14(8): 659. <https://doi.org/10.3390/d14080659>
- Vázquez-Baeza Y, Pirrung M, Gonzalez A, Knight R (2013) Emperor: A tool for visualizing highthroughput microbial community data. *GigaScience* 2(1): 1–16. <https://doi.org/10.1186/2047-217X-2-16>
- Wang L (2018) The countermeasures and suggestions of improving the *Cervus nippon* habitat in Jiangxi Taohongling National Nature Reserve. *The Journal of Hebei Forestry Science and Technology* 1: 68–70. <https://doi.org/10.16449/j.cnki.issn1002-3356.2018.01.020>
- Wang LC, Song XZ (2013) The Species Eco-Development Status of Chinese Sika Deer. China Animal Agriculture Association. China Deer Industry Development, Zhanjiang, 39–46. [In Chinese]
- Wang ZY, Meng DH, Luo Y, Teng LW, Gao H, Wang JF, Liu ZS (2019) Spring food-habits of red deer (*Cervus elaphus alashanicus*) in Helan Mountains, China. *Chinese Journal of Wildlife* 40(4): 825–831. <https://doi.org/10.19711/j.cnki.issn2310-1490.2019.04.002>
- Wang XF, Zhong YF, Zhan JW, Liu WH, Wu WG, Gao YM, Zhang C, Shao RQ, Cao KQ, Li YK (2021) Analysis on activity rhythm of *Lophura nycthemera* population in Taohongling Sika Deer National Nature Reserve based on infrared camera technology. *Modern Agricultural Science and Technology* 19: 182–184. [+194] <https://doi.org/10.5846/stxb201805251148>
- Xing XM, Ai C, Wang TJ, Li Y, Liu HT, Hu PF, Wang GW, Liu HM, Wang HL, Zhang RR, Zheng JJ, Wang XB, Wang L, Chang YX, Qian Q, Yu JH, Tang LX, Wu SG, Shao XJ, Li A, Cui P, Zhan W, Zhao S, Wu ZC, Shao XQ, Dong YM, Rong M, Tan YH, Cui XZ, Chang SZ, Song XC, Yang TG, Sun LM, Ju Y, Zhao P, Fan HH, Liu Y, Wang XH, Yang WY, Yang M, Wei T, Song SS, Xu JP, Yue ZG, Liang QQ, Li CY, Ruan J, Yang F (2022) The First High-Quality Reference Genome of Sika Deer Provides Insights for High-Tannin Adaptation. *Genomics, Proteomics & Bioinformatics*. <https://doi.org/10.1016/j.gpb.2022.05.008>

- Yao ZS, Xu XR, Xu P (2010) The Analysis of Food Plants of Sika Deer in Taohongling Nature Reserve, Jiangxi Province. Proceedings and Abstracts of the 9<sup>th</sup> National Symposium on Natural Medicinal Material Resources, Guangzhou (China), July 2010, 348–353. [In Chinese]
- Ye ZW (2015) Pharmacology of Chinese Medicine. Chongqing University Press, Chongqing, 10 pp. [In Chinese]
- Yin BF, Huai HY, Zhang YL, Zhou L, Wei WH (2007) Trophic niches of *Pantholops hodgsoni*, *Procapra picticaudata* and *Equus kiang* in Kekexili region. Chinese Journal of Ecology 18: 766–770. [In Chinese]
- Zhang LH, Piao HX, Jin Y (2011a) Research progress in evolution of Chinese sika deer population. Agricultural Science Journal of Yanbian University 33(1): 73–76. <https://doi.org/10.13478/j.cnki.jasyu.2011.01.016>
- Zhang CY, Wu JP, Huang XY (2011b) Evaluation of scatological analysis of sika deer food habits. Chinese Journal of Wildlife 32(4): 199–202. <https://doi.org/10.19711/j.cnki.issn2310-1490.2011.04.005>
- Zheng RQ, Bao YX (2004) Study methods and procedures for ungulate food habits. Acta Ecologica Sinica 7: 1532–1539. <https://doi.org/10.13287/j.1001-9332.202002.002>
- Zhong LQ, Zhi XL, Sun Y, Liu XX, Sun B, Zhou SC, Zhang WQ, Zhang MH (2020) Winter foraging of sympatric red deer and sika deer in northeast China: Diet composition, forage selection, bite diameter and browse intensity. Journal of Forest Research 25(4): 276–284. <https://doi.org/10.1080/13416979.2020.1762025>
- Zhou YX (2019) Diversity of mammals and birds, ungulates activity rhythm and habitat selection by Camera Trapping in the Taohongling. Master's thesis, Jiangxi Normal University, Jiangxi, China. [In Chinese]

## Supplementary material I

### Dietary of Sika deer, Reeves' muntjac and Chinese hare

Authors: Dandan Wang, Xiaolong Hu, Minling Li, Jie Liu, Ming Tang, Wuhua Liu, Jianwen Zhan, Yongtao Xu, Weiwei Zhang

Data type: data (excel document)

Copyright notice: This dataset is made available under the Open Database License (<http://opendatacommons.org/licenses/odbl/1.0/>). The Open Database License (ODbL) is a license agreement intended to allow users to freely share, modify, and use this Dataset while maintaining this same freedom for others, provided that the original source and author(s) are credited.

Link: <https://doi.org/10.3897/zookeys.1149.96936.suppl1>

# Taxonomic notes of subgenus *Velia* (*Cesavelia*) Koçak & Kemal, 2010 (Hemiptera, Heteroptera, Veliidae) from China, with description of one new species

Zezhong Jin<sup>1</sup>, Siying Fu<sup>1</sup>, Zhen Ye<sup>1</sup>

<sup>1</sup> Institute of Entomology, College of Life Sciences, Nankai University, Tianjin, 300071, China

Corresponding author: Zhen Ye ([yezhen1987331@nankai.edu.cn](mailto:yezhen1987331@nankai.edu.cn))

---

Academic editor: Wenjun Bu | Received 24 October 2022 | Accepted 4 February 2023 | Published 22 February 2023

---

<https://zoobank.org/12B248C0-791B-4DDD-B2E3-48AA2F531213>

---

**Citation:** Jin Z, Fu S, Ye Z (2023) Taxonomic notes of subgenus *Velia* (*Cesavelia*) Koçak & Kemal, 2010 (Hemiptera, Heteroptera, Veliidae) from China, with description of one new species. ZooKeys 1149: 37–52. <https://doi.org/10.3897/zookeys.1149.96680>

---

## Abstract

*Velia* (*Cesavelia*) *bui* **sp. nov.** from Hubei Province, China is described, and *Velia* (*Cesavelia*) *tonkina* Polhemus & Polhemus, 2003 is newly recorded from China. In addition, new distribution data for three species of *Velia* (*Cesavelia*), *V. longiconnexiva* Tran, Zettel & Buzzetti, 2009, *V. sinensis* Andersen, 1981 and *V. tonkina* Polhemus & Polhemus, 2003 are provided. Photographs of the habitus in dorsal and lateral views, metafemora of males, genitalic structures and habitats, along with a distribution map of this subgenus, are provided.

## Keywords

Distribution, morphology, new record, range extension, semiaquatic bugs, taxonomy

## Introduction

The genus *Velia* Latreille, 1804, includes three subgenera: *V.* (*Velia*) Latreille, 1804, *V.* (*Plesiavelia*) Tamanini, 1955 and *V.* (*Cesavelia*) Koçak & Kemal, 2010. The subgenus *Velia* s.str. is monotypic and only includes one extant species, *V.* (*Velia*) *rivulorum*

(Fabricius, 1775), which is distributed in the western Mediterranean (Tamanini 1947; Andersen 1995; Berchi et al. 2018). The subgenus *Plesiovelia* contains 28 taxa (23 species and 5 subspecies), distributed from western Europe to northwestern India, with extension to northern Africa (Andersen 1981, 1995b; Tran et al. 2009; Berchi et al. 2018). The subgenus *Cesavelia* is restricted to the Oriental Region, i.e., northern India, Nepal, central and southern China and northern Vietnam (Andersen 1981; Tran et al. 2009; Koçak and Kemal 2010; Basu et al. 2013). This subgenus was originally named *Haldwania* Tamanini, 1955 and this name was used in subsequent studies, e.g., Andersen (1981), Polhemus and Polhemus (1998), and Tran et al. (2009). It was then replaced by the present subgeneric name, because it was determined to be a junior homonym of *Haldwania* Beier, 1930 (Mantodea) (Koçak and Kemal 2010).

Morphologically, *Cesavelia* can be distinguished from the other subgenera by the relatively long antennal segment I (i.e., longer than width of head across eyes) and less stout hind femur (Tamanini 1955a, b, c; Andersen 1981; Berchi et al. 2018). Hitherto, ten species have been considered valid in this subgenus (Tamanini 1955b; Andersen 1981; Polhemus and Polhemus 1998; Tran et al. 2009; Basu et al. 2013), but only three species have been recorded from China before this study: *V. longiconnexiva* Tran, Zettel & Buzzetti, 2009, *V. sinensis* Andersen, 1981, and *V. yunnana* Tran, Zettel & Buzzetti, 2009. Here we report a new species *Velia (Cesavelia) bui* sp. nov. from Hubei Province of China, which extends the known distribution range of this subgenus eastward into central China. In addition, *V. tonkina* Polhemus & Polhemus, 2003 is recorded from China for the first time, and new distribution data for three species, *V. longiconnexiva*, *V. sinensis* and *V. tonkina* are provided. This paper also provides photographs of the habitus in dorsal and lateral view, metafemora of males, genitalic structures, habitats of species occurring in China, and a distribution map of this subgenus.

## Material and methods

All the specimens examined in this study are deposited in the Institute of Entomology, College of Life Sciences, Nankai University, Tianjin, China (NKUM). All measurements are given in millimeters (mm). The illustrations of specimens in dorsal view and structural details were captured using a Nikon SMZ1000 stereomicroscope equipped with a computer-controlled SPOTRT digital camera and Helicon software (Helicon Remote ver. 3.9.12 W and Helicon Focus ver. 7.7.5). The skeletal elements of genital segments were dissected after macerated with 5% KOH. The photographs of the dissected male genital segments were made using an OLYMPUS BX53 microscope equipped with a computer-controlled Canon OLYMPUS DP72 digital camera and cellSens Standard ver. 1.6 software.

## Taxonomic accounts

Family Veliidae Brullé, 1836

Subfamily Veliinae Brullé, 1836

Genus *Velia* Latreille, 1804

*Velia* (*Cesavelia*) *bui* sp. nov.

<https://zoobank.org/40E8683C-27BF-43A4-A29C-ACE62F1BA7C5>

Figs 1a–c, 3a, b, 5a, 6a, b, 7a, e, 8a–c, 9a, b

**Material examined.** *Holotype*: apterous ♂, CHINA, Hubei Province, Wufeng County, Houhe National Nature Reserve: 30.0869°N, 110.5520°E; 1085 m a.s.l.; 2015-VIII-8; Zhen Ye leg. (NKUM). *Paratypes*: 1 apterous ♀ 1 macropterous ♀, same data as holotype (NKUM).

**Diagnosis.** Body large, mainly brown. Connexiva straight in dorsal view, with dark yellow strips in male and brighter strips in female (Figs 1a–c, 3a, b), connexival spines sharp and dorsocaudally directed in female (Fig. 3a, b); abdominal segment VIII of male stout and ventrally concaved (Fig. 6a, b); proctiger of male with triangular dilations on each side and broadly rounded hind margin (Fig. 7a).

**Comparative notes.** *Velia bui* sp. nov. and *V. longiconnexiva* are similar in the coloration and size of the body. However, the female of *V. bui* sp. nov. can be easily distinguished from that of *V. longiconnexiva* by its nearly straight connexiva and relatively slender, straight, sharp, slightly directed dorsad connexival spines (Fig. 3a, b vs. 3c, d). The male of the new species can be distinguished from that of *V. longiconnexiva* by its relatively stout segment VIII in lateral view and slightly emarginated dorsal hind margin (Fig. 6a, b vs. 6c, d), the triangular lateral dilations and the broadly rounded hind margin of proctiger (Fig. 7a vs. 7b).

**Description of apterous male (holotype). Measurements.** Body: length 7.00, width 1.90. Head: length 0.58, width: 1.13, width about 1.95 times length. Antenna: 4.97 (1.63+1.13+1.13+1.08), length of antennal segment I about 1.44 times head width. Pronotum: width about 1.03 times length (length 1.48, width 1.53). Lengths of leg segments (femur: tibia: tarsus (tarsal segment I + segment II + segment III)): fore leg: 2.13: 2.13: 0.73 (0.05+0.25+0.43); middle leg: 3.13: 3.30: 1.88 (0.13+1.00+0.75), length of mesotarsus II about 1.33 times length of mesotarsus III; hind leg: 2.95: 3.38: 1.66 (0.08+0.95+0.63), length of metatarsus II about 1.51 times length of metatarsus III. Abdominal segment VIII: length about 1.67 times width (length 1.64, width 0.98).

**Color** (Fig. 1b). Body mainly brown, with scattered silvery pubescence. Pronotum with a row of black punctures near anterior margin and other punctures scattered on posterior lobe. Median part of anterior pronotal lobe and midline of pronotum dark orange; metanotum completely dark brown. Sides of abdomen dark brown, with dark orange stripes along connexiva. Silvery pubescence usually distinctly denser on

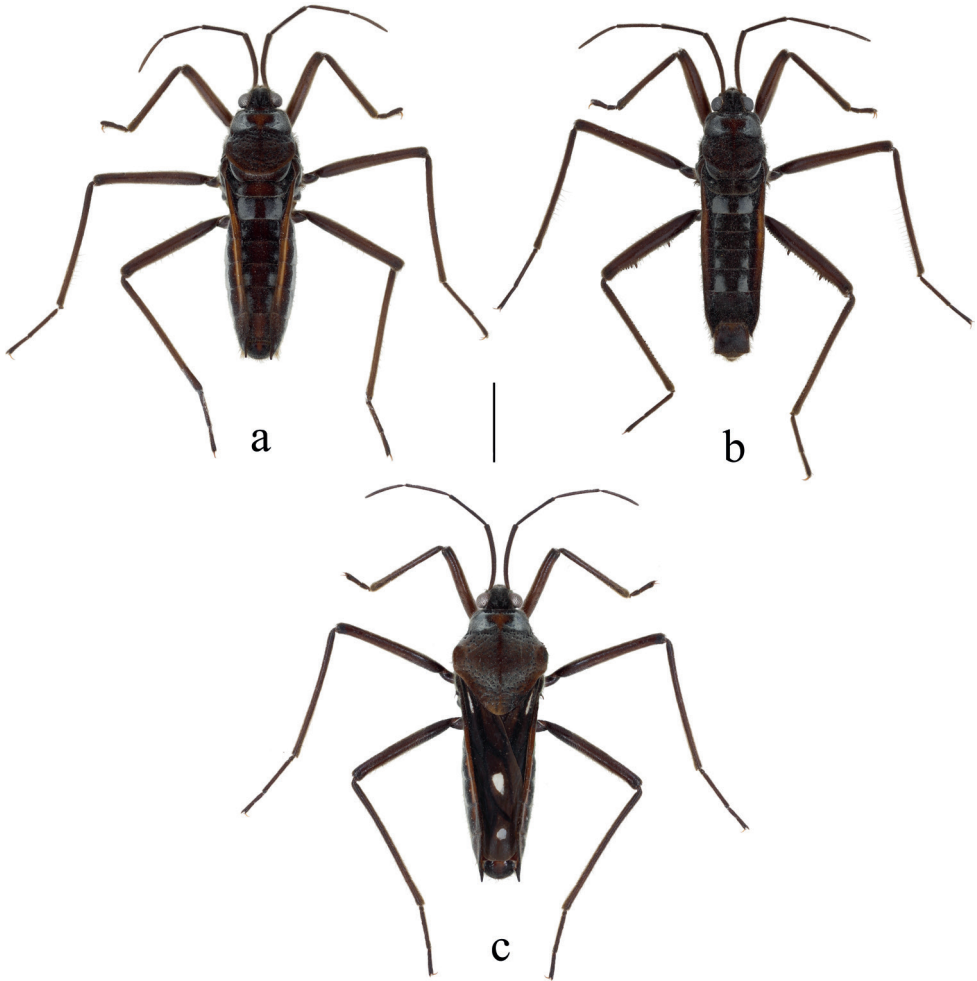


**Figure 1.** Habitus of females and male of *Velia (Cesavelia) bui* sp. nov. in dorsal view **a** apterous female **b** apterous male **c** macropterous female. Scale bar: 2.0 mm.

anterolateral corners of pronotum, lateral corners of metanotum and lateral parts of abdominal mediotergites.

**Structure.** Body relatively large, covered with dense, short pubescence. **Head** (Fig. 1b): triangular, almost perpendicular to thorax, without deflection; anteclypeus and postclypeus with dense, peg-like setae; antennal sockets prominent, antennal segment I much longer than head width, slightly thicker than antennal segments II–IV. **Thorax** (Fig. 1b): pronotum slightly wider than length, hind margin of pronotum broadly rounded, lateral parts of pronotum medially with distinct constrictions, middle part slightly raised and lateral parts of anterior pronotal lobe concaved; mesonotum completely hidden beneath pronotal lobe and hind part of metanotum visible in dorsal view; lateral evaporatoriums slender, with a cluster of suberect, thick setae on each side; legs mainly with decumbent or suberect setae, tarsi of fore legs short, tarsi of middle

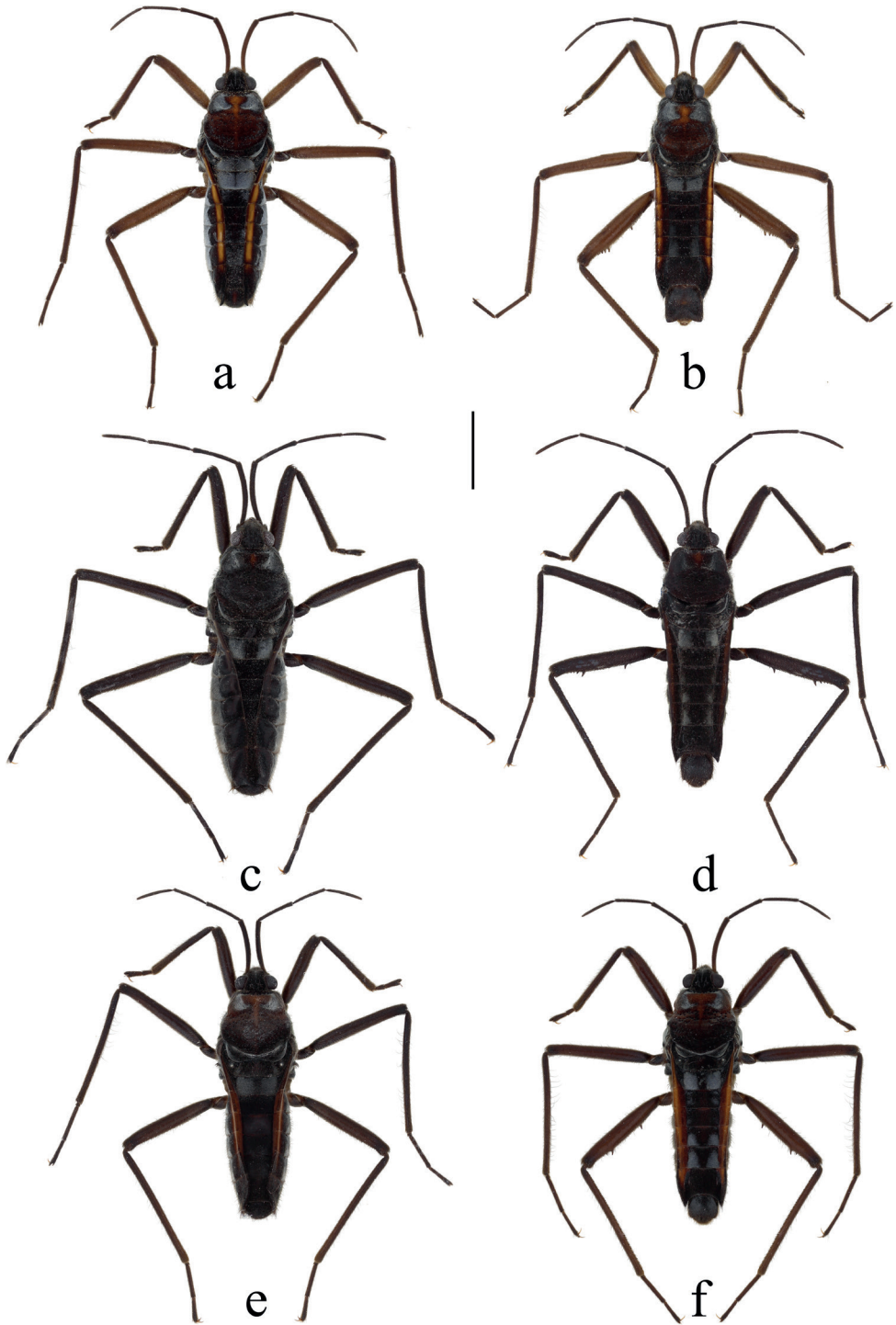


**Figure 2.** Habitus of females and males of *Velia* spp. in dorsal view (apterous form) **a** *V. longiconnexiva*, female **b** *V. longiconnexiva*, male **c** *V. sinensis*, female **d** *V. sinensis*, male **e** *V. tonkina*, female **f** *V. tonkina*, male. Scale bar: 2.0 mm.

and hind legs long and slender; profemora moderately incrassate, slightly curved and contracted subapically; mesofemora medially slender, mesotibiae slender and ventrally with a row of long, erect setae on each side; metafemora (Fig. 5a) relatively stout, ventrally with two rows of small teeth and two prominent long teeth on each side, metatibiae ventrally with two rows of small spines and dorsally with a row of suberect setae on each side. **Abdomen** (Figs 1b, 6a, b): relatively slender; mediotergite I concave laterally, mediotergites II–VII almost flat; connexiva moderately raised, almost parallel without convergence, connexival spines sharp, caudally pointed; abdominal segment VIII (Fig. 6a, b) relatively stout, ventrally concaved in lateral view, posteriorly with dense setae, dorsal hind margin of abdominal segment VIII medially emarginated. **Genital segments** (Figs 7a, 8a–c, 9a, b): relatively large and visible in vitro; proctiger (Fig. 7a) relatively flat, with a triangular dilation on each side, posteriorly with short, sparse setae; paramere (Fig. 8a–c) sickle-shaped, relatively slender, with thick setae on external side, apexes slightly blunt, subapical part with distinct dilation; endosoma (Fig. 9a, b) stout, apical ends of lateral sclerites distinctly constricted, dorsal sclerites weakly sclerotized, translucent and curved, secondary ventral sclerite slender, accessory sclerite absent.

**Description of apterous female. Measurements.** Body: length 7.30, width: 2.13. Head: length 0.80, width: 1.13, width about 1.41 times length. Antenna: 5.02 (1.63+1.13+1.13+1.13), length of antennal segment I about 1.44 times head width. Pronotum: width about 1.08 times length (length 1.70, width 1.83). Length of leg segments (femur: tibia: tarsus (tarsal segment I + segment II + segment III)): fore leg: 2.13: 2.13: 0.76 (0.08+0.25+0.43); middle leg: 3.13: 3.25: 1.89 (0.13+1.13+0.63), length of mesotarsus II about 1.79 times length of mesotarsus III; hind leg: 3.00: 3.38: 1.59 (0.08+0.88+0.63), length of metatarsus II about 1.40 times length of metatarsus III.

**Color** (Figs 1a, 3a, b). Similar to apterous male with following exceptions: hind margin of pronotum, median part of metanotum and all mediotergites dark orange. Stripes along connexiva much brighter.

**Structure.** Body slightly larger than apterous male. **Head** (Figs 1a, 3a, b): Similar to apterous male with following exceptions: the antennal segment I more bent. **Thorax** (Figs 1a, 3a, b): similar to apterous male with following exceptions: posterior pronotal lobe distinctly wider than anterior pronotal lobe; profemora much slender; metafemora slender, ventrally with two rows of small spines on each side, metatibiae ventrally without any spines or teeth. **Abdomen** (Figs 1a, 3a, b): similar to apterous male with following exceptions: relatively stout; connexiva gradually convergent toward abdominal apex, connexival spines long, slender and straight, slightly dorsocaudally directed. **Genital segments:** gonocoxae and gonapophyses semi-membranous, rami strongly sclerotized; proctiger (Fig. 7e) broad, sub-circle, posteriorly with short, sparse setae.

**Description of macropterous female. Measurements.** Body: length 7.50, width 2.38. Head: length 0.72, width 1.18, width about 1.64 times length. Antenna: 5.12 (1.68+1.13+1.18+1.13), length of antennal segment I about 1.42 times head width. Pronotum: width about 0.90 times length (length 2.63, width 2.38). Lengths of leg segments (femur: tibia: tarsus (tarsal segment I + segment II + segment III)): fore leg:

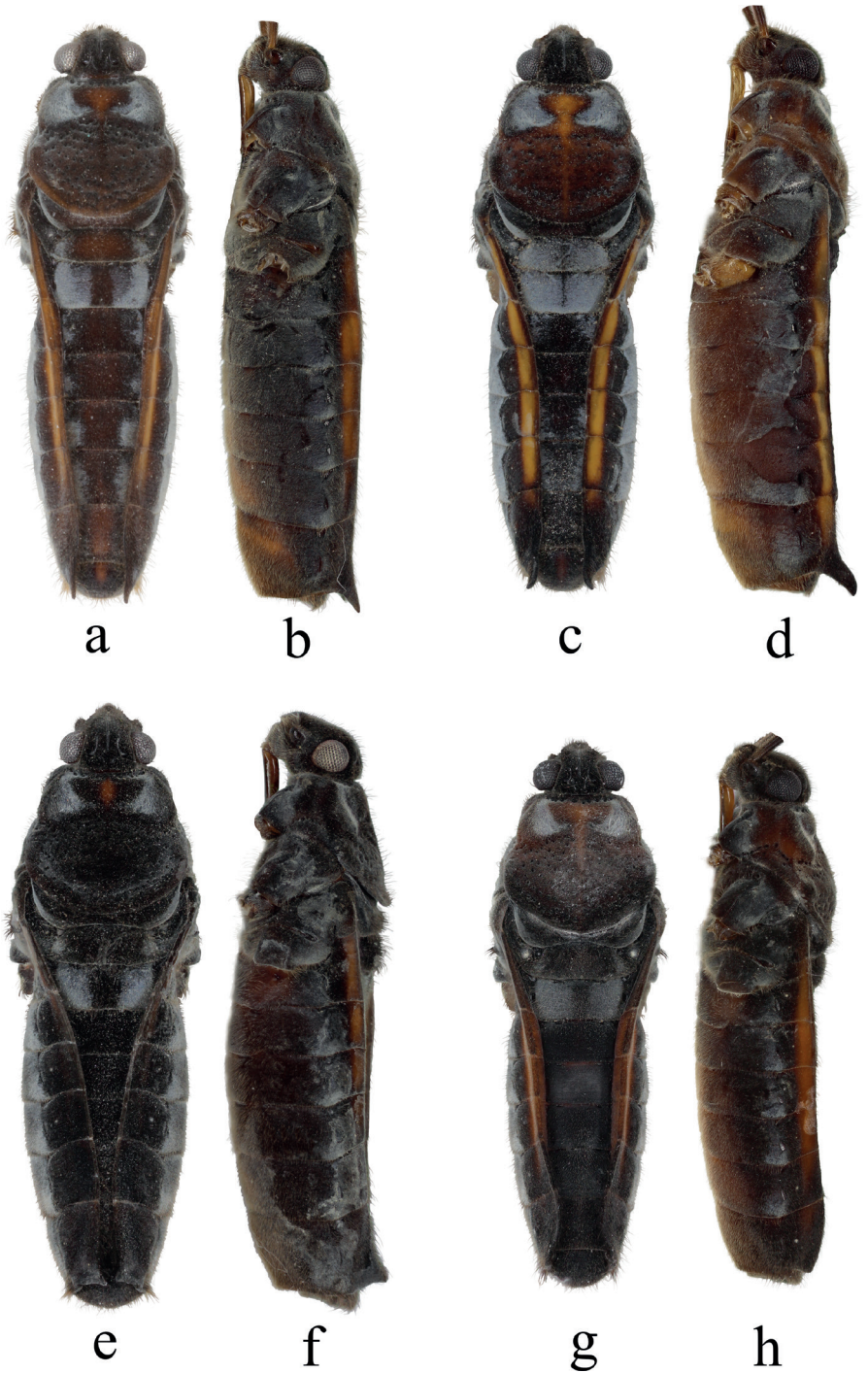


**Figure 3.** Bodies of *Velia* spp. (apterous female) **a** *V. bui* sp. nov., dorsal view **b** *V. bui* sp. nov., lateral view **c** *V. longiconnexiva*, dorsal view **d** *V. longiconnexiva*, lateral view **e** *V. sinensis*, dorsal view **f** *V. sinensis*, lateral view **g** *V. tonkina*, dorsal view **h** *V. tonkina*, lateral view. Scale bar: 2.0 mm.

2.13: 2.13: 0.71 (0.08+0.25+0.38); middle leg: 3.00: 3.38: 1.82 (0.05+1.04+0.73), length of mesotarsus II about 1.42 times length of mesotarsus III; hind leg: 3.00: 3.35: 1.64 (0.08+0.93+0.63), length of metatarsus II about 1.48 times length of metatarsus III. Wing: length: 4.65, width: 1.16.

**Color** (Fig. 1c). Similar to apterous female with following exceptions: hind margin of pronotum medially orangish; forewing brownish with dark brown veins and three white spots; sides of abdominal segments III–VI including connexiva with dark orange marks.

**Structure.** Body slightly larger than apterous female. **Head** (Fig. 1c): similar to apterous female. **Thorax** (Fig. 1c): similar to apterous female with following exceptions: pronotum large, nearly pentagonal, with broad posterior lobe completely covering the meso- and metanotum, humeral corners prominent; each forewing with three spots (Fig. 1c): a thin spot in first basal cell, a large teardrop-shaped spot in apical cell and a suborbicular spot between the free apical veins. **Abdomen and genital segments:** similar to apterous female.

**Macropterous male.** Unknown.

**Etymology.** The species is named in honor of Prof. Wenjun Bu (NKUM) for his outstanding contribution to the studies on Chinese fauna of Heteroptera, on the occasion of his 60<sup>th</sup> birthday.

**Distribution.** China (Hubei) (Fig. 11).

### *Velia longiconnexiva* Tran, Zettel & Buzzetti, 2009

Figs 2a, b, 3c, d, 5b, 6c, d, 7b, f, 8d–f, 9c, d

**Material examined.** 8 apterous ♂♂ 9 apterous ♀♀, CHINA, Guizhou Province, Leishan County, Leigongshan National Nature Reserve: 26.3827°N, 108.2277°E; 1700 m a.s.l.; 2013-VIII-3; Zhen Ye leg. (NKUM).

**Diagnosis.** Body large, mainly dark brown. Connexiva with dark yellow strips in male and brighter strips in female (Figs 2a, b, 3c, d), connexival spines of female long, dorsocaudally directed (Fig. 3c, d); abdominal segment VIII of male slender, dorsal hind margin strongly emarginated, ventrally concaved in lateral view (Fig. 6c, d); proctiger of male with sub-trapezoid dilations on each side and emarginated hind margin (Fig. 7b).

**Comparative notes.** See comparative notes of *V. bui* sp. nov.

**Distribution.** China (Guizhou) (Fig. 11).

### *Velia sinensis* Andersen, 1981

Figs 2c, d, 3e, f, 4a–l, 5c, 6e, f, 7c, g, 8g–i, 9e, f

**Material examined.** 2 apterous ♂♂ 2 apterous ♀♀, CHINA, Sichuan Province, Emei Mountain, Jiu Lao Dong Scenic area: 1800–1900 m a.s.l.; 1957-VII-22; Keren Huang leg. (NKUM). 5 apterous ♀♀, CHINA, Sichuan Province, Meishan City, Hongya County, Yanv Lake: 29.6335°N, 103.0858°E; 2013-VII-25; Xin Yu & Xubo Jiang leg.

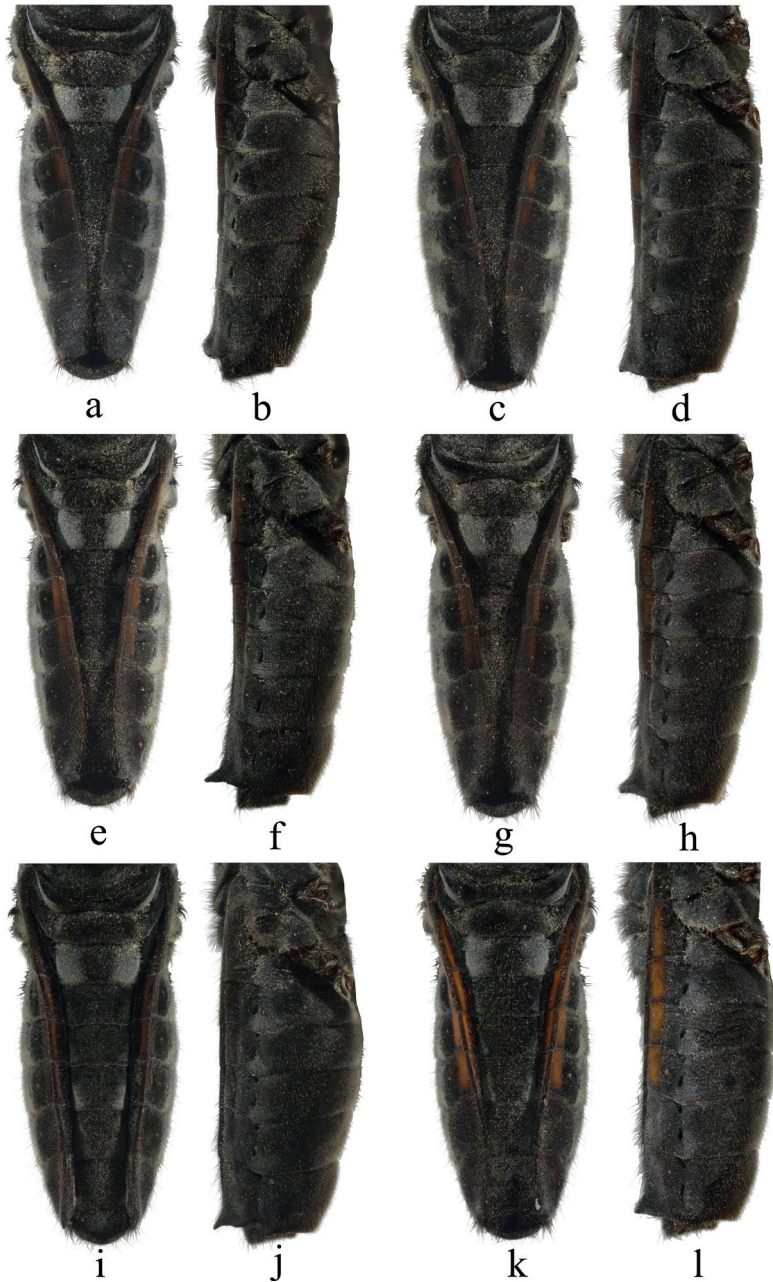


**Figure 4.** Abdomen of *V. sinensis* (females) from Qianfoshan National Nature Reserve, Mianyang City, Sichuan Province, China **a** connexiva strongly convergent type I, dorsal view **b** connexiva strongly convergent type I, lateral view **c** connexiva strongly convergent type II, dorsal view **d** connexiva strongly convergent type II, lateral view **e** connexiva moderately convergent type I, dorsal view **f** connexiva moderately convergent type I, lateral view **g** connexiva moderately convergent type II, dorsal view **h** connexiva moderately convergent type II, lateral view **i** connexiva slightly convergent type I, dorsal view **j** connexiva slightly convergent type I, lateral view **k** connexiva slightly convergent type II, dorsal view **l** connexiva slightly convergent type II, lateral view. Scale bar: 2.0 mm.

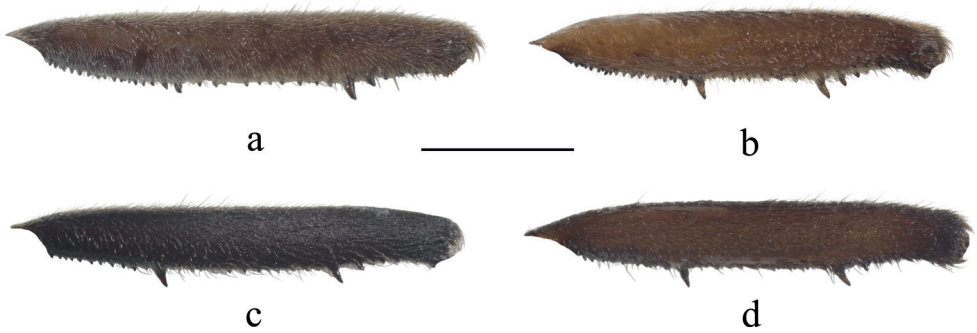


**Figure 5.** Metafemora of males, showing patterns of spines **a** *V. bui* sp. nov. **b** *V. longiconnexiva* **c** *V. sinensis* **d** *V. tonkina*. Scale bar: 1.0 mm.

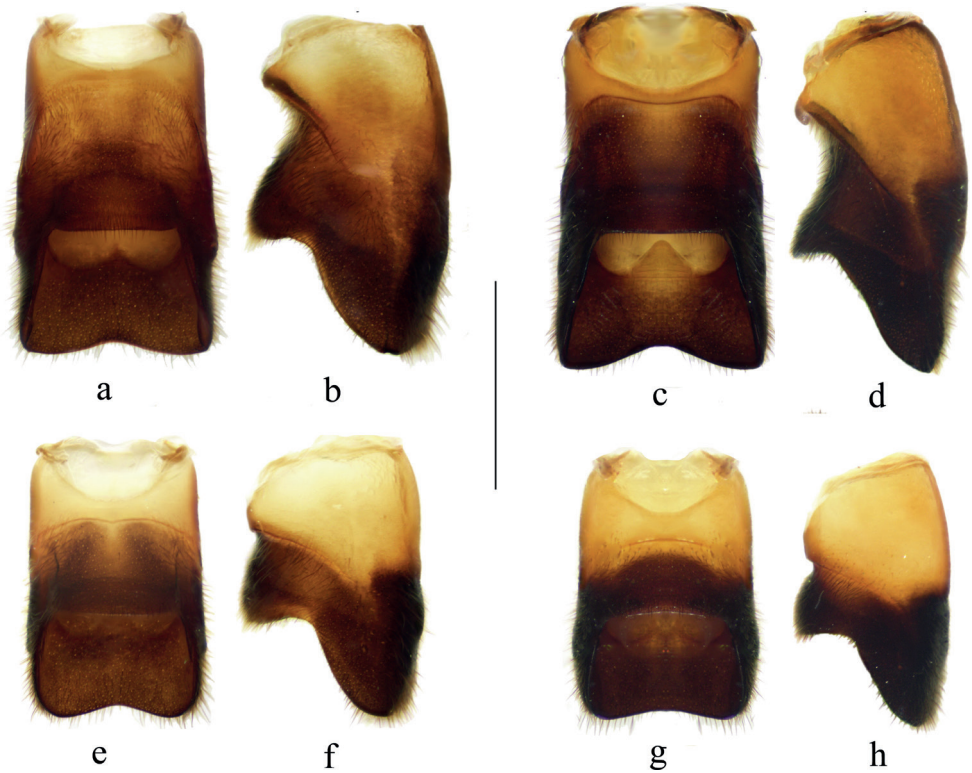


**Figure 6.** Abdominal segments VIII of males **a** *V. bui* sp. nov., ventral view **b** *V. bui* sp. nov., lateral view **c** *V. longiconnexiva*, ventral view **d** *V. longiconnexiva*, lateral view **e** *V. sinensis*, ventral view **f** *V. sinensis*, lateral view **g** *V. tonkina*, ventral view **h** *V. tonkina*, lateral view. Scale bar: 1.0 mm.

(NKUM). 1 apterous ♂ 7 apterous ♀♀, CHINA, Sichuan Province, Mianyang City, Qianfoshan National Nature Reserve: 29.8880°N, 103.0336°E; 2400 m a.s.l.; 2015-VII-17; Zhen Ye & Chenguang Zheng leg. (NKUM). 1 apterous ♂ 4 apterous ♀♀,

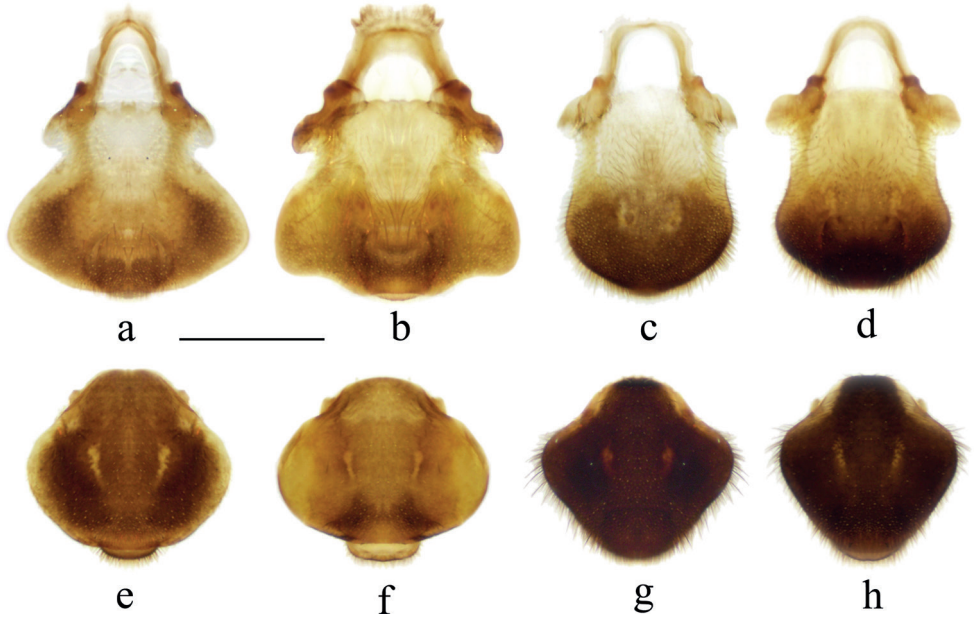


**Figure 7.** Proctigera of *Velia* spp. **a** *V. bui* sp. nov., male **b** *V. longiconnexiva*, male **c** *V. sinensis*, male **d** *V. tonkina*, male **e** *V. bui* sp. nov., female **f** *V. longiconnexiva*, female **g** *V. sinensis*, female **h** *V. tonkina*, female. Scale bar: 0.5 mm.

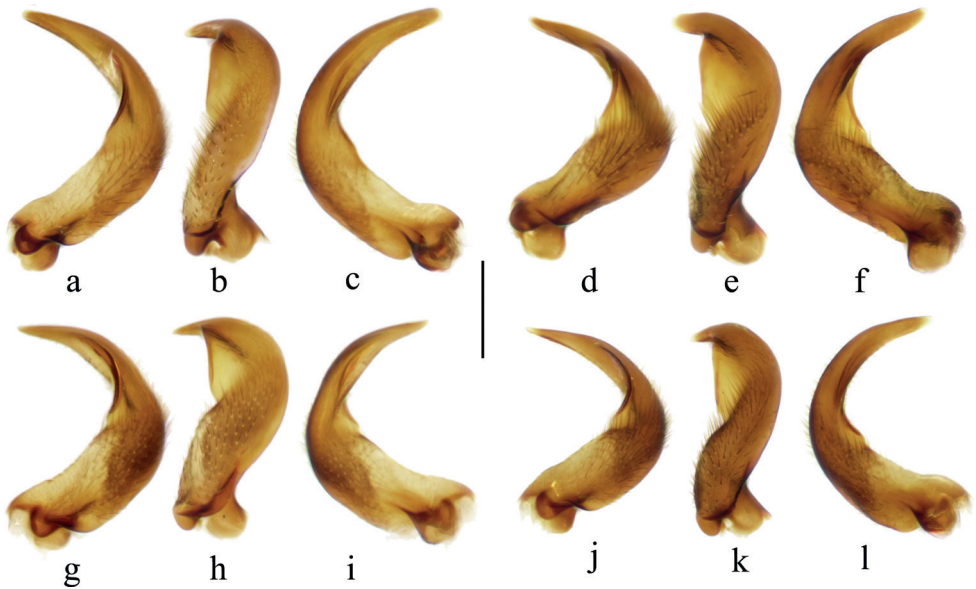


**Figure 8.** Parameres of males **a** *V. bui* sp. nov., external view **b** *V. bui* sp. nov., perpendicular view **c** *V. bui* sp. nov., internal view **d** *V. longiconnexiva*, external view **e** *V. longiconnexiva*, perpendicular view **f** *V. longiconnexiva*, internal view **g** *V. sinensis*, external view **h** *V. sinensis*, perpendicular view **i** *V. sinensis*, internal view **j** *V. tonkina*, external view **k** *V. tonkina*, perpendicular view **l** *V. tonkina*, internal view. Scale bar: 0.2 mm.

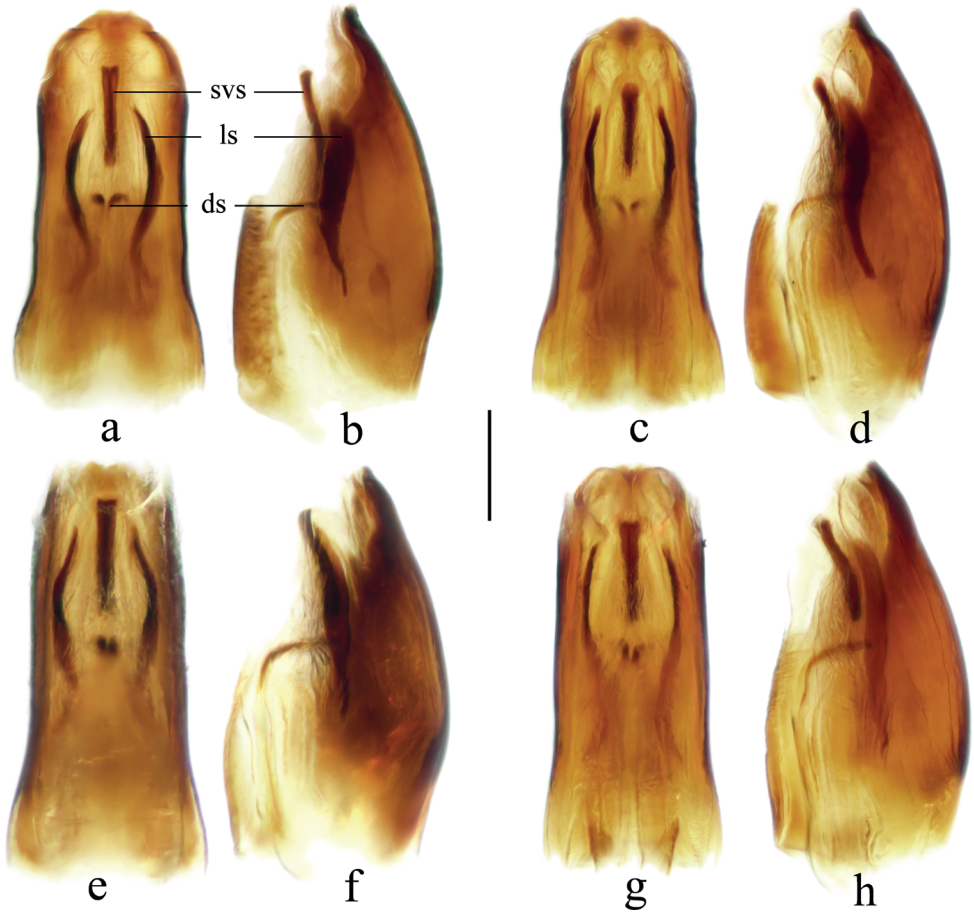


**Figure 9.** Endosomal structures of *Velia* spp. (males) **a** *V. bui* sp. nov., dorsal view **b** *V. bui* sp. nov., lateral view **c** *V. longiconnexiva*, dorsal view **d** *V. longiconnexiva*, lateral view **e** *V. sinensis*, dorsal view **f** *V. sinensis*, lateral view **g** *V. tonkina*, dorsal view **h** *V. tonkina*, lateral view. Scale bar: 0.2 mm. (ds = dorsal sclerite, ls = lateral sclerite, svs = secondary ventral sclerite).

CHINA, Sichuan Province, Dujiangyan City, Taian Town, Qingchenghoushan Scenic area: 30.9189°N, 103.4778°E; 918 m a.s.l.; 2014-VII-14; Zhen Ye, Yahui Zhen & Chenguang Zheng leg. (NKUM). 1 apterous ♂ 6 apterous ♀♀, CHINA, Sichuan Province, Ebian County, Xinchang Town, Yangziyan Village: 29.2478°N, 103.2631°E; 1022 m a.s.l.; 2017-VII-27; Chenguang Zheng leg. (NKUM).

**Diagnosis.** Body large, mainly dark brown to black, commonly dull (Figs 2c, d, 3e, f, 4a–l), but some individuals with conspicuous orange strips along connexiva (Fig. 4k, l); abdominal segment VIII of male small and slightly concaved ventrally (Fig. 6e, f); proctiger of male simple, with rounded hind margin (Fig. 7c).

**Comparative notes.** The comparison between *V. sinensis* and *V. tonkina* has been elucidated by Polhemus and Polhemus (2003) and Tran et al. (2009). In addition,

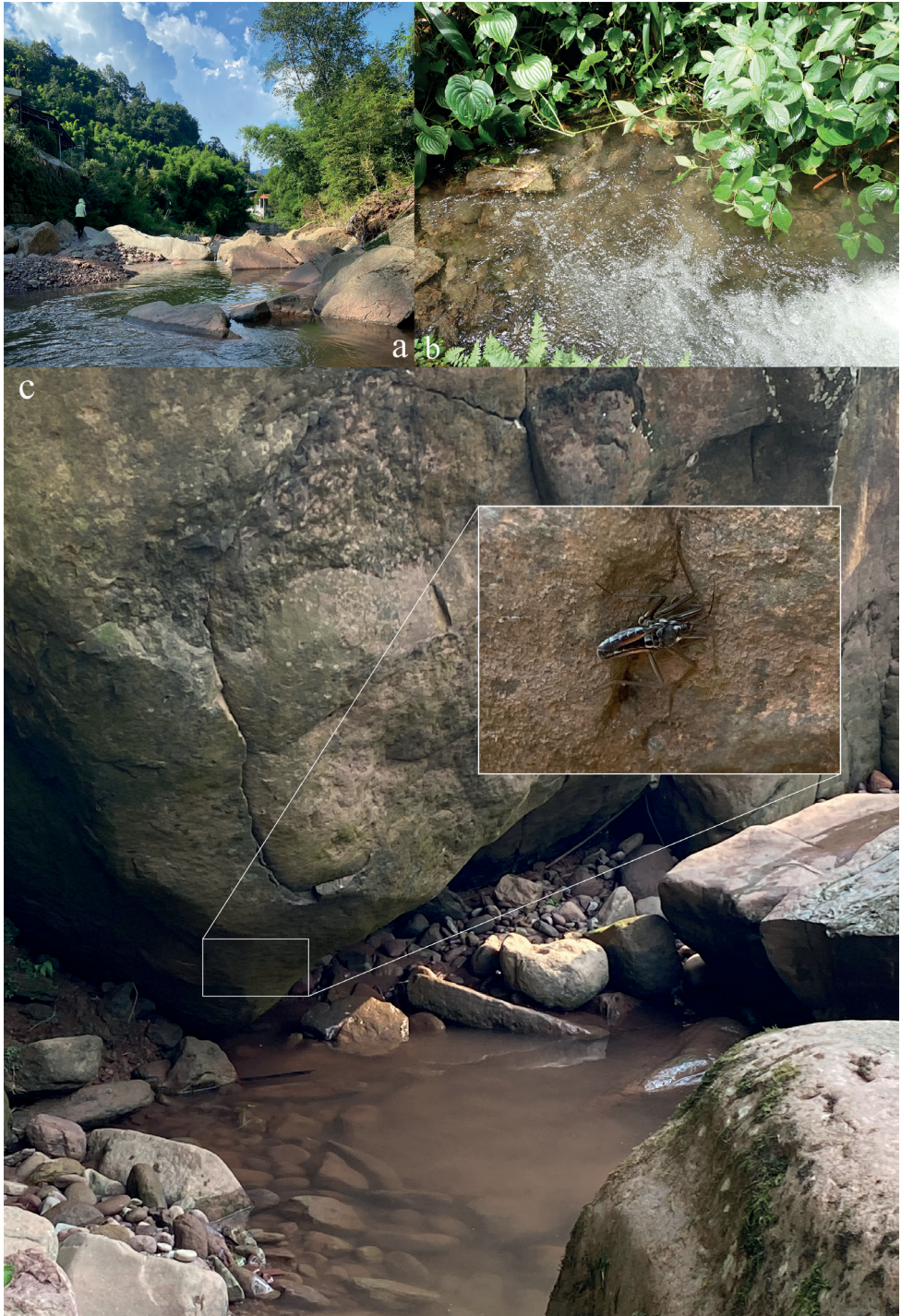


**Figure 10.** Photographs of habitats of *Velia* spp. **a** habitat of *V. sinensis* **b** habitat of *V. tonkina* **c** habitat of cryptic area on rock surfaces near the stream of *V. sinensis*.

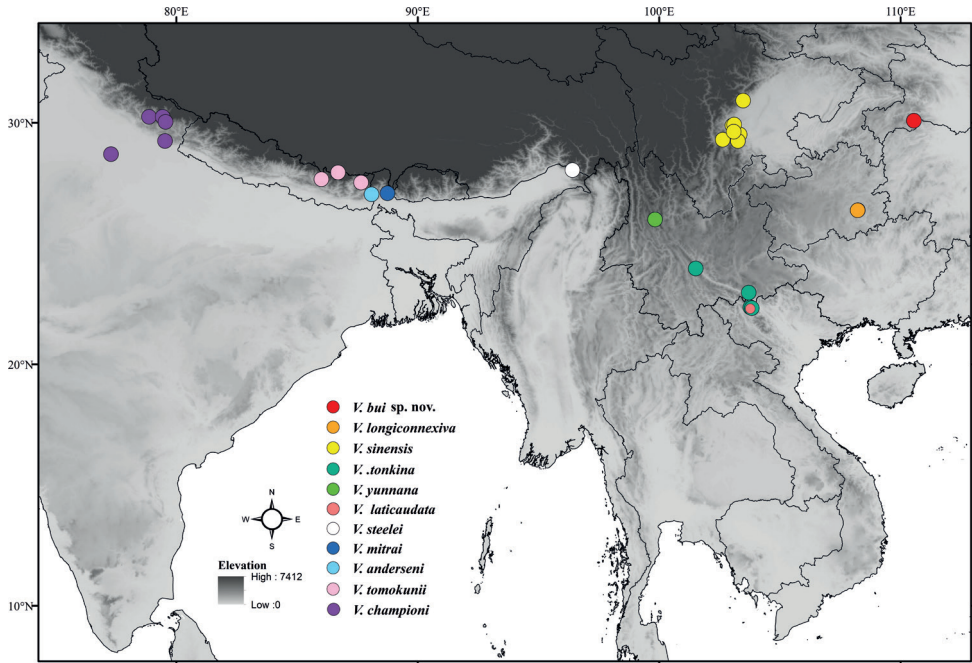


**Figure 11.** Geographical distribution of subgenus *Velia* (*Cesavelia*).

*V. sinensis* can be distinguished from *V. tonkina* by having the basal ends of the lateral sclerites in the endosoma slightly curved laterally (Fig. 9e). In contrast, *V. tonkina* has the basal ends of the lateral sclerites in the endosoma slightly curved inward (Fig. 9g).

**Habitats.** Some specimens of *V. sinensis* have been observed and collected in the shaded water surface and rock surface near streams (Fig. 10a, c).

**Distribution.** China (Sichuan) (Fig. 11).

### *Velia tonkina* Polhemus & Polhemus, 2003

Figs 2e, f, 3g, h, 5d, 6g, h, 7h, 8j–l, 9g, h

**Material examined.** 1 apterous ♂ 1 apterous ♀, CHINA, Yunnan Province, Yuxi City, Gasa Town, Shimexia Scenic area: 23.9688°N, 101.5127°E; 2013m a.s.l; 2016-VIII-01; Zhen Ye leg. (NKUM). 2 apterous ♀♀, CHINA, Yunnan Province, Honghe Pingbian Miao Autonomous County, Dweishan National Reserve: 22.9701°N, 103.7082°E; 2011-IV-16; Zhen Ye leg. (NKUM).

**Diagnosis.** Body large, mainly dark brown. Connexiva with dark orange strips (Figs 2e, f, 3g, h); connexival spines of female short, dorsocaudally directed, in some specimens strongly reduced (Fig. 3g, h); abdominal segment VIII of male small and ventrally concaved (Fig. 6g, h); proctiger of male simple, with broad rounded hind margin (Fig. 7d)

**Comparative notes.** See comparative notes of *V. sinensis* and in Tran et al. (2009).

**Habitats.** Some specimens of *V. tonkina* have been observed and collected in the shade of pools surface (Fig. 10b).

**Distribution.** China (Yunnan, first record for China), and Vietnam (Fig. 11).

## Discussion

Intraspecific variation among female individuals of *V. sinensis* and *V. tonkina* had been noticed and discussed by Tran et al. (2009). In this study, female specimens of *V. sinensis*, collected from one site (i.e., Qianfoshan National Nature Reserve, Mianyang City, Sichuan Prov., China), can be divided into three forms based on the levels of convergence of connexiva: (1) individuals with strongly convergent connexiva (Fig. 4a–d); (2) individuals with moderately convergent connexiva (Fig. 4e–h); and (3) individuals with slightly convergent connexiva (Fig. 4i–l). In addition, the connexival spines and the coloration of stripes along connexiva in the female collected from the same site above are also variable (Fig. 4a–l). Therefore, we speculate that the morphological variation at least within *V. sinensis* might not be attributable to the effects of geographical isolation. This phenomenon needs to be elucidated by subsequent studies based on molecular data.

## Acknowledgements

We express gratitude to Chenguang Zheng, Keren Huang, Xin Yu, Xubo Jiang for collecting specimens of *V. sinensis* for this research. We express our appreciation to Anh Duc Tran for his careful review and constructive comments. This study was supported by Natural Science Foundation of China (No. 31972872) and Fundamental Research Funds for the Central Universities, Nankai University (No. 20JJCQNJC01420).

## References

- Andersen NM (1981) A new genus of Veliinae and descriptions of new Oriental species of the subfamily (Hemiptera: Veliidae). *Entomologica Scandinavica* 12(3): 339–356. <https://doi.org/10.1163/187631281794709773>
- Andersen NM (1995) Infraorder Gerromorpha Popov, 1971 – semiaquatic bugs. In: Aukema B, Rieger C (Eds) *Catalogue of the Heteroptera of the Palaearctic Region* (Vol. 1). Netherlands Entomological Society, Amsterdam, 77–114.
- Basu S, Subramanian KA, Polhemus DA (2013) A new species of *Velia* (Hemiptera: Heteroptera: Veliidae) from West Bengal, India. *Zootaxa* 3693: 344–350. <https://doi.org/10.11646/zootaxa.3693.3.4>
- Berchi GM, Copilaş-Ciocianu D, Kment P, Buzzetti FM, Petrusek A, Rákosy L, Cianferoni F, Damgaard J (2018) Molecular phylogeny and biogeography of the West-Palaearctic *Velia*

- (Heteroptera: Gerromorpha: Veliidae). *Systematic Entomology* 43(2): 262–276. <https://doi.org/10.1111/syen.12273>
- Koçak AÖ, Kemal M (2010) Nomenclatural notes on the genus group names of the families Veliidae and Tingidae (Hemiptera). *Priamus* 12(6): 151–152.
- Polhemus JT, Polhemus DA (1998) Notes on Asian Veliinae (Heteroptera: Veliidae), with descriptions of three new species. *Journal of the New York Entomological Society* 106: 117–131.
- Polhemus DA, Polhemus JT (2003) A review of the Veliinae of Vietnam (Heteroptera: Veliidae) with description of a new *Velia* species. *Journal of the New York Entomological Society* 111(1): 29–40. [https://doi.org/10.1664/0028-7199\(2003\)111\[0029:AROTVO\]2.0.CO;2](https://doi.org/10.1664/0028-7199(2003)111[0029:AROTVO]2.0.CO;2)
- Tamanini L (1947) Contributo ad una revisione del genere *Velia* Latr. e descrizione di alcune specie nuove (Hemiptera, Heteroptera, Veliidae). *Memorie della Societa Entomologica Italiana* 26: 17–74.
- Tamanini L (1955a) IV Contributo allo studio del genere *Velia* Latr. con la descrizione di quattro nuove entità (Hem. Heter. Veliidae). *Bollettino della Società Entomologica Italiana* 85: 35–44.
- Tamanini L (1955b) Valore specifico delle *Velia* descritte da Fabriciuse posizione sistematica delle specie Europee e circummediterranee (Hem. Heter. Veliidae). V contributo allo studio del genere *Velia* Latr. *Memorie della Societa Entomologica Italiana* 33: 201–207.
- Tamanini L (1955c) Gen. *Velia* Lt. In: Stichel W (Ed.) *Illustrierte Bestimmungstabellen der Wanzen*. II. Europa 1. W. Stichel, Berlin, 125–148.
- Tran AD, Zettel H, Buzzetti FM (2009) Revision of the Oriental subgenus *Velia* (*Haldwania*) Tamanini, 1955 (Heteroptera: Veliidae), with descriptions of four new species. *Insect Systematics & Evolution* 40(2): 171–199. <https://doi.org/10.1163/187631209X433760>

# A new glassfrog species of the genus *Centrolene* (Amphibia, Anura, Centrolenidae) from Cordillera del Cóndor, southern Ecuador

Paul Székely<sup>1,2,3</sup>, María Córdova-Díaz<sup>1,4</sup>, Daniel Hualpa-Vega<sup>1,4</sup>,  
Santiago Hualpa-Vega<sup>1,4</sup>, Diana Székely<sup>1,2,3</sup>

**1** Museo de Zoología, Universidad Técnica Particular de Loja, San Cayetano Alto, calle París s/n, 110107, Loja, Ecuador **2** Laboratorio de Ecología Tropical y Servicios Ecosistémicos (EcoSs-Lab), Facultad de Ciencias Exactas y Naturales, Departamento de Ciencias Biológicas y Agropecuarias, Universidad Técnica Particular de Loja, San Cayetano Alto s/n, 110107, Loja, Ecuador **3** Research Center of the Department of Natural Sciences, Faculty of Natural and Agricultural Sciences, Ovidius University Constanța, Al. Universității no.1, 900470, Constanța, Romania **4** Fundación Green Jewel, Av. Pío Jaramillo y John Kennedy, Loja, Ecuador

Corresponding author: Paul Székely ([jpszekely@utpl.edu.ec](mailto:jpszekely@utpl.edu.ec))

Academic editor: U. García-Vázquez | Received 10 October 2022 | Accepted 3 February 2023 | Published 22 February 2023

<https://zoobank.org/028AD185-E485-4752-ACF1-E76AC0FBFB49>

**Citation:** Székely P, Córdova-Díaz M, Hualpa-Vega D, Hualpa-Vega S, Székely D (2023) A new glassfrog species of the genus *Centrolene* (Amphibia, Anura, Centrolenidae) from Cordillera del Cóndor, southern Ecuador. ZooKeys 1149: 53–84. <https://doi.org/10.3897/zookeys.1149.96134>

## Abstract

Based on an integrative taxonomical approach, using molecular, morphological, and bioacoustics data, a new species of glassfrog of the genus *Centrolene* is described from Refugio de Vida Silvestre El Zarza, southern Ecuador. *Centrolene zarza* **sp. nov.** is a medium sized species, easily distinguished from all other glassfrogs by its unique combination of characters, such as a shagreen dorsum with elevated warts corresponding to white spots, an evident tympanum, half or more than half of the upper parietal peritoneum covered by iridophores, iridophores absent on all visceral peritonea, including the pericardium, a lobed liver lacking iridophores, males with small projecting humeral spines, the outer edges of forearms and tarsus with a row of enameled warts that often continue into the external edges of Finger IV and/or Toe V, and white or yellowish white iris with thick black reticulations. The new species is closely related to a currently undescribed species and superficially resembles *C. condor*, *C. pipilata*, *C. solitaria*, *C. altitudinalis*, and *C. daidalea*. The tadpole and advertisement and courtship calls are described, and the threats to the species survival, mainly represented by habitat loss and contamination due to mining activities, are briefly discussed.

## Resumen

Se describe una nueva especie de rana de cristal del género *Centrolene*, del Refugio de Vida Silvestre El Zarza, sur del Ecuador, basada en un enfoque de taxonomía integrativa, utilizando datos moleculares, morfológicos y bioacústicos. La especie *Centrolene zarza* **sp. nov.** es de tamaño mediano, que se distingue fácilmente de todas las demás ranas de cristal por su combinación única de caracteres tales como dorso de piel rugosa con verrugas elevadas que corresponden a manchas blancas, tímpano evidente, la mitad o más del peritoneo parietal superior cubierto por iridóforos, iridóforos ausentes en todos los peritoneos viscerales, incluido el pericardio, hígado lobulado sin iridóforos, machos con pequeñas espinas humerales salientes, borde externo de los antebrazos y el tarso con hilera de verrugas esmaltadas que a menudo continúan en los bordes externos del Dedo IV y/o del Dedo V del pie, e iris blanco o blanco amarillento con reticulaciones negras gruesas. La nueva especie está estrechamente relacionada con una especie no descrita y se parece superficialmente a *C. condor*, *C. pipilata*, *C. solitaria*, *C. altitudinalis* o *C. daidalea*. Se describen renacuajos, cantos de aviso y cortejo, y se discuten brevemente las amenazas para su supervivencia, representadas por la pérdida de hábitat y la contaminación debido a las actividades mineras.

## Keywords

Amphibians, DNA, phylogenetics, tadpoles, tropical Andes, vocalizations

## Palabras claves

ADN, Andes tropicales, Anfibios, filogenética, renacuajos, vocalizaciones

## Introduction

The charismatic glassfrogs belong to the Neotropical family Centrolenidae Taylor, 1951 that currently contains ca. 150 species classified into 12 genera (Guayasamin et al. 2009, 2020). These generally small, arboreal frogs share a unique morphology and behavior that makes them readily distinguishable: a green dorsum in most species, completely or partially translucent venter (hence the name of glassfrogs), humeral spines in males of some species, out-of-water deposition of eggs along streams, and forward-directed eyes (Guayasamin et al. 2020). Ecuador, despite its small size, has the second largest number of glassfrogs after Colombia, with 63 species from ten genera, 20 of them being endemic to the country (Guayasamin et al. 2020, 2022).

*Centrolene* Jiménez De La Espada, 1872 is the type genus for the family Centrolenidae, and is the third richest in number of species, after *Nymphargus* Cisneros-Heredia & McDiarmid, 2007 and *Hyalinobatrachium* Ruiz-Carranza & Lynch, 1991a. Currently there are 24 described species in the genus, and six more are listed as incertae sedis (Guayasamin et al. 2009, 2020). For most of the *Centrolene* species some DNA sequences are available (Guayasamin et al. 2008; Castroviejo-Fisher et al. 2014; Twomey et al. 2014), and these were included in the latest phylogenetic analysis of the genus presented by Guayasamin et al. (2020). For three species we still lack molecular data: *Centrolene paezorum* Ruiz-Carranza, Hernández-Camacho & Ardila-Robayo, 1986

and *C. solitaria* (Ruiz-Carranza & Lynch, 1991c) from Colombia and *C. lemniscata* Duellman & Schulte, 1993 from Peru.

Currently, 12 *Centrolene* species have been reported from Ecuador, two being considered endemic (Guayasamin et al. 2020): *C. pipilata* (Lynch & Duellman, 1973) from the Amazonian slope of the Ecuadorian Andes, in the north and *C. condor* Cisneros-Heredia & Morales-Mite, 2008 from Cordillera del Cóndor, in the south. Additionally, four species are known from the Amazonian slopes of the Andes: *C. charapita* Twomey, Delia & Castroviejo-Fisher, 2014, *C. huilensis* Ruiz-Carranza & Lynch, 1995b, *C. medemi* (Cochran & Goin, 1970), and *C. sanchezi* Ruiz-Carranza & Lynch, 1991b. Herein we describe a new species of *Centrolene* from Cordillera del Cóndor, based on an integrative taxonomy approach, combining molecular, morphological and bioacoustics data.

## Materials and methods

### Specimen collection and study site

Field work was carried out between January 2020 and September 2022 in Refugio de Vida Silvestre El Zarza (Zamora Chinchipe province, southern Ecuador; 3.8341°S, 78.5458°W; datum WGS84; 1400–1680 m a.s.l.). Refugio de Vida Silvestre El Zarza (El Zarza wildlife refuge) is a national protected area founded in 2006 with the main aim of preserving some of Cordillera del Cóndor's biological richness, with emphasis on amphibians and the Amazonian tapir. The refuge protects 3696.31 ha of evergreen lower montane forest and important water systems. Field work was carried out during the day and night (usually between 12h00–01h00), through intensive visual encounter surveys and auditory surveys. The distribution map was designed with QGIS software and created using a digital elevation model obtained from JAXA/METI ALOS PALSAR Data (<https://search.asf.alaska.edu/>) and displayed via ASF DAAC.

All collected specimens were photographed alive, euthanized using 20% benzocaine, fixed in 10% formalin, and stored in 70% ethanol. Tissue samples for genetic analyses were preserved in 96% ethanol. Two egg clutches were collected and transported to the laboratory in order to raise and describe the tadpoles. Hatchlings and tadpoles were preserved in alcohol (as DNA samples) and 10% formalin (for the morphological analysis) in various developmental stages. Examined and referred specimens are housed at Museo de Zoología, Universidad Técnica Particular de Loja, Loja, Ecuador (MUTPL), Museo de Historia Natural Gustavo Orcés, Escuela Politécnica Nacional (MEPN), and Museo de Zoología, Pontificia Universidad Católica del Ecuador, Quito, Ecuador (QCAZ). Research permits were issued by the Ecuadorian Ministry of Environment (MAE-DNB-CM-2015-0016, MAAE-ARSFC-2020-0727, and MAATE-DBI-CM-2021-0181).

## Morphological analysis

For the description of qualitative and quantitative morphological characters, as well as the format of the description, we follow Cisneros-Heredia and McDiarmid (2007) and Guayasamin et al. (2020). Sex was determined by the presence of vocal slits, humeral spines and/or by gonadal inspection. Coloration of live specimens was based on field notes and digital photographs. All specimens were weighted (body mass: BM) before euthanasia using a My Weigh Triton T3 portable scale with 0.01 g precision. Measurements were taken under a stereo microscope, with a Vernier caliper, and rounded to the nearest 0.1 mm. Specimens were measured for the following morphometric variables:

- SVL** snout-vent length, distance from the tip of snout to posterior margin of vent;
- HW** head width, widest portion of the head, measured at level of jaw articulation;
- HL** head length, distance from the tip of snout to posterior angle of jaw articulation;
- IOD** interorbital distance, shortest distance between upper eyelids;
- IND** internarial distance, distance between the inner edges of the narial openings;
- EW** upper eyelid width, the perpendicular distance to the outer edge of the eyelid;
- ED** eye diameter, distance between anterior and posterior borders of eye;
- EN** eye-nostril distance, distance from posterior margin of nostril to anterior margin of eye;
- TD** tympanum diameter, horizontal distance between peripheral borders of tympanic annulus;
- FL** femur length, length of femur from vent to knee;
- TL** tibia length, length of flexed leg from knee to heel;
- FoL** foot length, distance from proximal margin of inner metatarsal tubercle to tip of Toe IV;
- HaL** hand length, distance from proximal edge of palmar tubercle to the tip of Finger III;
- 3DW** width of disc on Finger III, greatest width of disc of Finger III.

Measurements are given as mean  $\pm$  SD.

The developmental stages of embryos, hatchlings, and larvae were identified using the classification by Gosner (1960). Larval characters and description follow the terminology recommended by Mijares-Urrutia (1998), McDiarmid and Altig (1999), Anstis (2013), and Schulze et al. (2015). Photographs of tadpoles were taken of live specimens in a small glass tank and of the mouthparts on preserved specimens under a stereo microscope.

## Molecular analysis

Genomic extraction, amplification, and sequencing were as described in Székely et al. (2020) and the newly generated DNA sequences were deposited in GenBank

(Appendix 1). For the phylogenetic analysis we used sequences of two mitochondrial ribosomal genes (*12S* and *16S*rRNA) and one nuclear gene (*POMC*) from 36 individuals of 28 species corresponding to 27 different localities from Colombia, Ecuador, Peru, and Venezuela (Appendix 1). We used all the GenBank-available sequences for *Centrolene* and ten new sequences (for two species) generated by our study. As outgroups, we used all the available sequences of *Nymphargus*, as well as sequences of *Chimerella mariaelenae* (Cisneros-Heredia & McDiarmid, 2006), *Espadarana callistomma* (Guayasamin & Trueb, 2007), *Cochranella mache* Guayasamin & Bonaccorso, 2004, *Teratohyla midas* (Lynch & Duellman, 1973), *Sachatamia punctulata* (Ruiz-Carranza & Lynch, 1995a), *Rulyrana flavopunctata* (Lynch & Duellman, 1973), *Vitreorana helenae* (Ayarzagüena, 1992), *Celsiella vozmedianoii* (Ayarzagüena & Señaris, 1997), *Hyalinobatrachium aureoguttatum* (Barrera-Rodríguez & Ruiz-Carranza, 1989), and *Ikakogi tayrona* (Ruiz-Carranza & Lynch, 1991b). The tree was rooted with *Allophryne ruthveni* Gaige, 1926.

The sequences were edited, assembled, and aligned (MAFFT algorithm with the G-INS-i iterative refinement method; Katoh and Standley 2013) using the program Geneious Prime (Biomatters Ltd.). The edited alignments of *12S*, *16S* and *POMC* sequences were visually inspected to correct alignment errors in PhyDE (Müller et al. 2010), concatenated into a single matrix, and then used for the phylogenetic analyses. The analyses were based on a 2457 bp dataset (961 bp for *12S*, 895 bp for *16S*, and 601 bp for *POMC*). The aligned and concatenated matrix is available at <https://doi.org/10.5281/zenodo.7557286>.

We follow the glassfrog taxonomy proposed by Guayasamin et al. (2009). Phylogenetic relationships were inferred using both Maximum Likelihood (ML) and Bayesian Inference (BI). We used PartitionFinder v. 2.1.1 (Lanfear et al. 2017) to select the best partition scheme with the corrected Akaike Information Criterion (AICc) as a model of selection. PartitionFinder identified three partition schemes (best model in parentheses): *12S* and *16S* (GTR+I+G), *POMC* 1<sup>st</sup> position (TRN+G), and *POMC* 2<sup>nd</sup> and 3<sup>rd</sup> position (TRN+I+G). ML analyses were conducted in GARLI v. 2.1 (Zwickl 2006) performing 1000 tree searches (four independent searches, two with the “streefname” set to random and two set to stepwise, with 250 replicates each) and node support was assessed with 1000 bootstrap replicates. BI analysis was implemented in MrBayes 3.2.6 (Ronquist et al. 2012), the Markov chain Monte Carlo runs being performed twice, independently, for 70 million generations, with trees sampled every 1000 generations until convergence ( $p < 0.001$ ) and consensus trees were summarized after discarding the initial 25% as burn-in. More details about how tree searches were performed are presented in Székely et al. (2020). The phylograms were edited with FigTree (Rambaut 2014).

A priori, we deemed that a tree node had “strong support” when its bootstrap value was  $> 75$  and its Bayesian posterior probability was  $> 0.95$ , “moderate support” for 50–75 and 0.90–0.95, and “weak support” or non-resolved for values lower than 50 and 0.90, respectively (Vogel et al. 2020). Uncorrected genetic  $p$ -distances were calculated for *16S* with MEGA6 (Tamura et al. 2013) and are presented in Suppl. material 1.

## Bioacoustic analysis

We analyzed advertisement and courtship calls recorded in the field and in the laboratory. The calls were recorded in the field using an Olympus LS-11 Linear PCM Recorder and a RØDE NTG2 condenser shotgun microphone; in the laboratory we used a Tascam DR-100 MKIII Recorder with incorporated microphone. All recordings were made at 44.1 kHz sampling frequency and 16-bit resolution, in WAV file format. Air temperature and humidity were measured with a Lascar Electronics, model EL-USB-2-LCD data logger (accuracy:  $\pm 0.5$  °C;  $\pm 5\%$ ). All analyzed call recordings are deposited in original form, full length at Fonoteca UTPL (record IDs are provided in Suppl. material 2). Acoustic analysis was conducted using Raven Pro 1.6 (K. Lisa Yang Center for Conservation Bioacoustics at the Cornell Lab of Ornithology). We measured the temporal parameters from the oscillograms and the spectral parameters from spectrograms obtained with the Hanning window function, DFT: 512 samples, 3 dB filter bandwidth: 124 Hz, and a 50% overlap (Székely et al. 2020).

The terminology and procedures for measuring call parameters follow Cocroft and Ryan (1995), Toledo et al. (2015) and Köhler et al. (2017), with a call-centered approach to distinguish between a call and a note (sensu Köhler et al. 2017). The following temporal and spectral parameters were measured and analyzed: (1) call duration: time from the beginning to the end of a call (for both single-note and multi-note calls); in the case of single-note calls this is the same as a note duration; (2) inter-call interval: the interval between two consecutive calls, measured from the end of one call to the beginning of the consecutive call (only for multi-note calls); (3) call rate: number of calls/minute, measured as the time between the beginning of the first call and the beginning of the last call (only for multi-note calls); (4) pulse duration: time measured from one amplitude minimum to the next amplitude minimum of a pulse; (5) pulse rate: number of pulses/second, measured as the time between the beginning of the first pulse and the beginning of the last pulse; (6) dominant frequency: the frequency containing the highest sound energy, measured along the entire call; and (7) the 90% bandwidth, reported as frequency 5% and frequency 95%, or the minimum and maximum frequencies, excluding the 5% below and above the total energy in the selected call (Székely et al. 2020).

## Results

### Phylogeny

The Bayesian and Maximum likelihood phylogenetic trees showed very similar topologies, with minor differences in the position of some of the unresolved branches, mostly with stronger BI support (Fig. 1). We recovered *Centrolene* as monophyletic,

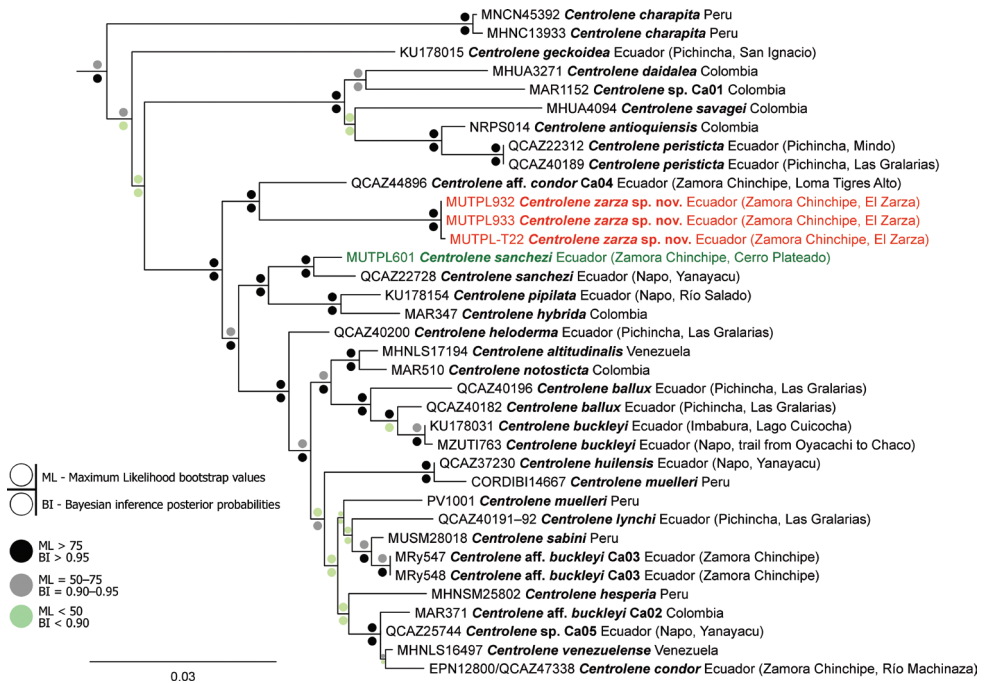


**Figure 1.** Maximum likelihood phylogram of *Centrolene*. The analysis is based on 2457 base pairs of concatenated mitochondrial DNA from *12S* and *16S*, and nuclear DNA from *POMC* gene fragments. Outgroup is not shown; the tree was rooted with *Allophryne ruthveni*. In red, the new species and in green a sequence newly generated by the present study. The catalog number, species name, country, and in the case of Ecuadorian species province and short locality names, are shown next to each terminal (associated data are listed in Appendix 1).

with strong support in the BI (posterior probabilities = 0.99), but with only moderate support in the ML analysis (bootstrap values = 65.4). Overall, the phylogenetic tree of our analysis showed the same topology as the last one constructed for the genus by Guayasamin et al. (2020), but with differences in the position of *C. charapita*, *C. geckoidea* Jiménez de la Espada, 1872 and of several unresolved branches. These differences are most likely a consequence of the different gene sampling scheme, as we used only three genes for our analysis.

The new species is closely related to an undescribed species, the candidate species Ca04 from Guayasamin et al. (2020) identified in their tree as *Centrolene aff. condor*. These two are the sister group of a branch that includes 15 species and three candidate new species and are part of a strongly supported clade (bootstrap values = 94.7; posterior probabilities = 1) that contains almost 3/4 of all the *Centrolene* species (Fig. 1). Uncorrected *p*-genetic distances for the gene *16S* between the new species and *Centrolene aff. condor* range from 3.4% to 3.6% and the other members of the genus from 4.0% to 9.9% (Suppl. material 1).

## Taxonomy

**Class Amphibia Blainville, 1816**

**Order Anura Duméril, 1805**

**Superfamily Centrolenoidea Taylor, 1951**

**Family Centrolenidae Taylor, 1951**

**Subfamily Centroleninae Taylor, 1951**

**Genus *Centrolene* Jiménez de la Espada, 1872**

***Centrolene zarza* sp. nov.**

<https://zoobank.org/BE900409-8243-4494-8B40-FE76C52BC571>

Figs 2–9

Common English name: Zarza Glassfrog

Common Spanish name: Rana de cristal del Zarza

**Etymology.** The specific name *zarza* is a noun in apposition and refers to the species' type locality: Refugio de Vida Silvestre El Zarza. This relatively small wildlife refuge conserves an impressive biodiversity with countless species of plants and birds, more than 50 species of amphibians and reptiles and several emblematic mammals, like the Amazonian tapir, jaguar, oncilla or the spectacled bear. It is surrounded by active mining concessions and thus fulfills an important role as a conservation island for the region, with an urgent need to expand connectivity between the reserve and neighboring conservation areas.

**Type material. *Holotype.*** MUTPL 932 (field no. SC 425; Figs 2, 3, 5A), an adult female from Ecuador, Zamora Chinchipe Province, Refugio de Vida Silvestre El Zarza, quebrada “Las Mariposas” (3.8341°S, 78.5458°W; datum WGS84), 1434 m a.s.l., collected by Joselyn Vinueza, Santiago Hualpa-Vega, María Córdova-Díaz, Daniel Hualpa-Vega, Angel Hualpa, Dalton Morocho, Luis León, and Ramiro Sarango on 10 October 2020.

***Paratypes.*** (1 female, 5 males). MUTPL 933 (field no. SC 428; Fig. 6C, D) an adult male from Refugio de Vida Silvestre El Zarza, quebrada “Las Mariposas” (3.8371°S, 78.5424°W), 1461 m a.s.l. collected by Luis León, Dalton Morocho, Ramiro Sarango, Santiago Hualpa-Vega, María Córdova-Díaz, Daniel Hualpa-Vega, Angel Hualpa and Joselyn Vinueza on 10 October 2020; MUTPL 1022 (field no. SC 435; Fig. 6E, F), MUTPL 1023 (field no. SC 436; Figs 4, 5B), and MUTPL 1024 (field no. SC 437), adult males from Refugio de Vida Silvestre El Zarza, quebrada “Las Mariposas” (3.8376°S, 78.5421°W), 1469 m a.s.l., collected by Santiago Hualpa-Vega, María Córdova-Díaz, Daniel Hualpa-Vega, Camilo López, Dalton Morocho, Dalton Bustán and Luis León on 24 January 2021; MUTPL 1050 (field no. SC 443) adult male and MUTPL 1051 (field no. SC 444; Fig. 6A, B) adult female from Refugio de Vida Silvestre El Zarza, quebrada “Las Mariposas” (3.8373°S, 78.5423°W), 1471 m a.s.l., collected by Santiago Hualpa-Vega, María Córdova-Díaz, Daniel Hualpa-Vega, Joselyn Vinueza, Luis León, Dalton Morocho and Álex Armijos on 13 March 2021.

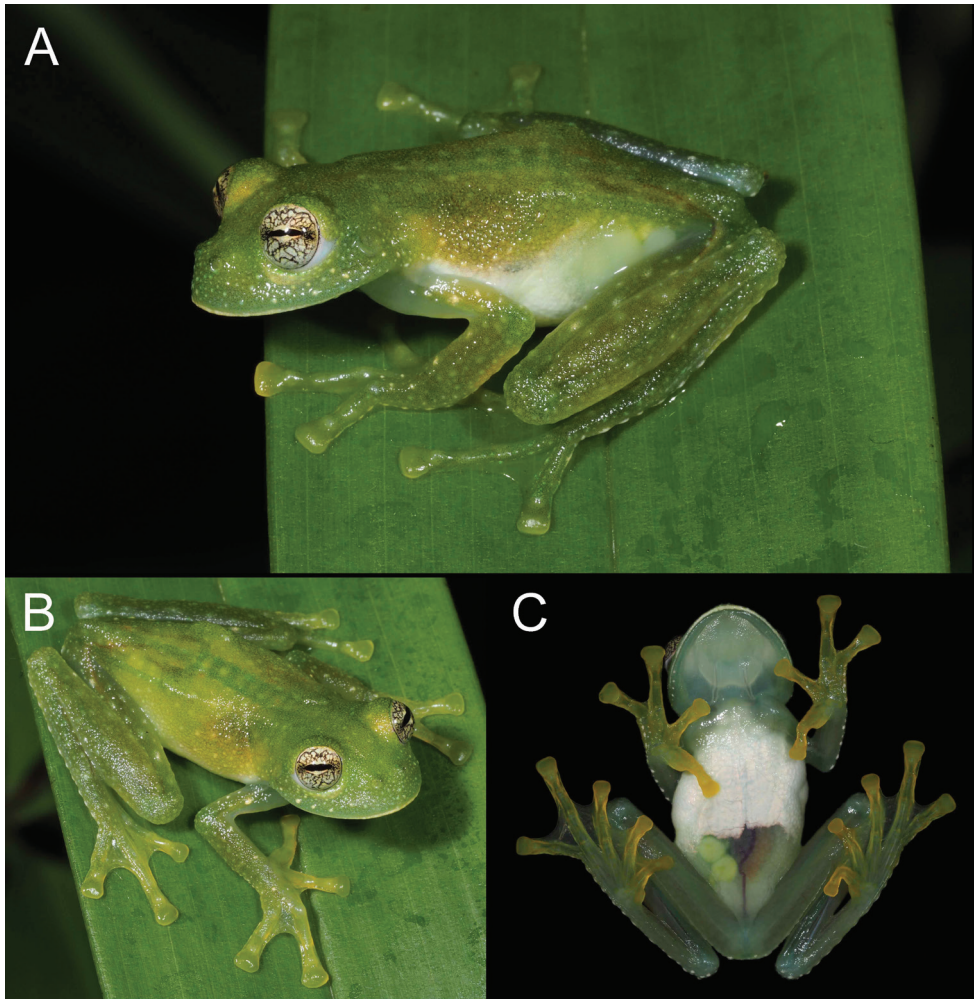


**Figure 2.** Holotype of *Centrolene zarza* sp. nov. (MUTPL 932, adult female), SVL 25.5 mm, in life **A** lateral view **B** dorsolateral view **C** ventral view.

**Diagnosis.** We assign this species to *Centrolene* based on phylogenetic evidence (Fig. 1) and on the general morphological similarity to other members of the genus (presence of humeral spines in males, liver divided into lobes and the hepatic peritoneum lacking an iridophore layer, and green bones in life). *Centrolene zarza* has the following combination of characters: (1) dentigerous processes of vomers ovoid, in transverse row between the choanae, separated medially by distance slightly lower than the width of processes; each process bearing 3–5 teeth; (2) snout rounded in dorsal view, sloping in profile; nostrils slightly elevated, producing depression in the internarial area; canthus rostralis not evident in dorsal view, rounded in cross section; (3) tympanic annulus and tympanic membrane evident but with coloration similar to that of surrounding skin;

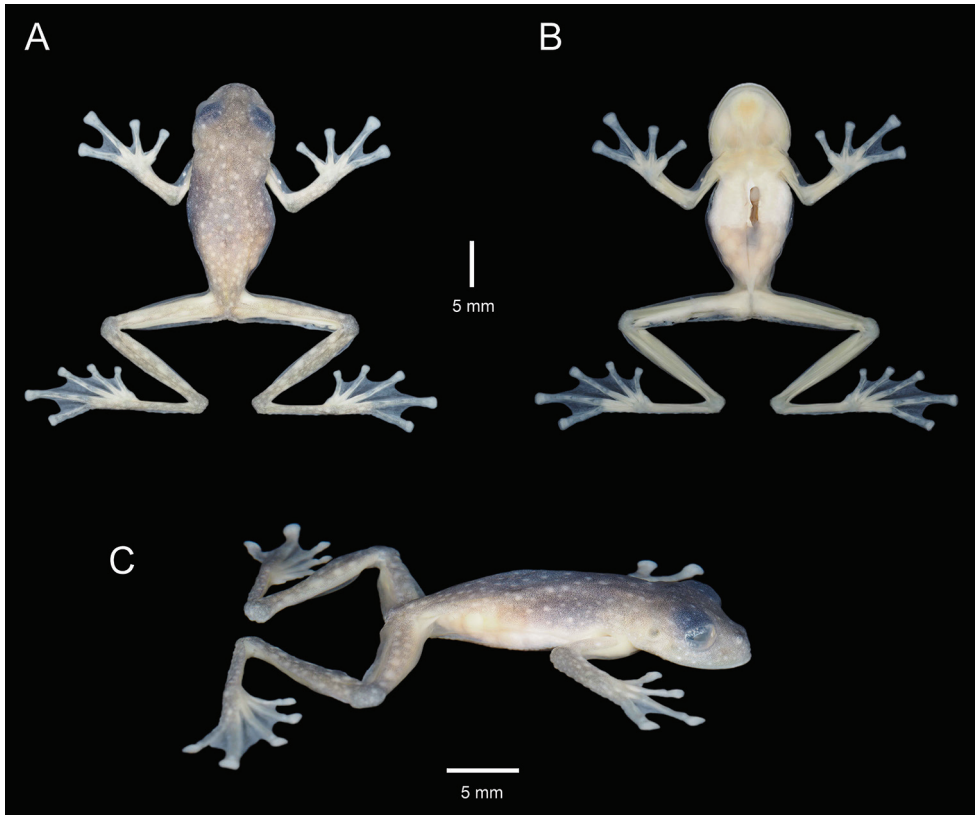


**Figure 3.** Holotype of *Centrolene zarza* sp. nov. (MUTPL 932, adult female) in preservative **A** dorsal view **B** ventral view **C** lateral view.

tympanum large, its diameter ~ 46% of eye diameter; weak supratympanic fold present, slightly concealing the upper margin of the tympanum; (4) dorsal skin shagreen with elevated, and some enameled, warts corresponding to white spots; (5) ventral skin coarsely areolate; ventral surfaces of thighs below vent with a pair of large, round, flat tubercles, flat tubercles (subcloacal warts); cloacal region bordered ventrally by many enameled, white, warts; (6) half or more than half of the upper parietal peritoneum covered by iridophores (condition P3); iridophores absent on all visceral peritonea, including the pericardium (condition V0); (7) liver lobed, lacking iridophores (condition H0); (8) adult males with small projecting humeral spines, round vocal slits and large subgular vocal sac; (9) webbing absent between Fingers I and II, basal between II and III, moderate between outer fingers: III2<sup>+</sup>–2IV; (10) webbing between toes moderate: I1<sup>-</sup>–2III1<sup>-</sup>–2III1<sup>-</sup>–2IV2–1<sup>+</sup>V; (11) outer edge of forearms and tarsus with row of enameled warts that often continue into the external edges of Finger IV and/or Toe V; fingers and toes with broad lateral fringes; (12) unpigmented Type I nuptial pads present in males; concealed prepollex; (13) Finger I shorter than Finger II; (14) diameter of eye ~ 2× wider than disc on Finger III; (15) in life, dorsum light green with many white

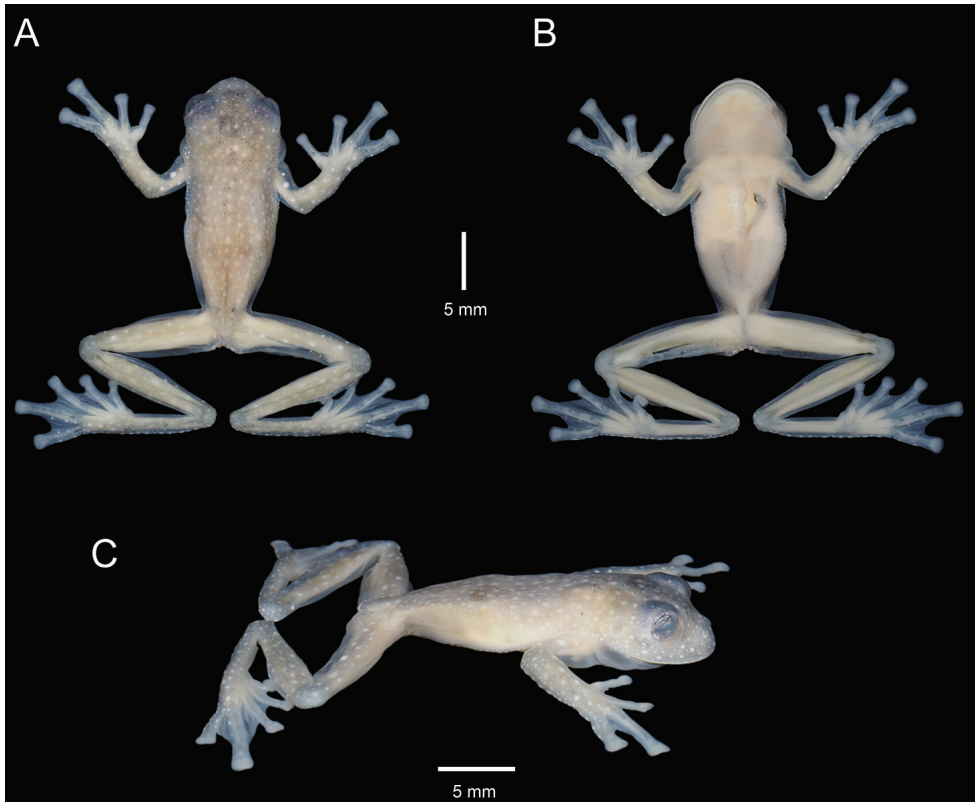


**Figure 4.** Paratype of *Centrolene zarza* sp. nov. (MUTPL 1023, adult male), SVL 23.2 mm, in preservative **A** dorsal view **B** ventral view **C** lateral view.

or whitish, elevated, spots and flecks of various sizes; bones green; (16) in preservative, dorsal surfaces greyish with white spots; (17) in life, iris white or yellowish white with thick and thin black reticulations; rounded points on the upper and lower side of the iris and no circumpupillary ring; (18) fingers and toes yellowish, usually lacking melanophores from the dorsal surfaces, except for Finger IV and Toes IV and V; (19) males call from the upper surfaces of leaves; advertisement call consisting of a high pitched, pulsed, single note, with every call/note featuring three clearly distinguishable pulses and a mean dominant frequency of 5309.8 Hz; courtship call composed by multi-noted, pulsed calls of usually five notes/call and a mean dominant frequency of 5127.4 Hz; (20) fighting behavior unknown; (21) egg clutches attached to the upper side of leaves; clutch size of 13–33 embryos ( $n = 2$ ); probably without parental care; (22) tadpoles with elongated, oval-depressed body; sinistral spiracle; vent tube situated medially, caudal and with dextral opening; tail 2.4× the length of the body; labial tooth row formula 0/2(1) in Gosner 26 but without tooth rows in Gosner 31; mostly pinkish coloration; (23) medium body size (sensu Guayasamin et al. 2020), SVL 25.5–27.0 mm in adult females ( $n = 2$ ) and 23.2–26.2 mm in adult males ( $24.1 \pm 1.21$ ,  $n = 5$ ).

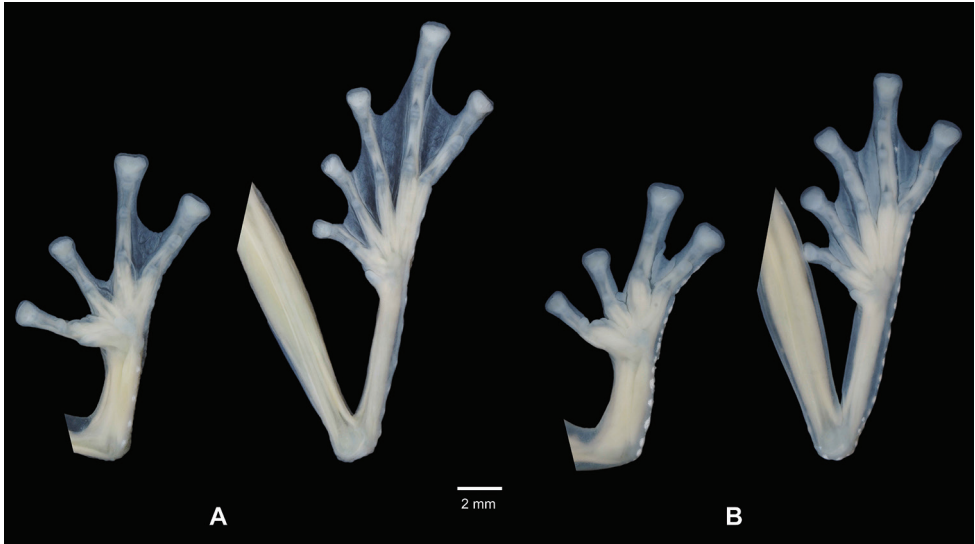


**Figure 5.** Palmar view of hand and plantar view of foot of **A** holotype of *Centrolene zarza* sp. nov. (MUTPL 932, adult female) and **B** paratype (MUTPL 1023, adult male) in preservative.

**Comparisons with similar species.** Due to its unique combination of characters, *Centrolene zarza* is easily distinguished from all other glassfrog species. The few congener species that generally resemble *C. zarza*, specifically that have green dorsum with white spots and/or flecks, are as follows: *C. condor*, has a very different general habitus with a more robust body, smaller eyes, less evident tympanum and dark bluish-black/brown flecks and punctuations along with the white flecks (vs. slender body, larger eyes, evident tympanic annulus and tympanic membrane and only white spots and/or flecks in *C. zarza*); *C. pipilata*, has a dorsum with yellowish-white flecks and diffuse dark green/black marks, and a distinct prepollex (vs. only white spots and/or flecks and concealed prepollex); *C. sanchezi*, has a smaller body size and the presence of white warts in an area that extends from below the eye to the insertion of the arm (vs. absence of the white warts); specimens of the *C. buckleyi* species complex that have white spots have less evident markings, dentigerous processes of vomers without teeth, less evident tympanum, condition V1 of the visceral peritonea and also live at much higher elevations of 2050–3070 m (vs. dentigerous processes of vomers with teeth and condition V0 of the visceral peritonea).

Some congener species have a similar habitus, but live in other countries: *C. solitaria* (one of the few species of *Centrolene* for which we lack molecular data) is endemic to the Andes of Colombia and has green spots along with the white flecks, iridophores covering parts of the gastrointestinal peritoneum and the males lack humeral spines (vs. only white spots and/or flecks, iridophores absent on all visceral peritonea and males with humeral spines); *C. altitudinalis* (Rivero, 1968) is endemic to Andes of Mérida State from Venezuela (Barrio-Amorós et al. 2019), and has golden brown iris

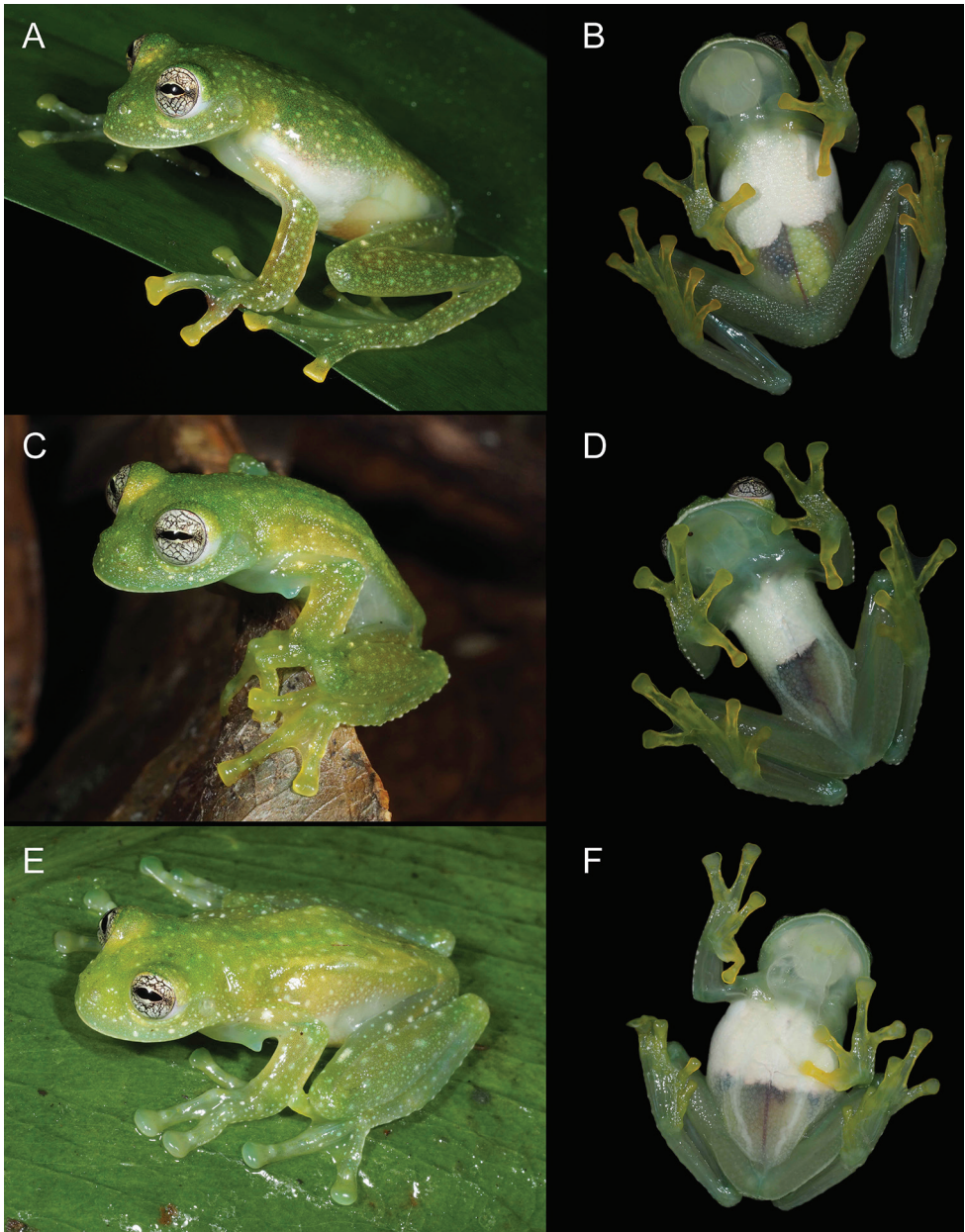


**Figure 6.** Morphological variation of *Centrolene zarza* sp. nov. in live specimens **A, B** female, paratype (MUTPL 1051) **C, D** male, paratype (MUTPL 933) **E, F** male, paratype (MUTPL 1022).

and lacks teeth on the dentigerous processes of vomers (vs. iris white or yellowish white with thick and thin black reticulations and dentigerous processes of vomers with teeth); *C. daidalea* (Ruiz-Carranza and Lynch 1991c), is reported from Colombia and

Venezuela, and has black spots along with the white ones, iridophores covering parts of the gastrointestinal peritoneum and the males lack humeral spines (vs. only white spots, iridophores absent on all visceral peritonea and males with humeral spines).

Somewhat similar species of the genus which live on the Pacific versant of the Ecuadorian Andes are *C. ballux* (Duellman & Burrowes, 1989), that has a minute body size, a distinct prepollex and lacks teeth on the dentigerous processes of vomers (vs. medium body size, concealed prepollex and dentigerous processes of vomers with teeth), and *C. heloderma* (Duellman, 1981) which has a unique pustular dorsum, condition V1 of the visceral peritonea and vomers lacking teeth (vs. shagreen dorsum with elevated warts, condition V0 of the visceral peritonea and vomers with teeth). Finally, species from other genera that superficially resemble *C. zarza* are *Cochranella resplendens* Lynch & Duellman, 1973, which has iridophores in pericardium and peritonea covering intestines and stomach and the males lack humeral spines (vs. iridophores absent on all visceral peritonea and males with humeral spines) and *Nymphargus posadae* (Ruiz-Carranza & Lynch, 1995a) that has almost indistinguishable tympanum, condition P2 and V1, and the males lack humeral spines (vs. evident tympanum, condition P3 and V0, and males with humeral spines).

**Description of the holotype.** Adult female (MUTPL 932; Figs 2, 3, 5A), medium sized, with many large and small yellowish white eggs. Head slightly narrower than the body, wider than long, head length 91% of head width, head width 34% of SVL, head length 31% of SVL; snout relatively short, snout to eye distance 13% of SVL, eye-nostril distance 24% of head length; snout rounded in dorsal view, sloping in profile; nostrils slightly elevated producing a shallow depression in the internarial area; canthus rostralis indistinct in dorsal view, rounded in cross section; loreal region slightly concave; lips non-flared; moderate sized eyes (sensu Guayasamin et al. 2020), eye diameter 11% of SVL, 34% of head length; eye-nostril distance 69% of eye diameter; eye diameter 93% of IOD; eyes directed anterolaterally at  $\sim 40^\circ$  from midline, slightly visible from below; upper eyelid width 85% of IOD; tympanic annulus and tympanic membrane evident, but the membrane with coloration similar to that of surrounding skin; tympanum oriented slightly dorsolaterally; tympanum large (sensu Guayasamin et al. 2020), its diameter  $\sim 46\%$  of eye diameter; weak supratympanic fold present, slightly concealing the upper margin of the tympanum; choanae large, ovoid, not concealed by palatal shelf of maxillary arch, closer to the distal margin of the dentigerous processes of vomers than to the margin of mouth; dentigerous processes of vomers ovoid, in transverse row between the choanae, separated medially by distance slightly lower than the width of processes; each process bearing three teeth; tongue just slightly longer as wide, not notched posteriorly, and only  $\sim 1/5$  of posterior part not adherent to the floor of mouth.

Skin of dorsal surfaces shagreen with elevated, and some enameled, warts corresponding to white spots; throat smooth; ventral skin coarsely areolate; ventral surfaces of thighs below vent with a pair of large, round, flat tubercles (subcloacal warts); cloacal opening directed posteriorly at upper level of thighs, no distinct cloacal sheath; cloacal region bordered ventrally by many enameled (white) warts.

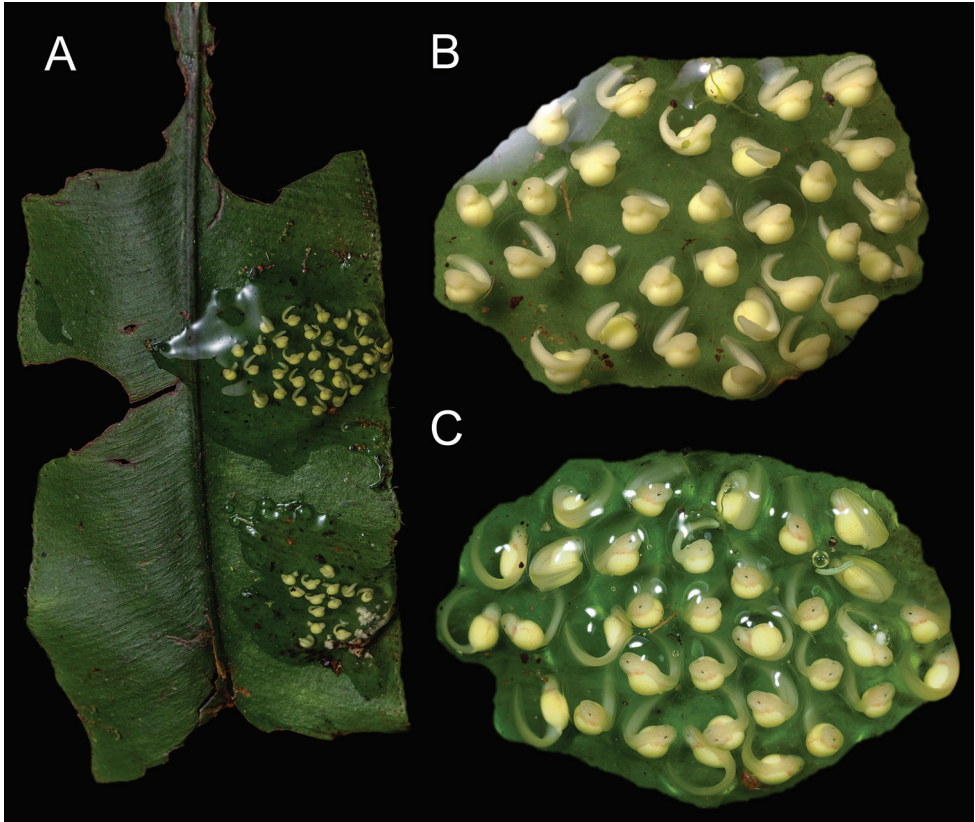


**Figure 7.** Egg-clutches of *Centrolene zarza* sp. nov. collected from the type locality (MUTPL-T22) **A** the egg-clutches attached to a leaf (10 June 2021) **B** hatchlings (sensu McDiarmid and Altig 1999) in stage Gosner 20 (10 June 2021) **C** hatchlings in stage Gosner 22 (13 June 2021).

Upper arm thin, forearm somewhat robust; outer edge of forearms with row of enameled warts that continue into the external edges of Finger IV; hand length 34% of SVL; palmar tubercle large, elliptical; thenar tubercle large, ovoid; subarticular tubercles prominent, round and round in section; numerous round palmar supernumerary tubercles present, much smaller than subarticular tubercles; relative lengths of fingers I < II < IV < III; concealed prepollex; fingers with broad lateral fringes; webbing absent between Fingers I and II, basal between II and III, moderate between outer fingers: III<sub>2</sub><sup>+</sup>–2IV (Fig. 5A); bulla absent; discs on fingers expanded, truncate; disc pads nearly triangular.

Hindlimbs long, slender; femur length 55% of SVL; tibia length 57% of SVL; foot length 48% of SVL; outer edge of tarsus with row of enameled warts that often continue into the external edges of Toe V; inner edge of tarsus bearing a long fold; inner metatarsal tubercle large, elliptical; outer metatarsal tubercle indistinct; subarticular tubercles rounded and flat; plantar supernumerary tubercles inconspicuous; relative length of toes I < II < III < V < IV; toes with broad lateral fringes; webbing between toes

moderate: I1<sup>-</sup>-2III1<sup>-</sup>-2III1<sup>-</sup>-2IV2-1<sup>+</sup>V (Fig. 5A); discs on toes expanded, truncate, lacking papillae; disc pads nearly triangular.

**Coloration of holotype.** In life (Fig. 2): dorsum light green, head and dorsal surfaces of arms and of hindlimbs darker green, with many white or whitish, elevated, spots and flecks of various sizes. The green vertebral column, sacrum, ileum, and urostyle visible through the skin (Fig. 2B). Flanks white or transparent (Fig. 2A); venter with more than half of the upper parietal peritoneum covered by white iridophores; lower parietal peritoneum transparent with part of the large intestine, urinary bladder, and some large yellowish white eggs visible (Fig. 2C); ventral vein red (Fig. 2C). Fingers and toes yellowish (more evident ventrally; Fig. 2C) lacking melanophores from the dorsal surfaces, except for Fingers III and IV and Toes IV and V. Iris yellowish white with thick and thin black reticulations and no circumpupillary ring. Bones green.

In preservative (Fig. 3): dorsal surfaces greyish with white spots; vertebral column, sacrum, ileum and urostyle no longer visible through the skin (Fig. 3A). Throat yellowish, upper parietal peritoneum on the venter white, lower part transparent (Fig. 3B). Melanophores absent from hands and feet, except few present on dorsal surfaces of Finger III and many on Finger IV and Toes IV and V.

**Measurements of holotype (in mm).** SVL 25.5; HW 8.7; HL 7.9; IOD 2.9; IND 2.1; EW 2.5; ED 2.7; EN 1.9; snout to eye distance 3.4; TD 1.4; FL 14.1; TL 14.5; FoL 12.2; HaL 8.6; 3DW 1.6.

**Body mass of holotype.** 1.05 g.

**Variation.** Morphometric variation is shown in Table 1. The females are larger, with slender bodies and longer limbs (Figs 3, 6A, B). The males have more robust bodies, slightly thicker forearms and have humeral spines (Figs 4, 6C–F). One male (MUTPL 1022, Fig. 6E) had a slightly little lighter dorsal coloration, but overall, no significant variation in dorsal coloration, iris coloration or pattern of the spots or flecks was observed between the encountered individuals. The green bones of limbs and vertebral column were visible dorsally, through the skin, in all specimens.

**Eggs and tadpoles.** Two egg clutches in stage Gosner 19 (Fig. 7) were collected from the type locality (3.8379°S, 78.5418°W; 1460 m a.s.l.) on 9 June 2021 (MUTPL-T22). Both egg clutches were attached to the upper side of a leaf at ~ 3 m above the stream. The clutches contained 13 and 33 embryos; no adults were observed guarding the eggs or in the near proximity. The tadpoles hatched in the laboratory after 5 days and survived for more than 6 months, until 2 January 2022. They developed well in the beginning, but halted their development at Gosner stage 31 (ca. 20 November), and unfortunately started to die in January 2022 without completing their metamorphosis. It is possible that the tadpoles died due to inadequate rearing conditions, or their death was produced by chytridiomycosis (see the discussion section).

The tadpoles of *C. zarza* (Fig. 8) belong to Type IV tadpole of Orton (1953), and the exotroph, lotic, and burrower ecomorphological guild of McDiarmid and Altig (1999). The following description is based on tadpoles at Gosner stages 26 and 31 (from the MUTPL-T22 series). For the tadpoles in Gosner stage 31 the total length was 26.9–34.7 mm ( $31.9 \pm 2.67$ ,  $n = 6$ ) and the body length was 8.2–10.4 mm ( $9.5 \pm 0.73$ ,  $n = 6$ ), body length being ~ 30% of total length.



**Figure 8.** Hatchlings (sensu McDiarmid and Altig 1999) and tadpoles of *Centrolene zarza* sp. nov. (MUTPL-T22) **A** Gosner stage 24 (26 June 2021) **B** Gosner stage 25 (5 August 2021) **C** Gosner stage 26 (23 August 2021) **D** Gosner stage 31 (20 November 2021).

Body elongated, oval-depressed, wider than high; snout rounded in dorsal view and sloped and rounded in lateral view. Eyes located on dorsal surface of head and C-shaped (at least until Gosner stage 31). Nostrils positioned dorsally, protruding, with very small narial apertures oriented anteriorly. Spiracle short, single, sinistral, located at the posterolateral region of the body; spiracular opening slightly below body axis, oriented posteriorly and upwards (dorsoposterior orientation). Vent tube situated medially, short, attached to the ventral fin (caudal), with a dextral opening directed postero-ventrally. Tail long,  $\sim 2.4\times$  the length of the body, with subacute tip. Dorsal fin originating at ca. mid-length of tail; myotomes of tail musculature weakly visible in the first half of tail length.

**Table 1.** Morphometric characters of *Centrolene zarza* sp. nov. Body mass (in grams), measurements (in mm) and morphological proportions (in percentages) of adult females and males; values are given as mean  $\pm$  SD (range). Female body mass includes eggs.

Character	Females (n = 2)	Males (n = 5)
Body mass (BM)	1.21 (1.05–1.37)	0.89 $\pm$ 0.08 (0.84–1.02)
Snout-vent length (SVL)	26.3 (25.5–27.0)	24.1 $\pm$ 1.21 (23.2–26.2)
Head width (HW)	9.1 (8.7–9.5)	8.4 $\pm$ 0.34 (7.9–8.7)
Head length (HL)	8.1 (7.9–8.4)	6.9 $\pm$ 0.43 (6.6–7.6)
Interorbital distance (IOD)	2.8 (2.8–2.9)	2.8 $\pm$ 0.13 (2.6–2.9)
Internarial distance (IND)	2.2 (2.1–2.2)	2.0 $\pm$ 0.09 (1.9–2.1)
Upper eyelid width (EW)	2.3 (2.1–2.5)	2.2 $\pm$ 0.24 (1.9–2.6)
Eye diameter (ED)	2.8 (2.7–3.0)	2.7 $\pm$ 0.18 (2.5–2.9)
Eye-nostril distance (EN)	2.0 (1.9–2.2)	1.8 $\pm$ 0.22 (1.6–2.1)
Tympanum diameter (TD)	1.3 (1.3–1.4)	1.2 $\pm$ 0.10 (1.2–1.4)
Femur length (FL)	14.8 (14.1–15.6)	13.2 $\pm$ 0.54 (12.7–14.0)
Tibia length (TL)	15.4 (14.5–16.2)	13.9 $\pm$ 0.49 (13.2–14.6)
Foot length (FoL)	12.5 (12.2–12.8)	11.5 $\pm$ 0.77 (10.6–12.7)
Hand length (HaL)	9.0 (8.6–9.5)	8.3 $\pm$ 0.31 (8.0–8.8)
Width of disc on Finger III (3DW)	1.6 (1.6–1.7)	1.4 $\pm$ 0.20 (1.1–1.6)
HW/SVL	33.9–35.0	32.6–36.9
HL/SVL	30.8–30.9	26.2–32.8
HL/HW	88.4–90.8	77.2–88.9
EN/HW	21.4–22.8	18.1–25.0
EN/HL	23.6–25.7	20.4–31.1
EN/IOD	63.8–78.2	55.4–71.9
ED/HW	31.2	31.6–33.3
ED/HL	34.4–35.3	37.5–43.2
ED/IOD	93.1–107.3	91.2–107.5
EN/ED	68.5–72.9	54.5–78.8
TD/ED	45.8–46.3	40.4–50.9
3DW/ED	57.4–57.6	44.0–58.2
EW/IOD	74.5–84.5	66.7–96.2
IND/IOD	72.4–80.0	64.9–76.9
IOD/HW	29.1–33.5	31.0–34.8
IOD/HL	32.9–36.9	36.8–43.2
FL/SVL	55.1–57.8	53.5–58.2
TL/SVL	56.9–60.0	55.6–60.6
FoL/SVL	47.4–47.8	45.7–50.6
HaL/SVL	33.7–35.0	33.0–35.8

Oral disc large (oral disc width  $\sim$  65% of body width), not emarginated, located near tip of snout, directed anteroventrally, protruding ventrally but not laterally (Fig. 8), beyond body. Marginal papillae uniserial, large, distributed around oral disc ( $\sim$  43–47 papillae); large part of the anterior (upper) margin of labium lacking papillae and instead having an involuted fold with smooth surface, but with a row of submarginal flattened papillae-like ridge in the proximity of the upper jaw sheath (Fig. 9). Upper jaw sheath broadly arched, slender (with less than half depth of upper jaw cartilages keratinized) and with serrated edge; lower jaw sheath slightly U-shaped, slender (with less than half depth of lower jaw cartilages keratinized) and with serrated edge (Fig. 9). Labial tooth row formula (LTRF) 0/2(1), P-1 with medial gap, and with a row

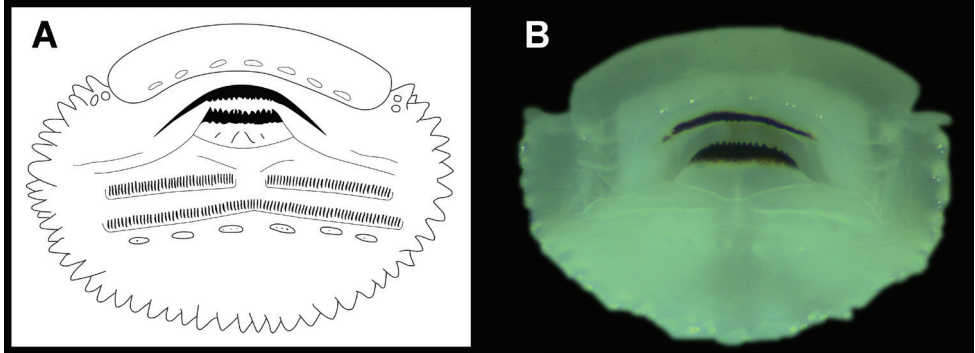


**Figure 9.** Oral apparatus of the tadpoles of *Centrolene zarza* sp. nov. (MUTPL-T22) **A** Gosner stage 26 **B** Gosner stage 31.

of submarginal flattened papillae-like ridge (composed by seven or eight papillae) on the posterior (lower) labium in Gosner stage 26 (Fig. 9A). However, in Gosner stage 31, all the tooth rows were lost and only the tooth (dermal) ridges were visible beside the submarginal ridge of papillae (Fig. 9B). It is not clear if the loss of the tooth rows is a natural process throughout the metamorphosis or it is caused by disease or other factors (see the discussion section).

General coloration varied in the different developmental stages (Fig. 8). Hatchlings (sensu McDiarmid and Altig 1999) in Gosner stage 24 were slightly pinkish but with a special green coloration of the abdomen (Fig. 8A). The tadpoles had a more evident pinkish coloration in Gosner stage 25 (Fig. 8B) and became almost red by the Gosner stage 26 (Fig. 8C). However, after a couple of months, by the Gosner stage 31, they had lost the reddish coloration and had the body just slightly pink and the tail almost brown (Fig. 8D). We do not know if this discoloration was a natural developmental process or the tadpoles were actually suffering from a disease or had other problems.

**Vocalizations.** On 3 September 2022 we recorded the calls of several males from the type locality (Refugio de Vida Silvestre El Zarza, quebrada “Las Mariposas”, Suppl. material 2). The males were calling (advertisement calls sensu Wells 2007) from above, at several meters high, in the vegetation bordering a small stream. For the description of these calls we used two recordings: FUTPL-A 263 and FUTPL-A 264 (the detailed information of each of the separate recordings is presented in the Suppl. material 2). Because the males were calling out of reach, up in the trees, we were not able to distinguish and pinpoint the calling males and so the recordings contain the calls of several males. Thus, the call description is based on the calls of probably three of the closest calling males. For this reason, we were not able to measure some of the temporal parameters, like the inter-call interval and call rate. We used for the analysis only the calls clearly distinguishable in each of the recordings, which were not overlapped by other calls. The advertisement call of *C. zarza* is characterized by a high pitched, pulsed, single note, with every call/note featuring 3 clearly distinguishable pulses (Fig. 10A–C). The calls had a duration of 0.242–0.318 s ( $0.268 \pm 0.02$ ,  $n = 17$ ), with a pulse du-

ration of 0.072–0.159 s ( $0.089 \pm 0.02$ ,  $n = 51$ ), and an average pulse rate of 11.8 pulses/s. The mean dominant frequency of the calls was 5309.8 Hz, with a mean 90% bandwidth of 5041.3–5487.2 Hz (Suppl. material 2). The fundamental frequency is not recognizable, and no harmonics are visible.

The call of paratype MUTPL 933 (FUTPL-A 261 and FUTPL-A 262) was recorded on 14 October 2020, on the first night that the specimen arrived in the laboratory. The animal was encountered in the type locality on a leaf at a height of 1.5 m near the stream while vocalizing. In laboratory, a recorder was left running all night, in order to record the call. The male was left in the same plastic bag in which it arrived from the field and had in its proximity, in a different bag, a female (the holotype). The male vocalized almost all night, but the call had a different structure from the typical advertisement call heard and recorded in the field (Fig. 10D–F). We identified this call as a courtship call (*sensu* Wells 2007), being composed not only by the single-noted calls, but mainly by multi-noted calls (usually of five notes/call, but up to six notes/call). The notes had the same structure as the single-noted calls, with the typical three pulses. Unfortunately, the pulses are not sufficiently visible in oscillograms or spectrograms in order to allow accurate measurements (Fig. 10D), probably due to the special conditions from the laboratory (echo from the walls, animal in plastic bag, etc.). The multi-noted calls had a duration of 0.581 to 1.905 s ( $1.300 \pm 0.45$ ,  $n = 18$ ), depending on the number of notes/calls. The individual notes had a duration similar to the ones from the single-noted calls of the advertisement calls, just slightly longer: 0.244–0.378 s ( $0.304 \pm 0.03$ ,  $n = 80$ ). The inter-call interval varied from 40.2 to 596.9 s ( $255.5 \pm 171.23$ ,  $n = 18$ ) and the call rate was  $\sim 0.23$  calls/min, or rather,  $\sim 14$  calls/hour (Suppl. material 2). The frequencies were slightly lower than the ones from the advertisement calls, with the mean dominant frequency of 5127.4 Hz, and a mean 90% bandwidth of 4914.7–5411.2 Hz (Suppl. material 2). The fundamental frequency was not recognizable, but 2 to 3 harmonics were visible, although these could be artificially produced by the echo from the walls in the laboratory (Fig. 10E).

It seems that in this species the males emit multi-note courtship calls when they detect the nearby presence of females and are used to interact with them, as in our case, where the male was probably aware of the female's presence. Similar behavior was observed in other glassfrog species (Greer and Wells 1980; Hutter et al. 2013) and it is well documented in various anuran species (see Wells 2007 for a detailed discussion). No multi-note calls were heard or recorded in the field but we did not witness any female-male interactions.

**Distribution.** *Centrolene zarza* is currently known only from Refugio de Vida Silvestre El Zarza, Zamora Chinchipe province, southern Ecuador (Fig. 11). The specimens were encountered at an altitudinal range between 1434 and 1480 m a.s.l. in an evergreen lower montane forest ecosystem.

**Natural history.** This is a (locally) common species in the sense that the species presence was detected (seen or heard), in the proper habitat, in large or moderate numbers, on more than 50% of the sampling days/nights (Székely et al. 2020). All specimens were encountered during the night, on the upper surfaces of leaves of the vegetation bordering two small streams (Fig. 12). Calling males were heard during January, March, June, October, and November, but intense activity (many males calling from

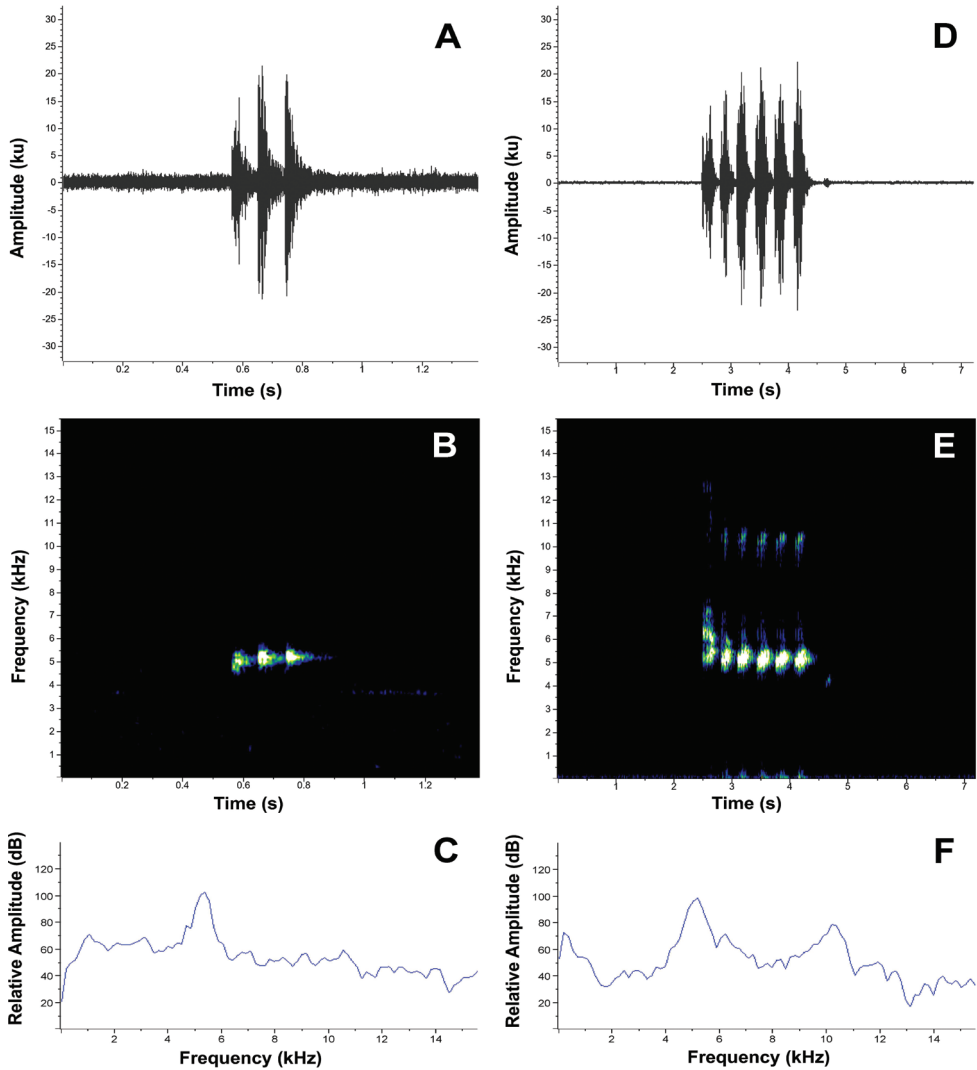


**Figure 10.** Vocalizations in *Centrolene zarza* sp. nov. Visual representation of the advertisement call (FUTPL-A 263; **A–C**) and courtship call (paratype MUTPL 933, FUTPL-A 261; **D–F**) **A** oscilogram of a single-noted call with the 3 pulses **B** spectrogram of a single-noted call **C** power spectrum of a single-noted call **D** oscilogram of a multi-noted call with 6 notes **E** spectrogram of a multi-noted call **F** power spectrum of a multi-noted call.

lower heights, 50 cm to 3 m above the streams) was recorded between October and March. The female paratype MUTPL 1051 was encountered nearby the calling male MUTPL 1050 at ~ 4 m high over the stream. However, no multi-note courtship calls were heard, nor was any direct interaction observed between these individuals. Observed syntopic glassfrog species were mainly *Espadarana audax* (Lynch & Duellman, 1973), in large numbers, but also *Nymphargus posadae*, *Chimerella mariaelenae*, and *Rulyrana mcdiarmidi* (Cisneros-Heredia, Venegas, Rada & Schulte, 2008).

**Conservation status.** *Centrolene zarza* is known, for now, from only two small streams inside the wildlife refuge, in an estimated area of less than 7 km<sup>2</sup>. Although this is a locally common species, which lives inside a nationally protected area, we recommend that *C. zarza* be categorized as Critically Endangered following the B1ab(i,ii,iii)+2ab(i,ii,iii) IUCN criteria (IUCN 2001) because: (1) its Extent of occurrence (EOO) and Area of occupancy (AOO) are estimated to be less than 7 km<sup>2</sup>; (2) it is known from only one locality; and (3) its habitats could be affected in the near future by mining activities (both legal or illegal), as the wildlife refuge is surrounded by active mining concessions.

## Discussion

### The *Centrolene condor* “problem”

The Condor Glassfrog (*C. condor*) was described by Cisneros-Heredia and Morales-Mite in 2008 with one male specimen collected in 2003 and without molecular data (Cisneros-Heredia and Morales-Mite 2008). Unfortunately, since then no additional specimens were encountered or collected from the type locality, Destacamento Militar Cóndor Mirador in the Zamora Chinchipe province (Fig. 11). Thus, the (molecular) identity of this species, and the relationships with its congeners are still unknown. Between March 2008 and July 2012 Ana Almendáriz and her team from Museo de Historia Natural Gustavo Orcés, Escuela Politécnica Nacional (MEPN), conducted several expeditions (as part of the socio-environmental studies of the area needed for a mining company) in the southern sector of the Cordillera del Cóndor, specifically in an area known as Alto Machinaza (Fig. 11; Almendáriz et al. 2014). From Alto Machinaza and nearby areas (such Río Machinaza – Sector Colibrí and Paquisha Alto, Fig. 11) they collected several specimens identified as *C. condor*. With the data collected in these expeditions Ana Almendáriz and Diego Batallas expanded the distribution range of the species with more than 30 km to the south, provided data on its habitat and tadpoles and described the call (Almendáriz and Batallas 2012). These animals are morphologically very similar to *C. condor*, but without molecular confirmation we cannot be sure they are the same species, especially since the same authors noted some small morphological differences compared with the original description. One of these specimens (EPN 12800/QCAZ 47338; the specimen is maintained in the MEPN collection) was sequenced by researchers from QCAZ and it is currently labeled as *C. condor* in the phylogenetical tree of Guayasamin et al. (2020) and our own study (Fig. 1). Another specimen collected from Loma Tigres Alto (Alto Machinaza; Fig. 11) as a tadpole, was sequenced and identified as *Centrolene* aff. *condor* (QCAZ 44896, the candidate species Ca04) in Guayasamin et al. (2020). However, this specimen, which is the sister species of *C. zarza*, is positioned in a different branch of the tree, far from the “*C. condor*” collected from almost the same location (Río Machinaza – Sector Colibrí).

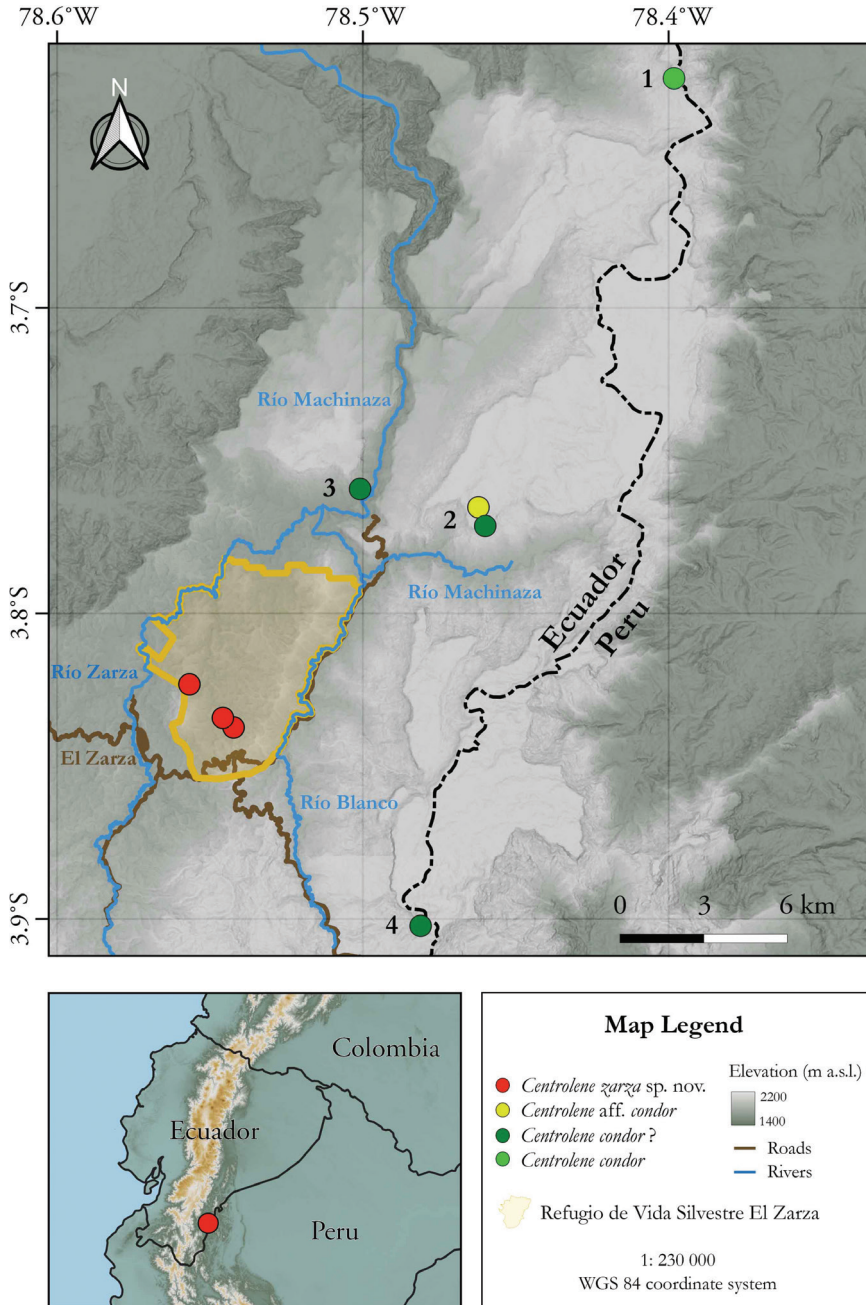


**Figure 11.** Distribution of *Centrolene zarza* sp. nov. Records are based on specimens deposited at the Museo de Zoología, Universidad Técnica Particular de Loja (MUTPL), Museo de Historia Natural Gustavo Orcés, Escuela Politécnica Nacional (MEPN) and Museo de Zoología, Pontificia Universidad Católica del Ecuador (QCAZ). 1. Destacamento Militar Cóndor Mirador, the type locality of *Centrolene condor*. 2. Alto Machinaza, with the two collecting sites, Loma Tigres Alto (yellow dot) and Loma Tigres Bajo (green dot). 3. Río Machinaza – Sector Colibrí. 4. Paquisha Alto.



**Figure 12.** Habitat of *Centrolene zarza* sp. nov. in the type locality. Refugio de Vida Silvestre El Zarza, quebrada “Las Mariposas”.

The fact that *C. zarza* is morphologically different from *C. condor* (see comparisons with similar species section) suggests that the current position of *C. condor* in the phylogenetic tree may be correct and that the specimens from Alto Machinaza and Paquisha Alto are indeed *C. condor* (or at least very similar, closely related species). For this reason, it is imperative that new material is collected from the type locality in order to clarify the exact position of *C. condor*. Unfortunately, this could be a difficult task to accomplish, as the whole area is already a mining company’s concession and access is restricted. Another option would be to obtain sequences from the formalized holotype using alternative extracting methods from degraded DNA (e.g., Bernstein and Ruane 2022).

## Conservation

The main threats for *C. zarza* are habitat loss and contamination due to mining activities, both legal and illegal. The whole southern sector of the Cordillera del Cóndor is threatened by imminent human colonization and settlement, agriculture and cattle raising, as well as gold and copper mining. The situation of Refugio de Vida Silvestre El Zarza, in this context, is of particular concern. For now, the wildlife refuge acts like a conservation island, being surrounded by large mining concessions and with active mining activities close to its northern borders. To make things worse, in recent years,

signs of illegal mining activities were recorded inside the refuge. These activities are conducted especially in the streams of the reserve, and could affect, particularly but not exclusively, the survival of the glassfrogs that live in the wildlife refuge, especially due to water contamination. Currently, there are 6 species and one potentially new species of glassfrogs recorded from the refuge, although still others might remain to be discovered in the future.

Another threat for the survival of *C. zarza* could be chytridiomycosis, the infectious fungal disease caused by *Batrachochytrium dendrobatidis* (*Bd*), that has been linked to worldwide amphibian population declines (Berger et al. 1998; Lips et al. 2006; Skerratt et al. 2007). We did not carry out a survey to detect the pathogen presence in the amphibian populations from the refuge, but the death of our tadpoles raised in the laboratory could be attributed to the infection. Several studies have established a relationship between *Bd* infection and the occurrence of anomalies in the oral apparatus of tadpoles in various amphibian species (Fellers et al. 2001; Drake et al. 2007; Vieira et al. 2013) as chytridiomycosis affects only the keratinized tissues, which are restricted to the oral region (jaw sheaths and teeth) of tadpoles (Marantelli et al. 2004). In our case, tadpoles in Gosner stage 26 had two rows of tooth but by Gosner stage 31, all the tooth rows were lost and only the dermal ridges were visible (Fig. 9). Rueda-Almonacid (1994) recorded something similar in the case of *C. geckoidea*, where the tadpoles in Gosner 22 (one month after hatching) had two incomplete tooth rows on the anterior labium and three tooth rows on the posterior labium but, three months after hatching, all the tooth rows were lost.

However, it is possible that the loss of tooth rows is a natural (developmental) process. This could be particularly true in our case, as we did not observe oral deformities in the form of dekeratinization (depigmentation) of mouthparts (which are the typical symptoms of *Bd* infection; Navarro-Lozano et al. 2018), just the loss of the tooth rows. Also, it is possible that the loss of tooth was caused by other factors, as there are studies that have indicated that oral deformities are not always related to *Bd* infection (Rachowicz 2002; Blaustein et al. 2005; Navarro-Lozano et al. 2018) and could be attributed to other factors, like low temperatures (Rachowicz 2002), water contamination (Rowe et al. 1998) or diet (McDiarmid and Altig 1999). In order to resolve this issue, we plan to implement a survey in the near future to confirm or not the pathogen's presence in the reserve and particularly in the threatened amphibian populations.

## Acknowledgements

We are grateful for the help and support offered by Ministerio del Ambiente, Agua y Transición Ecológica, Zona 7 and for the issued research permits (MAE-DNB-CM-2015-0016, MAAE-ARSFC-2020-0727 and MAATE-DBI-CM-2021-0181). Special thanks to the administrative personal and park rangers of Refugio de Vida Silvestre El Zarza: Washington Díaz, Luis León, Dalton Morocho, Álex Armijos, Dalton Bustán, Ángel Campoverde, Jomary Pineda, Edison Gálvez and Ramiro Sarango, whose

assistance was essential for the field work. Field and laboratory work was funded by Universidad Técnica Particular de Loja through the project “Descripción de nuevas especies de anfibios y reptiles del sur de Ecuador a partir de las colecciones del Museo de Zoología, UTPL”. We thank Jorge Brito and Manuel Morales-Mite for sharing their data with us and Monica Guerra (Museo de Historia Natural Gustavo Orcés, Escuela Politécnica Nacional) for providing access to the specimens in her care. We also thank Ángel Hualpa, Marek Castel, Joselyn Vinueza, Guillermo Enríquez, Marlon Vega, Camilo López, María José Rojas, and Andy Ruiz for help during fieldwork, and Pablo Córdova for his help with the digitization of the oral apparatus drawing. Finally, we want to thank Juan Manuel Guayasamin and Mauricio Ortega-Andrade for the useful comments and suggestions that improved our manuscript.

## References

- Almendáriz A, Batallas D (2012) Nuevos datos sobre la distribución, historia natural y el canto de *Centrolene condor* Cisneros-Heredia y Morales-Mite 2008 (Amphibia: Anura: Centrolenidae). *Revista Politécnica* 30: 42–53.
- Almendáriz A, Simmons JE, Brito J, Vaca-Guerrero J (2014) Overview of the herpetofauna of the unexplored Cordillera del Cóndor of Ecuador. *Amphibian & Reptile Conservation* 8: 45–64.
- Anstis M (2013) Tadpoles and frogs of Australia. New Holland Publishers, London, 829 pp.
- Ayarzagüena J (1992) Los centrolenidos de la Guayana Venezolana. *Publicaciones de la Asociación de Amigos de Doñana*. Sevilla 1: 1–46.
- Ayarzagüena J, Señaris JC (1997) Dos nuevas especies de *Cochranella* (Anura: Centrolenidae) para Venezuela. *Publicaciones de la Asociación de Amigos de Doñana* 8: 1–16.
- Barrera-Rodríguez M, Ruiz-Carranza PM (1989) Una nueva especie del género *Centrolenella* Noble, 1920 (Amphibia: Anura: Centrolenidae) de la Cordillera Occidental de Colombia. *Trianea* 3: 77–84.
- Barrio-Amorós C, Rojas-Runjaic F, Señaris J (2019) Catalogue of the amphibians of Venezuela: Illustrated and annotated species list, distribution, and conservation. *Amphibian & Reptile Conservation* 13: 1–198.
- Berger L, Speare R, Daszak P, Green DE, Cunningham AA, Goggin CL, Slocombe R, Ragan MA, Hyatt AD, McDonald KR, Hines HB, Lips KR, Marantelli G, Parkes H (1998) Chytridiomycosis causes amphibian mortality associated with population declines in the rain forests of Australia and Central America. *Proceedings of the National Academy of Sciences of the United States of America* 95(15): 9031–9036. <https://doi.org/10.1073/pnas.95.15.9031>
- Bernstein JM, Ruane S (2022) Maximizing molecular data from low-quality fluid-preserved specimens in natural history collections. *Frontiers in Ecology and Evolution* 10: 893088. <https://doi.org/10.3389/fevo.2022.893088>
- Blainville H-MD (1816) Prodrôme d’une nouvelle distribution systématique du règne animal. *Bulletin de la Société Philomathique de Paris* 3: 113–124.

- Blaustein AR, Romansic JM, Scheessele EA, Han BA, Pessier AP, Longcore JE (2005) Interspecific variation in susceptibility of frog tadpoles to the pathogenic fungus *Batrachochytrium dendrobatidis*. *Conservation Biology* 19(5): 1460–1468. <https://doi.org/10.1111/j.1523-1739.2005.00195.x>
- Castroviejo-Fisher S, Guayasamin JM, Gonzalez-Voyer A, Vilà C (2014) Neotropical diversification seen through glassfrogs. *Journal of Biogeography* 41(1): 66–80. <https://doi.org/10.1111/jbi.12208>
- Cisneros-Heredia DF, McDiarmid RW (2006) A new species of the genus *Centrolene* (Amphibia: Anura: Centrolenidae) from Ecuador with comments on the taxonomy and biogeography of glassfrogs. *Zootaxa* 1244: 1–32.
- Cisneros-Heredia DF, McDiarmid RW (2007) Revision of the characters of Centrolenidae (Amphibia: Anura: Athesphatanura), with comments on its taxonomy and the description of new taxa of glassfrogs. *Zootaxa* 1572(1): 1–82. <https://doi.org/10.11646/zootaxa.1572.1.1>
- Cisneros-Heredia DF, Morales-Mite M (2008) A new species of glassfrog from elfin forests of the Cordillera del Cóndor, southeastern Ecuador. *Herpetozoa* (Wien) 21: 49–56.
- Cisneros-Heredia DF, Venegas PJ, Rada M, Schulte R (2008) A new species of glassfrog (Anura: Centrolenidae) from the foothill Andean forests of Ecuador and Peru. *Herpetologica* 64(3): 341–353. <https://doi.org/10.1655/06-078.1>
- Cochran DM, Goin CJ (1970) Frogs of Colombia. *Bulletin – United States National Museum* 288: 1–655. <https://doi.org/10.5962/bhl.part.6346>
- Cocroft RB, Ryan MJ (1995) Patterns of advertisement call evolution in toads and chorus frogs. *Animal Behaviour* 49(2): 283–303. <https://doi.org/10.1006/anbe.1995.0043>
- Drake DL, Altig R, Grace JB, Walls SC (2007) Occurrence of oral deformities in larval anurans. *Copeia* 2007(2): 449–458. [https://doi.org/10.1643/0045-8511\(2007\)7\[449:OODIL\]2.0.CO;2](https://doi.org/10.1643/0045-8511(2007)7[449:OODIL]2.0.CO;2)
- Duellman WE (1981) Three new species of centrolenid frogs from the Pacific versant of Ecuador and Colombia. *Occasional Papers of the Museum of Natural History, University of Kansas* 88: 1–9.
- Duellman WE, Burrowes PA (1989) New species of frogs, *Centrolenella*, from the Pacific versant of Ecuador and southern Colombia. *Occasional Papers of the Museum of Natural History, University of Kansas* 132: 1–14.
- Duellman WE, Schulte R (1993) New species of centrolenid frogs from northern Peru. *Occasional Papers of the Museum of Natural History, University of Kansas* 155: 1–33.
- Duméril AMC (1805) *Zoologie Analytique, ou Méthode Naturelle de Classification des Animaux, Rendue plus Facile à l'Aide de Tableaux Synoptiques*. Allais, Paris, 344 pp. <https://doi.org/10.5962/bhl.title.44835>
- Fellers GM, Green DE, Longcore JE (2001) Oral chytridiomycosis in the mountain yellow-legged frog (*Rana muscosa*). *Copeia* 2001(4): 945–953. [https://doi.org/10.1643/0045-8511\(2001\)001\[0945:OCITMY\]2.0.CO;2](https://doi.org/10.1643/0045-8511(2001)001[0945:OCITMY]2.0.CO;2)
- Gaige HT (1926) A new frog from British Guiana. *Occasional Papers of the Museum of Zoology, University of Michigan* 176: 1–3.
- Gosner KL (1960) A simplified table for staging anuran embryos and larvae with notes on identification. *Herpetologica* 16: 183–190.

- Greer BJ, Wells KD (1980) Territorial and reproductive behavior of the tropical American frog *Centrolenella fleischmanni*. *Herpetologica* 36: 318–326.
- Guayasamin JM, Bonaccorso E (2004) A new species of Glass Frog (Centrolenidae: Cochranella) from the lowlands of northwestern Ecuador, with comments on the *Cochranella granulosa* group. *Herpetologica* 60(4): 485–494. <https://doi.org/10.1655/03-74>
- Guayasamin JM, Trueb L (2007) A new species of Glassfrog (Anura: Centrolenidae) from the lowlands of northwestern Ecuador, with comments on centrolenid osteology. *Zootaxa* 1447(1): 27–45. <https://doi.org/10.11646/zootaxa.1447.1.2>
- Guayasamin JM, Castroviejo-Fisher S, Ayarzagüena J, Trueb L, Vilà C (2008) Phylogenetic relationships of glassfrogs (Centrolenidae) based on mitochondrial and nuclear genes. *Molecular Phylogenetics and Evolution* 48(2): 574–595. <https://doi.org/10.1016/j.ympev.2008.04.012>
- Guayasamin JM, Castroviejo-Fisher S, Trueb L, Ayarzagüena J, Rada M, Vilà C (2009) Phylogenetic systematics of glassfrogs (Amphibia: Centrolenidae) and their sister taxon *Allophryne ruthveni*. *Zootaxa* 2100(1): 1–97. <https://doi.org/10.11646/zootaxa.2100.1.1>
- Guayasamin JM, Cisneros-Heredia DF, McDiarmid RW, Peña P, Hutter CR (2020) Glassfrogs of Ecuador: Diversity, evolution, and conservation. *Diversity (Basel)* 12(6): 222. <https://doi.org/10.3390/d12060222>
- Guayasamin JM, Brunner RM, Valencia-Aguilar A, Franco-Mena D, Ringler E, Medina Armijos A, Morochz C, Bustamante L, Maynard RJ, Culebras J (2022) Two new Glassfrogs (Centrolenidae: *Hyalinobatrachium*) from Ecuador, with comments on the endangered biodiversity of the Andes. *PeerJ* 10: e13109. <https://doi.org/10.7717/peerj.13109>
- Hutter CR, Esobar-Lasso S, Rojas-Morales JA, Gutiérrez-Cárdenas PDA, Imba H, Guayasamin JM (2013) The territoriality, vocalizations and aggressive interactions of the red-spotted glassfrog, *Nymphargus grandisonae* Cochran & Goin, 1970 (Anura: Centrolenidae). *Journal of Natural History* 47(47–48): 3011–3032. <https://doi.org/10.1080/00222933.2013.792961>
- IUCN (2001) IUCN Red List categories and criteria: Version 3.1. IUCN Species Survival Commission. IUCN, Gland, Switzerland and Cambridge, UK.
- Jiménez De La Espada M (1872) Nuevos batracios americanos. *Anales de la Sociedad Española de Historia Natural* 1: 85–88.
- Katoh K, Standley DM (2013) MAFFT multiple sequence alignment software version 7: Improvements in performance and usability. *Molecular Biology and Evolution* 30(4): 772–780. <https://doi.org/10.1093/molbev/mst010>
- Köhler J, Jansen M, Rodríguez A, Kok PJR, Toledo LF, Emmrich M, Glaw F, Haddad CFB, Rödel MO, Vences M (2017) The use of bioacoustics in anuran taxonomy: Theory, terminology, methods and recommendations for best practice. *Zootaxa* 4251(1): 1–124. <https://doi.org/10.11646/zootaxa.4251.1.1>
- Lanfear R, Frandsen PB, Wright AM, Senfeld T, Calcott B (2017) PartitionFinder 2: New methods for selecting partitioned models of evolution for molecular and morphological phylogenetic analyses. *Molecular Biology and Evolution* 34: 772–773. <https://doi.org/10.1093/molbev/msw260>

- Lips KR, Brem F, Brenes R, Reeve JD, Alford RA, Voyles J, Carey C, Livo L, Pessier AP, Collins JP (2006) Emerging infectious disease and the loss of biodiversity in a Neotropical amphibian community. *Proceedings of the National Academy of Sciences of the United States of America* 103(9): 3165–3170. <https://doi.org/10.1073/pnas.0506889103>
- Lynch JD, Duellman WE (1973) A review of the centrolenid frogs of Ecuador, with descriptions of new species. *Occasional Papers of the Museum of Natural History, University of Kansas* 16: 1–66. <https://doi.org/10.5962/bhl.part.29037>
- Marantelli G, Berger L, Speare R, Keegan L (2004) Distribution of the amphibian chytrid *Batrachochytrium dendrobatidis* and keratin during tadpole development. *Pacific Conservation Biology* 10(3): 173–179. <https://doi.org/10.1071/PC040173>
- McDiarmid RW, Altig R (1999) *Tadpoles: the biology of anuran larvae*. University of Chicago Press, Chicago, IL, USA, 444 pp.
- Mijares-Urrutia A (1998) Los renacuajos de los anuros (Amphibia) altoandinos de Venezuela: Morfología externa y claves. *Revista de Biología Tropical* 46: 119–143. <https://doi.org/10.15517/rbt.v46i1.19360>
- Müller J, Müller K, Neinhuis C, Quandt D (2010) PhyDe. *Phylogenetic Data Editor* 0: 9971. <http://www.phyde.de> [Accessed on 20 July 2022]
- Navarro-Lozano A, Sánchez-Domene D, Rossa-Feres DC, Bosch J, Sawaya RJ (2018) Are oral deformities in tadpoles accurate indicators of anuran chytridiomycosis? *PLoS ONE* 13(1): e0190955. <https://doi.org/10.1371/journal.pone.0190955>
- Orton GL (1953) The systematics of vertebrate larvae. *Systematic Zoology* 2(2): 63–75. <https://doi.org/10.2307/2411661>
- Rachowicz LJ (2002) Mouthpart pigmentation in *Rana muscosa* tadpoles: Seasonal changes without chytridiomycosis. *Herpetological Review* 33: 263–264.
- Rambaut A (2014) FigTree, Tree Figure Drawing Tool. v. 1.4.2. <http://tree.bio.ed.ac.uk/software/figtree> [Accessed on 13 July 2022]
- Rivero JA (1968) Los centrolénidos de Venezuela. *Memorias de la Sociedad de Ciencias Naturales La Salle* 28: 301–334.
- Ronquist F, Teslenko M, Van Der Mark P, Ayres DL, Darling A, Höhna S, Larget B, Liu L, Suchard MA, Huelsenbeck JP (2012) MrBayes 3.2: Efficient Bayesian phylogenetic inference and model choice across a large model space. *Systematic Biology* 61(3): 539–542. <https://doi.org/10.1093/sysbio/sys029>
- Rowe CL, Kinney OM, Congdon JD (1998) Oral deformities in tadpoles of the bullfrog (*Rana catesbeiana*) caused by conditions in a polluted habitat. *Copeia* 244–246(1): 244. <https://doi.org/10.2307/1447729>
- Rueda-Almonacid J (1994) Estudio anatómico y relaciones sistemáticas de *Centrolene geckoideum* (Salientia: Anura: Centrolenidae). *Trianca* 5: 133–187.
- Ruiz-Carranza PM, Lynch JD (1991a) Ranas Centrolenidae de Colombia I. Propuesta de una nueva clasificación genérica. *Lozania* 57: 1–30.
- Ruiz-Carranza PM, Lynch JD (1991b) Ranas Centrolenidae de Colombia II. Nuevas especies de *Centrolene* de la Cordillera Oriental y Sierra Nevada de Santa Marta. *Lozania* 58: 1–26.

- Ruiz-Carranza PM, Lynch JD (1991c) Ranas Centrolenidae de Colombia III. Nuevas especies del género *Cochranella* del grupo *granulosa*. *Lozania* 59: 1–18.
- Ruiz-Carranza PM, Lynch JD (1995a) Ranas Centrolenidae de Colombia V. Cuatro nuevas especies de *Cochranella* de la cordillera Central. *Lozania* 62: 1–23.
- Ruiz-Carranza PM, Lynch JD (1995b) Ranas Centrolenidae de Colombia VIII. Cuatro nuevas especies de *Centrolene* de la Cordillera Central. *Lozania*. 65: 1–16.
- Ruiz-Carranza PM, Hernández-Camacho J, Ardila-Robayo MC (1986) Una nueva especie colombiana del género *Centrolene* Jiménez de la Espada, 1872 (Amphibia: Anura) y redefinición del género. *Caldasia* 15: 431–444.
- Schulze A, Jansen M, Köhler G (2015) Tadpole diversity of Bolivia's lowland anuran communities: Molecular identification, morphological characterisation, and ecological assignment. *Zootaxa* 4016(1): 1–111. <https://doi.org/10.11646/zootaxa.4016.1.1>
- Skerratt LF, Berger L, Speare R, Cashins S, McDonald KR, Phillott AD, Hines HB, Kenyon N (2007) Spread of chytridiomycosis has caused the rapid global decline and extinction of frogs. *EcoHealth* 4(2): 125–134. <https://doi.org/10.1007/s10393-007-0093-5>
- Székely P, Eguiguren JS, Ordóñez-Delgado L, Armijos-Ojeda D, Székely D (2020) Fifty years after: A taxonomic revision of the amphibian species from the Ecuadorian biodiversity hotspot Abra de Zamora, with description of two new *Pristimantis* species. *PLoS ONE* 15(9): e0238306. <https://doi.org/10.1371/journal.pone.0238306>
- Tamura K, Stecher G, Peterson D, Filipski A, Kumar S (2013) MEGA6: Molecular Evolutionary Genetics Analysis Version 6.0. *Molecular Biology and Evolution* 30(12): 2725–2729. <https://doi.org/10.1093/molbev/mst197>
- Taylor EH (1951) Two new genera and a new family of tropical American frogs. *Proceedings of the Biological Society of Washington* 64: 33–40.
- Toledo LF, Martins IA, Bruschi DP, Passos MA, Alexandre C, Haddad CFB (2015) The anuran calling repertoire in the light of social context. *Acta Ethologica* 18(2): 87–99. <https://doi.org/10.1007/s10211-014-0194-4>
- Twomey EM, Delia J, Castroviejo-Fisher S (2014) A review of northern *Peruvian* glassfrogs (Centrolenidae), with the description of four new remarkable species. *Zootaxa* 3851(1): 1–87. <https://doi.org/10.11646/zootaxa.3851.1.1>
- Vieira C, Toledo L, Longcore J, Longcore J (2013) Body length of *Hylodes* cf. *ornatus* and *Lithobates catesbeianus* tadpoles, depigmentation of mouthparts, and presence of *Batrachochytrium dendrobatidis* are related. *Brazilian Journal of Biology* 73(1): 195–199. <https://doi.org/10.1590/S1519-69842013000100021>
- Vogel G, Nguyen TV, Lalremsanga HT, Biakzuala L, Hrima V, Poyarkov NA (2020) Taxonomic reassessment of the *Pareas margaritophorus-macularius* species complex (Squamata, Pareidae). *Vertebrate Zoology* 70: 547–569. <https://doi.org/10.26049/VZ70-4-2020-02>
- Wells KD (2007) *The Ecology and Behavior of Amphibians*. University of Chicago press, Chicago, USA, 1400 pp.
- Zwickl DJ (2006) Genetic algorithm approaches for the phylogenetic analysis of large biological sequence datasets under the maximum likelihood criterion. PhD Thesis, University of Texas, Austin, TX, USA.

## Appendix I

**Table A1.** Voucher, GenBank accession numbers and locality for the *Centrolene* species used in the phylogenetic analysis. With bold letters are marked the sequences generated by the present study. Ca01–Ca05 represent candidate new species from Guayasamin et al. (2020).

Species	Voucher number	GenBank accession no.			Locality
		<i>12S</i>	<i>16S</i>	<i>POMC</i>	
<i>Centrolene altitudinalis</i>	MHNLS 17194	EU663333	EU662974	EU663165	Venezuela: Mérida, Quebrada Albarregas
<i>Centrolene antioquiensis</i>	NRPS 014	EU663336	EU662977	EU663167	Colombia: Antioquia, Vereda El Roble
<i>Centrolene ballux</i>	QCAZ 40182	–	JX126954	–	Ecuador: Pichincha, Reserva Las Galarias, road Calacalí – La Independencia
<i>Centrolene ballux</i>	QCAZ 40196	KF639754	–	–	Ecuador: Pichincha, Reserva Las Galarias, road Calacalí – La Independencia
<i>Centrolene buckleyi</i>	KU 178031	EU663338	EU662979	EU663169	Ecuador: Imbabura, near Lago Cuicocha
<i>Centrolene buckleyi</i>	MZUTI 763	MH844843	MH844849	–	Ecuador: Napo, trail from Oyacachi to Chaco
<i>Centrolene</i> aff. <i>buckleyi</i> Ca02	MAR 371	EU663339	EU662980	EU663170	Colombia: Cundinamarca, Parque Nacional Chingaza
<i>Centrolene</i> aff. <i>buckleyi</i> Ca03	MRy 547	MH844838	MH844844	–	Ecuador: Zamora Chinchipe
<i>Centrolene</i> aff. <i>buckleyi</i> Ca03	MRy 548	MH844839	MH844845	–	Ecuador: Zamora Chinchipe
<i>Centrolene charapita</i>	MHNC 13933	KM068248	KM068256	–	Peru: Amazonas, La Oliva
<i>Centrolene charapita</i>	MNCN 45392	KF639760	KF534358	–	Peru: Amazonas, La Oliva
<i>Centrolene condor</i>	EPN 12800/ QCAZ 47338	–	MT225186	–	Ecuador: Zamora Chinchipe, Río Machinaza–Sector Colibrí
<i>Centrolene</i> aff. <i>condor</i> Ca04	QCAZ 44896	KF639755	JX126955	–	Ecuador: Zamora Chinchipe, Machinaza – Loma Tigres Alto
<i>Centrolene daidalea</i>	MHUA 3271	EU663366	EU663007	EU663192	Colombia: Cesar, Vereda San Cayetano
<i>Centrolene geckoidea</i>	KU 178015	EU663341	EU662982	–	Ecuador: Pichincha, 1 km SW San Ignacio
<i>Centrolene heloderma</i>	QCAZ 40200	KF639757	JX126956	–	Ecuador: Pichincha, Reserva Las Galarias, Río Santa Rosa
<i>Centrolene hesperia</i>	MHNSM 25802	EU663345	EU662986	KF639777	Peru: Cajamarca, Quebrada Chorro Blanco
<i>Centrolene huilensis</i>	QCAZ 37230	–	JX126959	–	Ecuador: Napo, Yanayacu Biological Station
<i>Centrolene hybrida</i>	MAR 347	EU663346	EU662987	EU663175	Colombia: Boyacá, Reserva Natural El Secreto
<i>Centrolene lynchi</i>	QCAZ 40191–92	KF639758	JX126957	–	Ecuador: Pichincha, Reserva Las Galarias, road Calacalí – La Independencia
<i>Centrolene muelleri</i>	CORDIBI 14667	–	KM068267	–	Peru: Amazonas, Puente – Vilcaniza
<i>Centrolene muelleri</i>	PV 1001	KF639759	JX126958	KF639778	Peru: Amazonas, Chachapoyas, Cataratas de Gokta
<i>Centrolene notosticta</i>	MAR 510	EU663351	EU662992	EU663180	Colombia: Norte de Santander, Vereda Piritama, Quebrada Piritama
<i>Centrolene persisticta</i>	QCAZ 22312	EU663352	EU662993	EU663181	Ecuador: Pichincha, Mindo Biology Station
<i>Centrolene persisticta</i>	QCAZ 40189	MT225171	–	–	Ecuador: Pichincha: Reserva Las Galarias
<i>Centrolene pipilata</i>	KU 178154	EU663353	EU662994	KF639779	Ecuador: Napo, Río Salado, 1 km upstream from Río Coca
<i>Centrolene sabini</i>	MUSM 28018	–	JX126960	–	Peru: Cusco, Parque Nacional Manu nearby Pilco Grande
<i>Centrolene sanchezi</i>	MUTPL 601	<b>OP751416</b>	<b>OP751399</b>	<b>OP753140</b>	Ecuador: Zamora Chinchipe, Reserva Biológica Cerro Plateado
<i>Centrolene sanchezi</i>	QCAZ 22728	EU663337	EU662978	EU663168	Ecuador: Napo, Yanayacu Biological Station
<i>Centrolene savagei</i>	MHUA 4094	EU663380	EU663020	EU663205	Colombia: Antioquia, Vereda El Retiro

Species	Voucher number	GenBank accession no.			Locality
		<i>12S</i>	<i>16S</i>	<i>POMC</i>	
<i>Centrolene venezuelense</i>	MHNLS 16497	EU663360	EU663001	EU663186	Venezuela: Mérida, Cordillera de Mérida
<i>Centrolene zarza</i>	MUTPL 932	<b>OP751417</b>	<b>OP751400</b>	<b>OP753141</b>	Ecuador: Zamora Chinchipe, Refugio de Vida Silvestre El Zarza
<i>Centrolene zarza</i>	MUTPL 933	<b>OP751418</b>	<b>OP751401</b>	<b>OP753142</b>	Ecuador: Zamora Chinchipe, Refugio de Vida Silvestre El Zarza
<i>Centrolene zarza</i>	MUTPL-T22	–	<b>OP751402</b>	–	Ecuador: Zamora Chinchipe, Refugio de Vida Silvestre El Zarza
<i>Centrolene</i> sp. Ca01	MAR 1152	KM068295	KM068295	–	Colombia: Chocó, Corregimiento de Balboa
<i>Centrolene</i> sp. Ca05	QCAZ 25744	MT225170	–	–	Ecuador: Napo, Yanayacu Biological Station

## Supplementary material 1

### Uncorrected genetic *p*-distances (%), for the mitochondrial gene *16S* for the *Centrolene* species

Authors: Paul Székely, María Córdova-Díaz, Daniel Hualpa-Vega, Santiago Hualpa-Vega, Diana Székely

Data type: xlsx file

Copyright notice: This dataset is made available under the Open Database License (<http://opendatacommons.org/licenses/odbl/1.0/>). The Open Database License (ODbL) is a license agreement intended to allow users to freely share, modify, and use this Dataset while maintaining this same freedom for others, provided that the original source and author(s) are credited.

Link: <https://doi.org/10.3897/zookeys.1149.96134.suppl1>

## Supplementary material 2

### Information regarding the *Centrolene zarza* sp. nov. call recordings and the bio-acoustic measurements

Authors: Paul Székely, María Córdova-Díaz, Daniel Hualpa-Vega, Santiago Hualpa-Vega, Diana Székely

Data type: xlsx file

Explanation note: Values are given as average  $\pm$  SD (range) and *n* = sample size.

Copyright notice: This dataset is made available under the Open Database License (<http://opendatacommons.org/licenses/odbl/1.0/>). The Open Database License (ODbL) is a license agreement intended to allow users to freely share, modify, and use this Dataset while maintaining this same freedom for others, provided that the original source and author(s) are credited.

Link: <https://doi.org/10.3897/zookeys.1149.96134.suppl2>

# New records of two roughy fish species of *Hoplostethus* and a confirmed record of *H. crassispinus* Kotlyar, 1980 (Trachichthyiformes, Trachichthyidae) from Taiwan

Yo Su<sup>1</sup>, Hsiu-Chin Lin<sup>1,2</sup>, Hsuan-Ching Ho<sup>3,4,5</sup>

**1** Department of Marine Biotechnology and Resources, National Sun Yat-sen University, Kaohsiung, Taiwan

**2** Doctoral Degree Program in Marine Biotechnology, National Sun Yat-sen University, Kaohsiung, Taiwan

**3** National Museum of Marine Biology & Aquarium, Pingtung, Taiwan

**4** Australian Museum, Sydney, Australia

**5** Department and Graduate Institution of Aquaculture, National Kaohsiung University of Science and Technology, Kaohsiung, Taiwan

Corresponding author: Hsuan-Ching Ho ([ogcoho@gmail.com](mailto:ogcoho@gmail.com))

---

Academic editor: Bruno Melo | Received 12 October 2022 | Accepted 2 February 2023 | Published 22 February 2023

---

<https://zoobank.org/6F1DC883-058A-4137-A554-E374F901D2E4>

---

**Citation:** Su Y, Lin H-C, Ho H-C (2023) New records of two roughy fish species of *Hoplostethus* and a confirmed record of *H. crassispinus* Kotlyar, 1980 (Trachichthyiformes, Trachichthyidae) from Taiwan. ZooKeys 1149: 85–101. <https://doi.org/10.3897/zookeys.1149.96233>

---

## Abstract

Two rarely caught species of the roughy fish genus *Hoplostethus* have been identified for the first time in the fish collections of Taiwan. The first, *H. grandperrini* Roberts & Gomon, 2012 was previously known only from two type specimens collected in the Southern Hemisphere off the coast of New Caledonia. Its distribution is now extended to the Northern Hemisphere off the coast of Pingtung, southern Taiwan. Our specimen represents the only record of this species since its initial description. The second, *H. robustispinus* Moore & Dodd, 2010 was originally described from a single specimen collected in the Philippines and was only known from the type locality and a single record off the Paracel Islands, South China Sea. This specimen represents the third record of the species since its original description. A single specimen of *H. crassispinus* Kotlyar, 1980, whose name has long appeared in the ichthyological literature of Taiwan and adjacent areas, was also identified as the first specimen-based record for Taiwan. Detailed descriptions of these species are provided and compared with available data of respective type specimens and related species, with intraspecific variations also discussed. Also included is a dichotomous key to all known species of the subgenus *Hoplostethus* in Taiwan.

## Keywords

Actinopterygii, biodiversity, distribution, ichthyofauna, taxonomy

## Introduction

The circumglobal roughy fish genus *Hoplostethus* is the most diverse group within the family Trachichthyidae, presently comprising 30 valid species (Su et al. 2022). They are characterized by having the combination of 3–8 dorsal-fin spines, lateral-line scales distinctly enlarged, body height >40% standard length (SL), and position of anus immediately before anal-fin origin (Kotlyar 1996). The genus *Hoplostethus* has been divided into four subgenera, with the nominate subgenus *Hoplostethus* differing from subgenera *Aulohoplostethus*, *Leiogaster*, and *Macrohoplostethus* by having light-colored pectoral fins, simple and unbranched pyloric caeca, 25–27 total vertebrae, enlarged abdominal scutes, and no striation area on the body (Kotlyar 1986; Su et al. 2022). *Hoplostethus robustispinus* Moore & Dodd, 2010 was described from a single specimen collected east of Calagua Islands, Philippines, and later known from another record near Paracel Islands, South China Sea (Moore and Dodd 2010; Kotlyar 2011). It is characterized by having thickened fin spines in adults, 16 or 17 pectoral-fin rays, 19 or 20 total developed gill rakers, a longer trunk (36.8–38.7% SL), 50–56 pyloric caeca, and all fins without black margin (Moore and Dodd 2010; Kotlyar 2011).

Another rarely caught species, *Hoplostethus grandperrini* Roberts & Gomon, 2012, was described based on two specimens collected off the coast of New Caledonia (Roberts and Gomon 2012). It is distinguished from congeners by having a whitish oral cavity, 17 or 18 pectoral-fin rays, 19 or 20 total gill rakers, a short pectoral fin, the tip of which does not reach a vertical position through the anal-fin origin, and a larger maximum body size, reaching 455 mm SL (Roberts and Gomon 2012). Due to their rarity in collections, no additional information on these two species exists since their original descriptions.

*Hoplostethus crassispinus* Kotlyar, 1980 was originally described from specimens collected from the Emperor Seamounts and was later identified based on specimens from the Kyushu-Palau ridge (Kotlyar 1980, 1986). Although this species has been recorded in Taiwan (e.g., Shen et al. 1993; Shen and Wu 2011; Koeda 2019), it has long been confused and attributed to an undescribed species (*H. sp.*, in Su et al. 2022). Therefore, the existence of this species in Taiwanese waters remains unknown.

In Taiwan, five species have been recorded: *H. crassispinus*, *H. japonicus* Hilgendorf, 1879, *H. mediterraneus* Cuvier, 1829, *H. roseus* Su, Lin & Ho, 2022, and *H. sp.* (Chen 1969; Shen et al. 1993; Shen and Wu 2011; Su et al. 2022). However, three of them were only recently recognized (*H. japonicus*, *H. roseus*, and *H. sp.*; Su et al. 2022). A thorough study of the genus is needed, as new species or new records are expected (Su et al. 2022).

Recently, three specimens were found in the fish collections in Taiwan. Based on their unique characters, the three specimens are here identified as *H. robustispinus*, *H. grandperrini*, and *H. crassispinus*, respectively. Detailed descriptions of the specimens and comparisons with their respective type specimens, and available data, are herein provided. Moreover, a dichotomous identification key for all known species of the subgenus *Hoplostethus* (including *H. sp.*, sensu Su et al. 2022) that occurs in Taiwan is also provided.

## Materials and methods

Methods for counts and measurements and description follow Su et al. (2022) except for the vertebral count, with the urostyle counted as the last vertebrae. Standard length (SL) and head length (HL) were used throughout, except where otherwise indicated. All measurements were made using digital calipers rounding to the nearest 0.1 mm, except for lengths longer than 150 mm, which were rounded to the nearest 1 mm by using a regular ruler. Paired-fin characters are presented as left/right. Counts of vertebrae and predorsal bones were determined by radiography. Specimens were deposited at the Academia Sinica, Biodiversity Research Center, Taipei, Taiwan (**ASIZP**), Fisheries Research Institute, Keelung, Taiwan (**FRIP**), and the Pisces Collection of the National Museum of Marine Biology and Aquarium, Pingtung, Taiwan (**NMMB-P**). Comparative materials including *Hoplostethus japonicus*, *H. roseus*, and *H. sp.*, are listed in Su et al. (2022).

## Results

### Family Trachichthyidae

#### *Hoplostethus* Cuvier, 1829

*Hoplostethus* Cuvier in Cuvier and Valenciennes 1829: 469 (type species: *Hoplostethus mediterraneus* Cuvier in Cuvier and Valenciennes 1829).

*Korsogaster* Parr, 1933: 9 (type species: *Korsogaster nanus* = *Hoplostethus mediterraneus*).

**Remarks.** *Hoplostethus* differs from other genera of Trachichthyidae in having the following combination of characters: body depth at dorsal-fin origin >40% SL; anus situated in front of anal-fin origin; dorsal-fin spines progressively longer posteriorly and longest at last spine; lateral-line scales distinctly larger than adjacent body scales, ca 2–3 times in size; light organ absent; and vomer usually without teeth (Kotlyar 1996; Su et al. 2022).

Kotlyar (1986) divided *Hoplostethus* into four subgenera, *Aulohoplostethus*, *Hoplostethus*, *Leiogaster*, and *Macrohoplostethus*, by their numbers of dorsal-fin soft rays, pyloric caeca, and total vertebrae, coloration of pectoral fin, simple or branched pyloric caeca, and the presence of stritiated area on body. Among those subgenera, the subgenus *Hoplostethus* is distinguished from other subgenera in having dorsal-fin soft rays 12–14 (vs 15–19 in *Macrohoplostethus*), total vertebrae 25–26 (vs 29–30 in *Macrohoplostethus*), pyloric caeca <50, simple and unbranched (vs >60, branched in *Macrohoplostethus*), pectoral fin pale (vs black in *Leiogaster*), and body without stritiated area (vs present in *Aulohoplostethus*).

Among the 30 valid species in *Hoplostethus*, one species is recognized under *Aulohoplostethus*, 19 under *Hoplostethus*, eight under *Leiogaster*, and two under *Macrohoplostethus*, respectively.

***Hoplostethus grandperrini* Roberts & Gomon, 2012**

Figs 1–3A; Tables 1, 2

English name: Grandperrin's roughy

Chinese name: 格蘭氏胸燧鯛

*Hoplostethus grandperrini* Roberts & Gomon, 2012: 351 (type locality: New Caledonia, Norfolk Ridge, 24°55'8.99"S, 168°20'56.99"E, depth 600–675 m).

*Hoplostethus* cf. *gigas*—Grandperrin and Lehodey 1992: 7, 26, 35.

**Material examined.** NMMB-P36039, 395 mm SL, off the coast of Shan-hai fishing port, Pingtung, southwestern Taiwan (ca 21°59'08.75"N, 120°42'42.03"E), 19 April 2014, hook and line, purchased by C.-W. Chang.

**Description of NMMB-P36039.** Meristic and morphometric values are provided in Tables 1, 2.

Dorsal-fin rays VI, 13; pectoral-fin rays 17/17; pelvic-fin rays I, 6/I, 6; anal-fin rays III, 9; principal caudal-fin rays 10+9=19, uppermost and lowermost rays unbranched; procurrent caudal-fin rays 7 dorsally and 7 ventrally; gill rakers on outer surface of first-gill arch 6+1+13=20; lateral-line scales 28; scale rows between dorsal-fin origin and lateral line 13, scale rows between anal-fin origin and lateral line 23; predorsal scales 24; abdominal scutes 17; vertebrae 11+16=27; pyloric caeca 44; pseudobranchial filaments 30; branchiostegal rays 8; supraneural and pterygiophore insertion formula: 0/0/2+1/1/1/1 (spinous dorsal fin only).

Body oblong, distinctly longer than deep, depth at dorsal-fin origin 2.0 in SL. Head large, its length 2.7 in SL, its height subequal to its length, 1.0 in HL; upper profile in front of dorsal fin slightly curved to back of head, with somewhat concave forehead, and abrupt downturn above maxilla; forehead broad, HF1 11.9 and HF2 5.6 in HL; eyes of moderate size, 3.7 in HL; snout length 4.6 in HL; space between eyes convex and broad, interorbital width 2.8 in HL; crests on head bones well developed and covered with rather long spinules.

Mouth large, posterior end of maxilla extending beyond vertical through posterior margin of eye. Nostrils right before anterior margin of eye, on horizontal about through center of eye; posterior nostril distinctly larger than anterior nostril; eyes rather ventrally placed, upper margin of eye on horizontal through lateral-line origin.

Most of lateral and medial surfaces of premaxilla and dentary covered with villiform teeth, those on medial surface rather conical; no teeth at symphyseal notch of premaxilla and knob at symphysis of dentaries. Narrow band of villiform teeth on palatine; vomer toothless. Gill rakers on first and second arch rod-shaped, laterally compressed, with small conical teeth on tips and inner surfaces; those in outer row of first arch longest; those on inner row of first arch and both inner and outer rows of second and third arches short; small tooth patches, forming bumps on midline of outer three arches; large tooth patches present on fourth ceratobranchial arch. Large, oval patch of villiform teeth on fifth ceratobranchial. Large, slightly oval



**Figure 1.** *Hoplostethus grandperrini* Roberts & Gomon, 2012. NMMB-P36039, 395 mm SL, Pingtung, Taiwan.

**Table 1.** Meristic data of *Hoplostethus grandperrini* and *H. robustispinus*. Data of other specimens were obtained from Kotlyar (2011), Moore and Dodd (2010), and Roberts and Gomon (2012). Paired-fin characters are presented as left/right.

	<i>Hoplostethus grandperrini</i>		<i>Hoplostethus robustispinus</i>		
	This study	Roberts and Gomon (2012)	This study	Moore and Dodd (2010)	Kotlyar (2011)
	NMMB-P36039	All types (n = 2)	FRIP 01364	Holotype	ZMMU-P22657
Dorsal-fin elements	VI, 13	VI, 13	VI, 13	VI, 14	VI, 13
Pectoral-fin elements	17/17	17–18	17/17	16–17	16/16
Pelvic-fin elements	I, 6/I, 6	I, 6	I, 6/I, 6	I, 6	N/A
Anal-fin elements	III, 9	III, 9	III, 9	III, 9	III, 9
Gill rakers	6+1+13=20	6+1+12–13=19–20	6+1+12=19	6+1+13=20	6+1+12=19
Pseudobranchial filaments	30	15 (n=1)	26	25–26	27–28
Lateral-line scales	28	29	28	28	28
Scale rows above lateral line	13	11–12	10	N/A	N/A
Scale rows below lateral line	23	26–35	27	N/A	N/A
Abdominal scutes	17	13–14	15	13	14
Predorsal scales	24	21–24	23	23	22
Pyloric caeca	44	N/A	N/A	56	50
Vertebrae	11+16	11+15	11+16	11+16	11+16

tooth patch on second pharyngobranchial. Large teardrop-like tooth patch on third pharyngeal arch.

Preopercular spine short, its tip not reaching pelvic-fin base. Longest gill raker 0.7 in eye diameter; gill filaments at angle of first gill arch very short, ca 4.3 in eye diameter, and ca 1.8 in length of longest pseudobranchial filaments.

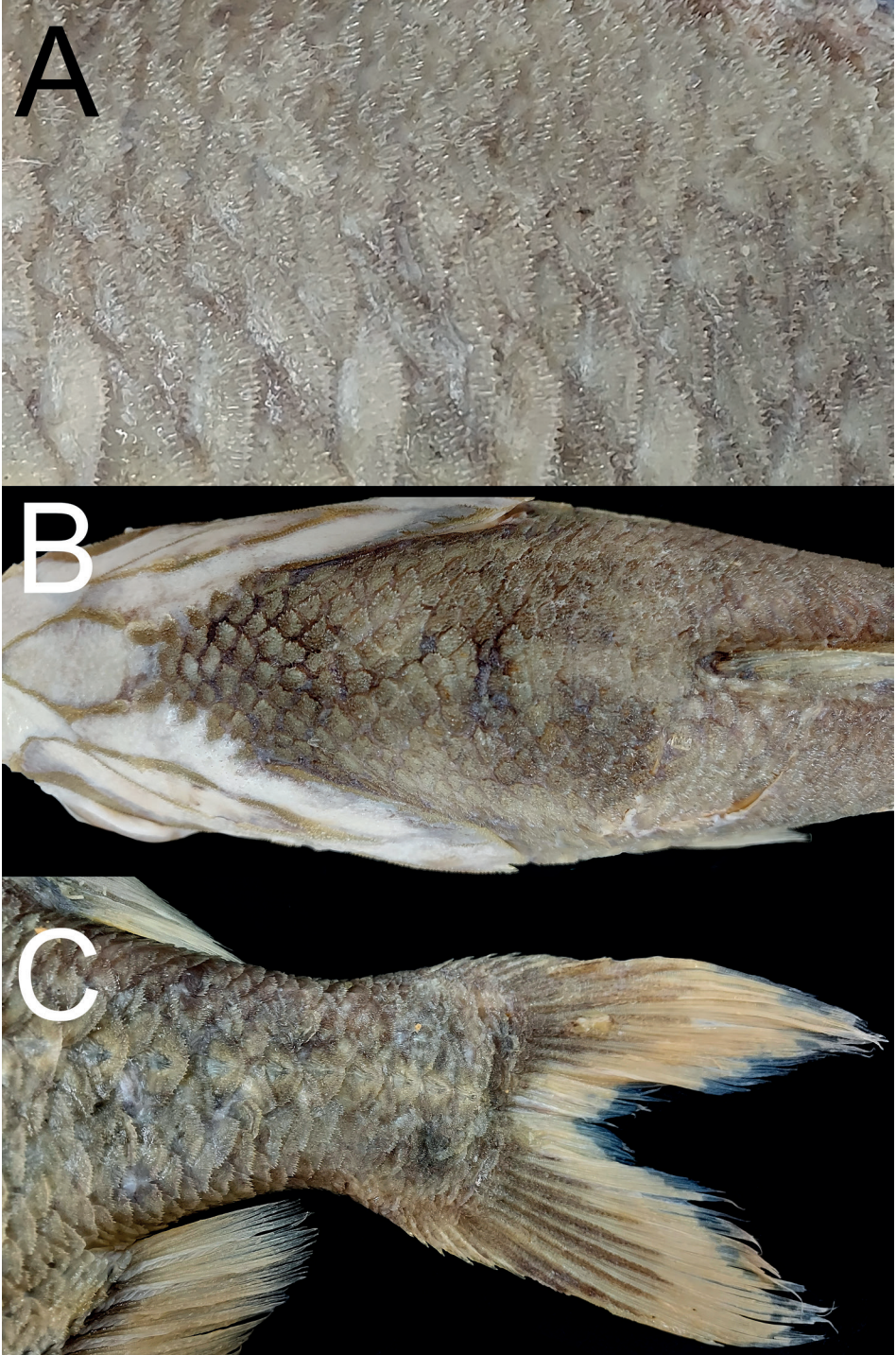


**Figure 2.** *Hoplostethus grandperrini*, NMMB-P36039, 395 mm SL **A** scales on the dorsal side of the body featuring long spinules **B** predorsal scales **C** caudal-fin pigmentation. Figs not to scale.

Body scales firmly attached, cycloid scales present on pectoral-fin region, elsewhere covered with ctenoid scales armored with rather long spinules (Fig. 2A); isthmus and gular region naked; lateral-line scales enlarged, ca 2–3 times size of body scales; center of each lateral-line scale without distinct spine; enlarged scales (scutes) covering abdomen region, their bases covered with body scales, all scutes with single tip; predorsal scales not enlarged and not forming distinct ridge (Fig. 2B).

Dorsal-fin spines progressively longer posteriorly, greatest increase in length from first to fourth spine; first ray unbranched, others branched; outer margin of dorsal-fin rays nearly straight. Pectoral fin truncated, slightly rounded; short, not reaching vertical through anal-fin origin. Pelvic fin short, reaching 11<sup>th</sup> abdominal scute. Pyloric caeca pale, unbranched.

**Coloration.** Fresh coloration unknown, presumably a reddish body color as shown by Roberts and Gomon (2012: fig. 6). Preserved specimen uniformly pale, slightly yellowish (Fig. 1), membranes on head region lighter than body color. Anal- and caudal-fin rays with black pigmentation near base (Fig. 2C). Oral cavity, including underside of tongue white, with very scarce black pigmentation (Fig. 3A). Inner side of opercle black. Peritoneum and stomach black.

**Distribution.** Previously, only type series collected between 600 and 675 m deep off the coast of New Caledonia were known. Our specimen represents the second record and a range extension to the Northern Hemisphere, suggesting a wide distribution in the western Pacific Ocean.

**Remarks.** The present specimen was identified as *H. grandperrini* by having a pale oral cavity, a short pectoral fin with its tip not reaching a vertical through the anal-fin origin, predorsal scales not enlarged and forming a distinct ridge, head bones covered with long spinules, ctenoid scales on body with rather long spinules, and a larger size, exceeding 300 mm SL (Roberts and Gomon 2012).

*Hoplostethus grandperrini* can be distinguished from other species of *Hoplostethus* co-occurring in Taiwan by having the following characters: a pale oral cavity, including the underside of the tongue (vs uniformly black oral cavity in both *H. japonicus* and *H. roseus*), a short pectoral fin with its tip not reaching a vertical through the anal-fin origin (vs a long pectoral fin exceeding beyond a vertical through the anal-fin origin in *H. japonicus* and *H. sp.*; sensu Su et al. 2022).

In comparison to the data provided by Roberts and Gomon (2012), our specimen has a higher number of abdominal scutes (17, vs 13–14) and pseudobranchial filaments (30, vs 15), a slightly lower number of lateral-line scales (28, vs 29) and fewer scale rows below the lateral line (23, vs 26–35), and some slightly different morphometric characters (e.g., smaller head length, prepectoral length, and prepelvic length; Tables 1, 2). These values are rather distinct, and additional research may reveal whether the Taiwanese population represents a different species. It is also notable that the forehead length (HF2) of our species is 6.7%, distinctly different from 41.0–44.2% SL provided by Roberts and Gomon (2012). Based on our previous data (e.g., 3.7–7.9% SL in specimens examined by Su et al. 2022), it is likely that they were referring to “head height” rather than “forehead height”.

***Hoplostethus robustispinus* Moore & Dodd, 2010**

Figs 3B–5; Tables 1, 2

English name: Thickspine roughy

Chinese name: 粗棘胸燧鯛

*Hoplostethus robustispinus* Moore & Dodd, 2010: 139 (type locality: east of Calagua Islands, Philippines, 14°18'00"N–14°47'00"N, 123°21'00"E–123°25'00"E, depth 648–660 m)–Kotlyar 2011: 484 (14°34'00"N, 112°06'00"E, South China Sea, depth 300 m).

**Material examined.** FRIP 01364, 241 mm SL, South China Sea, 30 April 1996, collected by D.-A. Lee.

**Description of FRIP 01364.** Meristic and morphometric data are provided in Tables 1, 2.

Dorsal-fin rays VI, 13; pectoral-fin rays 17/17; pelvic-fin rays I, 6/I, 6; anal-fin rays III, 9; principal caudal-fin rays 10+9=19, uppermost and lowermost rays unbranched; procurrent caudal-fin rays 7 dorsally and 7 ventrally; gill rakers on outer surface of first gill arch 6+1+12=19; lateral-line scales 28; scale rows between dorsal-fin origin and lateral line 10, scale rows between and anal-fin origin and lateral line 27; predorsal scales 23; abdominal scutes 15; vertebrae 11+16=27; pseudobranchial filaments 26; branchiostegal rays 8; supraneural and pterygiophore insertion formula: 0/0/2+1/1/1/1 (spinous dorsal fin only).

Body oblong, distinctly longer than deep, depth at dorsal-fin origin 2.1 in SL. Trunk large, length from pelvic-fin origin to anal-fin origin 2.5 in SL. Head large, its length 2.6 in SL, its height subequal to its length, 1.0 in HL; upper profile in front of dorsal fin rather flat, slightly curved to back of head, with somewhat rounded forehead, and abrupt downturn above maxilla; forehead broad, HF1 9.1 and HF2 6.2 in HL; eyes of moderate size, 3.5 in HL; snout length 4.9 in HL; space between eyes convex and broad, interorbital width 3.2 in HL; crests on head bones well developed and covered with small spinules.

Mouth large, posterior end of maxilla reaching vertical through posterior margin of eye. Nostrils right before anterior margin of eye, slightly above horizontal through center of eye; posterior nostril distinctly larger than anterior nostril; eyes rather dorsally placed, upper margin of eye on horizontal through lateral-line origin.

Most of lateral and medial surfaces of premaxilla and dentary covered with villiform teeth, those on medial surface rather conical; no teeth at symphyseal notch of premaxilla and knob at symphysis of dentaries. Narrow band of villiform teeth on palatine; vomer toothless. Gill rakers on first and second arch rod-shaped, laterally compressed; those in outer row of first arch longest; those on inner row of first arch and both inner and outer rows of second to fourth arches short.

Preopercular spine short, its tip not reaching pelvic-fin base. Longest gill raker 1.6 in eye diameter; gill filaments at angle of first gill arch very short, ca 5.9 in eye diameter, and ca 2.0 in length of longest pseudobranchial filaments.

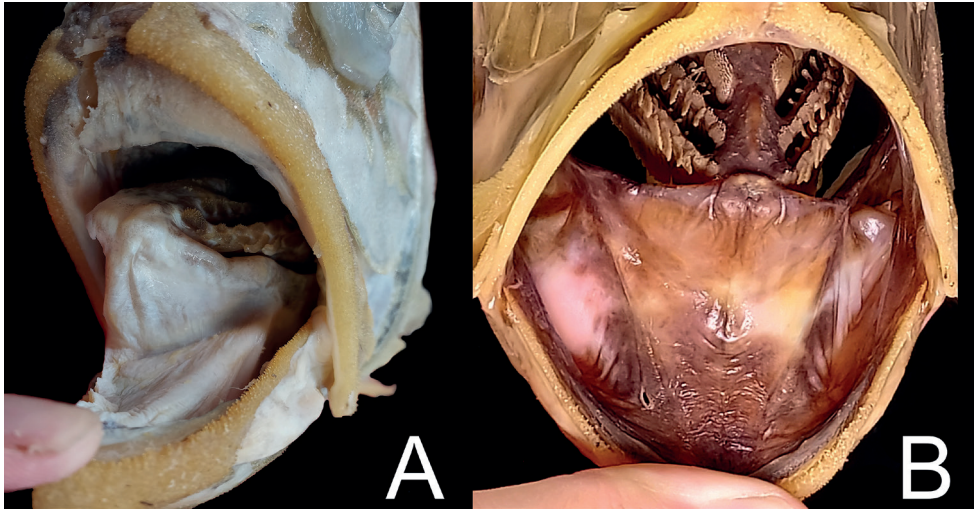


**Figure 3.** Coloration of oral cavities of *Hoplostethus* species **A** *H. grandperrini*, NMMB-P36039, 395 mm SL, preserved **B** *H. robustispinus*, FRIP01364, 241 mm SL, preserved.

Body scales firmly attached, cycloid scales present on pectoral-fin region, elsewhere covered with ctenoid scales; isthmus and gular region naked; lateral-line scales enlarged, ca 2–3 times size of body scales; center of each lateral-line scale without distinct spine; enlarged scales (scutes) covering abdomen region, their bases covered with body scales, all scutes with single tip; predorsal scales slightly enlarged and forming ridge.

Dorsal-fin spines progressively longer posteriorly, greatest increase in length from first to third spine; third to sixth spine extremely thickened, greatest width 5.6–8.9 in its length (Fig. 5A); first ray unbranched, others branched; outer margin of dorsal-fin rays nearly straight. Pectoral fin truncated, slightly rounded; short, not reaching vertical through anal-fin origin. Pelvic fin short, reaching eighth abdominal scute; its spine slightly thickened, greatest width 8.8 times in its length. Second and third anal-fin spines extremely thickened, greatest width 3.5–4.8 times in its length (Fig. 5B).

**Coloration.** Fresh condition of our specimen unknown, presumably a uniformly bright-red coloration as shown in Moore and Dodd (2010: fig. 3). Preserved specimen (Fig. 4) uniformly yellowish-brown, all fin spines paler than body color; fin-ray color similar to body color. Distal half of membrane between dorsal-fin spines black (Fig. 5A). Oral cavity, including underside of tongue mostly black, with some portions slightly whitish (Fig. 3B); inner side of opercle, and peritoneum black.

**Distribution.** Originally described from the Philippine Sea (Moore and Dodd 2010), and a later record reported from south to Paracel Islands in the South China Sea (14°34'00"N, 112°06'00"E) (Kotlyar 2011). Although the precise location of our specimen is unknown, it is presumed to be in the northern portion of the South China Sea, most likely near the Dong-sha Islands (Pratas Islands). Our specimen represents the third published record of the species and the first in Taiwan.

**Table 2.** Morphometric data of *Hoplostethus grandperrini* and *H. robustispinus*. Data of other specimens were obtained from Kotlyar (2011), Moore and Dodd (2010), and Roberts and Gomon (2012). Abbreviations: A, anal-fin; C, caudal-fin; D, dorsal-fin; GR, gill raker; HF, forehead height; HL, head length; P, pectoral-fin; V, pelvic-fin.

	<i>Hoplostethus grandperrini</i>			<i>Hoplostethus robustispinus</i>			
	This study		Roberts and Gomon (2012)	This study		Moore and Dodd (2010)	Kotlyar (2011)
	NMMB-P36039	All types (n = 2)		FRIP 01364	Holotype		ZMMU-P22657
SL (mm)	395		131–455	241		340	163
	%SL	%HL	%SL	%SL	%HL	%SL	%SL
HL	37.6		41.4–42.9	38.0		37.6	38.7
Head depth	39.5	105.2	N/A	37.8	99.3	40.1	43.5
Predorsal length	46.5	123.7	38.8–49.1	45.1	118.6	44.1	46.3
Prepectoral length	39.8	105.9	40.4–40.8	36.6	96.2	37.1	40.8
Prepelvic length	42.0	111.8	42.6–43.8	39.5	103.8	42.6	46.3
Prealanal length	67.6	180.0	73.2–76.7	72.6	190.8	69.6	76.1
Snout length	8.2	21.8	9.5–10.5	7.8	20.5	10.0	9.3
Eye diameter	10.1	26.8	9.6–12.5	11.0	28.8	9.4	11.7
Interorbital length	13.6	36.3	13.4–14.1	12.0	31.6	11.2	11.7
Upper-jaw length	25.6	68.1	26.3–30.4	25.9	68.2	24.9	26.1
Lower-jaw length	26.8	71.3	28.6–31.1	26.2	68.8	24.2	26.1
HF1	3.2	8.4	N/A	4.2	11.0	N/A	3.7
HF2	6.7	17.8	41.0–44.2	6.1	16.1	N/A	N/A
Postorbital length	18.5	49.3	22.0–22.4	19.6	51.4	18.8	18.4
P length	24.8	66.1	25.2–34.0	33.2	87.4	27.8	28.2
D–P length	32.9	87.5	N/A	36.0	94.5	N/A	N/A
D–V length	48.8	130.0	N/A	46.2	121.4	N/A	N/A
Body height	49.4	131.4	53.2–55.6	47.7	125.3	46.4	50.9
V length	18.5	49.4	N/A	21.3	56.1	19.5	23.0
V spine length	13.9	36.9	N/A	16.4	43.1	N/A	N/A
P–V length	14.3	38.1	15.8–18.3	10.7	28.0	N/A	10.4
D–A length	49.5	131.7	N/A	50.5	132.6	N/A	N/A
V–A length	32.1	85.6	35.5–42.4	39.3	103.4	38.7	36.8
D length	38.2	101.7	36.0–38.3	36.8	96.7	37.9	40.5
D height	18.0	48.0	N/A	broken		N/A	N/A
1 <sup>st</sup> D spine length	4.9	12.9	2.9–4.7	4.3	11.3	N/A	N/A
2 <sup>nd</sup> D spine length	7.2	19.1	4.1–8.9	7.0	18.5	N/A	N/A
Last D spine length	12.4	32.9	12.1–17.6	16.9	44.3	N/A	N/A
A length	15.8	42.1	15.8–18.3	17.8	46.7	16.1	19.0
A height	15.0	39.8	N/A	12.7	33.3	N/A	N/A
3 <sup>rd</sup> A spine length	9.7	25.7	7.7–13.3	12.4	32.6	N/A	N/A
Postanal length	23.1	61.5	N/A	22.5	59.1	N/A	20.9
Postdorsal length	27.3	72.6	N/A	22.7	59.8	N/A	23.9
Caudal-peduncle height	11.5	30.6	12.5–13.0	11.1	29.2	11.6	9.6
C length	25.4	67.5	N/A	broken		N/A	N/A
Longest GR	7.1	18.9	N/A	6.7	17.6	7.0	7.4
Gill filament at angle	2.4	6.3	N/A	1.9	4.9	N/A	N/A
Longest pseudobranchial filament	4.4	11.6	N/A	3.8	10.0	N/A	4.3

**Remarks.** Our specimen was identified as *H. robustispinus* by having thickened fin spines, a short pectoral fin that does not reach the vertical through the anal-fin origin, and a black oral cavity (Moore and Dodd 2010). *Hoplostethus robustispinus* can be separated from other co-occurring species in Taiwan based on its thickened fin spines, a distinct character for this species.



**Figure 4.** *Hoplostethus robustispinus* Moore & Dodd, 2010, FRIP 01364, 241 mm SL, South China Sea, Taiwan.

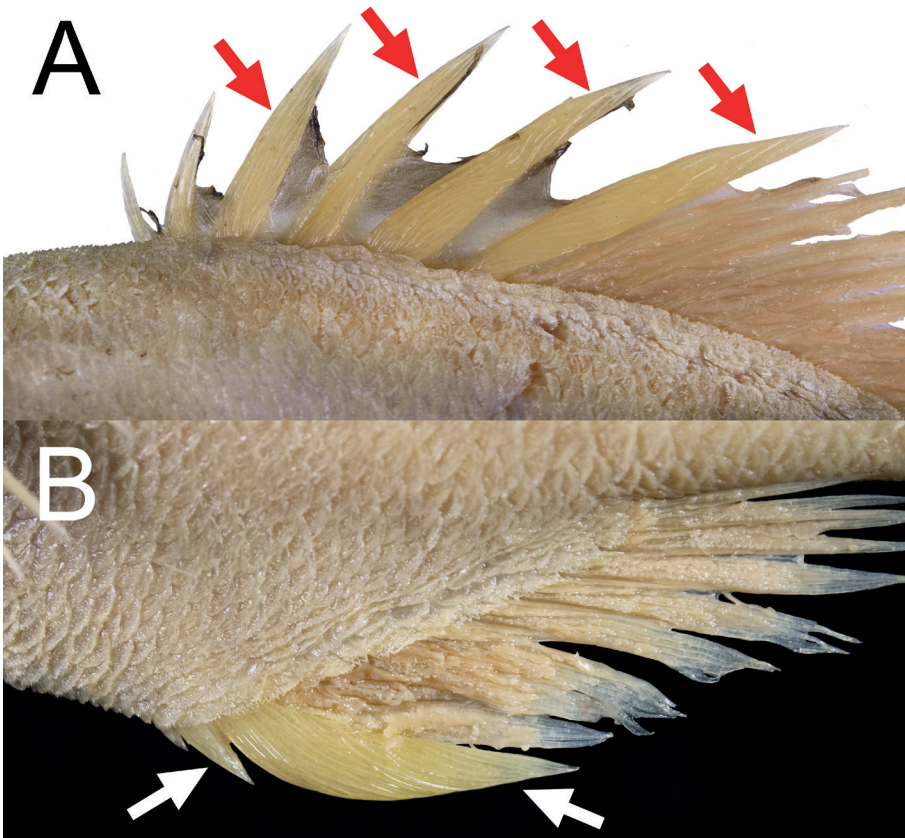


**Figure 5.** *Hoplostethus robustispinus*, FRIP 01364, 241 mm SL, showing thickened dorsal- (A) and anal- (B) fin spines (arrowed), and coloration of membranes between dorsal-fin spines (A).

Furthermore, our specimen has minor differences in meristic characters and body proportions compared to all known specimens (Moore and Dodd 2010; Kotlyar 2011) (Tables 1, 2), all of which can be attributed to intraspecific variation. Notably, it was stated that the holotype of *H. robustispinus* lacks black pigmentation on the membranes of the spinous dorsal fin, and Kotlyar (2011) stated that his specimen was reported as light-colored in his previous publication (Kotlyar 1986). However, our specimen possesses this character (Fig. 5A). This character must be confirmed when additional specimens are available.

### ***Hoplostethus crassispinus* Kotlyar, 1980**

Figs 6, 7; Tables 3, 4

Chinese name: 重胸燧鯛

*Hoplostethus crassispinus* Kotlyar, 1980: 1055 (type locality: Emperor Seamount Chain, Northwest Pacific, 31°05'00"N–32°01'00"N, 173°10'00"E–175°55'00"E, depth 280–360 m)–Kotlyar 1986: 127 (new record from Kyushu-Palau Ridge, 25°08'00"N, 135°41'10"E, depth 560–600 m); Kotlyar 1996: 152; Moore and Dodd 2010: 138; Kotlyar 2011: 152; Roberts and Gomon 2012: 341; Su et al. 2022: 10.

*Hoplostethus* sp.–Koeda et al. 2021: 17, fig. 5H (Ritto Seamount, western Mariana Ridge, western Pacific, 21°37'00"N–21°57'00"N, 141°53'00"E–142°13'00"E, depth 538 m).

**Material examined.** ASIZP 0065017, 86.3 mm SL, off the coast of Nanfang-ao fishing port, Yilan, northeastern Taiwan (ca 24°34'53.16"N, 121°52'12.21"E), 27 June 2004, bottom trawl, collected by H.-C. Ho.

**Description of ASIZP 0065017.** Meristic and morphometric data are provided in Tables 3, 4.

Dorsal-fin rays VI, 13; pectoral-fin rays 17/15; pelvic-fin rays I, 6/I, 6; anal-fin rays III, 9; principal caudal-fin rays 10+9, uppermost and lowermost rays unbranched; procurrent caudal-fin rays 7 dorsally and 7 ventrally; gill rakers on outer surface of first gill arch 5+1+12=18; lateral-line scales 28; predorsal scales 23; abdominal scutes 15; vertebrae 11+16=27; pseudobranchial filaments 24; branchiostegal rays 8; supraneural and pterygiophore insertion formula: 0/0/2+1/1/1/1 (spinous dorsal fin only).

Body oblong, distinctly longer than deep, depth at dorsal-fin origin 1.9 in SL. Head large, its length 2.7% in SL, its height slightly smaller than its length, 0.9% in HL; upper profile in front of dorsal fin rounded, slightly curved to back of head, with somewhat rounded forehead, and abrupt downturn above maxilla; forehead broad, HF1 9.4 and HF2 6.0 in HL; eyes rather large, 2.9 in HL; snout length 5.2 in HL; space between eyes convex and broad, interorbital width 3.3 in HL; crests on head bones well developed and covered with very tiny spinules.

Mouth large, posterior end of maxilla slightly reaching beyond vertical through posterior margin of eye. Nostrils right before anterior margin of eye, slightly higher



**Figure 6.** *Hoplostethus crassispinus* Kotlyar, 1980, ASIZP0065017, 86.3 mm SL, Yilan, Taiwan.

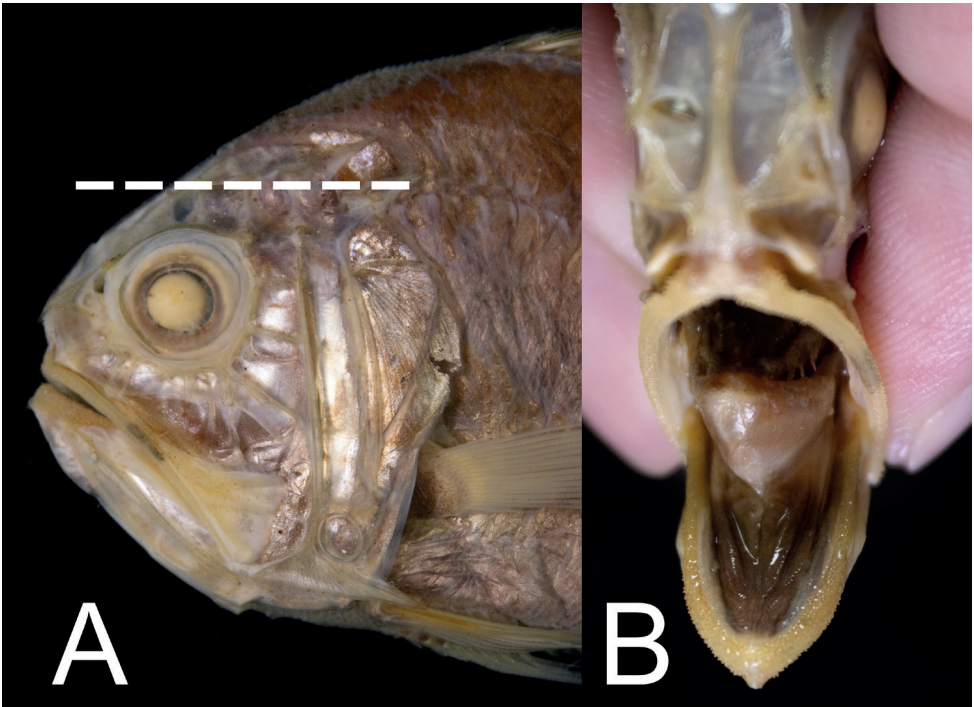


**Figure 7.** *Hoplostethus crassispinus*, ASIZP0065017, 86.3 mm SL **A** relative position of the eye and the horizontal level of lateral-line origin (white dashed line) **B** coloration of the oral cavity. Images not to scale.

than horizontal through center of eye; posterior nostril distinctly larger than anterior nostril; eyes rather ventrally placed, upper margin of eye distinctly lower than horizontal through lateral-line origin (Fig. 7A).

**Table 3.** Meristic data of *Hoplostethus crassispinus*. Data of type and other specimens were obtained from Kotlyar (1980) and Kotlyar (1986). Paired-fin characters are presented as left/right.

	<i>Hoplostethus crassispinus</i>		
	This study	Kotlyar (1980)	Kotlyar (1986)
	ASIZP 0065017	Types and non-types	All specimens (n = 16)
Dorsal-fin elements	VI, 13	VI–VII, 12–13	VI–VII, 12–13
Pectoral-fin elements	17/15	16–17	15–17
Pelvic-fin elements	I, 6/I, 6	I, 6	I, 6
Anal-fin elements	III, 9	III, 9	III–IV, 8–9
Gill rakers	5+1+12=18	6+1+11–13=18–20	6+1+11–13=18–20
Pseudobranchial filaments	27	N/A	23–28
Lateral-line scales	28	27–29	28–30
Abdominal scutes	15	11–15	10–15
Predorsal scales	23	N/A	21–23
Pyloric caeca	N/A	40–50	40–50
Vertebrae	11+16=27	10+16=26	10+16=26

Most of lateral and medial surfaces of premaxilla and dentary covered with villiform teeth; no teeth at symphyseal notch of premaxilla and knob at symphysis of dentaries. Narrow band of villiform teeth on palatine; vomer toothless. Gill rakers on first and second arch rod-shaped, laterally compressed; those in outer row of first arch longest; those on inner row of first arch and both inner and outer rows of second to fourth arches short.

Preopercular spine rather long, its tip reaching pelvic-fin base. Longest gill raker 1.4 in eye diameter; gill filaments at angle of first gill arch very short, ca 6.2 in eye diameter, and ca 1.9 in length of longest pseudobranchial filaments.

Body scales firmly attached, cycloid scales present on pectoral-fin region, elsewhere covered with ctenoid scales; isthmus and gular region naked; lateral-line scales enlarged, ca 2–3 times size of body scales; center of each lateral-line scale without distinct spine; enlarged scales (scutes) covering abdomen region, their bases covered with body scales, all scutes with single tip; predorsal scales enlarged and forming ridge.

Dorsal-fin spines progressively longer posteriorly, greatest increase in length from first to third spine; first ray unbranched, others branched; outer margin of dorsal-fin rays nearly straight. Pectoral fin truncated, slightly rounded; rather long, reaching to third anal-fin spine. Pelvic fin rather long, reaching 14<sup>th</sup> abdominal scute.

**Coloration.** Preserved specimen yellowish-brown (Fig. 6); all fin spines paler than body color. Membranes between dorsal-fin spines with black pigmentations. Oral cavity, including underside of tongue mostly black, with some portions slightly whitish (Fig. 7B). Inner side of opercle and peritoneum black. A recent study documented a reddish body color with a silvery abdomen (Koeda et al. 2021: 10).

**Distribution.** Originally described from the Emperor Seamount Chain (Kotlyar 1980) and subsequently recorded from the Kyushu-Palau Ridge (Kotlyar 1986). Although Kotlyar (2011) stated that this species may be restricted to these areas, our specimen confirmed the species' westward extension.

**Table 4.** Morphometric data of *Hoplostethus crassispinus*. Data of type and other specimens were obtained from Kotlyar (1980) and Kotlyar (1986). Abbreviations: A, anal-fin; C, caudal-fin; D, dorsal-fin; GR, gill raker; HF, forehead height; HL, head length; HT, holotype; NT, non-type; P, pectoral-fin; V, pelvic-fin.

	This study		Kotlyar (1980)	Kotlyar (1986)
	ASIZP 0065017		HT (PT; NT) (n = 5)	All specimens (n = 16)
SL (mm)	89.3		192 (136–161)	135–254
	%SL	%HL	%SL	%SL
HL	37.5		37.5 (36.0–37.1)	34.3–37.8
Head depth	40.6	108.1	41.6 (37.8–40.0)	37.8–44.0
Predorsal length	47.4	126.2	48.9 (46.4–47.5)	45.3–50.4
Prepectoral length	35.4	94.3	36.4 (36.8–39.2)	36.4–40.4
Prepelvic length	36.1	96.2	41.1 (40.4–45.0)	38.3–45.0
Prenal length	64.5	171.7	66.6 (66.9–73.3)	66.6–74.6
Snout length	7.2	19.1	9.4 (8.8–10.7)	7.9–10.7
Eye diameter	12.9	34.3	10.9 (11.0–11.4)	9.6–13.1
Interorbital length	11.5	30.7	11.4 (9.9–11.0)	9.9–12.0
Upper-jaw length	26.5	70.5	26.5 (24.4–26.0)	24.2–27.4
Lower-jaw length	26.7	71.1	27.0 (24.4–26.4)	24.2–27.8
HF1	4.0	10.6	3.1 (2.8–3.7)	2.5–4.5
HF2	6.2	16.6	N/A	N/A
Postorbital length	18.8	50.1	17.2 (14.7–16.3)	14.6–17.4
P length	30.6	81.4	30.2 (26.4–30.1)	25.6–30.9
D–P length	36.5	97.3	N/A	N/A
D–V length	50.5	134.6	N/A	N/A
Body height	52.4	139.5	51.5 (47.8–51.4)	47.8–53.7
V length	25.1	66.9	21.9 (18.6–22.5)	N/A
V spine length	18.7	49.8	N/A	N/A
P–V length	11.0	29.3	10.9 (8.8–11.2)	8.8–12.6
D–A length	54.4	144.9	N/A	N/A
V–A length	32.2	85.8	29.1 (27.1–37.3)	27.1–37.9
D length	40.7	108.4	40.0 (37.8–40.0)	37.0–42.2
D height	21.2	56.6	N/A	N/A
1 <sup>st</sup> D spine length	7.9	20.9	N/A	N/A
2 <sup>nd</sup> D spine length	broken		N/A	N/A
Last D spine length	20.2	53.8	N/A	N/A
A length	19.6	52.3	20.8 (18.6–20.6)	17.7–20.8
A height	16.1	42.8	N/A	N/A
3 <sup>rd</sup> A spine length	14.2	37.7	N/A	N/A
Postanal length	24.6	65.6	24.4 (21.4–24.2)	N/A
Postdorsal length	27.9	74.3	25.4 (24.3–25.7)	N/A
Caudal-peduncle height	13.4	35.8	14.0 (13.6–14.0)	N/A
C length	35.5	94.5	N/A	N/A
Longest GR	9.0	23.9	6.8 (6.2–6.6)	5.1–9.9
Gill filament at angle	2.1	5.5	N/A	N/A
Longest pseudobranchial filament	3.9	10.5	N/A	3.5–4.2

**Remarks.** The present specimen is identified as *H. crassispinus* by having a lower eye position, with the upper margin of the eye distinctly below the horizontal through lateral-line origin, a moderately long pectoral fin, with its end slightly exceeding the vertical through anal-fin origin, a blackish oral cavity, including the underside of the tongue, 15 or 17 pectoral-fin rays, and 18 total gill rakers. It can be distinguished from other Tai-

wanese species by its ventrally positioned eye, the upper margin of which is clearly below the horizontal through lateral-line origin (vs a more dorsally placed eye, the upper margin of the eye at the same horizontal through lateral-line origin in all species in Taiwan).

Although this species has long been thought to be part of the ichthyofauna of Taiwan (e.g., Shen et al. 1993; Shen and Wu 2011; Koeda 2019), the figures of these studies treated as “*H. crassispinus*” appear to be an undescribed species (*H. sp.*, in Su et al. 2022). *Hoplostethus crassispinus* differs from *H. sp.* in having total gill rakers 18–20 (vs 20–22 in *H. sp.*); predorsal scales 21–23 (vs 15–19); pyloric caeca 40–50 (vs 36); oral cavity blackish in adults (vs oral cavity whitish in adults); upper margin of the eye clearly below the horizontal through lateral-line origin (vs at the same horizontal level); gular region naked (vs gular region covered with ctenoid scales). As mentioned previously, the taxonomic study by Dr M. Gomon is ongoing, and we will await the publication of his findings (Su et al. 2022).

Compared to the morphological data provided by Kotlyar (1980, 1986), our specimen has very slight variations. Due to the fact that all other specimens are significantly larger than ours (135–254 vs 86.3 mm SL), these differences can be attributed to intraspecific variation. We discovered that an additional 136 mm SL specimen was used in Kotlyar’s (1980) description, but did not appear as a registered specimen anywhere in the article; therefore, this specimen is considered non-type material.

### Key to species of the subgenus *Hoplostethus* in Taiwan

- 1 Tip of caudal fin blackish..... *H. japonicus*
- Tip of caudal fin without or with very little black pigmentation ..... 2
- 2 Upper margin of eye below a horizontal through the lateral-line origin.....  
.....*H. crassispinus*
- Upper margin of eye on a horizontal through the lateral-line origin..... 3
- 3 Predorsal scales with the same size as adjacent body scales... *H. grandperrini*
- Predorsal scales enlarged, forming a distinct ridge ..... 4
- 4 Gular region covered with scales; oral cavity pale in adults .....  
..... *H. sp. (sensu Su et al. 2022)*
- Gular region naked; oral cavity blackish in adults ..... 5
- 5 Snout length 7.8–10.0% SL; caudal-fin base without brownish margin .....  
..... *H. robustispinus*
- Snout length 6.7–7.4% SL; caudal-fin base with brownish margin ..... *H. roseus*

### Acknowledgements

We thank J.-F. Huang, R.-Y. Hung, and S.-L. Ng for various contributions; S.-P. Huang (ASIZP), M.-Y. Lee, S.-C. Chuang, and S.-M. Yeh (FRIP) for specimen loans under their care; C.-W. Chang (NAMR) for providing useful information on the specimen of *H. grandperrini*; and P.-N. Lee and T.-W. Wu for curatorial assistance.

## Reference

- Chen JTF (1969) A Synopsis of the Vertebrates of Taiwan (Vol. 1). Commercial Books, Taipei, 548 pp.
- Cuvier G, Valenciennes A (1829) Histoire Naturelle des Poissons. Tome Quatrième. Livre Quatrième. Des Acanthoptérygiens à Joue Cuirassée. F.G. Levrault, Paris. v. 4: [i–xxvi +] 2 pp. [+ 1–518, pls 72–99, 97 bis.]
- Grandperrin R, Lehodey P (1992) Campagne BERYX 2 de pêche au chalut de fond sur trois monts sous-marins du Sud-Est de la Zone Economique de Nouvelle Calédonie (N.O. “Alis”, 22–31 octobre 1991). ORSTOM Rapports de Missions Sciences de la Mer. Biologie Marine 11: 1–40.
- Koeda K (2019) Family Trachichthyidae. In: Koeda K, Ho H-C (Eds) Fishes of Southern Taiwan. National Marine Museum of Biology and Aquarium, Checheng, 1400 pp.
- Koeda K, Takashima S, Yamakita T, Tsuchida S, Fujiwara Y (2021) Deep-sea fish fauna on the seamounts of southern Japan with taxonomic notes on the observed species. Journal of Marine Science and Engineering 9(11): e1294. <https://doi.org/10.3390/jmse9111294>
- Kotlyar AN (1980) A new species of the genus *Hoplostethus* (Trachichthyidae, Beryciformes) from the north-west Pacific. Zoologicheskii Zhurnal [Зоологический журнал] 59(7): 1054–1059. [In Russian]
- Kotlyar AN (1986) Systematics and distribution of species of the genus *Hoplostethus* Cuvier (Beryciformes, Trachichthyidae). Trudy Instituta Okeanologii Imeni P.P. Shirshova 121: 97–140. [In Russian]
- Kotlyar AN (1996) Beryciform Fishes of the World Ocean. VNIRO Publishing, Moscow, 368 pp. [In Russian]
- Kotlyar AN (2011) *Hoplostethus robustispinus* (Trachichthyidae) from the South China Sea. Journal of Ichthyology 51(6): 484–486. <https://doi.org/10.1134/S0032945211040096>
- Moore JA, Dodd KA (2010) A new species of the roughy genus *Hoplostethus* (Teleostei: Trachichthyidae) from the Philippines. Bulletin – Peabody Museum of Natural History 51(1): 137–144. <https://doi.org/10.3374/014.051.0103>
- Parr AE (1933) Deepsea Berycomorphi and Percomorphi from the waters around the Bahama and Bermuda islands (Scientific results of the third oceanographic expedition of the “Pawnee” 1927). Bulletin of the Bingham Oceanographic Collection Yale University 3(6): 1–51.
- Roberts CD, Gomon MF (2012) A review of giant roughies of the genus *Hoplostethus* (Beryciformes, Trachichthyidae), with descriptions of two new Australasian species. Memoirs of the Museum of Victoria 69: 341–354. <https://doi.org/10.24199/j.mmv.2012.69.08>
- Shen S-C [Ed.], Chen C-H, Lee S-C, Shao K-T, Mok H-K, Tseng C-S (1993) Fishes of Taiwan. Department of Zoology, National Taiwan University, Taipei, 960 pp.
- Shen S-C, Wu K-Y (2011) Fishes of Taiwan. National Museum of Marine Biology and Aquarium, Pingtung, 896 pp.
- Su Y, Lin H-C, Ho H-C (2022) *Hoplostethus roseus*, a new roughy fish from the western Pacific based on morphology and DNA barcoding (family Trachichthyidae). Journal of Fish Biology 101(3): 441–452. <https://doi.org/10.1111/jfb.15086>



# A new Asian leaf litter toad of the genus *Leptobrachella* (Amphibia, Anura, Megophryidae) from central south China

Jing Liu<sup>1\*</sup>, Shengchao Shi<sup>2\*</sup>, Shize Li<sup>1,2</sup>, Mengfei Zhang<sup>3</sup>,  
Sunjun Xiang<sup>4</sup>, Gang Wei<sup>5</sup>, Bin Wang<sup>2</sup>

**1** Department of Resources and Environment, Moutai Institute, Renhuai 564500, China **2** Chengdu Institute of Biology, Chinese Academy of Sciences, Chengdu 610041, China **3** Central South Inventory and Planning Institute of National Forestry and Grassland Administration, Changsha, Hunan 410014, China **4** College of Biological and Food Engineering, Huaihua University, Huaihua 418000, China **5** Biodiversity Conservation Key Laboratory, Guiyang College, Guiyang 550002, Guizhou, China

Corresponding author: Bin Wang ([wangbin@cib.ac.cn](mailto:wangbin@cib.ac.cn))

Academic editor: A. Crottini | Received 27 April 2022 | Accepted 23 January 2023 | Published 22 February 2023

<https://zoobank.org/6477696F-3600-4CA3-A1F2-A25715E64BFB>

**Citation:** Liu J, Shi S, Li S, Zhang M, Xiang S, Wei G, Wang B (2023) A new Asian leaf litter toad of the genus *Leptobrachella* (Amphibia, Anura, Megophryidae) from central south China. ZooKeys 1149: 103–134. <https://doi.org/10.3897/zookeys.1149.85895>

## Abstract

A new species of the Asian leaf litter toad genus *Leptobrachella* from central south China is described. Molecular phylogenetic analyses, based on mitochondrial 16S rRNA and nuclear RAG1 gene sequences indicated the new species as an independent clade in the genus. The new species could be distinguished from its congeners by a combination of the following characters: body of medium size (SVL 29.2–34.2 mm in 15 adult males and 34.4–43.1 mm in seven adult females); distinct black spots present on flanks; toes rudimentary webbed, with wide lateral fringes; ventral belly white with distinct nebulous brown speckling on ventrolateral flanks; skin on dorsum shagreened with fine tiny granules or short ridges; iris copper above, silver below; heels overlapped when thighs are positioned at right angles to the body; tibia-tarsal articulation reaches the middle eye; dorsal surface of tadpole semi-transparent light brown, spots on tail absent, keratodont row formula I: 3+3/2+2; I; call series basically consist of repeated long calls, at dominant frequency ( $5093 \pm 412$  Hz).

## Keywords

China, molecular phylogenetic analyses, morphology, new species, taxonomy

\* These authors contributed equally to this work.

## Introduction

The Asian leaf litter toads of the genus *Leptobranchella* Smith, 1925 (Anura, Megophryidae) are widely distributed from southern China west to north-eastern India and Myanmar, through mainland Indochina to peninsular Malaysia and the island of Borneo (Chen et al. 2018; Frost 2022). The toads inhabit the forest floor in montane evergreen forest. The taxa in the group had been classified into different genera, i.e. *Paramegophrys* Liu, 1964, *Carpophrys* Sichuan Biological Research Institute, 1977, *Leptolalax* Dubois, 1980, *Lalax* Delorme, Dubois, Grosjean & Ohler, 2006 and *Lalos* Dubois, Grosjean, Ohler, Adler & Zhao, 2010. Based on large-scale molecular phylogenetic analyses on this group, Chen et al. (2018) suggested that the above genera were synonymised with *Leptobranchella*. Currently, the genus *Leptobranchella* contains 95 species, of which, as noted, 34 species were described in the last five years (Frost 2022). The species diversity in the genus was indicated to be much underestimated and many cryptic species have not been described until now (Chen et al. 2018).

In recent years, we carried out a series of biodiversity surveys in Hunan and Guizhou Provinces, China and collected some specimens of *Leptobranchella*. Morphological comparisons, molecular phylogenetic analyses and bioacoustic comparisons consistently indicated these specimens as an undescribed species. We describe it herein as a new species.

## Materials and methods

### Specimens

A total of 22 specimens of the new species (Suppl. material 1) were collected from Tongdao and Suining County, Hunan Province and Congjiang County, Guizhou Province, China (Fig. 1). After taking photographs, they were euthanised using isoflurane and then the specimens were fixed in 10% buffered formalin. Tissue samples were taken and preserved separately in 95% ethanol prior to fixation. Specimens were deposited in Chengdu Institute of Biology, the Chinese Academy of Sciences (CIB, CAS), China.

### Molecular phylogenetic analyses

A total of 15 samples of the new species were used for molecular analyses (Table 1). For phylogenetic analyses, the corresponding gene sequences for all those related species, for which comparable sequences were available, were also downloaded from GenBank (Table 1), based on previous studies (Chen et al. 2018; Shi et al. 2021). Corresponding sequences of one *Leptobranchium huashen* Fei & Ye, 2005 and one *Megophrys glandulosa* (Fei, Ye & Huang, 1990) were downloaded and used as outgroups.

Total DNA was extracted using a standard phenol-chloroform extraction protocol (Sambrook et al. 1989). The mitochondrial 16S rRNA gene and nuclear DNA

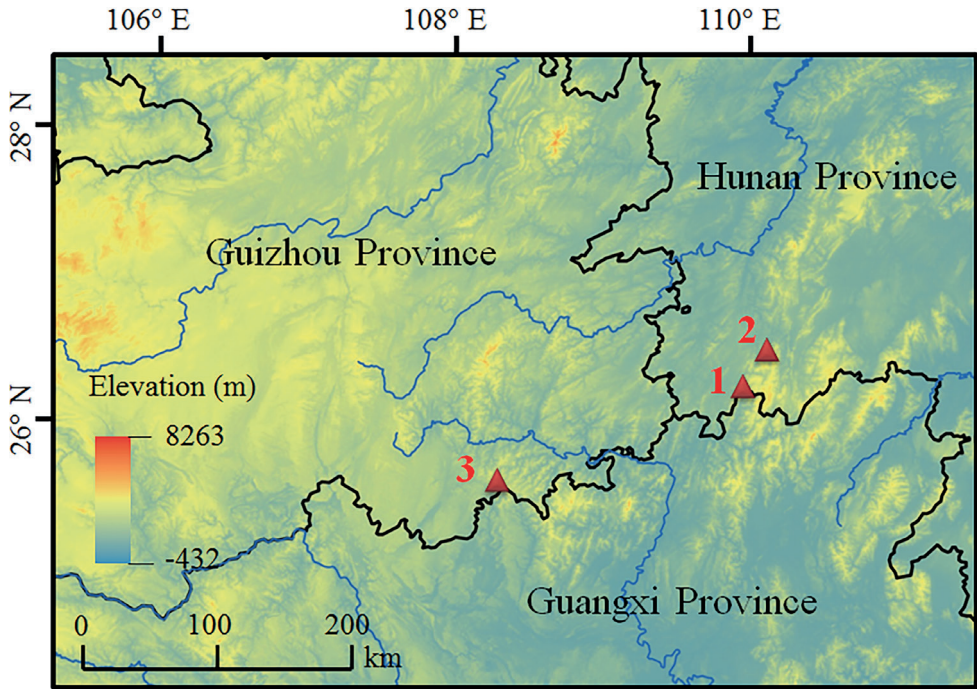


**Figure 1.** Sampling localities in this study. Localities 1–3 were all in China: 1, Tongdao County, Hunan Province; 2, Suining County, Hunan Province; 3, Congjiang County, Guizhou Province, China.

recombination activating gene 1 (RAG1) were amplified and the primers P7 (5'-CGC-CTGTTTACCAAAAACAT-3') and P8 (5'-CCGGTCTGAACTCAGATCACGT-3') for 16S were used following Simon et al. (1994) and RAG1\_F (5'-AGCTGCAGY-CARTACCAYAARATGTA-3') and RAG1\_R (5'-GCAAAGTTTCCGTTTCATTCT-CAT-3') for RAG1 were used following Mauro et al. (2004). Gene fragments were amplified under the following conditions: an initial denaturing step at 95 °C for 4 min; 36 cycles of denaturing at 95 °C for 30 sec, annealing at 51 °C/54 °C (16S/ RAG1) for 30 sec and extension at 72 °C for 70 sec, followed by a final extending step at 72 °C for 10 min. The fragments were sequenced on an ABI Prism 3730 automated DNA sequencer (Applied Biosystems, USA). New sequences were deposited in GenBank (for GenBank accession numbers, see Table 1).

Sequences were assembled and aligned using the Clustalw module in BioEdit v. 7.0.9.0 (Hall 1999) with default settings. Alignments were checked by eye and revised manually, if necessary. For the phylogenetic analyses, we constructed two sequence matrices for reconstructing the phylogenetic trees, i.e. mitochondrial 16S and RAG1 gene datasets. Phylogenetic analyses were conducted using Maximum Likelihood (ML) and Bayesian Inference (BI) methods, implemented in PhyML v. 3.0 (Guindon et al. 2010) and MrBayes v. 3.12 (Ronquist and Huelsenbeck 2003), respectively. We ran jModelTest v. 2.1.2 (Darriba et al. 2012) with Akaike and Bayesian Information

Criteria on the alignment, resulting in the best-fitting nucleotide substitution models of GTR + I + G for the 16S data and GTR + R for the RAG1 data. For the ML tree, branch supports were drawn from 10,000 non-parametric bootstrap replicates. In BI analyses, the parameters for each partition were unlinked and branch lengths were allowed to vary proportionately across partitions. Two runs each with four Markov chains were simultaneously run for 60 million generations with sampling every 1,000 generations. The first 25% trees were removed as the “burn-in” stage followed by calculations of Bayesian posterior probabilities and the 50% majority-rule consensus of the post burn-in trees sampled at stationarity. To detect the haplotype relationships and genetic isolation between the undescribed species and its related species on nuclear DNA, a haplotype network, based on RAG1 gene sequences, was constructed using the maximum parsimony method in TCS v.1.21 (Clement et al. 2000). Finally, genetic distance between *Leptobrachella* species, based on uncorrected *p*-distance model, was estimated on 16S gene using MEGA v.6.06 (Tamura et al. 2013).

## Morphological comparisons

All 22 specimens of the new taxon were measured. The terminology and methods followed Fei and Ye (2005), Mahony et al. (2011), Wang et al. (2019) and Shi et al. (2021). Measurements were made with a dial caliper to the nearest 0.1 mm (Watters et al. 2016) with digital calipers. Fourteen morphometric characters of adult specimens were measured:

- ED** eye diameter (distance from the anterior corner to the posterior corner of the eye);
- FL** foot length (distance from tarsus to the tip of the fourth toe);
- HDL** head length (distance from the tip of the snout to the articulation of jaw);
- HDW** head width (greatest width between the left and right articulations of jaw);
- HLL** hind-limb length (distance from tip of fourth toe to vent);
- IND** internasal distance (minimum distance between the inner margins of the external nares);
- IOD** interorbital distance (minimum distance between the inner edges of the upper eyelids);
- LAL** length of lower arm and hand (distance from the elbow to the distal end of the Finger IV);
- ML** manus length (distance from tip of third digit to proximal edge of inner palmar tubercle);
- SL** snout length (distance from the tip of the snout to the anterior corner of the eye);
- TL** tibia length (distance from knee to tarsus);
- TYD** maximal tympanum diameter;
- UEW** upper eyelid width (greatest width of the upper eyelid margins measured perpendicular to the anterior-posterior axis).

One tadpole specimen of the undescribed species was measured. Nineteen morphometric characters were measured for the tadpole:

<b>BH</b>	maximum body height;
<b>BL</b>	body length, from tip of snout to conjunction of body and tail;
<b>BW</b>	maximum body width;
<b>ED</b>	eye diameter (distance from the anterior corner to the posterior corner of the eye);
<b>IND</b>	internasal distance (minimum distance between the inner margins of the external nares);
<b>KRF</b>	keratodont row formula;
<b>LF</b>	maximum height of lower tail fin;
<b>NE</b>	distance between nostril and eye;
<b>ODW</b>	oral disc width;
<b>PP</b>	interpupilar distance;
<b>RN</b>	rostronarial distance;
<b>SN</b>	snout length, from tip of snout to the anterior corner of eye;
<b>SS</b>	distance from tip of snout to opening of spiracle;
<b>SU</b>	distance from snout to beginning of upper tail fin;
<b>TAL</b>	tail length;
<b>TMH</b>	maximum tail muscle height;
<b>TMW</b>	maximum tail muscle width;
<b>UF</b>	maximum height of upper tail fin;
<b>TH</b>	maximum tail height.

The new taxon was also compared with all other congeners of *Leptobrachella*, based on morphological characters. Comparative morphological data were obtained from literature (Table 2).

### Bioacoustics analyses

The advertisement calls of the new taxon were recorded from specimens CIB SSC1757, CIB SSC1754, CIB SSC1760, CIB LB20220311001, CIB LB20220311002 and CIB ZNY2022012. The advertisement call of the toad was recorded in the stream at ambient air temperature of 11.2–15.0 °C. Sony PCM-D50, Philips VTR 6900 digital sound recorder, Huawei Mate 30E Pro smart phone were used to record within 20 cm of the calling individual. The sound files in wave format were resampled at 48 kHz with sampling depth 24 bits. Terminology of advertisement call analyses and description followed Köhler et al. (2017) and Wang et al. (2019). Call recordings were analysed and visualised by Raven Pro 1.5 software (Cornell Laboratory of Ornithology, Ithaca, NY, USA) (window size 256 points, fast-Fourier transform, Hanning windows). Ambient temperature was taken by a digital hygrothermograph.

### Results

The aligned sequence matrix of 16S and RAG1 gene contained 498 bps and 888 bps, respectively. ML and BI analyses, based on the 16S gene matrix, resulted in essentially identical topologies (Fig. 2). All 15 samples of the undescribed species were clustered into one clade being deeply clustered into the *Leptobrachella* clade and seemly being sister to a clade comprising of *L. graminicola* and *L. yeae* (Fig. 2A). ML and BI analyses, based on the RAG1 gene matrix, also resulted in essentially identical topologies (Fig. 2B). In the RAG1 tree, eleven samples of the undescribed species were clustered together into an independent clade which was distantly divergent from other congeners. Four haplotypes were found for eleven samples of the undescribed species in the

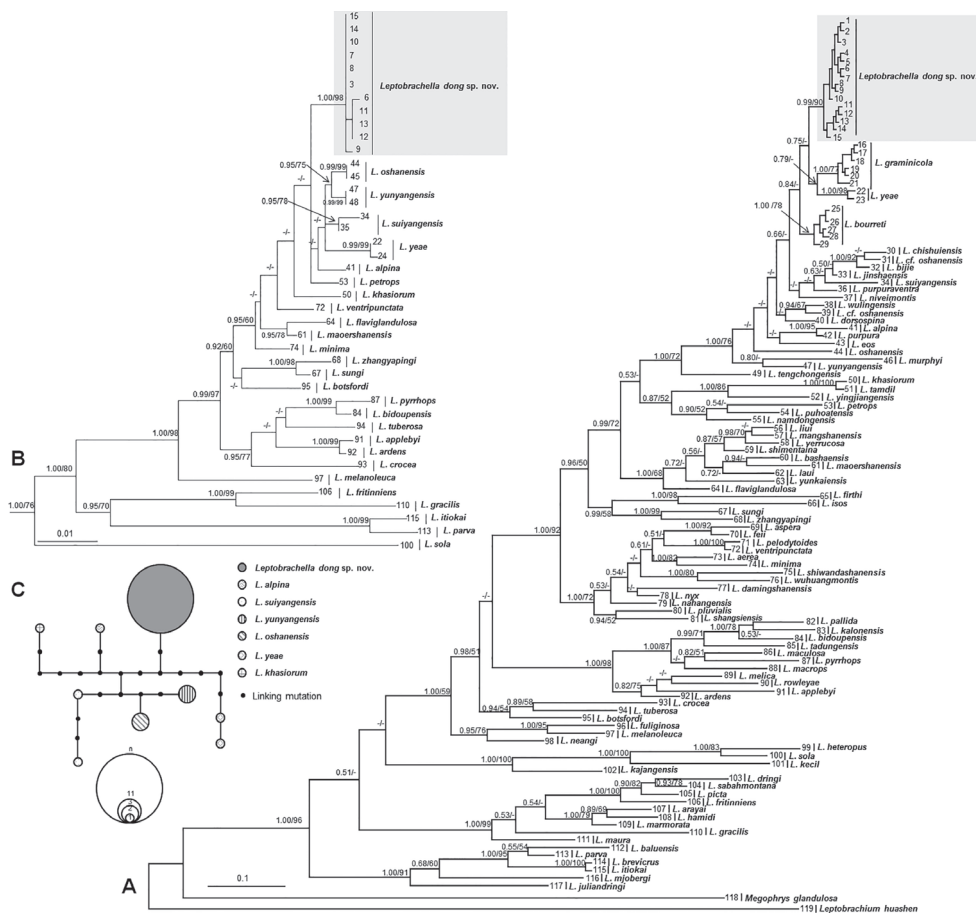


**Figure 2.** Phylogenetic trees of the genus *Leptobrachella* and a haplotype network constructed based on RAG1 gene sequences **A** maximum Likelihood (ML) tree reconstructed, based on mitochondrial 16S gene sequences **B** maximum Likelihood tree reconstructed, based on nuclear RAG1 gene sequences. Bayesian posterior probabilities (BPP) from BI analyses/ bootstrap supports (BS) from ML analyses are listed beside the nodes. The symbol “-” represents a value below 0.50/50. For information of samples 1–119, refer to Table 1 **C** the haplotype network constructed, based on RAG1 gene sequences.

RAG1 gene and there was no common haplotype between the undescribed species and its related species (Fig. 2C). The genetic distance of the *p*-distance model on the 16S gene within the specimens of the undescribed species ranged from 0.0% to 0.4%, being much lower than the interspecific genetic distance (all higher than 1.8%; Suppl. material 2). The smallest pairwise genetic divergence between the undescribed species and its congeners is 2.2% (vs. *L. bourreti*), being higher than or at the same level with that between some pairs of related species, such as *L. bijie* and *L. jinshaensis* (2.0%), *L. purpuraventra* and *L. jinshaensis* (2.1%).

The undescribed species could be identified from its congeners in a series of morphological and bioacoustics characters. For the detailed demonstration, based on morphological and bioacoustics comparisons, see the following section describing the new species.

Molecular phylogenetic analyses, morphological comparisons and bioacoustics analyses indicated that the specimens from Tongdao and Suining County, Hunan Province and Congjiang County, Guizhou Province, China represent an undescribed species which is described as follows.

## Taxonomic account

### *Leptobrachella dong* sp. nov.

<https://zoobank.org/EECEF9D0-E00F-49E3-B576-8E3A11C688DB>

Figs 3–5; Tables 1–4; Suppl. materials 1–3

**Type materials. Holotype.** CIB SSC1757, adult male (Figs 3, 4), collected by Shengchao Shi in Tongdao County (26.206674°N, 109.952695°E, ca. 790 m a.s.l.), Hunan Province, China on 2 April 2017.

**Paratypes.** Four adult males CIB SSC1754, CIB SSC1758, CIB SSC1759, CIB SSC1760, one adult female CIB SSC1755 and one tadpole CIB WB2020277 from the same place as holotype collected by Sheng-Chao Shi. Two adult males CIB LB20220305001 and CIB LB20220305003 and five adult females CIB LB20220306003, CIB LB20220306005, CIB LB20220305010, CIB LB20220306008 and CIB LB20220306009 collected by Shize Li from Congjiang County (25.572492°N, 108.274189°E, 1200 m a.s.l.), Guizhou Province, China on 6 March 2022. Two adult males CIB LB20220311001 and CIB LB20220311002 collected by Jing Liu from the same place as Congjiang County, Guizhou Province, China on 11 March 2022; One adult female CIB ZNY2022003 and two adult males CIB ZNY2022001 and CIB ZNY2022002 collected by Fu Shu and four adult males CIB ZNY2022010, CIB ZNY2022011, CIB ZNY2022012 and CIB ZNY2022013 collected by Keji Guo from the same place as Suining County (26.401561°N, 110.093467°E, 620 m a.s.l.), Hunan Province, China on 15 March 2022.

**Diagnosis.** *Leptobrachella dong* sp. nov. is assigned to the genus *Leptobrachella*, based on molecular data and the following morphological characters: medium size, rounded finger tips, the presence of an elevated inner palmar tubercle not continuous to the thumb, presence of macroglands on body (including supra-axillary, pectoral and femoral glands), vomerine teeth absent, tubercles on eyelids and anterior tip of snout with vertical white bar (Dubois 1983; Fei et al. 2009).

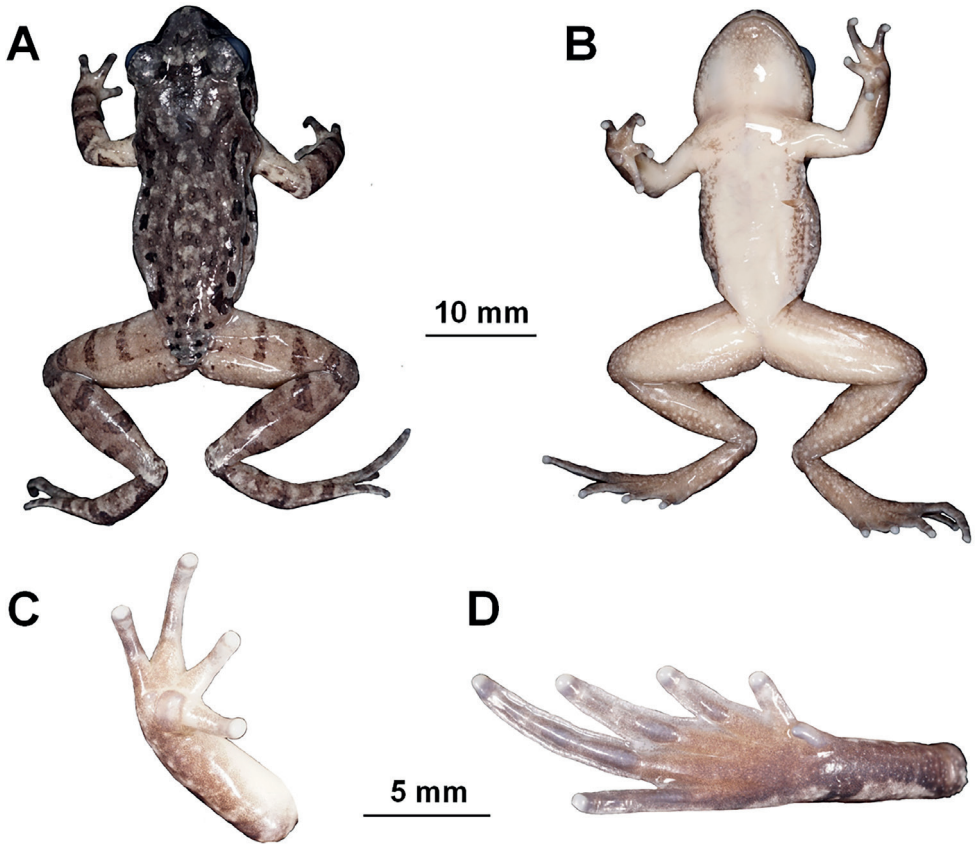


**Figure 3.** The holotype specimen CIB SSC1757 of *Leptobranchella dong* sp. nov. **A** dorsal view **B** ventral view **C** ventral view of hand **D** ventral view of foot.

*Leptobranchella dong* sp. nov. could be distinguished from its congeners by a combination of the following characters: (1) body of medium size (SVL 29.2–32.0 mm in 15 adult males and 37.4–43.1 mm in seven adult females); (2) distinct black spots present on flanks; toes rudimentary webbed, with wide lateral fringes; (3) ventral belly white with distinct nebulous brown speckling on ventrolateral flanks; (4) skin on dorsum shagreened with fine tiny granules or short ridges; (5) heels overlapped when thighs are positioned at right angles to the body; (6) tibia-tarsal articulation reaches the middle eye; (7) dorsal surface of tadpole semi-transparent light brown, spots on tail absent, keratodont row formula I: 3+3/2+2: I; (8) calls with two types, at dominant frequency ( $5.1 \pm 0.4$  kHz).

**Description of holotype.** Adult male. SVL in 32.0 mm. Head width almost equal with head length slightly (HDW / HDL 1.03); snout rounded in both ventral view and lateral view, projecting slightly beyond margin of the lower jaw; nostril closer to snout than eye; loreal region oblique; canthus rostralis indistinct; eyes large (ED / HDL 0.40), eye diameter slightly longer than snout length (ED / SL 1.07), eyes notably protuberant in both dorsal and lateral views, pupil vertical; tympanum distinct, rounded, tympanum diameter smaller than eye (TYD / ED 0.38), upper margin of tympanum in contact



**Figure 4.** Photos of the holotype CIB SSC1757 of *Leptobrachella dong* sp. nov. in life **A** dorsal view **B** ventral view **C** dorsolateral view **D** ventral view of hand **E** ventral view of foot.

with supratympanic ridge; vomerine teeth absent; tongue notched behind; supratympanic ridge distinct, extending from posterior corner of eye to supra-axillary gland.

Fore-limb relatively long (LAL / SVL 0.46), fingers long and slender (ML / SVL 0.25), webbing absent, lateral fringes on fingers narrow; relative finger lengths  $II < I < IV < III$ ; tips of fingers rounded and slightly swollen; subarticular tubercles absent on fingers, inner metacarpal tubercle large and rounded, separated from the smaller, round outer metacarpal; supra-axillary glands oval.

Hind-limb relatively long (HLL / SVL 1.53), heels overlapping when the tibias perpendicular to the body axis; tibio-tarsal articulation of adpressed limb reaching middle of eye, tibia length about half of snout-vent length (TL / SVL 0.49); relative toe length:  $I < II < V < III < IV$ ; toe tips rounded and slightly swollen; rudimentary webbing present between all five toes; wide lateral fringes present on all toes; dermal ridges under fourth toes interrupted; subarticular tubercles distinct under the base of II, III and IV toe; inner metatarsal tubercle oval and distinct, outer metatarsal tubercle absent (Fig. 3C).

**Table 1.** Information for samples used in molecular phylogenetic analyses in this study.

ID	Species	Locality	Voucher number	GenBank accession number	
				16S	RAG1
1	<i>Leptobranchella dong</i> sp. nov.	Tongdao County, Hunan Province, China	CIB SSC1758	OP764529	/
2	<i>Leptobranchella dong</i> sp. nov.	Tongdao County, Hunan Province, China	CIB SSC1757	OP764530	/
3	<i>Leptobranchella dong</i> sp. nov.	Tongdao County, Hunan Province, China	CIB WB2020277	OP764531	OP776448
4	<i>Leptobranchella dong</i> sp. nov.	Tongdao County, Hunan Province, China	CIB SSC1755	OP764532	/
5	<i>Leptobranchella dong</i> sp. nov.	Congjiang County, Guizhou Province, China	CIB LB20220305005	OP764533	/
6	<i>Leptobranchella dong</i> sp. nov.	Congjiang County, Guizhou Province, China	CIB LB20220306008	OP764534	OP776439
7	<i>Leptobranchella dong</i> sp. nov.	Congjiang County, Guizhou Province, China	CIB LB20220311002	OP764535	OP776441
8	<i>Leptobranchella dong</i> sp. nov.	Congjiang County, Guizhou Province, China	CIB LB20220311001	OP764536	OP776440
9	<i>Leptobranchella dong</i> sp. nov.	Congjiang County, Guizhou Province, China	CIB LB20220305001	OP764537	OP776449
10	<i>Leptobranchella dong</i> sp. nov.	Suining County, Hunan Province, China	CIB ZNY2022001	OP764538	OP776442
11	<i>Leptobranchella dong</i> sp. nov.	Suining County, Hunan Province, China	CIB ZNY2022002	OP764539	OP776443
12	<i>Leptobranchella dong</i> sp. nov.	Suining County, Hunan Province, China	CIB ZNY2022010	OP764540	OP776444
13	<i>Leptobranchella dong</i> sp. nov.	Suining County, Hunan Province, China	CIB ZNY2022011	OP764541	OP776445
14	<i>Leptobranchella dong</i> sp. nov.	Suining County, Hunan Province, China	CIB ZNY2022012	OP764542	OP776446
15	<i>Leptobranchella dong</i> sp. nov.	Suining County, Hunan Province, China	CIB ZNY2022013	OP764543	OP776447
16	<i>L. graminicola</i>	Mount Pu Ta Leng, Lao Cai, Vietnam	VNMN 010904	MZ224651	/
17	<i>L. graminicola</i>	Mount Pu Ta Leng, Lao Cai, Vietnam	VNMN 010905	MZ224648	/
18	<i>L. graminicola</i>	Mount Pu Ta Leng, Lao Cai, Vietnam	VNMN 010912	MZ224647	/
19	<i>L. graminicola</i>	Mount Pu Ta Leng, Lao Cai, Vietnam	VNMN 010908	MZ224653	/
20	<i>L. graminicola</i>	Mount Pu Ta Leng, Lao Cai, Vietnam	VNMN 010910	MZ224655	/
21	<i>L. graminicola</i>	Mount Pu Ta Leng, Lao Cai, Vietnam	VNMN 010909	MZ224649	/
22	<i>L. yeae</i>	Linggongli, Mount Emei, Sichuan Province, China	CIBEMGL19052104	MT957006	MT975979
23	<i>L. yeae</i>	Mount Emei, Sichuan Province, China	SYS a001830	KM014810	/
24	<i>L. yeae</i>	Mount Emei, Sichuan Province, China	CIBEM1867	/	MT975978
25	<i>L. bourreti</i>	Mount Pu Ta Leng, Lao Cai, Vietnam	VNMN 010916	MZ209167	/
26	<i>L. bourreti</i>	Bat Xat District, Lao Cai, Vietnam	ZMMU-A5636-02280	MH055872	/
27	<i>L. bourreti</i>	Sapa, Lao Cai Province, Vietnam	AMS R 177673	KR018124	/
28	<i>L. bourreti</i>	Ky Quan San, Lao Cai, Vietnam	AMS R 188515	MZ208835	/
29	<i>L. bourreti</i>	Sapa, Lao Cai, Vietnam	1999.566	KR827860	/
30	<i>L. chishuiensis</i>	Chishui National Nature Reserve, Chishui City, Guizhou Province, China	CIBCS20190518042	MT117054	/
31	<i>L. cf. oshanensis</i>	Changning County, Sichuan Province, China	CIB20050095	KC460337	/
32	<i>L. bijie</i>	Zhaozishan Nature Reserve, Bijie City, Guizhou Province, China	SYS a007314	MK414533	/
33	<i>L. jinshaensis</i>	Lengshuihe Nature Reserve, Jinsha County, Guizhou Province, China	CIB JS20200516001	MT814014	/
34	<i>L. suiyangensis</i>	Huoqiuba Nature Reserve, Suiyang County, Guizhou Province, China	GZNU20180606005	MK829649	OL800396

ID	Species	Locality	Voucher number	GenBank accession number	
				16S	RAG1
35	<i>L. suiyangensis</i>	Huoqiuba Nature Reserve, Suiyang County, Guizhou Province, China	GZNU20180606002	/	OL800395
36	<i>L. purpuraventra</i>	Wujing Nature Reserve, Bijie City, Guizhou Province, China	SYS a007081	MK414517	/
37	<i>L. niveimontis</i>	Daxueshan Nature Reserve, Yunnan Province, China	KIZ015734	MT302618	/
38	<i>L. wulingensis</i>	Tianquanshan Forest Park, Zhangjiajie, Hunan Province, China	CSUFT 177	MT530315	/
39	<i>L. cf. oshanensis</i>	Nanchuan District, Chongqing City, China	ZYC799	AY526215	/
40	<i>L. dorsospina</i>	Yushe Forest Park, Shuicheng County, Guizhou Province, China	SYS a004961	MW046194	/
41	<i>L. alpina</i>	Caiyanghe, Yunnan Province, China	KIZ049024	MH055867	MH056093
42	<i>L. purpura</i>	Yingjiang, Yunnan Province, China	SYS a006530	MG520354	/
43	<i>L. eos</i>	Boun Tay, Phongsaly, Laos	NCSM 80551	MH055887	/
44	<i>L. oshanensis</i>	Baoguoqi, Mount Emei, Sichuan Province, China	CIBEMS20190421BGS1	MT957023	MT975988
45	<i>L. oshanensis</i>	Shengshuige, Mount Emei, Sichuan Province, China	CIBEMS20190422SSG1-4		MT975985
46	<i>L. murphyi</i>	Doi Inthanon, Chiang Mai, Thailand	KIZ034039	MZ710519	/
47	<i>L. yunyangensis</i>	Qiyaoshan Nature Reserve, Yunyang County, Chongqing, China	GZNU20210622001	OL800364	OL800393
48	<i>L. yunyangensis</i>	Qiyaoshan Nature Reserve, Yunyang County, Chongqing, China	GZNU20210622002	/	OL800394
49	<i>L. tengchongensis</i>	Gaoligong Shan, Yunnan Province, China	SYS a004598	KU589209	/
50	<i>L. khasiorum</i>	Khasi Hills, Meghalaya, India	SDBDU 2009.329	KY022303	KY022348
51	<i>L. tamdil</i>	Mizoram, India	MZMU2224	MW665130	/
52	<i>L. yingjiangensis</i>	Yingjiang County, Yunnan Province, China	SYS a006533	MG520350	/
53	<i>L. petrops</i>	Ba Vi National Park, Ha Tay, Vietnam	ROM 13483	MH055901	MH056092
54	<i>L. puboatensis</i>	Pu Hu, Thanh Hoa, Vietnam	VNMN:2016 A.23	KY849587	/
55	<i>L. namdongensis</i>	Thanh Hoa Province, Vietnam	VNUF A.2017.37	MK965389	/
56	<i>L. liui</i>	Wuyi Shan City, Fujian Province, China	SYS a001597	KM014547	/
57	<i>L. mangshanensis</i>	Mangshan, Hunan Province, China	MSZTC201701	MG132196	/
58	<i>L. verrucosa</i>	Lianshan Bijiaoshan Nature Reserve, Guangdong, China	GEP a059	OP279589	/
59	<i>L. shimentaina</i>	Shimentai Nature Reserve, Guangdong, China	SYS a004712	MH055926	/
60	<i>L. bashaensis</i>	Basha Nature Reserve, Congjiang County, Guizhou Province, China	GIB196403	MW136294	/
61	<i>L. maershanensis</i>	Mao'er Shan, Guangxi Province, China	KIZ07614	MH055927	MH056099
62	<i>L. laui</i>	Shenzhen City, Guangdong Province, China	SYS a002450	MH055904	/
63	<i>L. yunkaiensis</i>	Dawuling Forest Station, Maoming City, Guangdong Province, China	SYS a004663	MH605584	/
64	<i>L. flavigliandulosa</i>	Xiaoqiaogou Nature Reserve, Yunnan Province, China	KIZ016072	MH055934	MH056098
65	<i>L. firithi</i>	Quang Nam Province, Vietnam	AMS R 171714	JQ739203	/
66	<i>L. isos</i>	Gia Lai, Vietnam	AMS R 176469	KT824767	/
67	<i>L. sungi</i>	Tam Dao, Vinh Phuc, Vietnam	ROM 20236	MH055858	MH056104
68	<i>L. zhangyapingi</i>	Chiang Mai, Thailand	KIZ07258	MH055864	MH056102
69	<i>L. aspera</i>	Huanglianshan Nature Reserve, Lyuchun, Yunnan, China	SYS a007743	MW046199	/
70	<i>L. feii</i>	Xiaoqiaogou Nature Reserve, Yunnan Province, China	KIZ048894	MT302634	/
71	<i>L. pelodytoides</i>	Tam Dao, Vinh Phu, Vietnam	ROM18282	EF397244	/
72	<i>L. ventripunctata</i>	Wenlong, Yunnan Province, China	KIZ013621	MH055824	MH056090
73	<i>L. aerea</i>	Vilabuly, Savannakhet, Laos	NCSM 76038	MH055809	/
74	<i>L. minima</i>	Doi Phu Fa, Nan, Thailand	KIZ024317	MH055852	MH056091

ID	Species	Locality	Voucher number	GenBank accession number	
				16S	RAG1
75	<i>L. shiwandashanensis</i>	Fangcheng City, Guangxi Province, China	NNU202103146	MZ326691	/
76	<i>L. wuhuangmontis</i>	Pubei County, Guangxi Province, China	SYS a003485	MH605577	/
77	<i>L. damingshanensis</i>	Guangxi Province, China	NNU202103281	MZ145229	/
78	<i>L. nyx</i>	Ha Giang, Vietnam	ROM 36692	MH055816	/
79	<i>L. nabhagensis</i>	Na Hang Nature Reserve, Tuyen Quang, Vietnam	ROM 7035	MH055853	/
80	<i>L. pluvialis</i>	Fansipan, Lao Cai, Vietnam	ROM 30685	MH055843	/
81	<i>L. shangsiensis</i>	Guangxi Province, China	NHMG1401032	MK095460	/
82	<i>L. pallida</i>	Lam Dong, Vietnam	UNS00511	KU530190	/
83	<i>L. kalonensis</i>	Binh Thuan Province, Vietnam	AMNH A191762	KR018115	/
84	<i>L. bidoupensis</i>	Bidoup-Nui Ba National Park, Lam Dong, Vietnam	ZMMU-A-4797-01454	MH055945	MH056110
85	<i>L. tadungensis</i>	Dak Nong Province, Vietnam	UNS00515	KR018121	/
86	<i>L. maculosa</i>	Ninh Thuan Province, Vietnam	AMS R 177660	KR018119	/
87	<i>L. pyrrophops</i>	Loc Bac, Lam Dong, Vietnam	ZMMU-A-4873-00158	MH055950	MH056109
88	<i>L. macrops</i>	Phu Yen, Vietnam	ZMMU-A5823	MG787993	/
89	<i>L. melica</i>	Ratanakiri, Cambodia	MVZ258198	HM133600	/
90	<i>L. rowleyae</i>	Da Nang City, Vietnam	ITBCZ2783	MG682552	/
91	<i>L. applebyi</i>	Phong Dien Nature Reserve, Thua Thien-Hue, Vietnam	KIZ010701	MH055947	MH056105
92	<i>L. ardens</i>	Kon Ka Kinh National Park, Gia Lai, Vietnam	ZMMU-NAP-06099	MH055949	MH056108
93	<i>L. crocea</i>	Thua Thien-Hue, Vietnam	ZMMU-NAP-02274	MH055955	MH056114
94	<i>L. tuberosa</i>	Kon Ka Kinh National Park, Gia Lai, Vietnam	ZMMU-NAP-02275	MH055959	MH056111
95	<i>L. botsfordi</i>	Fansipan, Lao Cai, Vietnam	AMS R 176540	MH055952	MH056088
96	<i>L. fuliginosa</i>	Phetchaburi, Thailand	KUHE 20197	LC201988	/
97	<i>L. melanoleuca</i>	Kapoe, Ranong, Thailand	KIZ018031	MH055967	MH056115
98	<i>L. neangi</i>	Veal Veng District, Pursat Province, Cambodia	CBC 1624	MT644613	/
99	<i>L. heteropus</i>	Larut, Perak, Malaysia	KUHE15487	AB530453	/
100	<i>L. sola</i>	Gunung Stong, Kelantan, Malaysia	KU RMB20973	MH055973	MH056119
101	<i>L. kecil</i>	Cameron, Malaysia	KUHE 52440	LC202004	/
102	<i>L. kajangensis</i>	Tioman, Malaysia	LSUHC 4431	LC202001	/
103	<i>L. dringi</i>	Gunung Mulu, Malaysia	KUHE:55610	AB847553	/
104	<i>L. sabahmontana</i>	Borneo, Malaysia	BORNEENSIS 12632	AB847551	/
105	<i>L. picta</i>	Borneo, Malaysia	UNIMAS 8705	KJ831295	/
106	<i>L. fritinniens</i>	Danum Valley Field Center, Sabah, Malaysia	FMNH 244800	MH055971	MH056118
107	<i>L. arayai</i>	Liwagu, Kinabalu, Malaysia	BORNEENSIS 22931	AB847558	/
108	<i>L. hamidi</i>	Bukit Lanjan, Selangor, Malaysia	KUHE17545	AB969286	/
109	<i>L. marmorata</i>	Borneo, Malaysia	KUHE53227	AB969289	/
110	<i>L. gracilis</i>	Bukit Kana, Sarawak, Malaysia	FMNH 273682	MH055972	MH056117
111	<i>L. maura</i>	Borneo, Malaysia	SP 21450	AB847559	/
112	<i>L. baluensis</i>	Tambunan, Sabah, Borneo, Malaysia	SP 21604	LC056792	/
113	<i>L. parva</i>	Mulu National Park, Sarawak, Malaysia	KUHE:55308	LC056791	MH056121
114	<i>L. brevicrus</i>	Gunung Mulu National Park, Sarawak, Malaysia	UNIMAS 8957	KJ831303	/
115	<i>L. itiokai</i>	Mulu National Park, Sarawak, Malaysia	KUHE:5589	LC137805	MH056120
116	<i>L. mjobergi</i>	Gading NP, Sarawak, Borneo, Malaysia	KUHE:47872	LC056787	/
117	<i>L. juliandringi</i>	Mulu NP, Sarawak, Borneo, Malaysia	KUHE 55333	LC056780	/
118	<i>Megophrys glandulosa</i>	Yunnan Province, China	KIZ048439	KX811762	MH056125
119	<i>Leptobranchium huasben</i>	Yunnan Province, China	KIZ049025	KX811931	MH056122

**Table 2.** References for morphological characters for congeners of the genus *Leptobrachella*.

ID	Species	Literature reviewed
1	<i>L. aerea</i> (Rowley, Stuart, Richards, Phimmachak & Sivongxay, 2010)	Rowley et al. (2010c)
2	<i>L. alpina</i> (Fei, Ye & Li, 1990)	Fei et al. (2009)
3	<i>L. applebyi</i> (Rowley & Cao, 2009)	Rowley and Cao (2009)
4	<i>L. arayui</i> (Matsui, 1997)	Matsui (1997)
5	<i>L. ardens</i> (Rowley, Tran, Le, Dau, Peloso, Nguyen, Hoang, Nguyen & Ziegler, 2016)	Rowley et al. (2016)
6	<i>L. aspera</i> Wang, Lyu, Qi & Wang, 2020	Wang et al. (2020)
7	<i>L. baluensis</i> Smith, 1931	Dring (1983); Eto et al. (2016)
8	<i>L. bashaensis</i> Lyu, Dai, Wei, He, Yuan, Shi, Zhou, Ean, Kuang, Guo, Wei & Yuan, 2020	Lyu et al. (2020)
9	<i>L. bidoupensis</i> (Rowley, Le, Tran & Hoang, 2011)	Rowley et al. (2011)
10	<i>L. bijie</i> Wang, Li, Li, Chen & Wang, 2019	Wang et al. (2019)
11	<i>L. bondangensis</i> Eto, Matsui, Hamidy, Munir & Iskandar, 2018	Eto et al. (2018)
12	<i>L. botsfordi</i> (Rowley, Dau & Nguyen, 2013)	Rowley et al. (2013)
13	<i>L. bourreti</i> (Dubois, 1983)	Ohler et al. (2011); Nguyen et al. (2021)
14	<i>L. brevicrus</i> Dring, 1983	Dring (1983); Eto et al. (2015)
15	<i>L. chishuiensis</i> (Li, Liu, Wei & Wang, 2020)	Li et al. (2020)
16	<i>L. crocea</i> (Rowley, Hoang, Le, Dau & Cao, 2010)	Rowley et al. (2010a)
17	<i>L. damingshanensis</i> Chen, Yu, Cheng, Meng, Wei, Zhou & Lu, 2021	Chen et al. (2021b)
18	<i>L. dorsospina</i> Wang, Lyu, Qi & Wang, 2020	Wang et al. (2020)
19	<i>L. dringi</i> (Dubois, 1987)	Inger et al. (1995); Matsui and Dehling (2012)
20	<i>L. eos</i> (Ohler, Wollenberg, Grosjean, Hendrix, Vences, Ziegler & Dubois, 2011)	Ohler et al. (2011)
21	<i>L. feii</i> (Chen, Yuan & Che, 2020)	Chen et al. (2020)
22	<i>L. firthi</i> (Rowley, Hoang, Dau, Le & Cao, 2012)	Rowley et al. (2012)
23	<i>L. flaviglandulosa</i> (Chen, Wang & Che, 2020)	Chen et al. (2020)
24	<i>L. fritinniensis</i> (Dehling & Matsui, 2013)	Dehling and Matsui (2013)
25	<i>L. fuliginosa</i> (Matsui, 2006)	Matsui (2006)
26	<i>L. fusca</i> Eto, Matsui, Hamidy, Munir & Iskandar, 2018	Eto et al. (2018)
27	<i>L. gracilis</i> (Günther, 1872)	Günther (1872); Dehling (2012b)
28	<i>L. graminicola</i> Nguyen, Tapley, Nguyen, Luong & Rowley, 2021	Nguyen et al. (2021)
29	<i>L. hamidi</i> (Matsui, 1997)	Matsui (1997)
30	<i>L. heteropus</i> (Boulenger, 1900)	Boulenger (1900)
31	<i>L. isos</i> (Rowley, Stuart, Neang, Hoang, Dau, Nguyen & Emmett, 2015)	Rowley et al. (2015a)
32	<i>L. itiokai</i> Eto, Matsui & Nishikawa, 2016	Eto et al. (2016)
33	<i>L. jinshaensis</i> Cheng, Shi, Li, Liu, Li & Wang, 2021	Cheng et al. (2021)
34	<i>L. juliandringi</i> Eto, Matsui & Nishikawa, 2015	Eto et al. (2015)
35	<i>L. kajangensis</i> (Grismer, Grismer & Youmans, 2004)	Grismer et al. (2004)
36	<i>L. kalonensis</i> (Rowley, Tran, Le, Dau, Peloso, Nguyen, Hoang, Nguyen & Ziegler, 2016)	Rowley et al. (2016)
37	<i>L. kecil</i> (Matsui, Belabut, Ahmad & Yong, 2009)	Matsui et al. (2009)
38	<i>L. khasiorum</i> (Das, Iron, Rangad & Hooroo, 2010)	Das et al. (2010)
39	<i>L. lateralis</i> (Anderson, 1871)	Anderson (1871); Humtsoe et al. (2008)
40	<i>L. laui</i> (Sung, Yang & Wang, 2014)	Sung et al. (2014)
41	<i>L. liui</i> (Fei & Ye, 1990)	Fei et al. (2009); Sung et al. (2014)
42	<i>L. macrops</i> (Duong, Do, Ngo, Nguyen & Poyarkov, 2018)	Duong et al. (2018)
43	<i>L. maculosa</i> (Rowley, Tran, Le, Dau, Peloso, Nguyen, Hoang, Nguyen & Ziegler, 2016)	Rowley et al. (2016)
44	<i>L. mangshanensis</i> (Hou, Zhang, Hu, Li, Shi, Chen, Mo & Wang, 2018)	Hou et al. (2018)
45	<i>L. maershanensis</i> (Yuan, Sun, Chen, Rowley & Che, 2017)	Yuan et al. (2017)
46	<i>L. marmorata</i> (Matsui, Zainudin & Nishikawa, 2014)	Matsui et al. (2014b)
47	<i>L. maura</i> (Inger, Lakim, Biun & Yambun, 1997)	Inger et al. (1997)
48	<i>L. melanoleuca</i> (Matsui, 2006)	Matsui (2006)
49	<i>L. melica</i> (Rowley, Stuart, Neang & Emmett, 2010)	Rowley et al. (2010b)
50	<i>L. minima</i> (Taylor, 1962)	Taylor (1962); Ohler et al. (2011)

ID	Species	Literature reviewed
51	<i>L. mjobergi</i> (Smith, 1925)	Eto et al. (2015)
52	<i>L. murphyi</i> Chen, Suwannapoom, Wu, Poyarkov, Xu, Pawangkhanant & Che, 2021	Chen et al. (2021a)
53	<i>L. namdongensis</i> (Hoang, Nguyen, Luu, Nguyen & Jiang, 2019)	Hoang et al. (2019)
54	<i>L. nahangensis</i> (Lathrop, Murphy, Orlov & Ho, 1998)	Lathrop et al. (1998)
55	<i>L. natunae</i> (Günther, 1895)	Günther (1895)
56	<i>L. neangi</i> Stuart & Rowley, 2020	Stuart and Rowley (2020)
57	<i>L. niveimontis</i> (Chen, Poyarkov, Yuan & Che, 2020)	Chen et al. (2020)
58	<i>L. nokrekensis</i> (Mathew & Sen, 2010)	Mathew and Sen (2010)
59	<i>L. nyx</i> (Ohler, Wollenberg, Grosjean, Hendrix, Vences, Ziegler & Dubois, 2011)	Ohler et al. (2011)
60	<i>L. oshanensis</i> (Liu, 1950)	Fei et al. (2009)
61	<i>L. pallida</i> (Rowley, Tran, Le, Dau, Peloso, Nguyen, Hoang, Nguyen & Ziegler, 2016)	Rowley et al. (2016)
62	<i>L. palmata</i> Inger & Stuebing, 1992	Inger and Stuebing (1992)
63	<i>L. parva</i> Dring, 1983	Dring (1983)
64	<i>L. pelodytoides</i> (Boulenger, 1893)	Boulenger (1893); Ohler et al. (2011)
65	<i>L. petrops</i> (Rowley, Dau, Hoang, Le, Cutajar & Nguyen, 2017)	Rowley et al. (2017a)
66	<i>L. picta</i> (Malkmus, 1992)	Malkmus (1992)
67	<i>L. pingbianensis</i> (Rao, Hui, Zhu & Ma, 2022)	Rao (2022 “2020”)
68	<i>L. platycephala</i> (Dehling, 2012)	Dehling (2012a)
69	<i>L. pluvialis</i> (Ohler, Marquis, Swan & Grosjean, 2000)	Ohler et al. (2000, 2011)
70	<i>L. puhoatensis</i> (Rowley, Dau & Cao, 2017)	Rowley et al. (2017b)
71	<i>L. purpuraventra</i> Wang, Li, Li, Chen & Wang, 2019	Wang et al. (2019)
72	<i>L. purpurus</i> (Yang, Zeng & Wang, 2018)	Yang et al. (2018)
73	<i>L. pyrrops</i> (Poyarkov, Rowley, Gogoleva, Vassilieva, Galoyan & Orlov, 2015)	Poyarkov et al. (2015)
74	<i>L. rowleyae</i> (Nguyen, Poyarkov, Le, Vo, Ninh, Duong, Murphy & Sang, 2018)	Nguyen et al. (2018)
75	<i>L. sabahmontana</i> (Matsui, Nishikawa & Yambun, 2014)	Matsui et al. (2014a)
76	<i>L. serasanae</i> Dring, 1983	Dring (1983)
77	<i>L. shangsiensis</i> Chen, Liao, Zhou & Mo, 2019	Chen et al. (2019)
78	<i>L. shimentaina</i> Wang, Lyu & Wang, 2022	Wang et al. (2022)
79	<i>L. shiwandashanensis</i> Chen, Peng, Pan, Liao, Liu & Huang, 2021	Chen et al. (2021c)
80	<i>L. sola</i> (Matsui, 2006)	Matsui (2006)
81	<i>L. sungi</i> (Lathrop, Murphy, Orlov & Ho, 1998)	Lathrop et al. (1998)
82	<i>L. suiyangensis</i> (Luo, Xiao, Gao & Zhou, 2020)	Luo et al. (2020)
83	<i>L. tadungensis</i> (Rowley, Tran, Le, Dau, Peloso, Nguyen, Hoang, Nguyen & Ziegler, 2016)	Rowley et al. (2016)
84	<i>L. tamdil</i> (Sengupta, Sailo, Lalremsanga, Das & Das, 2010)	Sengupta et al. (2010)
85	<i>L. tengchongensis</i> (Yang, Wang, Chen & Rao, 2016)	Yang et al. (2016)
86	<i>L. tuberosa</i> (Inger, Orlov & Darevsky, 1999)	Inger et al. (1999)
87	<i>L. ventripunctata</i> (Fei, Ye & Li, 1990)	Fei et al. (2009)
88	<i>L. verrucosa</i> Wang, Zeng, Lin & Li, 2022	Lin et al. (2022)
89	<i>L. wuhuangmontis</i> Wang, Yang & Wang, 2018	Wang et al. (2018)
90	<i>L. wulingensis</i> Qian, Xiao, Cao, Xiao & Yang, 2020	Qian et al. (2020)
91	<i>L. yeeae</i> Shi, Hou, Song, Jiang & Wang, 2021	Shi et al. (2021)
92	<i>L. yingjiangensis</i> (Yang, Zeng & Wang, 2018)	Yang et al. (2018)
93	<i>L. yunkaiensis</i> Wang, Li, Lyu & Wang, 2018	Wang et al. (2018)
94	<i>L. yunyangensis</i> Luo, Deng & Zhou, 2022	Luo et al. (2022)
95	<i>L. zhangyapingi</i> (Jiang, Yan, Suwannapoom, Chomdej & Che, 2013)	Jiang et al. (2013)

Dorsal skin relatively smooth with small tubercles and short folds; supra-axillary gland distinct and yellowish; pectoral gland small and indistinct; round femoral glands present and protuberant on rear of thigh, closer to knee than to vent; femoral adipose glands distinct, attached to inner side of skin on posterior ventral surface of thigh; ventral skin smooth; ventrolateral glands forming a distinct white line on flanks.

**Colouration of holotype in life.** In life, dorsal surface of head and trunk yellowish-brown, with distinct olive reverse-triangle dark markings between eyes connecting to a dark W-shaped marking between axillae that are fringed with greyish-white colour; elbow to upper arm distinctly yellowish-orange in colour on the dorsum; four transverse black bars present on dorsal surface of thighs and three on dorsal surface of lower arm; one dark blotch between nostril and eyes on loreal region and a dark blotch under the eye; supratympanic ridge reddish and a large black marking under supratympanic ridge; distinct dark blotches on flanks from groin to axilla, longitudinally in two rows; ventral surfaces light coloured; throat and ventral arms pinkish with cream speckling on margins; chest and belly cream white, on the lateral belly with dense brown speckling; ventral hind-limbs pinkish with sparse white glands; upper iris copper, lower iris silver.

**Preserved holotype colouration.** Dorsum of body and limbs fading to brown copper; transverse bars on limbs becoming more distinct. Ventral surface of body and limbs fading to cream white. Supra-axillary, femoral and pectoral glands fading to cream yellow.

**Variations.** Measurements and basic statistics of adult specimens are presented in Suppl. materials 1, 3, respectively. Females larger than males (29.2–34.2 mm in 15 adult males and 34.4–43.1 mm in seven adult females) and, in CIB LB20220311002, dark blotch between nostril and eyes on loreal region absent (Fig. 5A); in CIBSCC1754, a patch on the outside of the reverse-triangle dark markings between eyes (Fig. 5B); in CIB LB20220305005, no longitudinal stripes along dorsolateral body (Fig. 5C); in CIB LB20220306008, the colouration of head and anterior dorsum is darker than the posterior (Fig. 5D).

**Bioacoustics.** (Fig. 6; Suppl. material 3). Calls recorded at temperatures 11.2 to 15.0 °C. Descriptions based on six sequenced adults (Suppl. material 3) and 157 calls were measured. Dominant frequency of all type of calls is 4.4–5.6 kHz ( $5.1 \pm 0.4$  kHz), call duration is  $203.783 \pm 161.7$  ms, call interval is  $1238.3 \pm 2034.5$  ms, call repetition rate is  $1.61 \pm 0.9$  (calls/s). Additionally, the calls were of two types. The first type (type A) consists of repeated short notes (Fig. 6A, B), and the second type (type B) consists of two repeated short notes and with longer call duration ( $524.2 \pm 64.2$  ms) and shorter call interval ( $148.8 \pm 72.8$  ms) than type A (Fig. 6C, D). Amplitude of type A was largest at first pulse, drastic reducing in the following pulses; amplitude of second note of type A about half of the first note; amplitude of type B with highest pulse at the beginning of each note and decreasing towards to the end.

**Comparisons.** Compared with the 26 known congeners occurring south of the Isthmus of Kra, *Leptobrachella dong* sp. nov. could be distinguished from them by several characters: by having supra-axillary and ventrolateral glands, the new species differs from *L. arayai*, *L. dringi*, *L. fritinniens*, *L. gracilis*, *L. hamidi*, *L. heteropus*, *L. kajangensis*, *L. kecil*, *L. marmorata*, *L. maura*, *L. melanoleuca*, *L. picta*, *L. platycephala*, *L. sabahmontana*, and *L. sola* (vs. absent in the latter); by having rounded fingertips and moderate body size (29.2–34.2 mm in 15 adult males and 34.4–43.1 mm in seven adult females), the new species differs from the following species with pointed

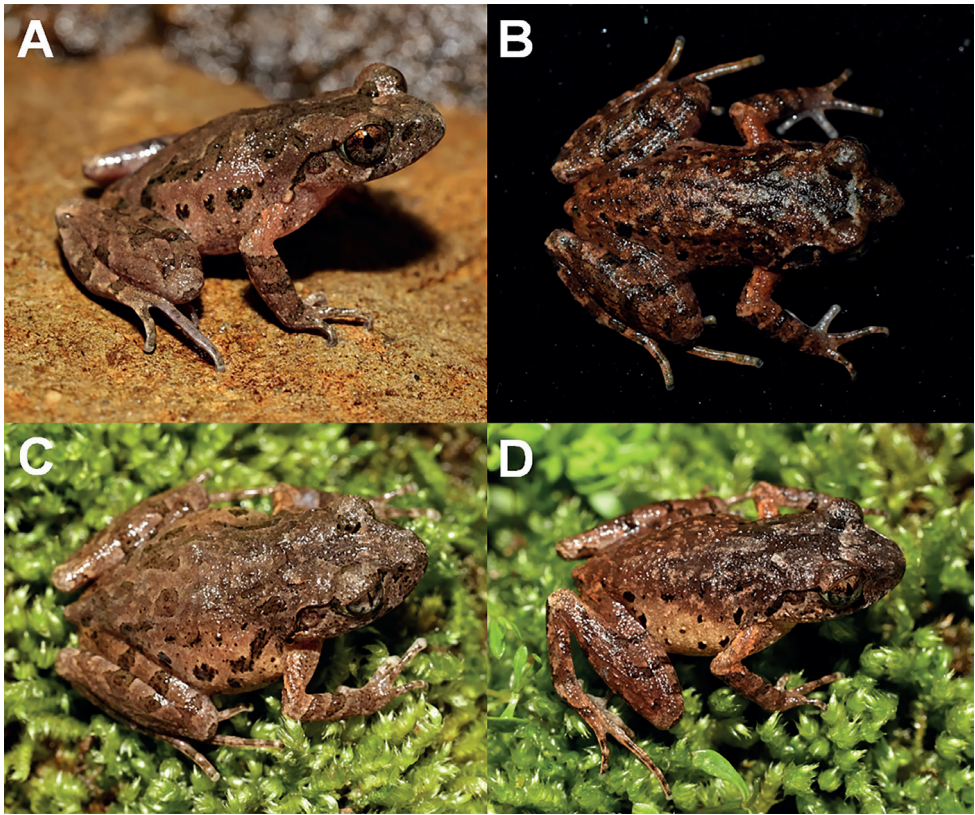


**Figure 5.** Colour variation in *Leptobrachella dong* sp. nov. **A** dorsolateral view of the male specimen CIB LB20220311002 **B** dorsal view of the male specimen CIB SCC1754 **C** dorsal view of the female specimen CIB LB20220305005 **D** dorsal view of the female specimen CIB LB20220306008.

**Table 3.** Basic statistics for the measurements of *Leptobrachella dong* sp. nov. Units in mm. See abbreviations for characters in the Materials and methods section.

Measurement	Male (n = 15)		Female (n = 7)	
	Ranging	Mean $\pm$ SD	Ranging	Mean $\pm$ SD
SVL	29.2–34.2	30.9 $\pm$ 1.4	34.4–43.1	39.4 $\pm$ 2.8
HDL	9.8–11.7	10.5 $\pm$ 0.6	11.8–13.8	12.7 $\pm$ 0.7
HDW	9.8–12.2	11.0 $\pm$ 0.7	12.4–14.5	13.7 $\pm$ 0.8
SL	4.0–5.0	4.5 $\pm$ 0.3	4.9–6.3	5.6 $\pm$ 0.4
IND	2.8–4.4	3.3 $\pm$ 0.4	3.4–4.7	4.3 $\pm$ 0.5
IOD	2.3–3.9	3.2 $\pm$ 0.5	3.4–4.1	3.6 $\pm$ 0.2
UEW	2.6–3.4	2.9 $\pm$ 0.2	2.9–4.3	3.6 $\pm$ 0.5
ED	3.6–4.4	4.1 $\pm$ 0.2	4.2–5.3	4.8 $\pm$ 0.4
TYD	1.5–2.2	1.7 $\pm$ 0.2	1.6–3.0	2.5 $\pm$ 0.4
LAL	13.5–15.5	14.6 $\pm$ 0.5	16.8–18.9	17.9 $\pm$ 0.9
ML	7.2–8.6	7.9 $\pm$ 0.4	8.6–10.5	9.6 $\pm$ 0.7
TL	14.5–16.4	15.2 $\pm$ 0.7	17.4–19.6	18.3 $\pm$ 0.8
FL	13.5–15.5	14.5 $\pm$ 0.6	17.4–19.4	17.9 $\pm$ 1.0
HLL	41.3–51.6	47.6 $\pm$ 3.1	54.6–62.5	58.4 $\pm$ 2.9

**Table 4.** Diagnosis characters on morphology of *Leptobrachella dong* sp. nov. from other congeners.

ID	Species	Male SVL (mm)	Female SVL (mm)	Black spots on flanks	Toes webbing	Fringes on toes	Ventral colouration	Dorsal skin texture
1	<i>Leptobrachella dong</i> sp. nov.	29.2–32.0	34.4–43.1	Yes	Rudimentary	Wide	White with distinct nebulous brown speckling on ventrolateral flanks	Shagreened with fine tubercles
2	<i>L. aerea</i>	25.1–28.9	27.1–38.6	No	Rudimentary	Wide	Near immaculate creamy-white; brown speckling on margins	Finely tuberculate
3	<i>L. alpina</i>	24.0–26.4	31.7–32.5	Yes	Rudimentary	Wide in males	Creamy-white with dark spots	Relatively smooth, some with small warts
4	<i>L. applebyi</i>	19.6–22.3	21.7	Yes	Rudimentary	No	Reddish-brown with white speckling	Smooth
5	<i>L. ardans</i>	21.3–24.7	25.4	Yes	No	No	Reddish-brown with white speckling	Smooth-finely shagreened
6	<i>L. aspera</i>	22.4	25.0–26.4	Yes	Rudimentary	Narrow	Creamy-white with distinct dark patches on chest and abdomen	Rough with dense conical granules, tubercles and glandular folds
7	<i>L. bashuensis</i>	22.9–25.6	27.1	Yes	Rudimentary	Narrow	Creamy-white chest and off-white belly with irregular black spots	Dorsal skin slightly shagreened with small tubercles and irregular brown stripes
8	<i>L. bidampensis</i>	23.6–24.6	29.2–29.4	Yes	Rudimentary	Weak	Reddish-brown with white speckling	Smooth
9	<i>L. bijije</i>	29.0–30.4	/	Yes	Rudimentary	Narrow	White with distinct nebulous greyish speckling on chest and ventrolateral flanks	Shagreened and granular
10	<i>L. bongfordi</i>	29.1–32.6	30.0–31.8	No	Rudimentary	Narrow	Reddish-brown with white speckling	Shagreened
11	<i>L. bourreti</i>	27.4–36.2	39.5–45.0	Yes	Rudimentary	Weak	Creamy-white	Relatively smooth, some with small warts
12	<i>L. chishuensis</i>	30.8–33.4	34.2	Yes	Rudimentary	Narrow	White with distinct nebulous greyish speckling on chest and ventrolateral flanks	Shagreened and granular
13	<i>L. crocea</i>	22.2–27.3	/	No	Rudimentary	No	Bright orange	Highly tuberculate
14	<i>L. damingshanensis</i>	33.6–34.4	/	Yes	Rudimentary	Narrow	Creamy-white ventral surface with small, creamy-white glands on throat, chest and belly, becoming more concentrated near lateral margin	Rough dorsal skin with sparse jacinth tubercles and some short longitudinal ridges
15	<i>L. dorsospina</i>	28.7–30.5	32.1–39.8	Yes	Rudimentary	Narrow	Greyish-white with black spots and orange pigmentations	Rough with dense conical granules, tubercles, glandular folds and conical spines
16	<i>L. eos</i>	33.1–34.7	40.7	No	Rudimentary	Wide	Creamy-white	Shagreened
17	<i>L. feii</i>	21.5–22.8	25.7	Yes	Rudimentary	Narrow	Creamy-white with black blotches	Shagreened with small tubercles and ridge
18	<i>L. firih</i>	26.4–29.2	25.7–36.9	No	Rudimentary	Wide in males	Creamy-white	Shagreened with fine tubercles
19	<i>L. flaviglandulosa</i>	23.0–27.0	29.3	Yes	Poorly developed	Narrow	Whitish, black speckling on margins	Shagreened with yellowish-brown tubercles
20	<i>L. fuliginosa</i>	28.2–30.0	/	Yes	Rudimentary	Weak	White with brown dusting	Nearly smooth, few tubercles
21	<i>L. grammicola</i>	23.1–24.6	28.6–32.9	No	Rudimentary	Wide	White with brown spots	Smooth, with many tubercles
22	<i>L. hao</i>	23.7–27.9	28.6–31.5	No	Rudimentary	Wide in males	Creamy-white with white dusting on margins	Mostly smooth, females more tuberculate

ID	Species	Male SVL (mm)	Female SVL (mm)	Black spots on flanks	Toes webbing	Fringes on toes	Ventral colouration	Dorsal skin texture
23	<i>L. jinshaensis</i>	29.7–31.2	/	Yes	No	Narrow	Cream yellow, presence of distinct nebulous greyish speckling on flanks	Shagreened and granular
24	<i>L. habonensis</i>	25.8–30.6	28.9–30.6	Yes	No	No	Pale, speckled brown	Smooth
25	<i>L. khasiorum</i>	24.5–27.3	31.2–33.4	Yes	Rudimentary	Wide	Creamy white	Isolated, scattered tubercles
26	<i>L. lateralis</i>	26.9–28.3	36.6	Yes	Rudimentary	No	Creamy white	Roughly granular
27	<i>L. laui</i>	24.8–26.7	28.1	Yes	Rudimentary	Wide	Creamy-white with dark brown dusting on margins	Round granular tubercles
28	<i>L. lui</i>	23.0–28.7	24.5–27.8	Yes	Rudimentary	Wide	Creamy-white with dark brown spots on chest and margins	Round granular tubercles with glandular folds
29	<i>L. macrops</i>	28.0–29.3	30.3	Yes	Rudimentary	No	Greyish-violet with white speckling	Roughly granular with larger tubercles
30	<i>L. maculosa</i>	24.2–26.6	27	Yes	No	No	Brown, less white speckling	Mostly smooth
31	<i>L. mungghanensis</i>	22.2–27.8	30.2	Yes	Rudimentary	Weak	White speckles on throat and belly	Nearly smooth
32	<i>L. maoershanensis</i>	25.2–30.4	29.1	Yes	Rudimentary	Narrow	Creamy-white chest and belly with irregular black spots	Longitudinal folds
33	<i>L. melica</i>	19.5–22.8	/	Yes	Rudimentary	No	Reddish-brown with white speckling	Smooth
34	<i>L. minima</i>	25.7–31.4	31.6–37.3	Yes	Rudimentary	No	Creamy-white	Smooth
35	<i>L. muiphyi</i>	23.2–24.9	29.3–32.1	Yes	Rudimentary	Wide	Creamy-white belly with small black spots on the margin	Shagreened with reddish tubercles and folds
36	<i>L. nahangensis</i>	40.8	/	Yes	Rudimentary	No	Creamy-white with light speckling on throat and chest	Smooth
37	<i>L. namdongensis</i>	30.9	32.1–35.3	Yes	Rudimentary	No	Creamy-white with brown dusting on margins	Finely tuberculate
38	<i>L. neangi</i>	/	35.4–36.3	Yes	Rudimentary (in females)	absent (in females)	Light purplish-grey with dark brown mottling on throat	Small, irregular bumps and ridges
39	<i>L. niveimontis</i>	22.5–23.6	28.5–28.7	Yes	Rudimentary	No	Ventral sides marbled with distinct irregular black speckling	Skin on dorsum scattered with fine reddish tubercles
40	<i>L. nobrekensis</i>	26.0–33.0	34.0–35.0	Yes	Rudimentary	unknown	White with distinct nebulous greyish speckling on chest and ventrolateral flanks	Tubercles and longitudinal folds
41	<i>L. nyx</i>	26.7–32.6	37.0–41.0	Yes	Rudimentary	No	Creamy-white with white and brown margins	Rounded tubercles
42	<i>L. oshanensis</i>	26.6–30.7	31.6	Yes	No	No	Whitish with no markings or only small, light grey spots	Smooth with few glandular ridges
43	<i>L. pallida</i>	24.5–27.7	/	No	No	No	Reddish-brown with white speckling	Tuberculate
44	<i>L. pelodyoides</i>	27.5–32.3	/	Yes	Wide	Narrow	Whitish	Small, smooth warts
45	<i>L. petrops</i>	23.6–27.6	30.3–47.0	No	No	Narrow	Immaculate creamy white	Highly tuberculate
46	<i>L. pluvialis</i>	21.3–22.3	25.5–33.5	Yes	Rudimentary	No	Dirty white with dark brown marbling	Smooth, flattened tubercles on flanks
47	<i>L. pubeoatensis</i>	24.2–28.1	27.3–31.5	Yes	Rudimentary	Narrow	Reddish-brown with white dusting	Longitudinal skin ridges
48	<i>L. purpurus</i>	25.0–27.5	/	Yes	Rudimentary	Wide	Dull white with indistinct grey dusting	Shagreened with small tubercles
49	<i>L. purpuraventura</i>	27.3–29.8	33.0–35.3	Yes	Rudimentary	Narrow	Grey purple with distinct nebulous greyish speckling on chest and ventrolateral flanks	Shagreened and granular

ID	Species	Male SVL (mm)	Female SVL (mm)	Black spots on flanks	Toes webbing	Fringes on toes	Ventral colouration	Dorsal skin texture
50	<i>L. pyrrophops</i>	30.3–33.9	30.8–34.3	Yes	Rudimentary	No	Reddish-brown with white speckling	Slightly shagreened
51	<i>L. novoleyae</i>	23.4–25.4	27.0–27.8	Yes	No	No	Pinkish milk-white to light brown chest and belly with numerous white speckles	Smooth with numerous tiny tubercles
52	<i>L. shangstensis</i>	24.9–29.4	30.8–35.9	Yes	Rudimentary	Narrow	ventral surface yellowish-creamy-white with marble texture	Smooth
53	<i>L. shiwandabananensis</i>	26.8–29.7	/	Yes	No	No	Creamy-white ventral surface with small, creamy-white glands on throat, chest and belly, becoming more concentrated near lateral margin	Shagreened with small raised tubercles and ridges
54	<i>L. sungi</i>	48.3–52.7	56.7–58.9	No or small	Wide	Weak	White	Granular
55	<i>L. suiyangensis</i>	28.7–29.7	30.5–33.5	Yes	Rudimentary	Narrow	Yellowish-creamy-white with marble texture chest and belly or with irregular light brown speckling	Shagreen with small granules
56	<i>L. naduensis</i>	23.3–28.2	32.1	Yes	No	No	Reddish-brown with white speckling	Smooth
57	<i>L. tamdi</i>	32.3	32.3	Yes	Wide	Wide	White	Weakly tuberculate
58	<i>L. tengchongensis</i>	23.9–26.0	28.8–28.9	Yes	Rudimentary	Narrow	White with dark brown blotches	Shagreened with small tubercles
59	<i>L. tuberosa</i>	24.4–29.5	30.2	No	Rudimentary	No	White with small grey spots/streaks	Highly tuberculate
60	<i>L. ventripunctata</i>	23.7–27.7	31.5–35.0	Yes	Rudimentary	No	Chest and belly with dark brown spots	Longitudinal skin ridges
61	<i>L. wuhuangmontis</i>	25.6–30.0	33.0–36.0	Yes	Rudimentary	Narrow	Greyish-white mixed by tiny white and black dots	Rough, scattered with dense conical tubercles
62	<i>L. wulingensis</i>	24.5–32.8	29.9–38.5	Yes	Rudimentary	Narrow	Creamy white, with distinct or indistinct brown speckling at margins	Shagreened with sparse large warts, sometimes with longitudinal ridges
63	<i>L. yue</i>	25.8–32.6	33.7–34.1	Yes	Rudimentary	Narrow	Ventral belly cream white with variable brown speckling	Dorsum relatively smooth with fine tiny granules or short ridges
64	<i>L. yingjiangensis</i>	25.7–27.6	/	Yes	Rudimentary	Wide	Creamy-white with dark brown flecks on chest and margins	Shagreened with small tubercles
65	<i>L. yunkatensis</i>	25.9–29.3	34.0–35.3	Yes	Rudimentary	Wide	Belly pink with distinct or indistinct speckling	Shagreened with short skin ridges and raised warts
66	<i>L. zhangyapingi</i>	45.8–52.5	/	No	Rudimentary	Wide	Creamy-white with white and brown	Mostly smooth with distinct tubercles
67	<i>L. pingbianensis</i>	28	30	Yes	Rudimentary	Unknown	Chest and belly with dark brown spots	Smooth
68	<i>L. shimentaina</i>	26.4–8.9	30.1–30.7	Yes	Rudimentary	Wide in males	Greyish-pink with distinct hazy brown speckling on chest and ventrolateral flanks	Round granular tubercles with glandular folds
69	<i>L. verrucosa</i>	23.2–25.9	/	Yes	Rudimentary	Narrow	Creamy-white with greyish-white and dark brown spots	Shagreened with numerous conical tubercles
70	<i>L. yuyangensis</i>	28.3–30.6	/	Yes	Rudimentary	Narrow	Light greyish-creamy-white, interspersed with light brown spots	Rough with sparse large warts, with short longitudinal ridges

fingertips and smaller body size: *L. baluensis* (14.9–15.9 mm in males), *L. bondangensis* (17.8 mm in male), *L. brevicrus* (17.1–17.8 mm in males), *L. fusca* (16.3 mm in male), *L. itiokai* (15.2–16.7 mm in males), *L. juliandringi* (17.0–17.2 mm in males), *L. mjobergi* (15.7–19.0 mm in males), *L. natunae* (17.6 mm in one adult male), *L. palmata* (14.4–16.8 mm in males), *L. parva* (15.0–16.9 mm in males) and *L. serasanae* (16.9 mm in female).

*Leptobranchella dong* sp. nov. could also be identified from 65 known *Leptobranchella* species occurring north of the Isthmus of Kra by some characters (see Table 4).

By having medium size of body (SVL 29.2–34.2 mm in males) *Leptobranchella dong* sp. nov. differs from the smaller males *L. aerea* (25.1–28.9 mm), *L. alpina* (24.0–26.4 mm), *L. applebyi* (19.6–22.3 mm), *L. ardens* (21.3–24.7 mm), *L. aspera* (22.4 mm), *L. bashaensis* (22.9–25.6 mm), *L. bidoupensis* (23.6–24.6), *L. crocea* (22.2–27.3 mm), *L. feii* (21.5–22.8 mm), *L. flaviglandulosa* (23.0–27.0 mm), *L. isos* (23.7–27.9 mm), *L. graminicola* (23.1–24.6 mm), *L. khasiorum* (24.5–27.3 mm), *L. lateralis* (26.9–28.3 mm), *L. laui* (24.8–26.7 mm), *L. liui* (24.8–26.7 mm), *L. maculosa* (24.2–26.6 mm), *L. mangshanensis* (22.22–27.76 mm), *L. maura* (26.1 mm), *L. melica* (19.5–22.8 mm), *L. murphyi* (23.2–24.9 mm), *L. niveimontis* (22.5–23.6 mm), *L. pallida* (24.5–27.7 mm), *L. petrops* (23.6–27.6 mm), *L. pluvialis* (21.3–22.3 mm), *L. puhoatensis* (24.2–28.1 mm), *L. pyrrhops* (25.0–27.5 mm), *L. rowleyae* (23.4–25.4 mm), *L. tadungensis* (23.3–28.2 mm), *L. tengchongensis* (23.9–26.0 mm), *L. ventripunctata* (23.7–27.7 mm) and *L. yingjiangensis* (25.7–27.6 mm) and differs from the larger in males *L. nahangensis* (40.8 mm), *L. platycephala* (35.1 mm), *L. sungi* (48.3–52.7 mm in males) and *L. zhangyapingi* (45.8–52.5 mm).

By having a larger size of body (SVL 34.4–43.1 mm in females), *Leptobranchella dong* sp. nov. differs from the smaller females *L. alpina* (31.7–32.5 mm), *L. applebyi* (21.7 mm), *L. ardens* (25.4 mm), *L. aspera* (25.0–26.4 mm), *L. bashaensis* (27.1), *L. botsfordi* (30.0–31.8 mm), *L. graminicola* (28.6–32.9 mm), *L. isos* (28.6–31.5 mm), *L. kalonensis* (28.9–30.6 mm), *L. khasiorum* (31.2–33.4 mm), *L. liui* (24.5–27.8 mm), *L. macrops* (30.3 mm), *L. maculosa* (27 mm), *L. mangshanensis* (30.2 mm), *L. maoershanensis* (29.1 mm), *L. murphyi* (29.3–32.1 mm), *L. macrops* (30.3 mm), *L. maoershanensis* (29.1 mm), *L. niveimontis* (28.5–28.7 mm), *L. oshanensis* (31.6 mm), *L. pluvialis* (25.5–33.5 mm), *L. puhoatensis* (27.3–31.5 mm), *L. rowleyae* (27.0–27.8 mm), *L. shimentaina* (30.1–30.7 mm), *L. suiyangensis* (30.5–33.5 mm), *L. tadungensis* (32.1 mm), *L. tamdil* (32.3 mm), *L. tengchongensis* (28.8–28.9 mm) and *L. tuberosa* (30.2 mm).

By having black spots on flanks, *Leptobranchella dong* sp. nov. differs from *L. aerea*, *L. botsfordi*, *L. crocea*, *L. eos*, *L. firthi*, *L. isos*, *L. pallida*, *L. petrops*, *L. tuberosa* and *L. zhangyapingi* (vs. lacking distinct black spots on the flanks in the latter).

By having rudimentary webbing, *Leptobranchella dong* sp. nov. differs from *L. ardens*, *L. jinshaensis*, *L. kalonensis*, *L. maculosa*, *L. oshanensis*, *L. pallida*, *L. petrops*, *L. rowleyae*, *L. shiwandashanensis* and *L. tadungensis* (vs. absent webbing in the latter).

By having wide fringes on toes, *Leptobranchella dong* sp. nov. differs from *L. applebyi*, *L. ardens*, *L. aspera*, *L. bashaensis*, *L. bidoupensis*, *L. bijie*, *L. botsfordi*, *L. bourreti*, *L. chishuiensis*, *L. crocea*, *L. damingshanensis*, *L. dorsospina*, *L. feii*, *L. flaviglandulosa*,

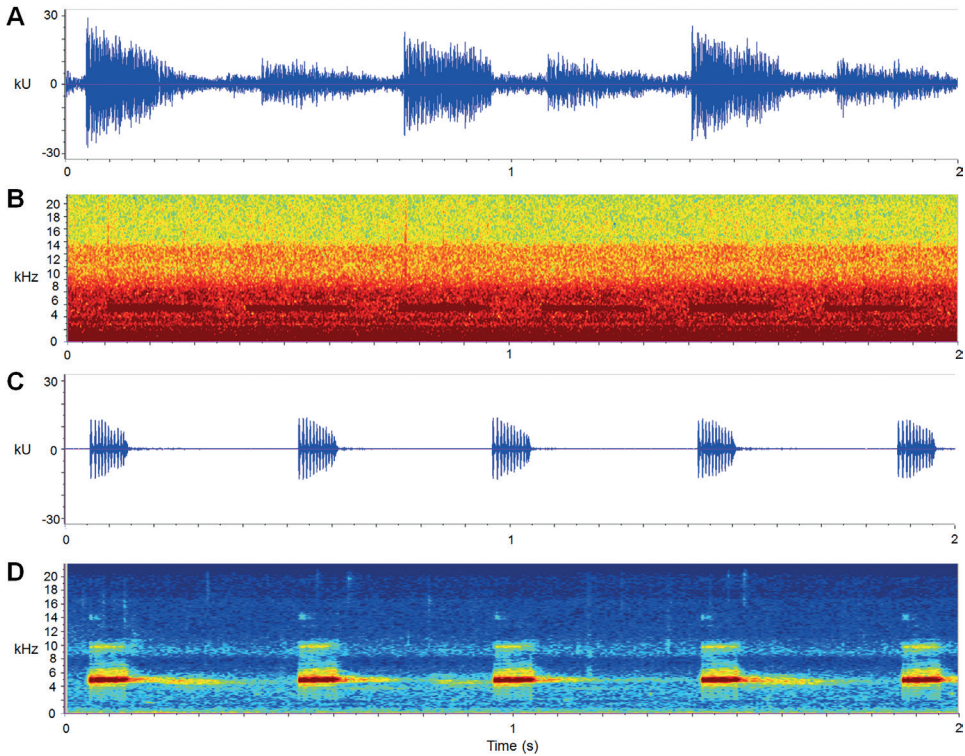


**Figure 6.** Advertisement calls of *Leptobrachella dong* sp. nov. **A, B** waveform and sonogram of the first call type (type A) over 2 seconds of the paratype CIB LB20220311002, respectively **C, D** waveform and sonogram of the second call type (type B) over 2 seconds of the holotype CIB SSC1757, respectively.

*L. fuliginosa*, *L. jinshaensis*, *L. kalonensis*, *L. lateralis*, *L. macrops*, *L. maculosa*, *L. mangshanensis*, *L. melica*, *L. minima*, *L. nahangensis*, *L. namdongensis*, *L. niveimontis*, *L. nyx*, *L. oshanensis*, *L. pallida*, *L. pelodytoides*, *L. petrops*, *L. pluvialis*, *L. puhoatensis*, *L. purpuraventra*, *L. pyrrhops*, *L. rowleyae*, *L. shangsiensis*, *L. shiwandashanensis*, *L. sungi*, *L. tengchongensis*, *L. tuberosa*, *L. ventripunctata*, *L. verrucosa*, *L. wuhuangmontis*, *L. wulingensis*, *L. yuae* and *L. yunyangensis* (vs. fringes on toes narrow or absent in the latter).

By having dorsal surface shagreened with fine tubercles, *Leptobrachella dong* sp. nov. differs from *L. applebyi*, *L. bidoupensis*, *L. kalonensis*, *L. melica*, *L. minima*, *L. nahangensis*, *L. pingbianensis*, *L. shangsiensis* and *L. tadungensis*, all of which have the dorsum smooth and *L. bourreti* (dorsum smooth with small warts), *L. fuliginosa* (dorsum smooth with fine tubercles), *L. liui* (dorsum with round tubercles), *L. macrops* (dorsum roughly granular with large tubercles), *L. maoershanensis* (dorsum shagreened with tubercles), *L. minima* (dorsum smooth), *L. neangi* (dorsum with small, irregular bumps and ridges), *L. nyx* (dorsum with round tubercles), *L. nokrekensis* (dorsum tubercles and longitudinal folds), *L. pelodytoides* (dorsum with small, smooth warts), *L. tamdil* (dorsum weakly tuberculate, with low, oval tubercles), *L. tuberosa* (dorsum highly tuberculate), *L. junkaiensis* (dorsum with raised warts) and *L. wuhuangmontis* (dorsum rough with conical tubercles).

The advertisement calls of *Leptobranchella dong* sp. nov. (Results and Fig. 3) differs from all other congeners occurring north of the Isthmus of Kra for which comparable acoustic data are available consisting of uniform and continuous calls with four to five pulses in each note. Of the congeners in the region with known calls, the new species can be separated from *L. purpurus*, *L. tuberosus*, *L. puhoatensis* and *L. yingjiangensis* by not having an invariably single-note call with irregular intervals. In addition, the dominant frequency of 4.4–5.6 kHz (at 11.2–15 °C) further distinguishes the call of *Leptobranchella dong* sp. nov. from that of the higher frequency calls of *L. aereus* (6.2–7.9 kHz at 22.4–25.7 °C), *L. yingjiangensis* (5.7–5.9 kHz at 19 °C), *L. isos* (5.9–6.2 kHz at 22.4–22.8 °C) and *L. ventripunctatus* (6.1–6.4 kHz at 15 °C) and the lower frequency calls of *L. applebyi* (4.0–4.3 kHz at 21.5 °C), *L. ardens* (3.1–3.4 kHz at 21.4–24.7 °C), *L. bidoupensis* (1.9–3.8 kHz at 19–21 °C), *L. botsfordi* (2.6–3.2 kHz at 14 °C), *L. croceus* (2.6–3.0 kHz at 21.6–25.1 °C), *L. fuliginosus* (2.1–2.8 kHz at 19.3–19.6 °C), *L. kalonensis* (2.8 kHz at 26.4 °C), *L. maculosus* (2.7–2.8 kHz at 23.3–24.1 °C), *L. melicus* (2.6–4.0 kHz at 26.1–26.2 °C), *L. pallidus* (2.4–2.7 kHz at 14.0–21.4 °C), *L. pyrrhops* (1.91–2.2 kHz at 25 °C), *L. rowleyae* (3.3–3.5 kHz at 21.5 °C), *L. tadungensis* (2.6–3.1 kHz at 12.9–22.3 °C) and *L. tuberosus* (2.6–2.8 kHz at 22.5–24.5 °C).

In mitochondrial DNA trees, *Leptobranchella dong* sp. nov. was clustered as an independent clade and sister to a clade comprising of *L. graminicola* and *L. yaeae*. The new species differs from *L. graminicola* by the following characters: body size larger with SVL 29.2–34.2 mm in adult males and 34.4–43.1 mm in adult females (vs. 23.1–24.6 mm in adult males and 28.6–32.9 mm in adult females); black spots on flanks present (vs. absent); ventral surface white with distinct nebulous brown speckling on ventrolateral flanks (vs. white with brown spots); dorsal surface shagreened with fine tubercles (vs. smooth, with many tubercles); and tibiotarsal articulation reaching to middle of eye (vs. anterior edge of eye). The new species differs from *L. yaeae* by having wide fringes on toes (vs. narrow); dorsal surface shagreened with fine tubercles (vs. relatively smooth with fine tiny granules or short ridges); and males with a pair of subgular internal vocal sacs (vs. internal single subgular vocal sac).

**Tadpoles (in mm).** Description based on sequenced tadpole CIB WB2020277 at Gosner stage 27 (Fig. 7). Body elliptical elongate in dorsal view; slightly depressed (BH / BW 1.5, BH 4.7, BL 14.7); eyes lateral (ED 0.9), nostril near to snout than eye (NE 2.9, RN 1.6, IND 2.4, SN 3.5); spiracle on left side of body (SS 7.8); keratodont formula I: 3+3/2+2: I; oral disc is cup-shaped with labial papillae (ODW 3.4); TOL 65.8 mm; tail fusiform, approximately 2.5 times as long as snout-vent length, tail height 18.2% of tail length (TH 6.4, TMH 4.6, TMW 3.8); dorsal fin low, arising behind the origin of the tail (SU 20.1); maximum tail depth near mid-length of tail and larger than body depth (TH / BL 1.4, UF 2.1, LF 1.3); the tip of tail rounded and without spots on dorsal of body.

**Secondary sexual characteristics.** Adult males with a pair of subgular vocal sacs (Fig. 8B), femoral adipose glands present on posterior surface of thigh and tiny transparent spines on chest during breeding season. Nuptial pads and spines absent on males.



**Figure 7.** The tadpole CIB WB2020277 of *Leptobrachella dong* sp. nov. in life **A** dorsal view **B** lateral view **C** ventral view **D** oral disc.

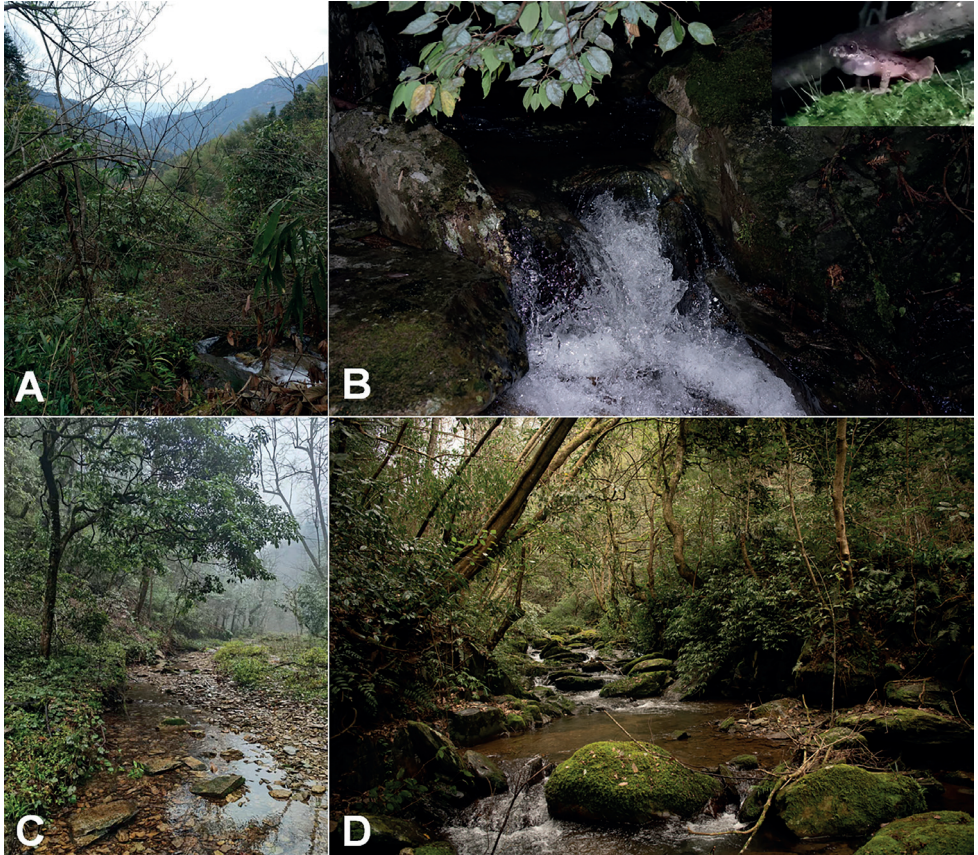


**Figure 8.** Habitats of *Leptobrachella dong* sp. nov. **A** landscape of the type locality Tongdao County, Hunan Province, China **B** a torrent mountain stream in the type locality (insert holotype CIB SSC1757 in life in the field) **C** habitat at the Congjiang County, Guizhou Province, China **D** habitat at the Suining County, Hunan Province, China.

**Ecology notes.** *Leptobrachella dong* sp. nov. has been found in three localities: Tongdao County and Suining County, Hunan Province and Congjiang County, Guizhou Province, China. Elevations recorded range from 620 m to 1200 m. Population from the Tongdao County inhabited a torrent stream covered by evergreen shrubs and the new species always found on the stones (Fig. 8A, B). Population from Congjiang County inhabited slow-flowing streams surrounded by evergreen broadleaf forest (Fig. 8C). Populations from Suining County, Hunan Province inhabited broad mountain stream surrounded by evergreen broadleaf forest (Fig. 8D). Tadpoles could be found at daytime and night. Gravid females were found by the streams in the type locality (2 April 2017) and Suining County (15 March 2022).

**Etymology.** This specific name “dong” refers to the Dong people, as the new species distributed in the concentrated area of Dong people. We suggest its English common name “Dong leaf litter toads” and Chinese name “Dong Zhang Tu Chan (侗掌突蟾)”.

## Discussion

South-western China was proposed as a biodiversity hotspot (Myers et al. 2000). In the past five years, 34 new species of the genus *Leptobrachella* have been discovered (Frost 2022), while the species of *Leptobrachella* have low vagility and an exclusive association with montane forests and their populations are often highly structured and underestimation of species diversity occurs in the genus, which suggests a high degree of localised diversification and micro-endemism (Fei et al. 2012; Chen et al. 2018). Therefore, a lot of cryptic species were proposed by molecular analyses in areas where surveys are weak (Chen et al. 2018).

This new species was found in three localities and the largest geographical distance between the localities is over 200 km. However, in this study, phylogenetic analyses, based on mitochondrial DNA, suggested the three populations as the same species and different from its congeners on a series of morphological characters. This perhaps indicated that the species have a widespread distribution. Further surveys are needed to evaluate the population status of the species.

## Acknowledgements

We are grateful for the kind help from Dong people, especially Zhen Shi and her families in Shangdong Village, Tongdao County, Hunan Province. We are grateful for the help of Fu Shu and Keji Guo of Central South Inventory and Planning Institute of National Forestry and Grassland Administration, Jingbo Long of Huangsang National Nature Reserve and Yongjian QIN of Forestry and Grassland Administration of Suining County for their help in fieldwork in Suining County, Hunan Province.

This work was supported by the Projects from the National Natural Science Foundation of China (Nos. 32270498, 31960099, 32260136, and 32070426); West Light Foundation of The Chinese Academy of Sciences (Grant No. 2021XBZG\_XBQNXZ\_A\_006); Special funds of Guiyang Bureau of Science and Technology for supporting the Guiyang College (GYKJ-GYU[2021]); Guizhou Provincial Science and Technology Projects (Nos. [2020]1Y083, ZK[2022]540 and [2020]4Y029); Forestry Science and Technology Research Project of Guizhou Forestry Department (No. [2020]13, J[2018]03 and [2022]41); Zunyi Bureau of Science and Technology (No. HZ[2020]319); Guizhou Provincial Department of Education Youth Science and Technology Talents Growth Project (Nos. KY[2018]470, KY[2018]452 and KY[2020]234); Science Research Project of Moutai Institute (No.myk2019009); and Biodiversity Survey of Suining County, Hunan Province.

## References

- Anderson J (1871) A list of the reptilian accession to the Indian Museum, Calcutta from 1865 to 1870, with a description of some new species. *Journal of the Asiatic Society of Bengal* 40: 12–39.
- Boulenger GA (1893) Concluding report on the reptiles and batrachians obtained in Burma by Signor L. Fea dealing with the collection made in Pegu and the Karin Hills in 1887–1888. *Annali del Museo Civico di Storia Naturale di Genova* 13: 304–347.
- Boulenger GA (1900) Descriptions of new batrachians and reptiles from the Larut Hills, Perak. *Annals and Magazine of Natural History, Series 7* 6(32): 186–193. <https://doi.org/10.1080/00222930008678356>
- Chen JM, Poyarkov Jr NJ, Suwannapoom C, Lathrop A, Wu YH, Zhou WW, Yuan ZY, Jin JQ, Chen HM, Liu HQ, Nguyen TQ, Nguyen SN, Duong TV, Eto K, Nishikawa K, Matsui M, Orlov NL, Stuart BL, Brown RM, Rowley J, Murphy RW, Wang YY, Che J (2018) Large-scale phylogenetic analyses provide insights into unrecognized diversity and historical biogeography of Asian leaf-litter frogs, genus *Leptolalax* (Anura: Megophryidae). *Molecular Phylogenetics and Evolution* 124: 162–171. <https://doi.org/10.1016/j.ympev.2018.02.020>
- Chen WC, Liao X, Zhou SC, Mo YM (2019) A new species of *Leptobranchella* (Anura: Megophryidae) from southern Guangxi, China. *Zootaxa* 4563(1): 067–082. <https://doi.org/10.11646/zootaxa.4563.1.3>
- Chen JM, Xu K, Poyarkov NA, Wang K, Yuan ZY, Hou M, Suwannapoom C, Wang J, Che J (2020) How little is known about “the little brown frogs”: description of three new species of the genus *Leptobranchella* (Anura: Megophryidae) from Yunnan. *Zoological Research* 41(3): 292–313. <https://doi.org/10.24272/j.issn.2095-8137.2020.036>
- Chen JM, Suwannapoom C, Wu YH, Poyarkov NJ, Xu K, Pawangkhanant P, Che J (2021a) Integrative taxonomy reveals a new species of *Leptobranchella* (Anura: Megophryidae) from the mountains of northern Thailand. *Zootaxa* 5052(2): 41–64. <https://doi.org/10.11646/zootaxa.5052.2.2>

- Chen WC, Yu GD, Cheng ZY, Meng T, Wei H, Zhou GY, Lu YW (2021b) A new species of *Leptobrachella* (Anura: Megophryidae) from central Guangxi, China. *Zoological Research* 42(6): 783–788. <https://doi.org/10.24272/j.issn.2095-8137.2021.179>
- Chen WC, Peng W, Pan W, Liao N, Liu Y, Huang Y (2021c) A new species of *Leptobrachella* Smith 1925 (Anura: Megophryidae) from southern Guangxi, China. *Zootaxa* 5020(3): 581–596. <https://doi.org/10.11646/zootaxa.5020.3.8>
- Cheng YL, Shi SC, Li J, Liu J, Li SZ, Wang B (2021) A new species of the Asian leaf litter toad genus *Leptobrachella* Smith, 1925 (Anura, Megophryidae) from northwest Guizhou Province, China. *ZooKeys* 1021: 81–107. <https://doi.org/10.3897/zookeys.1021.60729>
- Clement M, Posada D, Crandall KA (2000) TCS: A computer program to estimate gene genealogies. *Molecular Ecology* 9(10): 1657–1659. <https://doi.org/10.1046/j.1365-294x.2000.01020.x>
- Darriba D, Taboada GL, Doallo R, Posada D (2012) jModelTest 2: More models, new heuristics and parallel computing. *Nature Methods* 9(8): e772. <https://doi.org/10.1038/nmeth.2109>
- Das I, Tron RKL, Rangad D, Hooroo RN (2010) A new species of *Leptolalax* (Anura: Megophryidae) from the sacred groves of Mawphlang, Meghalaya, north-eastern India. *Zootaxa* 2339(1): 44–56. <https://doi.org/10.11646/zootaxa.2339.1.2>
- Dehling JM (2012a) Eine neue Art der Gattung *Leptolalax* (Anura: Megophryidae) vom Gunung Benom, Westmalaysia/A new species of the genus *Leptolalax* (Anura: Megophryidae) from Gunung Benom, Peninsular Malaysia. *Sauria* 34: 9–21.
- Dehling JM (2012b) Redescription of *Leptolalax gracilis* (Günther, 1872) from Borneo and taxonomic status of two populations of *Leptolalax* (Anura: Megophryidae) from Peninsular Malaysia. *Zootaxa* 3328(1): 20–34. <https://doi.org/10.11646/zootaxa.3328.1.2>
- Dehling JM, Matsui M (2013) A new species of *Leptolalax* (Anura: Megophryidae) from Gunung Mulu National Park, Sarawak, East Malaysia (Borneo). *Zootaxa* 3670(1): 33–44. <https://doi.org/10.11646/zootaxa.3670.1.2>
- Dring J (1983) Frogs of the genus *Leptobrachella* (Pelobatidae). *Amphibia-Reptilia* 4(2): 89–102. <https://doi.org/10.1163/156853883X00012>
- Dubois A (1983) Note préliminaire sur le genre *Leptolalax* Dubois, 1980 (Amphibiens, Anoures), avec diagnose d'une espèce nouvelle du Vietnam. *Alytes* 2: 147–153.
- Duong TV, Do DT, Ngo CD, Nguyen TQ, Poyarkov Jr NA (2018) A new species of the genus *Leptolalax* (Anura: Megophryidae) from southern Vietnam. *Zoological Research* 39: 181–196. <https://doi.org/10.24272/j.issn.2095-8137.2018.009>
- Eto K, Matsui M, Nishikawa K (2015) Description of a new species of the genus *Leptobrachella* (Amphibia, Anura, Megophryidae) from Borneo. *Current Herpetology* 34(2): 128–139. <https://doi.org/10.5358/hsj.34.128>
- Eto K, Matsui M, Nishikawa K (2016) A new highland species of dwarf litter frog genus *Leptobrachella* (Amphibia, Anura, Megophryidae) from Sarawak. *Raffles Bulletin of Zoology*. Singapore 64: 194–203.
- Eto K, Matsui M, Hamidy A, Munir M, Iskandar DT (2018) Two new species of the genus *Leptobrachella* (Amphibia: Anura: Megophryidae) from Kalimantan, Indonesia. *Current Herpetology* 37(2): 95–105. <https://doi.org/10.5358/hsj.37.95>

- Fei L, Ye CY (2005) The key and illustration of Chinese. Sichuan Publishing House of Science and Technology. Chongqing, China.
- Fei L, Ye CY, Huang YZ (1990) Key to Chinese Amphibians. Publishing House for Scientific and Technological Literature. Chongqing, China.
- Fei L, Hu SQ, Ye CY, Huang YZ (2009) Fauna Sinica. Amphibia (Vol. 2) Anura. Science Press, Beijing.
- Fei L, Ye CY, Jiang JP (2012) Colored atlas of Chinese amphibians and their distributions. Sichuan Publishing House of Science and Technology, Chengdu.
- Frost DR (2022) Amphibian Species of the World: an Online Reference. Version 6.1. American Museum of Natural History, New York. <http://research.amnh.org/herpetology/amphibia/index.html> [Accessed 4 Nov 2022]
- Grismer LL, Grismer JL, Youmans TM (2004) A new species of *Leptolalax* (Anura: Megophryidae) from Pulau Tioman, West Malaysia. *Asiatic Herpetological Research* 10: 8–11.
- Guindon S, Dufayard JF, Lefort V, Anisimova M, Hordijk W, Gascuel O (2010) New algorithms and methods to estimate maximum-likelihood phylogenies: assessing the performance of PhyML 3.0. *Systematic Biology* 59(3): 07–321. <https://doi.org/10.1093/sysbio/syq010>
- Günther A (1872) On the reptiles and amphibians of Borneo. *Proceedings of the Scientific Meetings of the Zoological Society of London* 1872: 586–600.
- Günther A (1895) Te reptiles and batrachians of the Natuna Islands. *Novitates Zoologicae* 2: 499–502.
- Hall TA (1999) BIOEDIT: A user-friendly biological sequence alignment editor and analysis program for Windows 95/98/NT. *Nucleic Acids Symposium Series* 41(41): 95–98. <https://doi.org/10.1021/bk-1999-0734.ch008>
- Hoang CV, Nguyen TT, Luu VQ, Nguyen TQ, Jiang JP (2019) A new species of *Leptobranchella* Smith 1925 (Anura: Megophryidae) from Thanh Hoa Province, Vietnam. *Raffles Bulletin of Zoology*. Singapore 67: 536–556. <https://doi.org/10.26107/RBZ-2019-0042>
- Hou YM, Zhang MF, Hu F, Li SY, Shi SC, Chen J, Mo XY, Wang B (2018) A new species of the genus *Leptolalax* (Anura, Megophryidae) from Hunan, China. *Zootaxa* 4444(3): 247–266. <https://doi.org/10.11646/zootaxa.4444.3.2>
- Humtsoe LN, Bordoloi S, Ohler A, Dubois A (2008) Rediscovery of a long known species, *Ixalus lateralis* Anderson, 1871. *Zootaxa* 1921(1): 24–34. <https://doi.org/10.11646/zootaxa.1921.1.2>
- Inger RF, Stuebing RB (1992 [“1991”]) A new species of frog of the genus *Leptobranchella* Smith (Anura: Pelobatidae), with a key to the species from Borneo. *Raffles Bulletin of Zoology*. Singapore 39: 99–103.
- Inger RF, Stuebing RB, Tan F (1995) New species and new records of anurans from Borneo. *Raffles Bulletin of Zoology*. Singapore 43: 115–132.
- Inger RF, Lakim M, Biun A, Yambun P (1997) A new species of *Leptolalax* (Anura: Megophryidae) from Borneo. *Asiatic Herpetological Research* 7: 48–50. <https://doi.org/10.5962/bhl.part.18855>
- Inger RF, Orlov N, Darevsky I (1999) Frogs of Vietnam: A report on new collections. *Fieldiana. Zoology* 92: 1–46.

- Jiang K, Yan F, Suwannapoom C, Chomdej S, Che J (2013) A new species of the genus *Leptolalax* (Anura: Megophryidae) from northern Thailand. *Asian Herpetological Research* 4(2): 100–108. <https://doi.org/10.3724/SPJ.1245.2013.00100>
- Köhler J, Jansen M, Rodríguez A, Kok P, Toledo LF, Emmrich M, Glaw F, Haddad CFB, Rödel MO, Vences M (2017) The use of bioacoustics in anuran taxonomy: Theory, terminology, methods and recommendations for best practice. *Zootaxa* 4251(1): 1–124. <https://doi.org/10.11646/zootaxa.4251.1.1>
- Lathrop A, Murphy RW, Orlov N, Ho CT (1998) Two new species of *Leptolalax* (Anura: Megophryidae) from northern Vietnam. *Amphibia-Reptilia* 19(3): 253–267. <https://doi.org/10.1163/156853898X00160>
- Li SZ, Liu J, Wei G, Wang B (2020) A new species of the Asian leaf litter toad genus *Leptobranchella* (Amphibia, Anura, Megophryidae) from southwest China. *ZooKeys* 943: 91–118. <https://doi.org/10.3897/zookeys.943.51572>
- Lin SS, Li YH, Lu YH, Su HL, Wu SB, Zhang QQ, Mo MJ, Xiao SJ, Pan Z, Pan HJ, Zeng ZC, Wang J (2022) A new species of the genus *Leptobranchella* (Anura, Megophryidae) from northwestern Guangdong Province, China. *Herpetozoa* 35: 165–178. <https://doi.org/10.3897/herpetozoa.35.e89981>
- Liu CC (1950) Amphibians of western China. *Fieldiana Zoology Memoires* 2: 1–397. [+ 10 pl] <https://doi.org/10.5962/bhl.part.4737>
- Luo T, Xiao N, Gao K, Zhou J (2020) A new species of *Leptobranchella* (Anura, Megophryidae) from Guizhou Province, China. *ZooKeys* 923: 115–140. <https://doi.org/10.3897/zookeys.923.47172>
- Luo T, Wang WF, Peng D, Lei B, Deng HQ, Ji SN, Huang HQ, Zhou J (2022) A new species of the Asian Leaf Litter Toad genus *Leptobranchella* (Amphibia, Anura, Megophryidae) from Chongqing City, Southwest China. *Asian Herpetological Research* 13: 75–95. <https://doi.org/10.16373/j.cnki.ahr.210052>
- Lyu JC, Dai LL, Wei PF, He YH, Yuan ZY, Shi WL, Zhou SL, Ran SY, Kuang ZF, Guo X, Wei G, Yuan G (2020) A new species of the genus *Leptobranchella* Smith, 1925 (Anura, Megophryidae) from Guizhou, China. *ZooKeys* 1008: 139–157. <https://doi.org/10.3897/zookeys.1008.56412>
- Mahony S, Sengupta S, Kamei RG, Biju SD (2011) A new low altitude species of *Megophrys* Kuhl and van Hasselt (Amphibia: Megophryidae), from Assam, Northeast India. *Zootaxa* 3059(1): 36–46. <https://doi.org/10.11646/zootaxa.3059.1.2>
- Malkmus R (1992) *Leptolalax pictus* sp. nov. (Anura: Pelobatidae) vom Mount Kinabalu/NordBorneo. *Sauria* 14: 3–6.
- Mathew R, Sen N (2010 [“2009”]) Description of a new species of *Leptobranchium* Tschudi, 1838 (Amphibia: Anura: Megophryidae) from Meghalaya, India. *Records of the Zoological Survey of India* 109(3): 91–108. <https://doi.org/10.26515/rzsi/v109/i3/2009/158996>
- Matsui M (1997) Call characteristics of Malaysian *Leptolalax* with a description of two new species (Anura: Pelobatidae). *Copeia* 1997(1): 158–165. <https://doi.org/10.2307/1447851>
- Matsui M (2006) Three new species of *Leptolalax* from Thailand (Amphibia, Anura, Megophryidae). *Zoological Science* 23(9): 821–830. <https://doi.org/10.2108/zsj.23.821>

- Matsui M, Dehling JM (2012) Notes on an enigmatic Bornean megophryid, *Leptolalax dringi* Dubois, 1987 (Amphibia: Anura). *Zootaxa* 3317(1): 49–58. <https://doi.org/10.11646/zootaxa.3317.1.4>
- Matsui M, Belabut DM, Ahmad N, Yong HS (2009) A new species of *Leptolalax* (Amphibia, Anura, Megophryidae) from Peninsular Malaysia. *Zoological Science* 26(3): 243–247. <https://doi.org/10.2108/zsj.26.243>
- Matsui M, Zainudin R, Nishikawa K (2014a) A new Species of *Leptolalax* from Sarawak, Western Borneo (Anura: Megophryidae). *Zoological Science* 31(11): 773–779. <https://doi.org/10.2108/zs140137>
- Matsui M, Nishikawa K, Yambun P (2014b) A new *Leptolalax* from the mountains of Sabah, Borneo (Amphibia, Anura, Megophryidae). *Zootaxa* 3753(3): 440–452. <https://doi.org/10.11646/zootaxa.3753.5.3>
- Mauro DS, Gower DJ, Oommen OV, Wilkinson M, Zardoya R (2004) Phylogeny of caecilian amphibians (Gymnophiona) based on complete mitochondrial genomes and nuclear RAG1. *Molecular Phylogenetics and Evolution* 33(2): 413–427. <https://doi.org/10.1016/j.ympev.2004.05.014>
- Myers N, Mittermeier RA, Mittermeier CG, Da Fonseca GAB, Kent J (2000) Biodiversity hotspots for conservation priorities. *Nature* 403(6772): 853–858. <https://doi.org/10.1038/35002501>
- Nguyen LT, Poyarkov Jr NA, Le DT, Vo BD, Ninh HT, Duong TV, Murphy RW, Sang NV (2018) A new species of *Leptolalax* (Anura: Megophryidae) from Son Tra Peninsula, central Vietnam. *Zootaxa* 4388(1): 1–21. <https://doi.org/10.11646/zootaxa.4388.1.1>
- Nguyen LT, Tapley B, Nguyen CT, Luong HV, Rowley JJJ (2021) A new species of *Leptobranchella* (Anura, Megophryidae) from Mount Pu Ta Leng, northwest Vietnam. *Zootaxa* 5016(3): 301–332. <https://doi.org/10.11646/zootaxa.5016.3.1>
- Ohler A, Marquis O, Swan S, Grosjean S (2000) Amphibian biodiversity of Hoang Lien Nature Reserve (Lao Cai Province, northern Vietnam) with description of two new species. *Herpetozoa* 13(1/2): 71–87.
- Ohler A, Wollenberg KC, Grosjean S, Hendrix R, Vences M, Ziegler T, Dubois A (2011) Sorting out *Lalos*: Description of new species and additional taxonomic data on megophryid frogs from northern Indochina (genus *Leptolalax*, Megophryidae, Anura). *Zootaxa* 3147(1): 1–83. <https://doi.org/10.11646/zootaxa.3147.1.1>
- Poyarkov NJ, Rowley JJ, Gogoleva SI, Vassilieva AB, Galoyan EA, Orlov NL (2015) A new species of *Leptolalax* (Anura: Megophryidae) from the western Langbian Plateau, southern Vietnam. *Zootaxa* 3931(2): 221–252. <https://doi.org/10.11646/zootaxa.3931.2.3>
- Qian TY, Xia X, Cao Y, Xiao NW, Yang DD (2020) A new species of *Leptobranchella* (Anura: Megophryidae) Smith, 1925 from Wuling Mountains in Hunan Province, China. *Zootaxa* 4816(4): 491–526. <https://doi.org/10.11646/zootaxa.4816.4.4>
- Rao DQ (2022 [“2020”]) *Atlas of Wildlife in Southwest China: Amphibian*. Beijing Publishing House, Beijing.
- Ronquist FR, Huelsenbeck JP (2003) MrBayes3: Bayesian phylogenetic inference under mixed-models. *Bioinformatics* 19(12): 1572–1574. <https://doi.org/10.1093/bioinformatics/btg180>

- Rowley JJ, Cao TT (2009) A new species of *Leptolalax* (Anura: Megophryidae) from central Vietnam. *Zootaxa* 2198(1): 51–60. <https://doi.org/10.11646/zootaxa.2198.1.5>
- Rowley JJ, Hoang DH, Le TTD, Dau VQ, Cao TT (2010a) A new species of *Leptolalax* (Anura: Megophryidae) from Vietnam and further information on *Leptolalax tuberosus*. *Zootaxa* 2660: 33–45.
- Rowley JJ, Stuart BL, Neang T, Emmett DA (2010b) A new species of *Leptolalax* (Anura: Megophryidae) from northeastern Cambodia. *Zootaxa* 2567(1): 57–68. <https://doi.org/10.11646/zootaxa.2567.1.3>
- Rowley JJ, Stuart BL, Richards SJ, Phimmachak S, Sivongxay N (2010c) A new species of *Leptolalax* (Anura: Megophryidae) from Laos. *Zootaxa* 2681(1): 35–46. <https://doi.org/10.11646/zootaxa.2681.1.3>
- Rowley JJ, Le DTT, Tran DTA, Hoang DH (2011) A new species of *Leptobranchella* (Anura: Megophryidae) from southern Vietnam. *Zootaxa* 2796(1): 15–28. <https://doi.org/10.11646/zootaxa.2796.1.2>
- Rowley JJ, Hoang HD, Dau VQ, Le TTD, Cao TT (2012) A new species of *Leptolalax* (Anura: Megophryidae) from central Vietnam. *Zootaxa* 3321(1): 56–68. <https://doi.org/10.11646/zootaxa.3321.1.4>
- Rowley JJ, Dau VQ, Nguyen TT (2013) A new species of *Leptolalax* (Anura: Megophryidae) from the highest mountain in Indochina. *Zootaxa* 3737(4): 415–428. <https://doi.org/10.11646/zootaxa.3737.4.5>
- Rowley JJ, Stuart BL, Neang T, Hoang HD, Dau VQ, Nguyen TT, Emmett DA (2015a) A new species of *Leptolalax* (Anura: Megophryidae) from Vietnam and Cambodia. *Zootaxa* 4039(3): 401–417. <https://doi.org/10.11646/zootaxa.4039.3.1>
- Rowley JJ, Tran DTA, Le DTT, Dau VQ, Peloso PLV, Nguyen TQ, Hoang HD, Nguyen TT, Ziegler T (2016) Five new, microendemic Asian Leaf-litter Frogs (*Leptolalax*) from the southern Annamite mountains, Vietnam. *Zootaxa* 4085(1): 63–102. <https://doi.org/10.11646/zootaxa.4085.1.3>
- Rowley JJ, Dau VQ, Hoang HD, Le DTT, Cutajar TP, Nguyen TT (2017a) A new species of *Leptolalax* (Anura: Megophryidae) from northern Vietnam. *Zootaxa* 4243(3): 544–564. <https://doi.org/10.11646/zootaxa.4243.3.7>
- Rowley JJ, Dau VQ, Cao TT (2017b) A new species of *Leptolalax* (Anura: Megophryidae) from Vietnam. *Zootaxa* 4273(1): 61–79. <https://doi.org/10.11646/zootaxa.4273.1.5>
- Sambrook J, Fritsch EF, Maniatis T (1989) *Molecular Cloning: a Laboratory Manual*. Cold Spring Harbor Laboratory Press, New York.
- Sengupta S, Sailo S, Lalremsanga HT, Das A, Das I (2010) A new species of *Leptolalax* (Anura: Megophryidae) from Mizoram, north-eastern India. *Zootaxa* 2406(1): 56–68. <https://doi.org/10.11646/zootaxa.2406.1.3>
- Shi SC, Hou YM, Song ZB, Jiang JP, Wang B (2021) A new leaf litter toad of *Leptobranchella* Smith, 1925 (Anura, Megophryidae) from Sichuan Province, China with supplementary description of *L. oshanensis*. *Asian Herpetological Research* 12(2): 143–166. <https://doi.org/10.16373/j.cnki.ahr.200118>

- Simon C, Frati F, Beckenbach A, Crespi B, Liu H, Flook P (1994) Evolution, weighting and phylogenetic utility of mitochondrial gene sequences and a compilation of conserved polymerase chain reaction primers. *Annals of the Entomological Society of America* 87(6): 651–701. <https://doi.org/10.1093/aesa/87.6.651>
- Stuart BL, Rowley JJJ (2020) A new *Leptobranchella* (Anura: Megophryidae) from the Cardamom Mountains of Cambodia. *Zootaxa* 4834(4): 556–572. <https://doi.org/10.11646/zootaxa.4834.4.4>
- Sung YH, Yang JH, Wang YY (2014) A new species of *Leptolalax* (Anura: Megophryidae) from southern China. *Asian Herpetological Research* 5(2): 80–90. <https://doi.org/10.3724/SPJ.1245.2014.00080>
- Tamura K, Stecher G, Peterson D, Fiipiski A, Kumar S (2013) MEGA6: Molecular Evolutionary Genetics Analysis Version 6.0. *Molecular Phylogenetics and Evolution* 28: 2725–2729. <https://doi.org/10.1093/molbev/mst197>
- Taylor EH (1962) The amphibian fauna of Thailand. *The University of Kansas Science Bulletin* 43: 265–599. <https://doi.org/10.5962/bhl.part.13347>
- Wang J, Yang JH, Li Y, Lyu ZT, Zeng ZC, Liu ZY, Ye YH, Wang YY (2018) Morphology and molecular genetics reveal two new *Leptobranchella* species in southern China (Anura, Megophryidae). *ZooKeys* 776: 105–137. <https://doi.org/10.3897/zookeys.776.22925>
- Wang J, Li YL, Li Y, Chen HH, Zeng YJ, Shen JM, Wang YY (2019) Morphology, molecular genetics, and acoustics reveal two new species of the genus *Leptobranchella* from northwestern Guizhou Province, China (Anura, Megophryidae). *ZooKeys* 848: 119–154. <https://doi.org/10.3897/zookeys.848.29181>
- Wang J, Lyu ZT, Qi S, Zeng ZC, Zhang WX, Lu LS, Wang YY (2020) Two new *Leptobranchella* species (Anura, Megophryidae) from the Yunnan-Guizhou Plateau, southwestern China. *ZooKeys* 995: 97–125. <https://doi.org/10.3897/zookeys.995.55939>
- Wang J, Qi S, Dai KY, Lyu ZT, Zeng ZC, Chen HH, Li YQ, Zhao YY, Wang YZ, Wang YY (2022) A new *Leptobranchella* species (Anura, Megophryidae) from South China, with comments on the taxonomic status of *L. chishuiensis* and *L. purpurus*. *Zoosystematics and Evolution* 98(1): 165–180. <https://doi.org/10.3897/zse.98.73162>
- Watters JL, Cummings ST, Flanagan RL, Siler CD (2016) Review of morphometric measurements used in anuran species descriptions and recommendations for a standardized approach. *Zootaxa* 4072(4): 477–495. <https://doi.org/10.11646/zootaxa.4072.4.6>
- Yang JH, Wang YY, Chen GL, Rao DQ (2016) A new species of the genus *Leptolalax* (Anura: Megophryidae) from Mt. Gaoligongshan of western Yunnan Province, China. *Zootaxa* 4088: 379–394. <https://doi.org/10.11646/zootaxa.4088.3.4>
- Yang JH, Zeng ZC, Wang YY (2018) Description of two new sympatric species of the genus *Leptolalax* (Anura: Megophryidae) from western Yunnan of China. *PeerJ* 6(e4586): 1–32. <https://doi.org/10.7717/peerj.4586>
- Yuan ZY, Sun RD, Chen JM, Rowley JJ, Wu ZJ, Hou SB, Wang SN, Che J (2017) A new species of the genus *Leptolalax* (Anura: Megophryidae) from Guangxi, China. *Zootaxa* 4300(4): 551–570. <https://doi.org/10.11646/zootaxa.4300.4.5>

## Supplementary material 1

### Measurements of adult specimen of *Leptobrachella dong* sp. nov.

Author: Bin Wang

Data type: table (excel document)

Explanation note: Morphological data. Units in mm. See abbreviations for characters in the Materials and methods section.

Copyright notice: This dataset is made available under the Open Database License (<http://opendatacommons.org/licenses/odbl/1.0/>). The Open Database License (ODbL) is a license agreement intended to allow users to freely share, modify, and use this Dataset while maintaining this same freedom for others, provided that the original source and author(s) are credited.

Link: <https://doi.org/10.3897/zookeys.1149.85895.suppl1>

## Supplementary material 2

### Uncorrected p-distance between *Leptobrachella* species on the 16S rRNA gene

Author: Bin Wang

Data type: table (excel document)

Explanation note: Genetic distance. The values below 3% are coloured in red.

Copyright notice: This dataset is made available under the Open Database License (<http://opendatacommons.org/licenses/odbl/1.0/>). The Open Database License (ODbL) is a license agreement intended to allow users to freely share, modify, and use this Dataset while maintaining this same freedom for others, provided that the original source and author(s) are credited.

Link: <https://doi.org/10.3897/zookeys.1149.85895.suppl2>

## Supplementary material 3

### Call data

Author: Bin Wang

Data type: table (excel document)

Explanation note: Call measurements (mean  $\pm$  standard deviation) of *Leptobrachella dong* sp. nov.

Copyright notice: This dataset is made available under the Open Database License (<http://opendatacommons.org/licenses/odbl/1.0/>). The Open Database License (ODbL) is a license agreement intended to allow users to freely share, modify, and use this Dataset while maintaining this same freedom for others, provided that the original source and author(s) are credited.

Link: <https://doi.org/10.3897/zookeys.1149.85895.suppl3>

# Description of two new species of the leafhopper genus *Pediopsis* Burmeister (Hemiptera, Cicadellidae, Eurymelinae, Macropsini) from China

Hu Li<sup>1,2</sup>, Ran-Huai Dai<sup>2</sup>, Michael D. Webb<sup>3</sup>

**1** Shaanxi Key Laboratory of Bio-resources, School of Biological Science & Engineering, Shaanxi University of Technology, Qinling-Bashan Mountains Bioresources Comprehensive Development C.I.C., State Key Laboratory of Biological Resources and Ecological Environment of Qinling-Bashan, Shaanxi, 723000, Hanzhong, China **2** Institute of Entomology of Guizhou University, The Provincial Key Laboratory for Agricultural Pest Management of Mountainous Region, Guizhou, 550025, Guiyang, China **3** The Natural History Museum, SW7 5BD, London, UK

Corresponding author: Ran-Huai Dai ([lihu@snut.edu.cn](mailto:lihu@snut.edu.cn), [rh dai69@163.com](mailto:rh dai69@163.com))

Academic editor: Pavel Stoev | Received 30 January 2022 | Accepted 25 January 2023 | Published 22 February 2023

<https://zoobank.org/F2942BEA-1D8C-490C-93DC-EF66B9EBBCCC>

**Citation:** Li H, Dai R-H, Webb MD (2023) Description of two new species of the leafhopper genus *Pediopsis* Burmeister (Hemiptera, Cicadellidae, Eurymelinae, Macropsini) from China. ZooKeys 1149: 135–144. <https://doi.org/10.3897/zookeys.1149.81434>

## Abstract

Two new leafhopper species of *Pediopsis* Burmeister, *Pediopsis albopicta* Li & Dai, **sp. nov.** from Hunan and Guizhou provinces of central China and *Pediopsis pianmaensis* Li & Dai, **sp. nov.** from Yunnan Province of southwestern China, are described and illustrated. Ambiguity in the original description of *P. bannaensis* Yang & Zhang is discussed, and figures of the female holotype of *P. femorata* Hamilton are provided for the first time. A checklist and key to Chinese species of *Pediopsis* are also given.

## Keywords

Auchenorrhyncha, Homoptera, morphology

## Introduction

The leafhopper genus *Pediopsis* Burmeister, belonging to the tribe Macropsini of the subfamily Eurymelinae (*sensu* Dietrich and Thomas 2018), was established by Burmeister (1838) as a subgenus of *Bythoscopus* Germar; it was subsequently raised to the level

of genus and *Jassus tiliae* Germar, 1831 was designated as its type species by Kirkaldy (1903). Many authors (Anufriev 1971; Hamilton 1980; Tishechkin 1997; Cai et al. 2005; Dai and Li 2013; Yang and Zhang 2015; Yang et al. 2016) have described new species or proposed new combinations in the genus worldwide, increasing the number of species to 19, of which six are known from China (Dai et al. 2018). In this paper, two new species of *Pediopsis* from China are described, ambiguity in the original description of *P. bannaensis* Yang & Zhang is discussed, and the status of *P. femorata* Hamilton is commented on. Figures of the female holotype of *P. femorata* for the first time are provided. In addition, a checklist and key to the Chinese species of *Pediopsis* are given.

## Materials and methods

Specimens studied were collected by netting. External morphology was observed under Olympus SZX7 and BX43 microscopes. Male terminalia preparations were macerated in a boiling solution of 8% NaOH for ~ 5 min. Habitus images of adults were obtained by using a KEYENCE VHX-1000 system. Genitalia drawings were created and edited utilizing Adobe Illustrator CS6 and Photoshop CS6 based on line drawings of specimens.

The higher classification and morphological terminology used in this work follows Hamilton (1980) and Dietrich and Thomas (2018). Body length is measured from the apex of the head to the end of the folded forewings and presented in millimeters (mm).

Type specimens of the new species and other material examined are deposited in the Institute of Entomology, Guizhou University, Guiyang, China (**GUGC**).

## Systematics

### Genus *Pediopsis* Burmeister

*Bythoscopus* (*Pediopsis*) Burmeister, 1838: 11.

*Pediopsis*–Kirkaldy 1903: 214; Hamilton 1980: 902.

**Type species.** *Jassus tiliae* Germar, 1831, by subsequent designation of Kirkaldy (1903).

**Distribution.** Palaearctic, Oriental, Nearctic, and Australian regions.

**Remarks.** *Pediopsis* can be distinguished by the following combination of features: head across eyes usually distinctly narrower than pronotum, face wider than long, lora relatively large, pronotum frontally declivous and usually with strongly oblique striations, male pygofer without spines or processes, dorsal connective usually strongly developed. The traditional separation of *Pediopsis* from *Pedionis* (Hamilton 1980) is followed here, but, as more species become known, the two genera may be synonymized. The difficulty in defining *Pediopsis* is apparent from the fact that the genus was keyed out in two places in Hamilton's (1980) key. At present, the most reliable feature to separate the two genera is the presence or absence of processes or spines on the ventral margin of the male pygofer (absent in *Pediopsis* and present in *Pedionis*).

Checklist to species of *Pediopsis* from China

- P. albopicta* Li & Dai, sp. nov. Figs 1–11. Distribution. China (Hunan and Guizhou provinces).
- P. bannaensis* Yang & Zhang, 2015: 488, figs 29–39. Distribution. China (Yunnan Province), Thailand.
- P. cudraniaae* Cai & Wang, 2005: 206, fig. 1. Distribution. China (Shandong Province).
- P. femorata* Hamilton, 1980: 919; Figs 22–26. Distribution. China (Taiwan).
- P. kurentsovi* Anufriev, 1971: 95, figs 4–6; 1976: 133. Distribution. China (Hebei, Heilongjiang provinces), Russia.
- P. ningxiaensis* Dai & Li, 2013: 961, figs 22–31. Distribution. China (Ningxia Province).
- P. tiliae* (Germar, 1831: 14), Hamilton 1980: 903, fig. 62. Distribution. Widespread in Palaearctic region.
- P. pianmaensis* Li & Dai, sp. nov. Figs 12–21. Distribution. China (Yunnan Province).

Key to species of *Pediopsis* recorded in China

- 1 Fore margin of head and pronotum in dorsal view strongly arched forward (Fig. 22).....***P. femorata***
- Fore margin of head and pronotum in dorsal view moderately arched forward .....**2**
- 2 Mesonotum with white tip and veins of forewings with white spots (Fig. 1); aedeagal shaft very short (Fig. 10) ..... ***P. albopicta***
- Mesonotum without white tip and veins of forewings without white spots; aedeagal shaft short to long .....**3**
- 3 Species mainly dark (Fig. 12); forewing with two subapical cells (Fig. 14).....  
..... ***P. pianmaensis***
- Species mainly pale, sometimes forewing with distinct brown markings; forewings with two or three subapical cells (Fig. 4) ..... **4**
- 4 Dorsal connective with process near midlength or subbasally.....**5**
- Dorsal connective with process absent .....**7**
- 5 Dorsal connective with well-developed process near midlength, caudodorsally twisted Y-shaped (see Yang and Zhang 2015: fig. 39) ..... ***P. bannaensis***
- Dorsal connective with weakly developed process subbasally, straight (see Anufriev 1971: fig. 4; Dai and Li 2013: figs 31, 34) .....**6**
- 6 Forewing distinctly marked with brown; aedeagal shaft slender (see Anufriev 1971: fig. 6; Dai and Li 2013: fig. 32) ..... ***P. kurentsovi***
- Forewing weakly marked with brown; aedeagal shaft not slender (see Dai and Li 2013: fig. 29)..... ***P. ningxiaensis***
- 7 Dorsal connective clearly twisted dorsally in lateral aspect (see Hamilton 1980: fig. 62).....***P. tiliae***
- Dorsal connective clearly twisted ventrally in lateral aspect (Fig. 16).....  
..... ***P. cudraniaae***

***Pediopsis albopicta* Li & Dai, sp. nov.**

<https://zoobank.org/75EF8204-6352-4FD0-81AC-965941C9C833>

Figs 1–11

**Examined material.** *Holotype* ♂, CHINA: Hunan Province, Badagongshan National Natural Reserve, Tianpingshan, 5.viii.2013, collected by Hu Li. *Paratypes* 1 ♂, same data as holotype, except 3.viii.2013; 1 ♀, Guizhou Province, Shiqian County, Fodingshan National Natural Reserve, 15.viii.1991, collected by Xiang-Sheng Chen.

**Description.** *Body color* (Figs 1–3). Body background color black to dark brown. Head and face (Fig. 3) yellowish, with dark spots or stripes, frontoclypeus slightly milky white, eyes dark brown with reddish tinge, fading to gray; ocelli dark; apex of anteclypeus and gena black. Pronotum (Fig. 1) with anterior half dark brown, posterior half gray, striations on surface darker. Mesonotum (Fig. 1) evenly black with white tip. Forewing (Figs 1, 2) brown, with several transparent patches at midlength and subapically; veins black with clear white spots. Legs yellowish with black or brown patches.

*Body appearance* (Figs 1–4). Head across eyes (Fig. 1) clearly narrower than pronotum; crown short with anterior and posterior margins almost parallel. Face (Fig. 3) as long as wide across eyes, surface with clear punctures and striations, central region slightly tumid frontally, distance between ocelli relatively large, approximately 8× that from ocellus to adjacent eye. Pronotum (Figs 1, 2) broad, 2.4× wider than long, with strongly oblique striations. Mesonotum (Fig. 1) 1.5× longer than pronotum. Forewing (Figs 1, 2, 4) with three subapical and four apical cells, venation prominent.

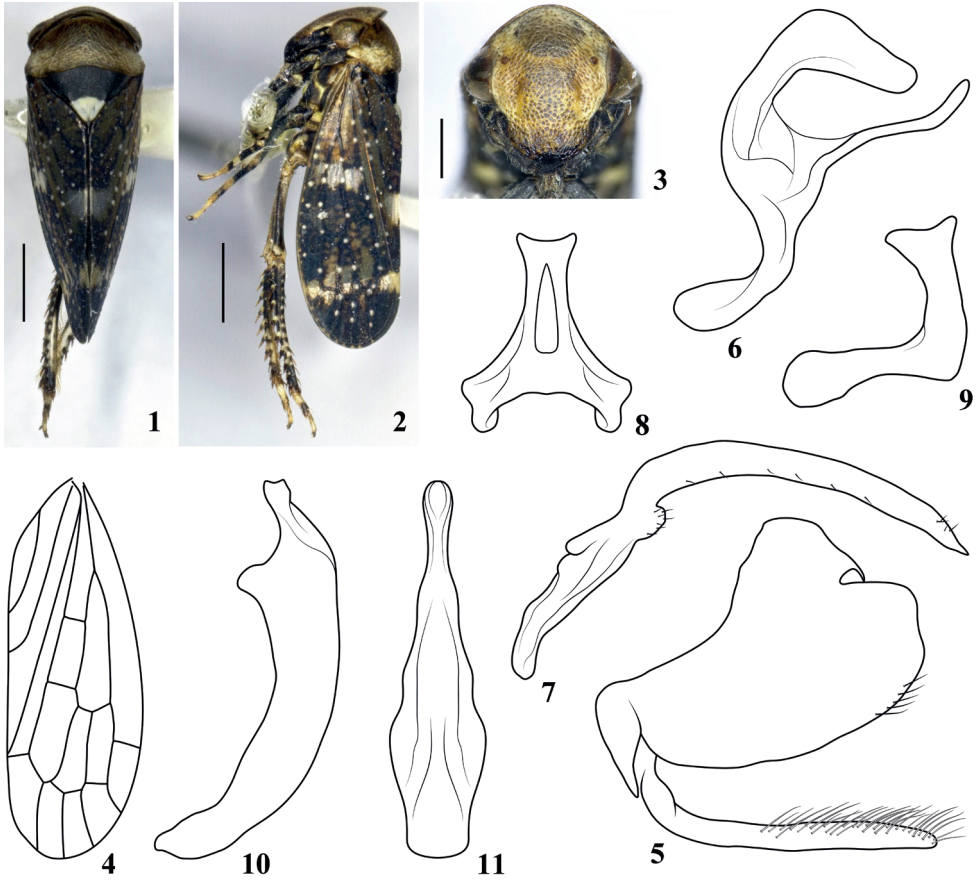
*Male genitalia* (Figs 5–11). Pygofer (Fig. 5) broad basally, lobe short and stout, caudal margin truncated, slightly depressed medially, ventral margin smoothly curved, with scattered marginal setae. Subgenital plate (Fig. 5) slender, of equal width throughout length, with relatively long hair-like setae, its length as long as ventral margin of pygofer. Dorsal connective (Fig. 6) strongly developed, S-shaped, with long slender process produced on ventral margin directed caudad and twisted. Style (Fig. 7) with apophysis stout, angled dorsally at basal 1/3, gradually tapering to pointed apex, with few marginal setae. Connective as in Figs 8, 9. Aedeagus (Figs 10, 11) with basal apodeme and shaft short, the latter shorter than 1/2 length of whole aedeagus, tapered in lateral view to truncate apex, bent dorsally.

**Measurement.** Body length (including tegmen): 4.3 mm.

**Distribution.** China (Hunan and Guizhou provinces).

**Etymology.** The specific epithet of the new species is derived from the Latin words *albus* (white) and *picta* (spot), referring to the white tip of the mesonotum and white spots on the forewing veins.

**Remarks.** This species can be readily separated from other congeners by the contrasting color pattern of its mesonotum, white spotted forewing veins, and different shape of the aedeagus and dorsal connective.



**Figures 1–11.** *Pediopsis albopicta* sp. nov. **1** male habitus, dorsal view **2** male habitus, lateral view **3** face **4** forewing **5** male pygofer and subgenital plate, lateral view **6** dorsal connective, lateral view **7** style, lateral view **8** connective, ventral view **9** connective, lateral view **10** aedeagus, lateral view **11** aedeagus, ventral view. Scale bars: 1 mm (**1, 2**); 0.5 mm (**3**).

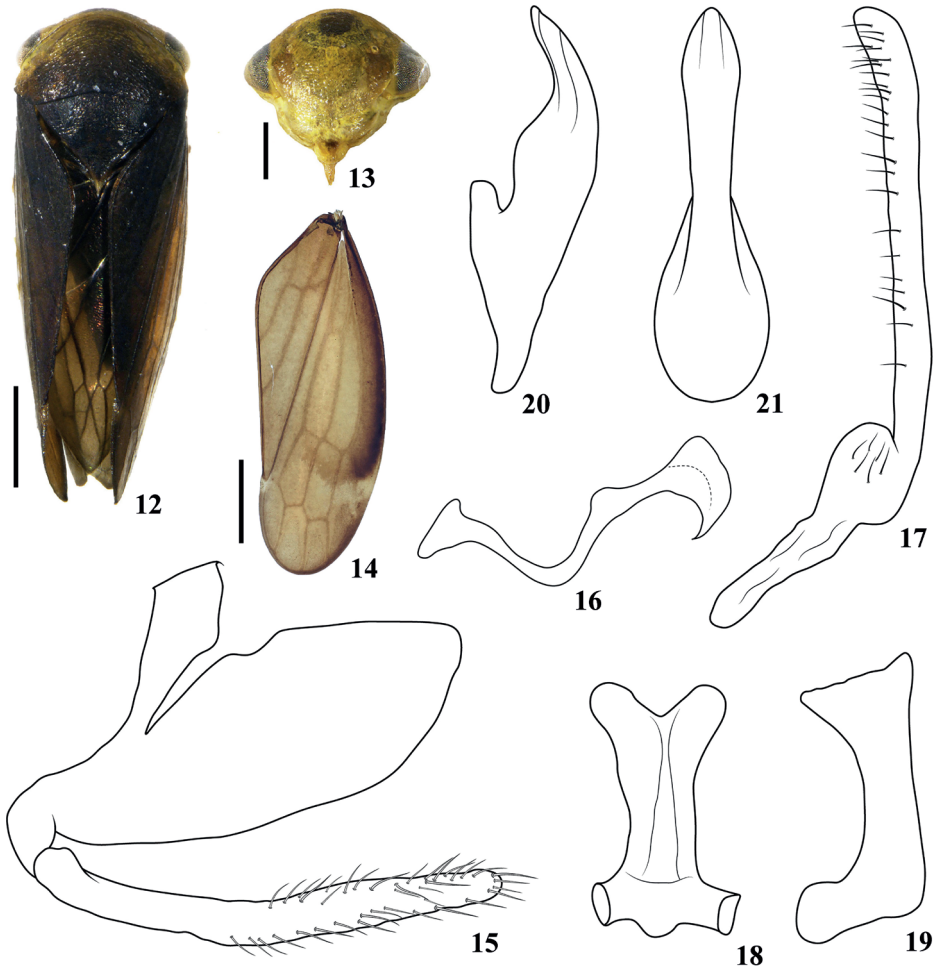
***Pediopsis pianmaensis* Li & Dai, sp. nov.**

<https://zoobank.org/F032A413-DF1C-4426-91C5-DE6DF8487C88>

Figs 12–21

**Examined material.** *Holotype* ♂, CHINA: Yunnan Province, Lushui City, Pianma Town, 26°0'34"N, 98°37'55"E, 26.v.2019, collected by Jia-Jia Wang and Chao Zhang.

**Description.** *Body color* (Figs 12–14). Specimen from alcohol. Yellowish to dark brown, striations on head, face, and pronotum same color as those of ground color. Head (Figs 12, 13) yellowish, face with dark brown spot at upper central region, eyes brown with gray tinge, ocelli yellow, lower parts of ocelli slightly brown, anteclypeus with brown macula. Pronotum (Fig. 12) yellowish on anterior areas, especially those



**Figures 12–21.** *Pediopsis pianmaensis* sp. nov. **12** male habitus, dorsal view **13** face **14** forewing **15** male pygofer and subgenital plate, lateral view **16** dorsal connective, lateral view **17** style, lateral view **18** connective, dorsal view **19** connective, lateral view **20** aedeagus, later view **21** aedeagus, ventral view. Scale bars: 1 mm (**12, 14**); 0.5 mm (**13**).

near eyes, then gradually darkening to almost black at posterior part. Mesonotum (Fig. 12) evenly black, with small yellowish tip. Forewing (Fig. 12) dark brown to almost black on basal part, veins black. Legs yellow with brown markings.

**Body appearance** (Fig. 12). Head across eyes (Fig. 13) slightly narrower than pronotum; crown short, almost parallel sided. Face (Fig. 13) including eyes  $1.2\times$  wider than its length; distance between ocelli nearly  $4\times$  that from ocellus to adjacent eye. Pronotum (Fig. 12)  $2.2\times$  wider than long, with striations nearly transverse. Mesonotum (Fig. 12)  $1.3\times$  longer than pronotum. Forewing (Fig. 14) with two subapical and three apical cells, venation prominent.

**Male genitalia** (Figs 15–21). Pygofer (Fig. 15) slightly prolonged caudally. Subgenital plate (Fig. 15) slender, slightly longer than ventral margin of pygofer, apical 1/2 with scattered setae. Dorsal connective (Fig. 16) relatively simple, S-shaped with apex broad and tapering to acute ventrally directed tip. Style (Fig. 17) with apophysis relatively straight, slightly widening to truncate apex, with marginal setae. Connective as in Figs 18, 19. Aedeagus (Figs 20, 21) with dorsal apodeme and preatrium short, shaft in lateral view broad basally, thereafter tapered to upturned apex, in ventral view expanded distally with conically rounded apex.

**Measurement.** Body length (including tegmen): 5.1 mm.

**Distribution.** China (Yunnan Province).

**Etymology.** The specific epithet refers to the type locality of the new species, Pianma Town (Yunnan Province), combined with the Latin suffix *-ensis*, meaning “pertaining to”.

**Remarks.** The new species can be distinguished from all other congeners by its darker body color, forewing with two ante-apical cells, simple aedeagus, and S-shaped dorsal connective.

### *Pediopsis bannaensis* Yang & Zhang

*Pediopsis bannaensis* Yang & Zhang, 2015: 488, figs 29–39.

**Remarks.** This species was described from the holotype and paratype male from China deposited in the Northwest A&F University, Yangling, China (NWFU) and three male paratypes from Thailand in the Illinois Natural History Survey, Champaign, USA (INHS). However, there are some ambiguities in the original description. Firstly, if the genitalia are drawn accurately, two different species appear to have been figured. The genitalia of one species were shown undissected in fig. 33 of the original description, and based on the aedeagus, the dissected parts of another species were shown in figs 34–39. The aedeagus shown in fig. 33 is the one described, i.e., “Aedeagus strongly tapered from wide base to narrow apex in lateral aspect”. Enquiries made by one of us (Webb) indicate that there are three (not two) Chinese specimens of the species present in the NWFU collection, with the original type data, all without type labels. Of these specimens only one is dissected and matches fig. 33. Other enquiries made regarding the paratypes in INHS indicate that their aedeagi also match fig. 33. All type series specimens match the habitus images in the original description with respect to general appearance and color pattern, particularly the long dark basal triangles of the mesonotum. However, unaccountably none match the actual specimen imaged based on the leg position in the lateral habitus figure (Yang and Zhang 2015: fig. 30). It is suggested that the dissected specimen in NWFU be regarded as the holotype even though we do not know what specimen provided the external images, which are of a better specimen.

***Pediopsis femorata* Hamilton**

Figs 22–26

*Pediopsis femorata* Hamilton, 1980: 919.*Pediopsoides femorata*–Huang and Viraktamath 1993: 365, misapplication?*Pediopsis femorata*–Dai et al. 2018: 188.

**Remarks.** This species was described based on the female type from Taiwan island, China. Subsequently, Huang and Viraktamath (1993) moved it into *Pediopsoides* Matsumura according to their own specimens from Taiwan. However, Dai et al. (2018) studied the material examined by Hamilton (1980) and Huang and Viraktamath (1993) and considered Huang and Viraktamath's (1993) identification of *Pediopsoides femorata* to be a misidentification and gave it a new name; it may or may not be a new species of *Pediopsoides* (see Li et al. in prep.).



**Figures 22–26.** Female holotype of *Pediopsis femorata* Hamilton **22** habitus, dorsal view **23** labels **24** face, frontal view **25** habitus, lateral view **26** habitus, ventral view. Scale bars: 1 mm. Images © North Carolina State University.

## Acknowledgements

We are very grateful to Dr Dmitri Yu. Tishechkin (M.V. Lomonosov Moscow State University, Moscow) for comments about the status of the new species described here, and to Dr Matt Bertone (North Carolina State University, Raleigh) for taking photos of *Pediopsis femorata*. We thank Drs Xiang-Sheng Chen, Jia-Jia Wang, and Chao Zhang (GUGC) for providing specimens for our study. This project was supported by a National Natural Science Foundation of China (No. 32000329), a Scientific Research Program Funded by Shaanxi Provincial Education Department (No. 21JK0568), and a “City-University Co-construction” Scientific Research Project for State Key Laboratory of Biological Resources and Ecological Environment of Qinling-Bashan (No. SXJ-2102).

## References

- Anufriev GA (1971) New and little-known leafhoppers (Homoptera, Auchenorrhyncha) from the Far East of the U.S.S.R. and neighboring countries. *Entomologicheskoe Obozrenie* 50(1): 95–116. [in Russian with English summary]
- Anufriev GA (1976) Notes on the genus *Psammoterrix* HPT. With descriptions of two new species from Siberia and the Far East (Homoptera, Cicadellidae). *Reichenbachia* 16(9): 129–134.
- Burmeister HCC (1838) *Genera Quaedam Insectorum. Iconibus Illustravit et Descripsit Hermannus Burmeister. A. Burmeister, Berlini*, 48 pp. <https://doi.org/10.5962/bhl.title.8144>
- Cai B, Wang ZQ, Liu CH, Yan JH (2005) A new species of leafhopper injurious to *Tricuspid Cudrania* (Homoptera: Cicadellidae: Macropsinae). *Canye Kexue* 31(2): 206–207. [in Chinese with English summary]
- Dai R-H, Li H (2013) Notes on the leafhopper genus *Pediopsis* (Hemiptera: Cicadellidae: Macropsinae) with description of one new species from China. *The Florida Entomologist* 96(3): 957–963. <https://doi.org/10.1653/024.096.0333>
- Dai R-H, Li H, Li Z-Z (2018) *Macropsinae from China* (Hemiptera: Cicadellidae). China Agriculture Press, Beijing, 240 pp.
- Dietrich CH, Thomas MJ (2018) New eurymelinae leafhoppers (Hemiptera, Cicadellidae, Eurymelinae) from Eocene Baltic amber with notes on other fossil Cicadellidae. *ZooKeys* 726: 131–143. <https://doi.org/10.3897/zookeys.726.21976>
- Germar EF (1831) *Cercopis mactata* Germ. *Tettigonia concinna* Germ. *Augusti Ahrensii Fauna Insectorum Europae* 14: 11–15.
- Hamilton KGA (1980) Contributions to the study of the world Macropsini (Rhynchota: Homoptera: Cicadellidae). *Canadian Entomologist* 112(9): 875–932. <https://doi.org/10.4039/Ent112875-9>
- Huang KW, Viraktamath CA (1993) The Macropsine Leafhoppers (Homoptera: Cicadellidae) of Taiwan. *Chinese Journal of Entomology* 13: 361–373.

- Kirkaldy GW (1903) On the nomenclature of the genera of the Rhynchota; Heteroptera, and auchenorrhynchous Homoptera – Part V. *Entomologist* 36: 213–216.
- Tishechkin DYu (1997) A new species of the genus *Pediopsis* (Homoptera: Cicadinea: Cicadellidae: Macropsinae) from Malaysia. *Russian Entomological Journal* 6(3–4): 29–30.
- Yang L, Zhang Y (2015) New records and synonymy in the genus *Macropsidius* (Hemiptera, Cicadellidae, Macropsinae) from China and description of a new *Pediopsis* species. *Zootaxa* 4021(3): 487–492. <https://doi.org/10.11646/zootaxa.4021.3.9>
- Yang L, Dietrich CH, Zhang Y (2016) Two new *Pediopsis* species and a new *Ruandopsis* species (Hemiptera: Cicadellidae: Macropsinae) from Madagascar. *Zootaxa* 4173(2): 174–182. <https://doi.org/10.11646/zootaxa.4173.2.8>

# Performance of intron 7 of the $\beta$ -fibrinogen gene for phylogenetic analysis: An example using gladiator frogs, *Boana* Gray, 1825 (Anura, Hylidae, Cophomantinae)

Ruth Amanda Estupiñán<sup>1,2</sup>, Sávio Torres de Farias<sup>2,3</sup>, Evonnildo Costa Gonçalves<sup>4</sup>,  
Mauricio Camargo<sup>1</sup>, Maria Paula Cruz Schneider<sup>5</sup>

**1** Instituto Federal da Paraíba, Campus, João Pessoa, Paraíba, PB. CEP 58015-435, Brazil **2** Programa de Pós-graduação em Ciências Biológicas (Zoologia), Departamento de Sistemática e Evolução, Universidade Federal da Paraíba, João Pessoa, PB. CEP 58051-900, Brazil **3** Laboratório de Genética Evolutiva – Paulo Leminski, Departamento de Biologia Molecular, Universidade Federal da Paraíba, João Pessoa, PB. CEP 58051-900, Brazil **4** Laboratório de Tecnologia Biomolecular-LTB, Instituto de Ciências Biológicas, Universidade Federal do Pará, Belém, PA. CEP 66075-110, Brazil **5** Centro de Genômica e Biologia de Sistemas, Universidade Federal do Pará, Belém, PA, CEP 66075-110, Brazil

Corresponding author: Ruth Amanda Estupiñán ([ruthamanda.estupinan@gmail.com](mailto:ruthamanda.estupinan@gmail.com))

Academic editor: Uri García-Vázquez | Received 21 April 2022 | Accepted 22 July 2022 | Published 22 February 2023

<https://zoobank.org/4767C7D0-49CA-4D64-A07C-1FFFAD20836B>

**Citation:** Estupiñán RA, Torres de Farias S, Gonçalves EC, Camargo M, Cruz Schneider MP (2023) Performance of intron 7 of the  $\beta$ -fibrinogen gene for phylogenetic analysis: An example using gladiator frogs, *Boana* Gray, 1825 (Anura, Hylidae, Cophomantinae). ZooKeys 1149: 145–169. <https://doi.org/10.3897/zookeys.1149.85627>

## Abstract

*Boana*, the third largest genus of Hylinae, has cryptic morphological species. The potential applicability of *b-fibrinogen intron 7 – FGBI7* is explored to propose a robust phylogeny of *Boana*. The phylogenetic potential of *FGBI7* was evaluated using maximum parsimony, MrBayes, and maximum likelihood analysis. Comparison of polymorphic sites and topologies obtained with concatenated analysis of *FGBI7* and other nuclear genes (*CXCR4*, *CXCR4*, *RHO*, *SIAH1*, *TYR*, and *28S*) allowed evaluation of the phylogenetic signal of *FGBI7*. Mean evolutionary rates were calculated using the sequences of the mitochondrial genes *ND1* and *CYTB* available for *Boana* in GenBank. Dating of *Boana* and some of its groups was performed using the RelTime method with secondary calibration. *FGBI7* analysis revealed high values at informative sites for parsimony. The absolute values of the mean evolutionary rate were higher for mitochondrial genes than for *FGBI7*. Dating of congruent *Boana* groups for *ND1*, *CYTB*, and *FGBI7* revealed closer values between mitochondrial genes and slightly different values from those of *FGBI7*. Divergence times of basal groups tended to be overestimated when mtDNA was used and were more accurate when nDNA

was used. Although there is evidence of phylogenetic potential arising from concatenation of specific genes, *FGBI7* provides well-resolved independent gene trees. These results lead to a paradigm for linking data in phylogenomics that focuses on the uniqueness of species histories and ignores the multiplicities of individual gene histories.

### Keywords

Anura evolutionary rate, divergence time, gladiator frogs, indels, nuclear DNA, nucleotide substitution rate, phylogenetic hypothesis, polymorphic sites

## Introduction

Using only one type of trait, such as mitochondrial DNA (mtDNA), to detect phylogenetic relationships can lead to noise (Rubinoff and Holland 2005). Frog mitochondrial DNA (mtDNA) has high sequence evolution rates and many gene arrangements, making it difficult to find conserved regions (Zhang et al. 2013). The low mutation rates in mtDNA may also limit the ability to distinguish related species (Ballard and Whitlock 2004; Nabholz et al. 2008, 2009).

Introns in nuclear protein coding genes have several properties that make them useful for phylogenetic analyses of recently evolved vertebrates (Igea et al. 2010; Schmitz et al. 2017). Because they are flanked by conserved exons, they are easily amplified by polymerase chain reaction (PCR) in a variety of taxa that provide sites for PCR primers (Prychitko and Moore 2003). Introns evolve more slowly than mtDNA (Prychitko and Moore 1997, 2000; Johnson and Clayton 2000) and more rapidly than nuclear exon sequences (Hughes and Yeager 1997; Li 1997).

To obtain data on robust phylogenetic and temporal divergence in phylogeographic studies of frogs, nuclear intron data have often been used in conjunction with mtDNA data (Zhang et al. 2013; Lourenço et al. 2015; Faivovich et al. 2021; Pereyra et al. 2021). Rapidly evolving noncoding introns are used to resolve problematic nodes at the species, genus, and family levels (Prychitko and Moore 1997; Igea et al. 2010; Folk et al. 2015), and they show more robust and congruent phylogenetic signals than exons (Chen et al. 2017).

The small size of aligned base pairs (bp) and low genetic variability (variable site dataset) of *FGBI7* resulted in few informative traits and discordance between mtDNA and nuclear DNA (nDNA) (Gonçalves et al. 2007; Velo-Antón et al. 2008; Brunes et al. 2010, 2014; Prado et al. 2012; Maia-Carvalho et al. 2014; Menezes et al. 2016, 2020). These results are in contrast with previous studies related to *FGBI7* in amphibians. Thus, *FGBI7* is a valuable marker for assessing phylogenetic relationships at the family level and is likely suitable for phylogenetic analyses between closely related taxa that have recently diverged (Sequeira et al. 2006; Teixeira et al. 2015).

With 99 taxa, the Neotropical gladiator frogs of *Boana* Gray, 1825, constitute the third largest genus within Hylinae (Frost 2023). The phenotypically very similar species and lack of reliable diagnostic characters difficult the precise identity of *Boana*.

Studies of cariology, morphology, vocalizations, and molecular characters have revealed cryptic species, new species, and changes in the classification of *Boana* groups (Caminer and Ron 2014, 2020; Duellman et al. 2016; Fouquet et al. 2016, 2021; Orrico et al. 2017; Ferro et al. 2018; Peloso et al. 2018; Pinheiro et al. 2019a; Lyra et al. 2020; Faivovich et al. 2021).

Two questions prompted us to conduct this study: 1) Is *FGBI7* a phylogenetic signal for *Boana* with more robust topologies than other nuclear genes? 2) Does *FGBI7* contribute to explaining the phylogeny of *Boana*? To answer these questions, we reconstructed the evolutionary history of *Boana* using several molecular markers, including *FGBI7*.

## Materials and methods

### Taxonomic sampling and DNA isolation

DNA samples were obtained from captured specimens and donations from herpetological collections (Appendix 1: Table A1). Samples included taxa from most known species groups of *Boana* (Pinheiro et al. 2019a; Faivovich et al. 2021).

Total DNA extraction from muscle or liver tissue was performed using the SDS -proteinase K/phenol-chloroform extraction method (Sambrook and Rusell 2001). *FGBI7* was sequenced on tissues from twenty-four *Boana* species (ingroup), three taxa of *Aplastodiscus*, one sample of *Bokermannohyla circumdata*, one sample of *Nesorohyla kanaima*, and one of *Callimedusa tomopterna* (outgroups). Primers 5'-CCATGACAATACACAACGGC-3' and 5'-ACCACCATCCACCACCATC-3' were designed based on the sequence of *Xenopus laevis* (Roberts et al. 1995). After selecting the most conserved regions of *FGBI7*, the NCBI Primer- BLAST tool was used to design the target-specific primers (Ye et al. 2012). The amplification protocol was based on a 25- $\mu$ L solution of 0.5–2.0  $\mu$ L of the DNA template, 2.5  $\mu$ L of 10 $\times$  PCR buffer, 0.5  $\mu$ L of each primer (10 pmol/ $\mu$ L), 0.5–1.5  $\mu$ L of MgCl<sub>2</sub>, 1  $\mu$ L of the dNTPs, and 0.15  $\mu$ L of Ex Taq DNA polymerase. The PCR protocol included 3 min at 94 °C, 35 (or 30) cycles of 1 min at 94 °C, 1 min at 60 °C (or 59 s and 55 °C), and 1 min at 72 °C, and a final extension at 75 °C for 5 min.

### Sequencing and alignment

PCR products were sequenced using a MegaBACE automated DNA sequencer (GE Healthcare) and the DYEnamic ET dye terminator kit (GE Healthcare) according to the manufacturer's instructions. Each sample was sequenced with both forward and reverse primers to confirm the observed mutations.

After searching available data in GenBank, we compared the phylogenetic signal of *FGBI7* with that of C-X-C motif chemokine receptor 4 (*CXCR4*), single exon of recombination activating gene 1 (*CXCR4*), exon 1 of Rhodopsin (*RHO*), seven-in-absentia homolog 1 (*SIAH1*), exon 1 of Tyrosinase (*TYR*), and 28S ribosomal rDNA.

Sequence alignments were made using MAFFT version 7 (Katoh and Standley 2013). Alignments were edited using BioEdit (Hall 1999). Exon sequences were then concatenated using Sequence Matrix 1.7.8 (Vaidya et al. 2011) and subjected to various phylogenetic analysis methods using the same parameters as for individual genes. Genes were concatenated, although some sequences within the *Boana* taxa were not available. Missing bases that corresponded to unsequenced data were marked with a question mark.

To compare polymorphic sites and basic sequence statistics, *Boana* sequences were analyzed for conserved, variable, parsimony-informative, and singleton sites using MEGA X (Kumar et al. 2018). The number of sites without missing data (Pb\*) was calculated for all genes by adding the conserved sites (C-S), singleton sites (S-S), and informative parsimony sites (P-I).

## Phylogenetic analysis

Each set of sequences for each marker was analyzed using maximum parsimony (**MP**), Bayesian analysis (**MB**), and maximum likelihood (**ML**). MP was performed in the TNT Willi Hennig Society Edition (Goloboff and Catalano 2016), and phylogenetic trees were constructed using the New Technology Search routine. Parameters selected included sectorial search, ratchet, drift, and tree fusing. A specific search was performed with an initial setting of 100 levels and run 100 times to define the minimum sequence length. Deletions were considered as a fifth base type.

Support for clades was tested using a jackknife procedure with a removal rate of 0.36, which is the most congruent value with bootstrapping (Farris et al. 1996), with absolute frequencies of 50 RAS + TBR per replicate for a total of 1,000 replicates. Consistency indices (CI), retention indices (RI), and rescaled consistency indices (CR) were calculated.

MB analysis of the evolutionary model were performed using MEGA X. For sequences with many gaps, the “use all sites” setting was selected (Tamura et al. 2011). Bayesian and Akaike information criteria were used to select the most appropriate nucleotide substitution model (Posada and Buckley 2004). The MB was run in MrBayes 3.2.7 (Ronquist et al. 2012), and sequences were considered as individual partitions for each model.

One run consisted of two repeated Monte Carlo Markov chains. The run was based on considering four chains, and the default settings for the state frequency priors (statefreqpr) were set as fixed (equal) and the substitution rate priors (ratepr) were set as variable. The other priors were set to default settings, and 85 million generations were performed (with a burn-in fraction of 0.25). Stabilization of the resulting parameters was assessed using Tracer version 1.7 (Rambaut et al. 2018) and Bayesian probability theory.

The ML analysis was performed with MEGA X software (Kumar et al. 2018) using the best substitution model generated with the same program. Bootstrap support values were used to estimate clade support based on 1,000 replicates. Missing data and gaps were included in the analyses using the “use all sites” commands. Tree inference

options included nearest neighbor replacement and initial tree for ML with automatic configuration (default: NJ /BioNJ); system resource use, number of threads 1.

Phylogenetic trees were compared for each marker based on their topology and monophyletic groups defined for *Boana* (Faivovich et al. 2005, 2021; Pinheiro et al. 2019a). Trees were edited in Inkscape 0.48.5, FigTree V 1.4.4 (Rambaut 2016), and MEGA X.

## Mean evolutionary rates of *ND1*, *CYTB*, and *FGBI7* nuclear genes

Mean evolutionary rates for *Boana* species were based on mitochondrial and informative genes such as *ND1* and *CYTB* from GenBank (Zhang et al. 2013). For phylogenetic inference ML, the sequences of each gene were submitted to the MEGA X software. Molecular dating for each tree, including the *FGBI7* obtained, was performed using the RelTime method (Tamura et al. 2018), a fast and powerful dating algorithm very similar to the results obtained by the Bayesian method (Mello et al. 2017; Mello 2018).

To establish a chronological scale for clade/lineage evolution, the divergence times established by Duellman et al. (2016) were used to calibrate the phylogenetic trees of the mitochondrial genes *ND1*, *CYTB*, and *FGBI7*. The following three divergence times were used for the *ND1* tree: I – divergence between *Aplastodiscus* and *Boana*, at 34.2 Ma; II – divergence of *Boana pulchella* group from the other *Boana* groups, at 22.6 Ma; and III – separation between *Boana pellucens* and *Boana rufitela*, at 5.30 Ma. The *FGBI7*-based phylogenetic tree was calibrated with the same divergence time of 34.2 Ma. The *CYTB*-based phylogenetic tree was calibrated with the divergence time between *Bokermannohyla* and *Aplastodiscus* + *Boana* of 36.8 Ma.

Divergence times were calibrated with a normal distribution and 95% confidence interval. Relative evolution rate values for each node were obtained using RelTime-Rate. Absolute evolution rates were obtained by dividing the relative rates by the scaling factor (ratio of absolute times/relative times) (Tamura et al. 2018). Mean evolutionary rates were calculated based on the absolute rates of all clades of *ND1*, *CYTB*, and *FGBI7*. After setting the calibration conditions, the “use all sites” option was selected to include all gaps and missing data in the branch length calculation (Mello 2018).

## Results

### FGBI7 DNA sequences

The average length of the *FGBI7* sequences examined was 478 base pairs. The sequences contained both single and multiple insertions and deletions. *FGBI7* sequences of 710 bp were recorded for *Boana albomarginata*, *Boana albopunctata*, *Boana lanciformis*, and *Boana raniceps*. Alignment of long (710bp) and short sequences (478 bp) revealed short and larger deletions (230–438 positions). However, polymorphism was detected when comparing the long and short sequences.

## Nuclear DNA (nDNA) contribution to the phylogeny of *Boana*

In this study, new *FGBI7* sequences were generated for 24 *Boana* taxa. For comparison of singleton and parsimony informative sites, available sequences for 11 nuclear genes and two mitochondrial genes were retrieved from GenBank. The low number of available sequences for *c-myc2*, *c-myc3*, *H3a*, *KIAA1239*, and *POMC* for a large number of *Boana* taxa prevented their inclusion in the phylogenetic analysis of the group. *CXCR4*, *RHO*, *SIAH1*, *TYR*, and *28S* were used for the phylogenetic evaluation of *Boana* (Table 1).

### Polymorphic sites

Informative singleton and parsimony sites comprised between 36% and 63% of all sites. The percentage of singleton sites was generally high for all genes. The percentage of parsimony-informative sites relative to the total number of sites, excluding missing data-Pb\* for each of the compared genes, showed that the data based on *FGBI7*, *TYR*, and *CXCR4* gave more sensitive and highly informative performance (Table 1). Although the P-I percentage did not differ between concatenated genes (C-genes) and *FGBI7*, the percentage of P-I/Pb\* parsimony-informative sites was higher for *FGBI7*. With the exception of *28S*, the frequency of A+T was higher than 50% for all genes, with *FGBI7* having the highest value.

**Table 1.** Comparative polymorphic sites and basic sequence statistics in *Boana* nDNA.

	<i>CXCR4</i>	<i>FGBI7</i>	<i>RAG1</i>	<i>RHO</i>	<i>SIAH1</i>	<i>TYR</i>	<i>28S</i>	C-genes	C-genes (1)	<i>ND1</i>	<i>Cyt b</i>
S	30	24	19	51	26	29	26	58	50	58	53
Pb	676	478	428	316	397	532	823	3650	1686	941	385
Pb*	675	466	428	316	397	532	786	3606	1673	941	385
C-S	497	286	368	254	358	387	691	2817	1153	445	198
S-S(%)	70(39)	85(47)	35(58)	27(44)	18(46)	53(37)	53(56)	358(46)	220(42)	42(8)	20(11)
P-I(%)	108(61)	95(53)	25(42)	35(56)	21(54)	92(63)	42(44)	424(54)	300(58)	454(92)	167(89)
PIS(%) (100*P-I/Pb*)	16	20.39	5.84	11.08	5.29	17.29	5.34	11.76	17.93	99.51	99.56
AT (%)	50.4	60.4	55.8	54.5	51.3	51.9	42.5	51.3	53.2	59.5	59.3
CG (%)	49.6	39.6	44.2	45.5	48.7	48.1	57.5	48.7	46.8	40.5	40.7

C-genes = concatenated genes. C-genes (1) = concatenated (*TYR*, *FGBI7*, *CXCR4*) S = Species number. Pb = aligned base pairs. Pb\* = Total number of sites, excluding missing data. C-S = conserved sites; S-S = singleton variable sites; P-I = parsimony-informative sites. PIS = Parsimony-informative sites excluding missing data. AT (%) = adenine-thymine frequency, CG (%) = cytosine-guanine frequency.

### Phylogenetic hypothesis

The support values of several nodes were low, ranging from 0 to 50 in all 21 trees generated by the three phylogenetic methods applied (MP, MB, and ML) (Fig. 1). Analysis of the seven nDNA markers using three different phylogenetic methods led to conflicting hypotheses about the monophyly of *Boana*. Seven groups of *Boana* were more frequently classified as monophyletic by the three methods using *TYR*, *FGBI7*, and *CXCR4*.

*FGBI7* suggests monophyly of *B. pellucens* group, similar to *CXCR4*, which also supports polyphyly of *B. punctata*. All groups examined were polyphyletic for 28S (Table 2).

The MP and consistency indices for all nDNAs analyzed were > 0.5. The CI and CR indices showed a similar trend for all nDNA, indicating a lower degree of homoplasies with an increase in their values (Table 3).

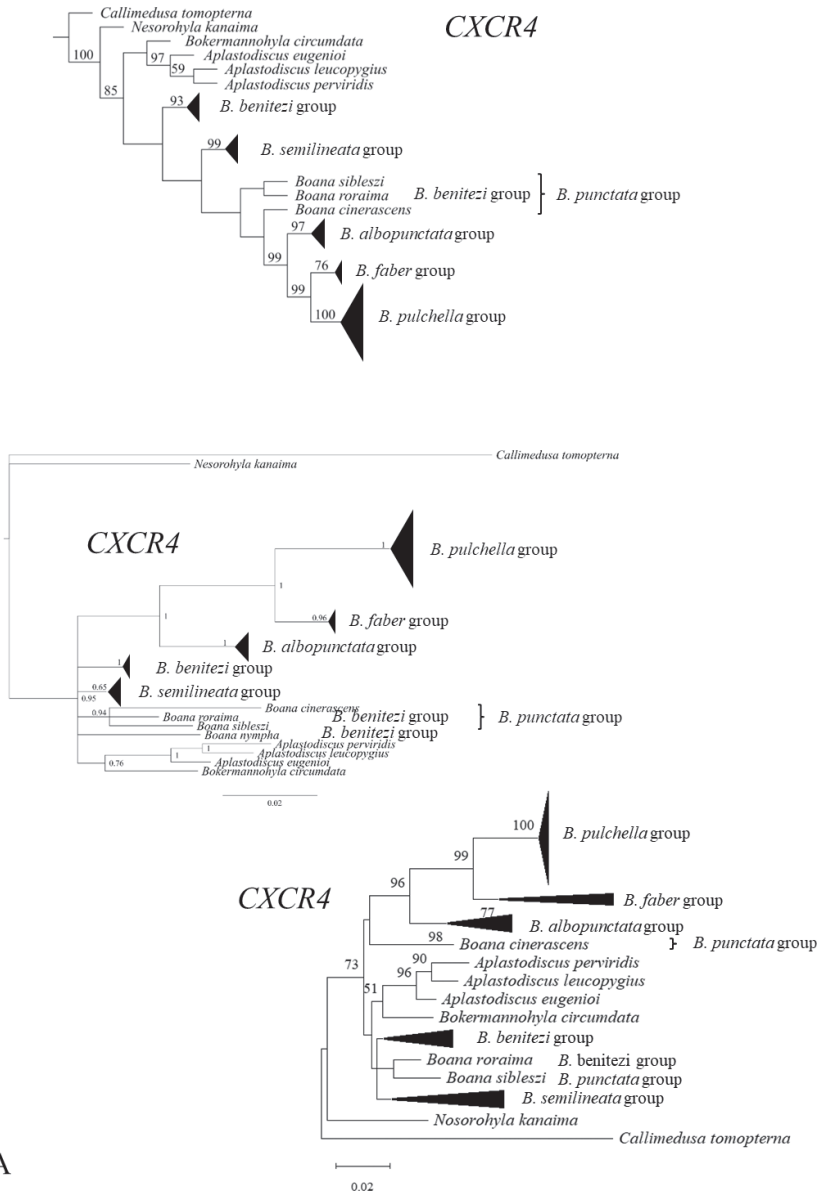
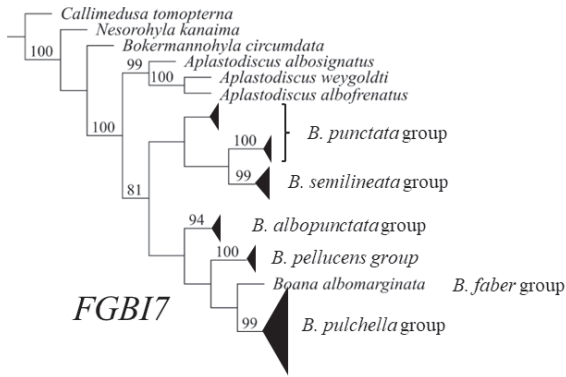
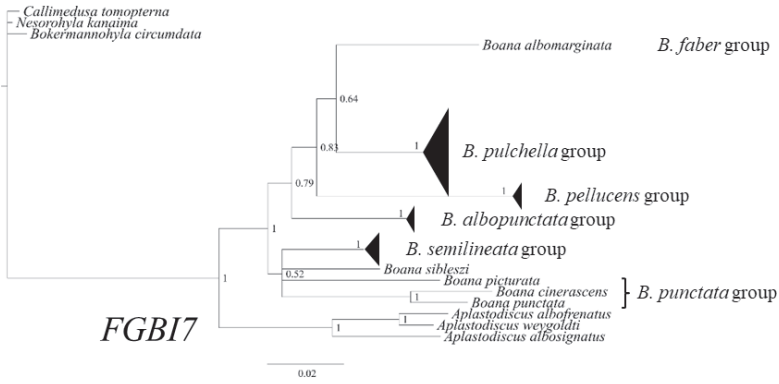


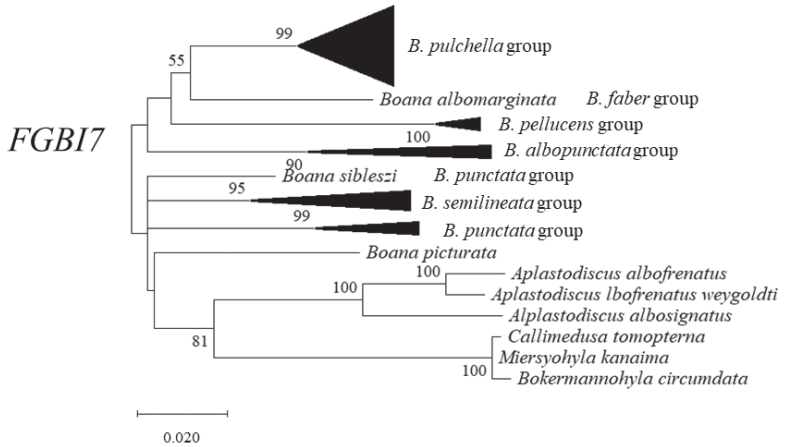
**Figure 1.** Phylogenetic trees corresponding to the studied markers provided more sensitive and highly informative performance (**A** *CXCR4* **B** *FGBI7* **C** *TYR*), and the methods used—MP, MB, and ML, corresponding to the first, second, and third trees for each marker, respectively). For Jackknife support values from the MP method, and bootstrap support values for the ML method, values below 50% were not presented.



FGBI7



FGBI7



FGBI7

B

Figure 1. Continued.

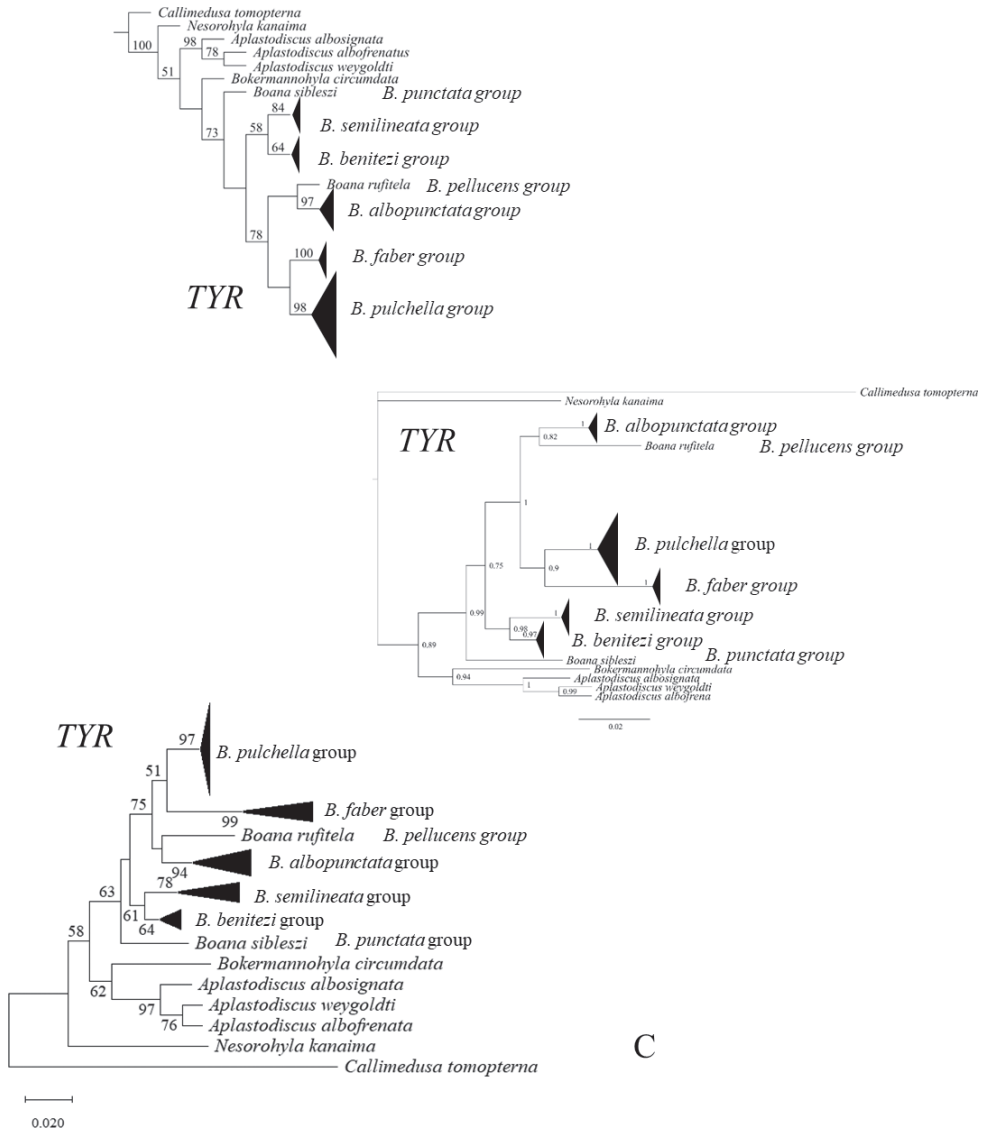


Figure 1. Continued.

**Table 2.** Monophyletic species groups recovered by the three phylogenetic methods for single and concatenated gene phylogeny.

	<i>CXCR4</i>	<i>FGBI7</i>	<i>CXCR4</i>	<i>RHO</i>	<i>SIAHI</i>	<i>TYR</i>	<i>28S</i>	<i>C-gene</i>
<i>Boana</i>	MP	MP, MB	*	*	MP, MB, ML	MP, MB, ML	*	*
<i>B. albopunctata</i> group	MP, MB, ML	MP, MB, ML	–	*	*	MP, MB, ML	*	*
<i>B. benitezi</i> group	–	–	*	*	–	MP, MB, ML	*	MP
<i>B. faber</i> group	MP, MB, ML	–	–	MP, ML	–	MP, MB, ML	*	MP, MB, ML
<i>B. pellucens</i> group	–	MP, MB, ML	–	–	–	–	–	MP, MB, ML
<i>B. pulchella</i> group	MP, MB, ML	MP, MB, ML	MP	*	MP, MB, ML	MP, MB, ML	*	*
<i>B. punctata</i> group	*	*	–	*	–	–	*	*
<i>B. semilineata</i> group	MP, MB, ML	MP, MB, ML	–	MP	–	MP, MB, ML	*	MP, MB, ML

MP: monophyletic group by maximum parsimony; MB: monophyletic group by MrBayes; ML: monophyletic by maximum likelihood; \*: polyphyletic groups identified by the three methods; -: absent groups or a single representative species.

**Table 3.** Consistency and retention indices of individual and concatenated genes.

	<i>CXCR4</i>	<i>FGBI7</i>	<i>CXCR4</i>	<i>RHO</i>	<i>SIAHI</i>	<i>TYR</i>	<i>28S</i>	<i>C-genes</i>
CI	0.607	0.802	0.797	0.615	0.745	0.563	0.669	0.635
RI	0.782	0.857	0.791	0.729	0.819	0.655	0.577	0.714
CR	0.475	0.687	0.630	0.448	0.610	0.369	0.386	0.453

CI = consistency; RI = retention; CR = rescaled consistency indices

## Mean evolutionary rate

*ND1* and *CYTB* gene sequence data available for *Boana* in GenBank were obtained for 58 and 53 species, respectively. The nucleotide substitution model GTR+G+I was run with MEGA X to generate the phylogenies. The T92+G model was chosen for the phylogenetic analysis of *FGBI7*. The absolute values of the mean evolutionary rates for *ND1*, *CYTB*, and *FGBI7* were  $1.235198E^{-2} \pm 3.61903E^{-3}$ , coefficient of variation – CV = 29%;  $1.2796789E^{-2} \pm 4.6661189E^{-3}$ , CV = 36.4%; and  $1.920083E^{-3} \pm 1.07878E^{-3}$ ; CV = 56% replacement/site/million years, respectively.

Comparison of dating results between congruent *Boana* groups for *ND1*, *CYTB*, and *FGBI7* showed divergence among the three genes, with some values being most similar among mitochondrial genes. However, the results diverged to a lesser extent from those obtained for the nuclear gene *FGBI7*. The dating results for the *B. pulchella* group revealed divergence times of 14.28 Ma (*ND1*), 15.22 Ma (*CYTB*), and 10 Ma (*FGBI7*). In addition, the *B. punctata* group (*B. cinerascens* and *B. punctata*) showed dating results of 11.44 Ma (*ND1*), 15.13 Ma (*CYTB*), and 9.12 Ma (*FGBI7*), and the *B. albopunctata* group showed divergence times of 21.94 Ma (*ND1*), 13.50 Ma (*CYTB*), and 16.32 Ma (*FGBI7*) (Fig. 2).

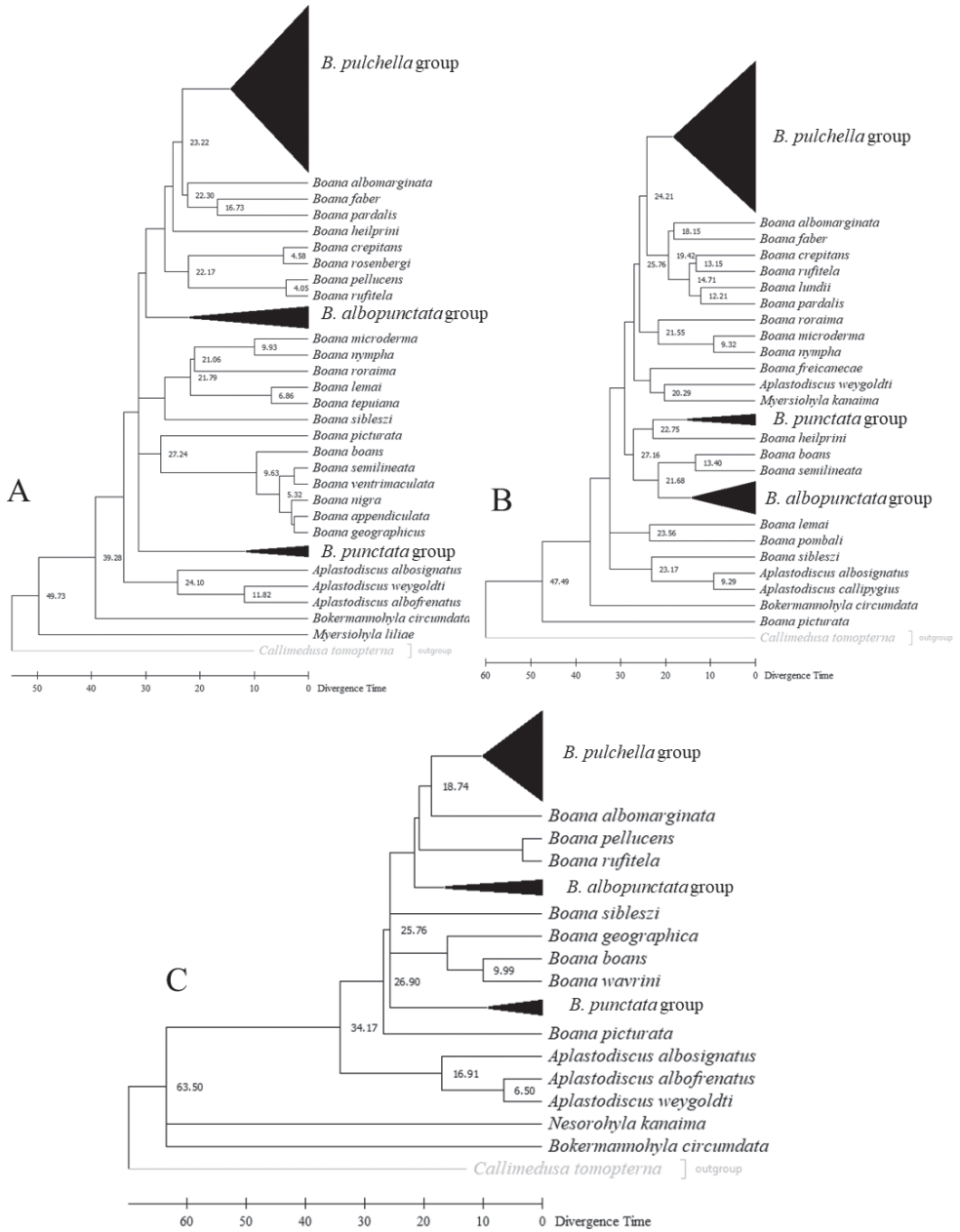


**Figure 2.** Molecular dating of gene trees **A** *ND1* **B** *CYTB* **C** *FGFI7* using the RelTime method in MEGA X.

## Discussion

While we explored the potential applicability of *FGBI7* in reconstructing the phylogeny of *Boana* clades, our goal was to include a growing number of informative sites for future analyses, to contribute to the understanding of phylogenetic signal, and to investigate the robustness of a combination of mitochondrial and nuclear data.

Despite the short sequence (478 bp) observed in the present study, the *FGBI7*-based analyses were highly consistent with the previously proposed phylogenetic hypothesis based on the concatenation of mitochondrial and nuclear genes previously proposed for *Boana* groups (Faivovich et al. 2013, 2021; Pinheiro et al. 2019a). The phylogeny MP best agreed with these studies, showing *B. punctata* group as polyphyletic and the groups *B. semilineata* group, *B. albopunctata* group, *B. pellucens* group, *B. faber* group, and *B. pulchella* group as monophyletic.

Similar groupings were also observed among species. Some support values, such as those of *B. semilineata* group, *B. pellucens* group, and *B. pulchella* group, were very close to those determined by Pinheiro et al. (2019a).

The response of the CI and CR indices obtained by the MP analysis showed a lower degree of homoplasy for *FGBI7*. Therefore, a higher degree of parsimony compared with the congruent hypothesis generated considering the *TYR* and *CXCR4* genes and using different analysis methods supports the use of *FGBI7* in phylogenetic analysis of *Boana*.

The observed variation between the CR indices obtained for the analyzed genes can be attributed to the phylogenetic signal of indels (Miklós et al. 2004; Granados et al. 2013). Indels are a valuable source of phylogenetic information that can influence the phylogenetic outcome and have less homoplasy than nucleotides (Houde et al. 2019). The phylogenetic utility of indels may vary between individual genes; therefore, the phylogenetic weight of a single indel compared to that of a nucleotide should be explored (Pasko et al. 2011). The number, size, and distribution of indels within a sequence likely reflect the complex phenomena that lead to their accumulation over an evolutionary period and the different approaches used to analyze the available data (Houde et al. 2019).

The lowest proportion of parsimony-informative sites identified for C-genes is due to the noise of concatenation with *28S* and *RHO*. After the data for these genes were removed from the analysis (C-genes (1)), the information signal increased, although it remained lower than that of *FGBI7*. Typically, it is believed that informativeness about species history is maximized by allowing concatenation of multiple independent loci to obtain a hypothesis congruent with the species tree. However, concatenation of sequence data can bias the phylogeny if the number of gene trees that match the species tree is small. In these cases, species tree approaches can provide better-resolved phylogenies when a large number of loci are used (Edwards et al. 2007).

However, when gene tree and species tree data support a robust and congruent hypothesis (Granados et al. 2013; Ai and Kang 2015), it is possible that species trees can be resolved using only two or three few loci. These results lead to a paradigm for combining data in phylogenomics that focuses on the uniqueness of species histories and ignores the diversity of individual gene histories.

The concatenated C-gene and C-gene (1) phylogenies in MP yielded very similar clades, but the C-gene tree is not supported by bootstrap values; the C-gene (1) tree showed some high support values. The *FGBI7* tree, on the other hand, showed a larger number of bootstrap values compared to the C-gene trees (1). Tonini et al. (2015) concluded that phylogeneticists should continue to make explicit comparisons between the results of modern and classical methods.

The low reliability values obtained for multiple bootstrap and jackknife nodes and single gene trees, such as the concatenated alignment of the seven genes, indicate low robustness of the estimated topology. The low bootstrap values could be due to the small sample size and the generation of bias by signals generated by a few genes. Bootstrap values and similar support values increase with increasing numbers of sites sampled (Phillips et al. 2004).

Congruence was observed not only at the tips of trees but also at deeper inner branches. Chen et al. (2003) proposed a reliable alternative strategy in which only one bootstrap value is considered as the threshold for clade significance. In this alternative strategy, the same clade repeatedly derived from different data sets is accepted even at low bootstrap values, rather than a strongly supported clade derived from a single data set. Congruence analysis reveals different evolutionary signals in the underlying collection of genes and allows for a more conservative interpretation of phylogenomic signals (Thiergart et al. 2014). The use of *FGBI7* proved to be a complementary technique for resolving the *Boana* phylogeny. By confirming specific clades within the *Boana* phylogeny, the use of integrated traits may be better suited to elucidate the history of a clade (Salichos and Rokas 2013).

The congruence between the topology resulting from the use of *FGBI7* in this study and the results reported by Pinheiro et al. (2019a) and Faivovich et al. (2021) may be due to the design of a specific primer for *FGBI7* analysis. Other studies have also shown satisfactory results with the use of *FGBI7*-specific primers for different study groups (Sequeira et al. 2006; Teixeira et al. 2015). Designing PCR primers to screen primers against a user-selected database avoids nonspecific amplification and highlights a variable sequence of the marker to establish relationships. Although the design of specific primers is time consuming (Small et al. 2004), it has significant advantages over universal primers, particularly in terms of gene amplification, sequence quality and variation, and searching for a phylogenetic signal (Cai and Ma 2016).

Intraspecific variability in body color, description of new species, and research on declining taxa of the Hylidae (AmphibiaWeb 2021; IUCN 2021) are challenges for future studies that should be addressed using integrative trait taxonomy (Hillis 2019; Pinheiro et al. 2019b). Despite the short sequence observed in the *FGBI7*-based analysis, this is a versatile gene that can be used to address a variety of phylogenetic and taxonomic questions. The elucidation of taxa thought to be geographically widespread that are in fact cryptic species, such as *Boana* (Estupiñán et al. 2016; Fouquet et al. 2016; Caminer et al. 2017; Orrico et al. 2017; Cryer et al. 2019), and the agreement with previously proposed phylogenetic hypotheses supported by the informative sites for parsimony demonstrate the high performance of *FGBI7*.

This study also showed that *FGBI7* for *Boana* has lower mean evolutionary rates than mitochondrial genes (*ND1* and *CYTB*). The substitution rates in this study are consistent with previous reports in which nuclear genes typically had lower substitu-

tion rates than mitochondrial genes (Zheng et al. 2011; Near et al. 2012; Stöck et al. 2012). The mtDNA and nDNA evolution rates in this study were similar to those estimated by Ehl et al. (2019). These authors estimated evolution rates from  $E^{-2}$  to  $E^{-3}$  for mtDNA and from  $E^{-3}$  to  $E^{-4}$  for nDNA. However, the amplitude of evolutionary rates was lower for *FGBI7* compared with mtDNA.

The divergence dates of the *FGBI7* data were close to those obtained by Fouquet et al. (2021) for *B. punctata* group (*B. cinerascens* + *B. punctata*) ( $\bar{x} = 9.66 \pm 0.76$  Ma) and *B. albopunctata* ( $\bar{x} = 16.8 \pm 0.70$  Ma). Divergence times for *B. fasciata* were determined by Duellman et al. (2016), Feng et al. (2017), and Fouquet et al. (2021). Although Feng et al. (2017) criticized the geological dating method used by Duellman et al. (2016) and instead calibrated their dating data with fossil records, their results differed significantly from those of Fouquet et al. (2021), who used the same calibration method. Duellman et al. (2016) and Fouquet et al. (2021) found mean divergence times of  $4.71 \pm 1.06$  Ma for *B. fasciata*, while those for *CYTB* were overestimated by 13.22 Ma.

Assuming that the divergence threshold for *Neobatrachus* from Gondwana is 145 Ma and that for Hylidae is 70 Ma, and based on nDNA data and calibration of the fossil record, the origin of *Boana* is estimated to be 25 Ma (Feng et al. 2017). Using a threshold of 62 Ma and based on nDNA and mtDNA data, Duellman et al. (2016) estimated the origin of *Boana* to be 34 Ma, with a mean diversification rate within their groups of  $19.1 \pm 4.6$  Ma. This estimate is close to the divergence time calculated by Fouquet et al. (2021) for *B. albopunctata* (17.3 Ma) and by *FGBI7* in the present study.

Recent divergence times inferred from mtDNA sequences tend to overestimate times for basal clades (Maddin et al. 2012). On the other hand, estimates of divergence times for more recent nodes based on nuclear loci are inaccurate because significantly fewer mutations have accumulated between comparatively young lineages (Wilke et al. 2009). Another way to address this divergence is to compare these results with additional evidence. The considerable amplitude between the appearance of *Boana* is estimated to be 30 Ma and the onset of divergence of the Amazonian clade of *B. albopunctata* group is estimated to be 10 Ma. This limits our understanding of divergence times using only a single type of molecular marker. We propose that *FGBI7* should be used for anuran clades that originated between 30 and 70 Ma, while mtDNA should be used for clades that originated between 25 and 30 Ma and diverged until recently ( $< 2$  Ma). Thus, it is possible to construct an nDNA-based time tree for a reduced set of taxa representing all genera, reconstruct different lineage-level time trees using mtDNA data, and compare the performance of the different approaches (Ehl et al. 2019).

The use of *FGBI7* in this study showed that, unlike other nuclear genes already used to generate phylogenetic hypotheses of Anura (e.g.: Wiens et al. 2010; Pyron and Wiens 2011; Duellman et al. 2016) or in the phylogenies of *Boana* and some of their groups (Faivovich et al. 2013, 2021; Caminer and Ron 2014; Pinheiro et al. 2019a; Lyra et al. 2020), has great potential to reveal relationships between lineages of very close clades.

The topology, total informative sites, and parsimony sites of *FGBI7*, in combination with mitochondrial genes, allow the clarification of new lineages already proposed by other authors such as Fouquet et al. (2021), Vasconcellos et al. (2021), and Rainha et al. (2021), contributing to future studies on *Boana* evolution and systematics.

Although estimating divergence times for clades is a difficult task (Mello 2018), the approach proposed in this study estimated the average evolutionary rate for *Boana* using two mitochondrial genes and *FGBI7*. Therefore, we recommend the use of *FGBI7* for the analysis of clades such as *Boana* with temporal ranges between 30 and 70 Ma and the use of the mtDNA genes for lineages with thresholds from the origin of *Boana*, between 25 and 30 Ma, to recent times (< 2 Ma).

## Acknowledgements

We extend our gratitude to researchers for sample donations, to Maria Silvanira R. Barbosa for her assistance with laboratory procedures, to Daniel Fernandes Vilar Cardoso from CIMIR-RE at the Federal Institute of Paraíba for providing appropriate hardware for analysis, and to Beatriz Mello from Genetics Department – Federal University of Rio de Janeiro, for her assistance in the calculation of mean evolutionary rates and molecular dating using the RelTime method in MEGA X. We would also like to thank the Brazilian Environment Ministry, which financed the MMA/PROBIO-Brazil project “Diversity of vertebrates on the upper Marmelos River (BX 044)” and CAPES for providing a graduate RAET stipend. Collection licenses: 301 062/2003-CGFAU/LIC issued by the Brazilian Institute for the Environment and Renewable 302 Natural Resources (IBAMA).

## References

- Ai B, Kang M (2015) How Many Genes are Needed to Resolve Phylogenetic Incongruence?. *Evolutionary Bioinformatics* 11(1): 185–188. <https://doi.org/10.4137/EBO.S26047>
- AmphibiaWeb (2021) University of California, Berkeley, CA, USA. <https://amphibiaweb.org>
- Ballard JWO, Whitlock MC (2004) The incomplete natural history of mitochondria. *Molecular Ecology* 13(4): 729–744. <https://doi.org/10.1046/j.1365-294X.2003.02063.x>
- Berneck BVM, Haddad CFB, Lyra ML, Cruz CAG, Faivovich J (2016) The green clade grows: a phylogenetic analysis of *Aplastodiscus* (Anura: Hylidae). *Molecular Phylogenetics and Evolution* 97: 213–223. <https://doi.org/10.1016/j.ympev.2015.11.014>
- Brunes TO, Sequeira F, Haddad CFB, Alexandrino J (2010) Gene and species trees of a Neotropical group of treefrogs: Genetic diversification in the Brazilian Atlantic Forest and the origin of a polyploid species. *Molecular Phylogenetics and Evolution* 57(3): 1120–1133. <https://doi.org/10.1016/j.ympev.2010.08.026>
- Brunes TO, Alexandrino J, Baêta D, Zina J, Haddad CFB, Sequeira F (2014) Species limits, phylogeographic and hybridization patterns in Neotropical leaf frogs (Phyllomedusinae). *Zoologica Scripta* 43(6): 586–604. <https://doi.org/10.1111/zsc.12079>
- Cai L, Ma H, (2016) Using nuclear genes to reconstruct angiosperm phylogeny at the species level: A case study with Brassicaceae species. *Journal of Systematics and Evolution* 54(4): 438–452. <https://doi.org/10.1111/jse.12204>

- Caminer MA, Ron S (2014) Systematics of treefrogs of the *H. calcaratus* and *H. fasciatus* species complex (Anura, Hylidae) with the description of four new species. *ZooKeys* 370: 1–68. <https://doi.org/10.3897/zookeys.370.6291>
- Caminer MA, Ron SR (2020) Systematics of the *Boana semilineata* species group (Anura: Hylidae), with description of two new species from Amazonian Ecuador. *Zoological Journal of the Linnean Society* 190(1): 149–180. <https://doi.org/10.1093/zoolinnean/zlaa002>
- Caminer MA, Milá B, Jansen M, Fouquet A, Venegas PJ, Chávez G, Loughheed SC, Ron SR (2017) Systematics of the *Dendropsophus leucophyllatus* species complex (Anura: Hylidae): Cryptic diversity and the description of two new species. *PLoS ONE* 12(4): e0176902. <https://doi.org/10.1371/journal.pone.0176902>
- Chen WJ, Bonillo C, Lecointre G (2003) Repeatability of clades as a criterion of reliability: A case study for molecular phylogeny of Acanthomorpha (Teleostei) with larger number of taxa. *Molecular Phylogenetics and Evolution* 26(2): 262–288. [https://doi.org/10.1016/S1055-7903\(02\)00371-8](https://doi.org/10.1016/S1055-7903(02)00371-8)
- Chen MY, Liang D, Zhang P (2017) Phylogenomic resolution of the phylogeny of laurasiatherian mammals: Exploring phylogenetic signals within coding and noncoding sequences. *Genome Biology and Evolution* 9(8): 1998–2012. <https://doi.org/10.1093/gbe/evx147>
- Cryer J, Wynne F, Price SJ, Puschendorf R (2019) Cryptic diversity in *Lithobates warszewitschii* (Amphibia, Anura, Ranidae). *ZooKeys* 838: 49–69. <https://doi.org/10.3897/zookeys.838.29635>
- Duellman WE, Marion AB, Hedges SB (2016) Phylogenetics, classification, and biogeography of the treefrogs (Amphibia: Anura: Arboranae). *Zootaxa* 4104(4): 1–109. <https://doi.org/10.11646/zootaxa.4104.1.1>
- Edwards SV, Liu L, Pearl DK (2007) High-resolution species trees without concatenation. *Proceedings of the National Academy of Sciences of the United States of America* 104(14): 5936–5941. <https://doi.org/10.1073/pnas.0607004104>
- Ehl S, Vences M, Veitha M (2019) Reconstructing evolution at the community level: A case study on Mediterranean amphibians. *Molecular Phylogenetics and Evolution* 134: 211–225. <https://doi.org/10.1016/j.ympev.2019.02.013>
- Estupiñán RA, Ferrari SF, Gonçalves EC, Barbosa MSR, Vallinoto M, Schneider MPC (2016) Evaluating the diversity of Neotropical anurans using DNA barcodes. *ZooKeys* 637: 89–106. <https://doi.org/10.3897/zookeys.637.8637>
- Faivovich J, Haddad CFB, Garcia PCA, Frost DR, Campbell JA, Wheeler WC (2005) Systematic review of the frog family Hylidae with special reference to Hylinae: Phylogenetic analysis and taxonomic revision. *Bulletin of the American Museum of Natural History* 294(1): 1–240. [https://doi.org/10.1206/0003-0090\(2005\)294\[0001:SROTFF\]2.0.CO;2](https://doi.org/10.1206/0003-0090(2005)294[0001:SROTFF]2.0.CO;2)
- Faivovich J, Haddad CFB, Baeta D, Jungfer KH, Alvares GFR, Brandao RA, Sheil C, Barrientos LS, Barrio-Amoros CL, Cruz CAG, Wheeler WC (2010) The phylogenetic relationships of the charismatic poster frogs, Phyllomedusinae (Anura, Hylidae). *Cladistics* 26(3): 227–261. <https://doi.org/10.1111/j.1096-0031.2009.00287.x>
- Faivovich J, McDiarmid RW, Myers CW (2013) Two new species of *Myersiophyla* (Anura: Hylidae) from Cerro de la Neblina, Venezuela, with comments on other species of the genus. *American Museum Novitates* 3792(3792): 1–63. <https://doi.org/10.1206/3792.1>
- Faivovich J, Pinheiro PDP, Lyra ML, Pereyra MO, Baldo D, Muñoz A, Reichle S, Brandão RA, Giarretta AA, Thomé MTC, Chaparro JC, Baêta D, Widholzer RL, Baldo J, Lehr E,

- Wheeler WC, Garcia PCA, Haddad CFB (2021) Phylogenetic relationships of the *Boana pulchella* group (Anura: Hylidae). *Molecular Phylogenetics and Evolution* 155: 1–18. <https://doi.org/10.1016/j.ympev.2020.106981>
- Farris JS, Albert VA, Kallersjo AM, Lipscomb D, Kluge AG (1996) Parsimony jackknifing outperforms neighbour joining. *Cladistics* 12(2): 99–124. <https://doi.org/10.1111/j.1096-0031.1996.tb00196.x>
- Feng YJ, Blackburn DC, Lianga D, Hillis DM, Waked DB, Cannatella DC, Zhang P (2017) Phylogenomics reveals rapid, simultaneous diversification of three major clades of Gondwanan frogs at the Cretaceous–Paleogene boundary. *Proceedings of the National Academy of Sciences of the United States of America* 114(29): E5864–E5870. <https://doi.org/10.1073/pnas.1704632114>
- Ferro JM, Cardozo DE, Suárez P, Boeris JM, Blasco Zúñiga A, Barbero G, Gomes A, Gazoni T, Costa W, Nagamachi CY, Rivera M, Parise-Maltempo PP, Wiley JE, Pieczarka JC, Haddad CFB, Faivovich J, Baldo D (2018) Chromosome evolution in Cophomantini (Amphibia, Anura, Hylinae). *PLoS ONE* 13(2): e0192861. <https://doi.org/10.1371/journal.pone.0192861>
- Folk RA, Mandel JR, Freudenstein JV (2015) A protocol for targeted enrichment of intron-containing sequence markers for recent radiations: A phylogenomic example from *Heuchera* (Saxifragaceae). *Applications in Plant Sciences* 3(8): 1500039. <https://doi.org/10.3732/apps.1500039>
- Fouquet A, Martínez Q, Zeidler L, Courtois EA, Gaucher P, Blanc M, Lima JD, Souza SM, Rodrigues MT, Kok PJR (2016) Cryptic diversity in the *Hypsiboas semilineatus* species group (Amphibia, Anura) with the description of a new species from the eastern Guiana Shield. *Zootaxa* 4084(1): 079–104. <https://doi.org/10.11646/zootaxa.4084.1.3>
- Fouquet A, Marinho P, Réjaud A, Carvalho TR, Caminer MA, Jansen M, Rainha RN, Rodrigues MT, Werneck FP, Lima AP, Hrbek T, Giaretta AA, Venegas PJ, Chávez G, Ron S (2021) Systematics and biogeography of the *Boana albopunctata* species group (Anura, Hylidae), with the description of two new species from Amazonia. *Systematics and Biodiversity* 0(4): 1–38. <https://doi.org/10.1080/14772000.2021.1873869>
- Frost DR (2023) *Amphibian Species of the World: an Online Reference*. Version 6.1. American Museum of Natural History, New York, USA. <https://amphibiansoftheworld.amnh.org/index.php>
- Goloboff P, Catalano S (2016) TNT version 1.5, with a full implementation of phylogenetic morphometrics. *Cladistics* 32(3): 221–238. <https://doi.org/10.1111/cla.12160>
- Gonçalves H, Martínez Solano I, Ferrand N, García-París M (2007) Conflicting phylogenetic signal of nuclear vs mitochondrial DNA markers in midwife toads (Anura, Discoglossidae, *Alytes*) deep coalescence or ancestral hybridization? *Molecular Phylogenetics and Evolution* 44(1): 494–500. <https://doi.org/10.1016/j.ympev.2007.03.001>
- Granados MC, Wanke S, Salomo K, Goetghebeur P, Samain MS (2013) Application of the phylogenetic informativeness method to chloroplast markers: A test case of closely related species in tribe Hydrangeae (Hydrangeaceae). *Molecular Phylogenetics and Evolution* 66(1): 233–242. <https://doi.org/10.1016/j.ympev.2012.09.029>
- Hall TA (1999) BioEdit: A user-friendly biological sequence alignment editor and analysis program for Windows 95/98/NT. *Nucleic Acids Symposium Series* 41: 95–98.
- Hillis MD (2019) Species delimitation in herpetology. *Journal of Herpetology* 53(1): 3–12. <https://doi.org/10.1670/18-123>

- Houde P, Braun EL, Narula N, Minjares U, Mirarab S (2019) Phylogenetic signal of indels and the Neoavian radiation. *Diversity* 11(7): e108. [23 pp] <https://doi.org/10.3390/d11070108>
- Hughes AL, Yeager M (1997) Coordinated amino acid changes in the evolution of mammalian defensins. *Journal of Molecular Evolution* 44(6): 675–682. <https://doi.org/10.1007/PL00006191>
- Igea J, Juste J, Castresana J (2010) Novel intron markers to study the phylogeny of 697 closely related mammalian species. *BMC Ecology and Evolution* 10: e369. <https://doi.org/10.1186/1471-2148-10-369>
- IUCN (2021) The IUCN Red List of Threatened Species. Version 2021-1. <https://www.iucn-redlist.org>
- Johnson, KP, Clayton DH (2000) Nuclear and mitochondrial genes contain similar phylogenetic signal for pigeons and doves (Aves: Columbiformes). *Molecular Phylogenetics and Evolution* 14(1):141–151. <https://doi.org/10.1006/mpev.1999.0682>
- Katoh K, Standley DM (2013) MAFFT multiple sequence alignment software 4 version 7: Improvements in performance and usability. *Molecular Biology and Evolution* 30(4): 772–780. <https://doi.org/10.1093/molbev/mst010>
- Kumar S, Stecher G, Li M, Knyaz C, Tamura K (2018) MEGA X: Molecular Evolutionary Genetics Analysis across computing platforms. *Molecular Biology and Evolution* 35(6): 1547–1549. <https://doi.org/10.1093/molbev/msy096>
- Li WH (1997) *Molecular Evolution*. Sinauer Associates, Sunderland, Massachusetts, 457 pp.
- Lourenço LB, Targueta CP, Baldo D, Nascimento J, Garcia PCA, Andrade GV, Haddad CFB, Recco-Pimentel SM (2015) Phylogeny of frogs from the genus *Physalaemus* (Anura, Leptodactylidae) inferred from mitochondrial and nuclear gene sequences. *Molecular Phylogenetics and Evolution* 92: 204–216. <https://doi.org/10.1016/j.ympev.2015.06.011>
- Lyra ML, Lourenço AC, Pinheiro PDP, Pezutti TL, Baeta D, Barlow A, Hofreiter M, Pombal Jr JP, Haddad CFB, Faivovich J (2020) High throughput DNA sequencing of museum specimens sheds light on the long missing species of the *Bokermannohyla claresignata* group (Anura: Hylidae: Cophomantini). *Zoological Journal of the Linnean Society* 190(4): 1235–1255. <https://doi.org/10.1093/zoolinnean/zlaa033>
- Maddin HC, Russell AP, Anderson JS (2012) Phylogenetic implications of the morphology of the braincase of caecilian amphibians (Gymnophiona). *Zoological Journal of the Linnean Society* 166(1): 160–201. <https://doi.org/10.1111/j.1096-3642.2012.00838.x>
- Maia-Carvalho BM, Goncalves H, Ferrand N, Solano IM (2014) Multilocus assessment of phylogenetic relationships in *Alytes* (Anura, Alytidae). *Molecular Phylogenetics and Evolution* 79: 270–278. <https://doi.org/10.1016/j.ympev.2014.05.033>
- Mello B (2018) Estimating TimeTrees with MEGA and the TimeTree Resource. *Molecular Phylogenetics and Evolution* 35(9): 2334–2342. <https://doi.org/10.1093/molbev/msy133>
- Mello B, Tao Q, Tamura K, Kumar S (2017) Fast and Accurate Estimates of Divergence Times from Big Data. *Molecular Phylogenetics and Evolution* 34(1): 45–50. <https://doi.org/10.1093/molbev/msw247>
- Menezes L, Canedo C, Batalha-Filho H, Garda AA, Gehara M, Napoli MF (2016) Multilocus Phylogeography of the Treefrog *Scinax eurydice* (Anura, Hylidae) Reveals a Plio-Pleistocene Diversification in the Atlantic Forest. *PLoS ONE* 11(6): e0154626. <https://doi.org/10.1371/journal.pone.0154626>

- Menezes L, Batalha-Filho H, Garda AA, Napoli MF (2020) Tiny treefrogs in the Pleistocene: Phylogeography of *Dendropsophus oliveirai* in the Atlantic Forest and associated enclaves in northeastern Brazil. *Journal of Zoological Systematics and Evolutionary Research* 59(1): 179–194. <https://doi.org/10.1111/jzs.12422>
- Miklós I, Lunter GA, Holmes I (2004) A “Long Indel” model for evolutionary sequence alignment. *Molecular Biology and Evolution* 21(3): 529–540. <https://doi.org/10.1093/molbev/msh043>
- Nabholz B, Glémin S, Galtier N (2008) Strong variations of mitochondrial mutation rate across mammals – the longevity hypothesis. *Molecular Biology and Evolution* 25(1): 120–130. <https://doi.org/10.1093/molbev/msm248>
- Nabholz B, Glémin S, Galtier N (2009) The erratic mitochondrial clock: Variations of mutation rate, not population size, affect mtDNA diversity across mammals and birds. *BMC Evolutionary Biology* 9(54): 1–13. <https://doi.org/10.1186/1471-2148-9-54>
- Near TJ, Eytan RI, Dornburg A, Kuhn KL, Moore JA, Davis MP, Wainwright PC, Friedman M, Smith WL (2012) Resolution of ray-finned fish phylogeny and timing of diversification. *Proceedings of the National Academy of Sciences of the United States of America* 109(34): 13698–13703. <https://doi.org/10.1073/pnas.1206625109>
- Orrico VGD, Nunes I, Mattedi C, Fouquet A, Lemos AW, Rivera–Correa M, Lyra ML, Loebmann D, Pimenta BVS, Caramaschi U, Rodrigues MT, Haddad CFB (2017) Integrative taxonomy supports the existence of two distinct species within *Hypsiboas crepitans* (Anura: Hylidae). *Salamandra* 53: 99–113. <http://www.salamandra-journal.com/>
- Pasko L, Ericson PGP, Elzanowski A (2011) Phylogenetic utility and evolution of indels: A study in neognathous birds. *Molecular Phylogenetics and Evolution* 61(3): 760–771. <https://doi.org/10.1016/j.ympev.2011.07.021>
- Peloso PLV, Oliveira RMD, Sturaro MJ, Rodrigues MT, Lima-Filho GR, Bitar YOC, Wheeler WC, Aleixo A (2018) Phylogeny of Map Tree Frogs, *Boana semilineata* species group, with a new Amazonian species (Anura: Hylidae). *South American Journal of Herpetology* 13(2): 150–169. <https://doi.org/10.2994/SAJH-D-17-00037.1>
- Pereyra MO, Blotto BL, Baldo D, Chaparro JC, Ron SR, Elias-Costa AJ, Iglesias PP, Venegas PJ, Thomé MTC, Ospina-Sarria JJ, Maciel NM, Rada M, Kolenc F, Borteiro C, Rivera-Correa M, Rojas-Runjaic FJM, Moravec J, De La Riva I, Wheeler WC, Castroviejo-Fisher S, Grant T, Haddad CFB, Faivovich J (2021) Evolution in the Genus *Rhinella*: A Total Evidence Phylogenetic Analysis of Neotropical True Toads (Anura: Bufonidae). *Bulletin of the American Museum of Natural History* 447(1): 1–156. <https://doi.org/10.1206/0003-0090.447.1.1>
- Phillips MJ, Delsuc F, Penny D (2004) Genome-scale phylogeny and the detection of systematic biases. *Molecular Phylogenetics and Evolution* 21(7): 1455–1458. <https://doi.org/10.1093/molbev/msh137>
- Pinheiro PP, Kok PJR, Noonan BPD, Means B, Haddad CFB, Faivovich J (2019a) A new genus of Cophomantini, with comments on the taxonomic status of *Boana liliae* (Anura: Hylidae). *Zoological Journal of the Linnean Society* 185(1): 226–245. <https://doi.org/10.1093/zoolinnean/zly030>
- Pinheiro HT, Moreau CS, Daly M, Rocha LA (2019b) Will DNA barcoding meet taxonomic needs? *Science* 365(6456): 873–874. <https://doi.org/10.1126/science.aay7174>

- Posada D, Buckley TR (2004) Model selection and model averaging in phylogenetics: Advantages of Akaike information criterion and Bayesian approaches over likelihood ratio tests. *Systematic Biology* 53(5): 793–808. <https://doi.org/10.1080/10635150490522304>
- Prado CPA, Haddad CFB, Zamudio KR (2012) Cryptic lineages and Pleistocene population expansion in a Brazilian Cerrado frog. *Molecular Ecology* 21(4): 921–941. <https://doi.org/10.1111/j.1365-294X.2011.05409.x>
- Prychitko TM, Moore WS (1997) The utility of DNA sequences of an intron from the b-fibrinogen gene in phylogenetic analysis of woodpeckers (Aves: Picidae). *Molecular Phylogenetics and Evolution* 8(2): 193–204. <https://doi.org/10.1006/mpev.1997.0420>
- Prychitko TM, Moore WS (2000) Comparative evolution of the mitochondrial cytochrome b gene and nuclear  $\beta$ -fibrinogen intron 7 in woodpeckers. *Molecular Phylogenetics and Evolution* 17(7): 1101–1111. <https://doi.org/10.1093/oxfordjournals.molbev.a026391>
- Prychitko TM, Moore WS (2003) Alignment and phylogenetic analysis of  $\beta$ -fibrinogen intron 7 sequences among avian orders reveal conserved regions within the intron. *Molecular Biology and Evolution* 20(5): 762–771. <https://doi.org/10.1093/molbev/msg080>
- Pyron RA, Wiens JJ (2011) A large-scale phylogeny of Amphibia including over 2800 species, and a revised classification of extant frogs, salamanders, and caecilians. *Molecular Phylogenetics and Evolution* 61(2): 543–583. <https://doi.org/10.1016/j.ympev.2011.06.012>
- Rainha RN, Martinez PA, Moraes LJCL, Castro KMSA, Réjaud A, Fouquet A, Leite RN, Rodrigues MT, Werneck FP (2021) Subtle environmental variation affects phenotypic differentiation of shallow divergent treefrog lineages in Amazonia. *Biological Journal of the Linnean Society* 134(1): 177–197. <https://doi.org/10.1093/biolinnean/blab056>
- Rambaut A (2016) FigTree, tree figure drawing tool. Available from Version 1 (4) 3. <http://tree.bio.ed.ac.uk/software/figtree>
- Rambaut A, Drummond AJ, Xie D, Baele G, Suchard MA (2018) Posterior summarization in Bayesian phylogenetics using Tracer 1.7. *Systematic Biology* 67(5): 901–904. <https://doi.org/10.1093/sysbio/syy032>
- Roberts LR, Nichols LA, Holland LJ (1995) cDNA and amino-acid sequences and organization of the gene encoding the BI3 subunit of fibrinogen from *Xenopus laevis*. *Gene* 160(2): 223–228. [https://doi.org/10.1016/0378-1119\(95\)00188-C](https://doi.org/10.1016/0378-1119(95)00188-C)
- Ronquist F, Teslenko M, van der Mark P, Ayres DL, Darling A, Höhna S, Larget B, Liu L, Suchard MA, Huelsenbeck JP (2012) MrBayes 3.2: Efficient Bayesian phylogenetic inference and model choice across a large model space. *Systematic Biology* 61(3): 539–542. <https://doi.org/10.1093/sysbio/sys029>
- Rubinoff D, Holland BS (2005) Between Two Extremes: Mitochondrial DNA is neither the Panacea nor the Nemesis of Phylogenetic and Taxonomic Inference. *Systematic Biology* 54(6): 952–961. <https://doi.org/10.1080/10635150500234674>
- Salichos L, Rokas A (2013) Inferring ancient divergences requires genes with strong phylogenetic signals. *Nature* 497(7449): 327–331. <https://doi.org/10.1038/nature12130>
- Sambrook JF, Russell DW (2001) *Molecular cloning: a laboratory manual*. Cold Spring Harbor Laboratory Press, New York, 2344 pp.
- Schmitz U, Pinello N, Jia F, Alasmari S, Ritchie W, Keightley MC, Shini S, Lieschke GJ, Wong JLL, Rasko JEJ (2017) Intron retention enhances gene regulatory complexity in vertebrates. *Genome Biology* 18(216): 1–15. <https://doi.org/10.1186/s13059-017-1339-3>

- Sequeira F, Ferrand N, Harris DJ (2006) Assessing the phylogenetic signal of the nuclear beta-fibrinogen intron 7 in salamandrids (Amphibia: Salamandridae). *Amphibia-Reptilia* 27(3): 409–418. <https://doi.org/10.1163/156853806778190114>
- Small RL, Cronn RC, Wendel JF (2004) Use of nuclear genes for phylogeny reconstruction in plants. *Australian Systematic Botany* 17(2): 145–170. <https://doi.org/10.1071/SB03015>
- Stöck M, Dufresnes CS, Litvinchuk N, Lymberakis P, Biollay S, Berroneau M, Borzée A, Ghali K, Ogielska M, Perrin N (2012) Cryptic diversity among Western Palearctic tree frogs: Postglacial range expansion, range limits, and secondary contacts of three European tree frog lineages (*Hyla arborea* group). *Molecular Phylogenetics and Evolution* 65(1): 1–9. <https://doi.org/10.1016/j.ympev.2012.05.014>
- Tamura K, Peterson D, Peterson N, Stecher G, Nei M, Kumar S (2011) Mega 5: Molecular evolutionary genetics analysis using maximum likelihood, evolutionary distance, and maximum parsimony methods. *Molecular Biology and Evolution* 28(10): 2731–2739. <https://doi.org/10.1093/molbev/msr121>
- Tamura K, Tao Q, Kumar S (2018) Theoretical Foundation of the RelTime Method for Estimating Divergence Times from Variable Evolutionary Rates. *Molecular Phylogenetics and Evolution* 35(7): 1770–1782. <https://doi.org/10.1093/molbev/msy044>
- Teixeira JI, Martínez-Solano D, Buckley P, Tarroso M, García-París M, Ferrand N (2015) Genealogy of the nuclear  $\beta$ -fibrinogen intron 7 in *Lissotriton boscai* (Caudata, Salamandridae) concordance with mtDNA and implications for phylogeography and speciation. *Contributions to Zoology* 84(3): 193–215. <https://doi.org/10.1163/18759866-08403002>
- Thiery T, Landan G, Martin WF (2014) Concatenated alignments and the case of the disappearing tree. *BMC Ecology and Evolution* 14: e266. <https://doi.org/10.1186/s12862-014-0266-0>
- Tonini J, Moore A, Stern D, Shcheglovitova M, Ortí G (2015) Concatenation and Species Tree Methods Exhibit Statistically indistinguishable Accuracy under a Range of Simulated Conditions Version 1. *PLoS Currents* 9: 7. <https://doi.org/10.1371%2Fcurrents.tol.34260cc27551a527b124ec5f6334b6be>
- Vaidya G, Lohman DJ, Meier R (2011) SequenceMatrix: Concatenation software for the fast assembly of multigene datasets with character set and codon information. *Cladistics* 27(2): 171–180. <https://doi.org/10.1111/j.1096-0031.2010.00329.x>
- Vasconcellos MM, Colli GR, Cannatella DC (2021) Paleotemperatures and recurrent habitat shifts drive diversification of treefrogs across distinct biodiversity hotspots in sub-Amazonian South America. *Journal of Biogeography* 48(2): 305–320. <https://doi.org/10.1111/jbi.13997>
- Velo-Antón G, Martínez-Solano I, García-París M (2008)  $\beta$  fibrinogen intron 7 variation in *Discoglossus* (Anura: Discoglossidae) implications for the taxonomic assessment of morphologically cryptic species. *Amphibia-Reptilia* 29(4): 523–533. <https://doi.org/10.1163/156853808786230460>
- Wiens JJ, Kuczynski CA, Hua X, Moen DS (2010) An expanded phylogeny of treefrogs (Hylidae) based on nuclear and mitochondrial sequence data. *Molecular Phylogenetics and Evolution* 55(3): 871–882. <https://doi.org/10.1016/j.ympev.2010.03.013>
- Wilke T, Schulthei R, Albrecht C (2009) As time goes by: A simple fool's guide to molecular clock approaches in invertebrates. *American Malacological Bulletin* 27(1/2): 25–45. <https://doi.org/10.4003/006.027.0203>

- Ye J, Coulouris G, Zaretskaya I, Cutcutache I, Rozen S, Madden T (2012) Primer-BLAST: A tool to design target-specific primers for polymerase chain reaction. *BMC Bioinformatics* 13(134): 1–11. <https://doi.org/10.1186/1471-2105-13-S6-S1>
- Zhang P, Liang D, Mao R-L, Hillis DM, Wake DB, Cannatella DC (2013) Efficient Sequencing of Anuran mtDNAs and a Mitogenomic Exploration of the Phylogeny and Evolution of Frogs. *Molecular Biology and Evolution* 30(8): 1899–1915. <https://doi.org/10.1093/molbev/mst091>
- Zheng Y, Peng R, Kuro-o M, Zeng X (2011) Exploring patterns and extent of bias in estimating divergence time from mitochondrial DNA sequence data in a particular lineage: A case study of salamanders (Order Caudata). *Molecular Biology and Evolution* 28(9): 2521–2535. <https://doi.org/10.1093/molbev/msr072>

## Appendix I

**Table A1.** Voucher information, localities, and GenBank accession numbers for the sequences analyzed for this study.

Species	<i>CXCR4</i>	<i>Intron 7</i>	<i>RAG-1</i>	<i>RHO</i>	<i>SIAHI</i>	<i>Tyr</i>	<i>28S</i>	Voucher and source literature of sequences
<i>Boana aguilari</i>	MT824211			MT824337			KF751464	Faivovich et al. (2013, 2021)
<i>Boana albomarginata</i>	KF751476	OQ448590	AY844384	AY844568	AY844794		AY844218	MRT 5870; Jussara, Bahia, Brazil. Faivovich et al. (2005, 2013)
<i>Boana albopunctata</i>		OQ448612		AY844569	AY844795	AY844041		MRT 8229, Petrolina, Goiás, Brazil. Faivovich et al. (2005)
<i>Boana balzani</i>	MT824213	OQ448599	AY844395	AY844582	AY844806		AY844226	MNCN/ADN 5785, Camino a San Onofre, Carrasco, Cochabamba, Bolivia. Faivovich et al. (2005, 2021)
<i>Boana benitezi</i>	KF751477		AY844396	AY844583			AY844227	Faivovich et al. (2005, 2013)
<i>Boana bischoffi</i>	MT824219	OQ448607	AY844398		MT824343		MT824526	AF 327, Fazenda Intervales, Estado de São Paulo. Faivovich et al. (2005, 2021)
<i>Boana boans</i>	KF751478	OQ448591		AY844588	AY844809	AY844055	AY844231	MPEG 17385, Arredores da Fazenda passo Formoso, Manicoré, Amazonas. Faivovich et al. (2005, 2013)
<i>Boana botumirim</i>				MT824344				Faivovich et al. (2021)
<i>Boana buriti</i>		OQ448601		MT824346	MT824484			CHUNB 30653, Brasília, Distrito Federal. Faivovich et al. (2021)
<i>Boana caingua</i>	KF751479	OQ448602		MT824352	AY844812	AY844057	AY844234	AF 515, Ribeirão Grande São Paulo, São Paulo. Faivovich et al. (2005, 2013, 2021)
<i>Boana calcarata</i>							AY844235	Faivovich et al. (2005)
<i>Boana cambui</i>				MT824356	MT824486	MT824534		Faivovich et al. (2021)
<i>Boana cinerascens</i>	KF751480	OQ448595		AY844610			DQ283466	RAET 505, Estação Científica Ferreira Penna, Melgaço, Pará, Brazil. Faivovich et al. (2005, 2013)
<i>Boana cipoensis</i>				MT824357	MT824487			Faivovich et al. (2021)
<i>Boana cordobae</i>	KF751481		AY844411	MT824460	MT824516	AY844066	AY844244	Faivovich et al. (2005, 2013, 2021)
<i>Boana crepitans</i>	KF751482			AY844601			AY844067	Faivovich et al. (2005, 2013)
<i>Boana curupi</i>	MT824227			MT824359	MT824489			Faivovich et al. (2021)
<i>Boana ericae</i>			AY844416	AY844605			MT824537	Faivovich et al. (2005, 2021)

Species	CXCR4	Intron 7	RAG-1	RHO	SLAH1	Tyr	28S	Voucher and source literature of sequences
<i>Boana faber</i>				AY844607				Faivovich et al. (2005)
<i>Boana fasciata</i>	KX200378			AY844608				Faivovich et al. (2005); Feng et al. (2017)
<i>Boana freicanecae</i>	MT824217			MT824366		MT824538		Faivovich et al. (2021)
<i>Boana geographica</i>		OQ448611						QCAZ 16809: Estación Científica Yasuni. PUCE, Laguna, Orellana, Ecuador. in confirmation process
<i>Boana gladiator</i>	MT824212			MT824368				Faivovich et al. (2021)
<i>Boana goiana</i>				MT824372	MT824491	MT824541		Faivovich et al. (2021)
<i>Boana guentheri</i>	MT824245	OQ448608		MT824373	MT824492		AY844253	CFBH 3386: Terra de Areia, Rio Grande do Sul, Brazil. Faivovich et al. (2005, 2021)
<i>Boana heilprini</i>				AY844613				Faivovich et al. (2005)
<i>Boana jaguarivaivensis</i>				MT824374	MT824494			Faivovich et al. (2021)
<i>Boana joaquina</i>	KF751484	OQ448605	AY844421	MT824376			AY844256	CFBH 1068: Urubici, Santa Catarina, Brazil. Faivovich et al. (2005, 2013, 2021)
<i>Boana lanciformis</i>				AY844619		AY844081	AY844258	Faivovich et al. 2005
<i>Boana lemai</i>	KF751485		AY844423	AY844620		AY844082	AY844259	Faivovich et al. (2005, 2013)
<i>Boana leptolineata</i>	MT824246	OQ448604	AY844424	AY844621	AY844839	AY844083	AY844260	CFBH 8504: São Francisco de Paula, Rio Grande do Sul, Brazil. Faivovich et al. (2005, 2021)
<i>Boana lundii</i>				AY844623		AY844085	AY844262	Faivovich et al. (2005)
<i>Boana marginata</i>	KF751486		AY844426	AY844624		MT824542	AY844263	Faivovich et al. (2005, 2013, 2021)
<i>Boana marianitae</i>		OQ448610	AY844427	MT824378	AY844843			MNCN/ADN 5901: Camino a Bella Vista, Florida, Santa Cruz, Bolivia. Faivovich et al. (2005, 2021)
<i>Boana melanopleura</i>	KF751487	OQ448600		MT824379	HM444787			MTD-TD 1146: Huancabamba, Pasco, Peru. Faivovich et al. (2013, 2021)
<i>Boana multifasciata</i>	GQ365986		AY844436	AY844633		AY844093	AY844270	Faivovich et al. (2005, 2010)
<i>Boana nympha</i>	KF751488			AY844661		AY844112	AY844289	Faivovich et al. (2005, 2013)
<i>Boana pardalis</i>				AY844637				Faivovich et al. (2005)
<i>Boana pellicens</i>		OQ448597						QCAZ 15354: Via Toachi-Chiriboga. Poza junto a carretera cerca del Rio Orito, Ecuador.
<i>Boana picturata</i>		OQ448594						QCAZ 15549:3 Km from Durango, em el cruce de la vá San Lorenzo e outra carretera X, Esmeraldas, Ecuador.
<i>Boana poaju</i>				MT824380	MT824495			Faivovich et al. (2021)
<i>Boana polytaenia</i>	MT824241	OQ448606	AY844443	MT824429	MT824508		MT824547	CFBH 8394: Cristina, MG. Faivovich et al. (2005, 2021)
<i>Boana pombali</i>	MT824247			MT824431	MT824511		MT824552	Faivovich et al. (2021)
<i>Boana prasina</i>				MT824436			MT824554	Faivovich et al. (2021)
<i>Boana pulchella</i>		OQ448609	AY844445	MT824443	MT824513	MT824557	AY844278	CHUNB 37686: Pilar do Sul, Estado de São Paulo, Brazil. Faivovich et al. (2005, 2021)
<i>Boana punctata</i>		OQ448596		AY844645				QCAZ18185: Estación Biológica Jatun Sacha, Napo. Faivovich et al. (2005)
<i>Boana raniceps</i>	KF751489	OQ448613		AY844646	AY844863	AY844103		MRT 6706: UHE Lajeado Tocantins. Faivovich et al. (2005, 2013)
<i>Boana riojana</i>	MT824238		AY844447	MT824462	MT824518		AY844279	Faivovich et al. (2005, 2021)
<i>Boana roraima</i>	KF751490		AY844448	AY844650		AY844104	AY844280	Faivovich et al. (2005, 2013)

Species	CXCR4	Intron 7	RAG-1	RHO	SLAH1	Tyr	28S	Voucher and source literature of sequences
<i>Boana rufifela</i>		OQ448598		AY844652	AY844867	AY844105	AY844282	CHP-STRI:5114: Quebrada Guabalito, Palmarazo, Parque Nacional General de División Omar Torrijos Herrera, Provincia de Coclé. Faivovich et al. (2005)
<i>Boana semigutata</i>		OQ448603	AY844452	MT824466	MT824519	MT824559	AY844285	CFBH 242: Piraquara, Paraná, Brazil. Faivovich et al. (2005, 2021)
<i>Boana semilineata</i>	KF751491		AY844453	AY844656		AY844108	AY844286	Faivovich et al. (2005, 2013)
<i>Boana sibleszi</i>	KF751492	OQ448593	AY844455	AY844658	AY844873	AY844110	AY844288	ROM 39561: Mount Ayanganna, Guyana. Faivovich et al. (2005, 2013)
<i>Boana stellae</i>	MT824229			MT824475		MT824567		Faivovich et al. (2021)
<i>Boana stenocephala</i>				MT824479	MT824520	MT824563		Faivovich et al. (2021)
<i>Boana warrini</i>		OQ448592						RAET 502: Estação Científica Ferreira Penna, Melgaço, Pará, Brazil
<i>Aplastodiscus albofrenatus</i>		OQ448614	KU184083	KU184111	KU184149	KU184246		AF 101: Rio de Janeiro, Rio de Janeiro, Brazil. Berneck et al. (2016)
<i>Aplastodiscus albosignatus</i>		OQ448616	AY844385	KU184114	AY844796	AY844042	AY844219	CFBH 7711: Parque Estadual Serra do Mar, Santa Virginia, São Luís do Paraitinga, São Paulo, Brazil. Faivovich et al. (2005)
<i>Aplastodiscus eugenioi</i>	KF751465							Faivovich et al. (2013)
<i>Aplastodiscus leucopygius</i>	KF751466						AY844261	Faivovich et al. (2005; 2013)
<i>Aplastodiscus perviridis</i>	KF751467						AY844201	Faivovich et al. (2005, 2013)
<i>Aplastodiscus weygoldti</i>		OQ448615	AY844467	KU184124	AY844887	KU184257		AF 68: São Paulo do Aracá, Espírito Santo, Brazil. Faivovich et al. (2005)
<i>Bokermannohyla circumdata</i>	KF751468	OQ448619	AY844409		AY844817	AY844064	AY844242	IT-H0562, MZUSP 93551: Juquitiba, Estado de São Paulo. Berneck et al. (2016); Faivovich et al. (2005; 2013)
<i>Callimedusa tomopterna</i>	GQ366024	OQ448618	AY844497	AY844715		AY844157	AY844328	MPEG 17368, Near Fazenda Passo Formoso, Manicoré, Amazonas, Brazil. Faivovich et al. (2010, 2005)
<i>Callimedusa vaillanti</i>					AY844921			Faivovich et al. (2005)
<i>Myersiobyla liliae</i>			MH251236					Pinheiro et al. (2019a)
<i>Myersiobyla inparquesi</i>							AY844291	Faivovich et al. (2005)
<i>Nesorobyla kanaima</i>	GQ365994	OQ448617		AY844617	MH251240	AY844079		ROM 39586: Mount Ayanganna, Guyana. Faivovich et al. (2005, 2010); Pinheiro et al. (2019a)

AF: Laboratório de Citogenética de Vertebrados. Depto. Genética e Biologia Evolutiva, Instituto de biologia, Universidade de São Paulo.

CHP- STRI: Circulo Herpetologico de Panama-Smithsonian Tropical Research Institute

CFBH: Célio F. B. Haddad. Coleção de anfíbios, SP, Brazil

CHUNB: Coleção herpetológica, Universidade de Brasília, Brazil

MNCN: Museu Nacional de Ciências Naturales, Spain

MPEG: Museu Paraense Emílio Goeldi, Brazil

MRT: Miguel Trefaut Urbano Rodrigues, Universidade de São Paulo, Brazil.

MTD-TD: Museum für Tierkunde, Germany.

MZUSP: Museu de Zoologia, Universidade de São Paulo, Brazil

QCAZ: Colección de anfibios del Museo de Zoología, Pontificia Universidad Católica del Ecuador

RAET: Ruth Amanda Estupiñán Tristancho, Brazil

ROM: Royal Ontario Museum, Centre for Biodiversity and Conservation Biology: Herpetology, Canada

## Supplementary material I

### Phylogenetic trees and molecular dating of gene trees

Authors: Ruth Amanda Estupiñán, Sávio Torres de Farias, Evonnildo Costa Gonçalves, Mauricio Camargo, Maria Paula Cruz Schneider

Data type: pdf file

Explanation note: Phylogenetic trees corresponding to the studied markers (a. CXCR4, b. FGBI7, c. RAG-1, d. RHO, e. TYRF.SIAH1, g. 28SandC-genes), and the methods used – MP, MB, and ML, corresponding to the 1<sup>st</sup>, 2<sup>nd</sup>, and 3<sup>rd</sup> trees for each marker, respectively). For Jackknife support values from the MP method, and bootstrap support values for the ML method, values below 50% were not presented. Molecular dating of gene trees. a. ND1. b. CYTB, and c. FGBI7 using the Rel-Timemethod in MEGA X.

Copyright notice: This dataset is made available under the Open Database License (<http://opendatacommons.org/licenses/odbl/1.0/>). The Open Database License (ODbL) is a license agreement intended to allow users to freely share, modify, and use this Dataset while maintaining this same freedom for others, provided that the original source and author(s) are credited.

Link: <https://doi.org/10.3897/zookeys.1149.85627.suppl1>



# Revision of the genus *Charitoprepes* Warren (Lepidoptera, Crambidae), with the description of a new species from China

Shi-Qi Huang<sup>1</sup>, Xi-Cui Du<sup>1</sup>

<sup>1</sup> College of Plant Protection, Southwest University, Chongqing, China

Corresponding author: Xi-Cui Du ([duxicui@hotmail.com](mailto:duxicui@hotmail.com))

---

Academic editor: R. Mally | Received 27 November 2022 | Accepted 8 February 2023 | Published 23 February 2023

---

<https://zoobank.org/C742BDB9-3733-4545-83A9-C9457A1C6659>

---

**Citation:** Huang S-Q, Du X-C (2023) Revision of the genus *Charitoprepes* Warren (Lepidoptera, Crambidae), with the description of a new species from China. ZooKeys 1149: 171–179. <https://doi.org/10.3897/zookeys.1149.98065>

---

## Abstract

The genus *Charitoprepes* is revised based on morphological characteristics, and *Charitoprepes aciculata* sp. nov. is described as new from China. Additionally, the female genitalia of *C. lubricosa* are described for the first time based on new material. The differences among species of this genus are diagnosed, along with images of adults and their genitalia.

## Keywords

*Charitoprepes aciculata* sp. nov., genitalia, Pyraloidea, Spilomelinae

## Introduction

The genus *Charitoprepes* was erected by Warren (1896) with *Charitoprepes lubricosa* Warren, 1896 from India as the type species. Hampson (1896) synonymized *Charitoprepes* with *Heterocnephes* Lederer, 1863, which was followed by other authors for more than 100 years. *Charitoprepes* was treated as valid genus by Kim et al. (2014), with *C. lubricosa* as the only species. Mally et al. (2019) transferred *Heterocnephes apicipicta* to *Charitoprepes* based on morphological characteristics and, until now, this genus only contained two known species (Nuss et al. 2023). The genus is distributed in China, India, Japan, and South Korea (Inoue 1963; Wang et al. 2003; Choi 2010; Kim et al. 2014).

*Charitoprepes* species are easily distinguished from those of other genera in having an elongated elliptical black patch at the apex of the greyish brown forewings. Species in this genus are externally very similar, but they can be distinguished by their genitalia. In this study, the morphological characteristics of this genus are revised, and one new species is described from China.

## Materials and methods

The specimens were collected using a light trap and killed with ethyl acetate or ammonium hydroxide. The specimens, including the type material of the new species, are deposited in the College of Plant Protection, Southwest University, Chongqing, China (SWU). The corresponding author examined the type specimen of *Charitoprepes lubricosa* deposited in Natural History Museum, London, United Kingdom (NHMUK). Genitalia preparation mainly follows Li and Zheng (1996). Images of the adults were photographed using a digital camera (Nikon P7700), and images of the genitalia were captured with a digital camera (Leica DFC 450) attached to a digital microscope (Leica M205 A). The terminology mainly follows Maes (1995) and Mally et al. (2019).

## Taxonomy

### *Charitoprepes* Warren, 1896

*Charitoprepes* Warren, 1896: 136. Type species: *Charitoprepes lubricosa* Warren, 1896, by original designation.

**Diagnosis.** This genus is distinguished by the greyish-brown body and wings; the forewing with an elongated, elliptical, black patch at the apex. This genus can be distinguished from *Heterocnephes* by its labial palpi bent and upturned normally, the corpus bursae with two thin, band-like signa present or absent. In *Heterocnephes*, however, the second segment of labial palpi is inflated and nearly oblong, along with its third segment protruded forward (Wang 1980), the corpus bursae has two round signa, and the valva is broader than that of *Charitoprepes*.

**Generic characteristics. Adult.** Body and wings greyish brown. Frons rounded. Antenna filiform, with sparse cilia ventrally. Labial palpi bent and upturned. Maxillary palpi filiform. Forewing with orbicular and discoidal stigma present, an elongated, elliptical, black patch along costa at apex; length of cell approximately half of wing; discocellulars arcuately incurved;  $R_{S1}$  very close to  $R_{S2+S3}$ ;  $R_{S2}$  anastomosed with  $R_{S3}$  approximately three-fifths beyond cell;  $M_2$ ,  $M_3$  and  $CuA_1$  originating from posterior angle of the cell and uniformly spaced at base. Hindwing with length of cell half of wing; discocellulars strongly, arcuately incurved; Rs anastomosed with Sc+R at long distance;  $M_1$  and Rs shortly stalked at base beyond cell;  $M_2$ ,  $M_3$  and  $CuA_1$  originating from posterior angle of cell (Fig. 1A, B). Legs shiny white. Middle tibia with distal

inner spur approximately twice length of outer spur; hind tibia with inner proximal spur approximately triple length of outer proximal spur, and inner distal spur approximately twice length of outer distal spur. Tympanal organs with fornix tympani surface projecting from the tympanic frame. Praecinctorium strongly bifid (Fig. 1C).

**Male genitalia.** Uncus long and thin, with the distal part swollen and covered with minute setae. Valva broad. Fibula spine-like and downcurved. Sacculus sclerotized, with an apical triangular process overlapping with the fibula. Saccus broad and rounded, tapered terminally. Cornutus present and diverse.

**Female genitalia.** Apophyses anteriores as long as apophyses posteriores, or longer. Ductus bursae varies from short and broad to long and thin. Corpus bursae elliptical or oval. A pair of thin, band-like signa present or absent.

**Distribution.** China, India, Japan, South Korea (Fig. 2).

**Remarks.** According to Kim et al. (2014), this genus can be identified by an elongated, elliptical, black patch at apex of forewing and dark brown, discoidal stigma on the hindwing. In *C. aciculata* sp. nov., however, the discoidal stigma on the hindwing is absent. Therefore, the morphological characteristics of *Charitoprepes* have been revised in this study, with supplementary wing venation and genitalia characteristics.

### Key to species of *Charitoprepes* based on morphology and genitalia

- 1        Discoidal stigma absent on hindwing; phallus slender and extremely elongated, with an elongated, needle-like cornutus..... *C. aciculata* sp. nov.
- Discoidal stigma present on hindwing; phallus short and stout..... 2
- 2        Phallus with a spicate cornutus ..... *C. lubricosa*
- Phallus with two fusiform cornuti..... *C. apicipicta*

### *Charitoprepes lubricosa* Warren, 1896

Figs 1A, 3A, B, 4A, B

*Charitoprepes lubricosa* Warren, 1896: 136. Type locality: India (Meghalaya). Type depository: NHMUK.

*Heterocnephes lubricosa*: Hampson, 1896: 265.

**Material examined.** *Holotype*, ♀ INDIA, Khasis, X. 1894, Nat. Coll. (NHMUK).

**Additional material.** CHINA, **Chongqing Municipality**, 4 ♂♂, 2 ♀♀, Chengkou County, Dongan Town, Xingtian Village, 1300 m elev., 30 June 2013, Gui-Qing He & Li-Jun Xu leg., Genitalia slide no. HSQ22163 ♀; 1 ♂, Jinfo Mountain, 696 m elev., 18 May 2017, Ji-Ping Wan & Qiu-Long Yang leg., Genitalia slide no. HSQ22166 ♂; 2 ♂♂, Simian Mountain, 900 m elev., 18 July 2012, Gui-Qing He leg., wing slide no. HSQ22003; **Guangdong Prov.**, 1 ♂, Nanling Nature Reserve, Babao Reserve Station, 1070 m elev., 23 August 2010, Xi-Cui Du leg.; **Sichuan Prov.**, 1 ♀, Xuyong County, Guandou Town, 501 m elev., 29 August 2013, Li-Jun Xu leg.; **Yunnan Prov.**, 1 ♂, Xishuangbanna Dai Autonomous Prefecture, Yaoqu Town, 780 m elev.,

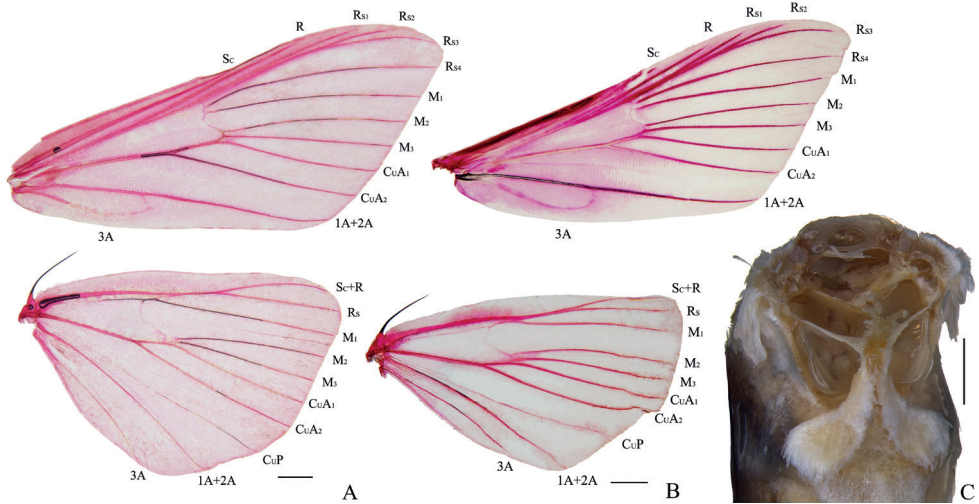


**Figure 1.** Wing venation and tympanal organs of *Charitoprepes* **A**, **C** *C. lubricosa* **B** *C. aciculata* sp. nov. Upper is forewing, lower is hindwing. Scale bars: 1.0 mm (**A**, **B**); 0.5 mm (**C**).



**Figure 2.** Distribution of *Charitoprepes* spp. (*C. lubricosa*: orange triangles; *C. apicipicta*: green triangles; *C. aciculata* sp. nov.: blue triangles).

26 May 2015, Man-Fei Tao leg., Genitalia slide no. HSQ22160 ♂; **Zhejiang Prov.**, 2 ♂♂, 1 ♀, Tianmu Mountain, 400 m elev., 26 July 2011, Xi-Cui Du leg.

**Description. Adult** (Fig. 3A, B). Body and wings pale greyish brown. Forewing length 10.0–14.0 mm, wingspan 21.0–29.0 mm. Frons pale greyish brown, white laterally; vertex white. Antenna brown, scape white ventrally. Labial palpi with first segment white, second and third segments brown. Maxillary palpi white, brown near

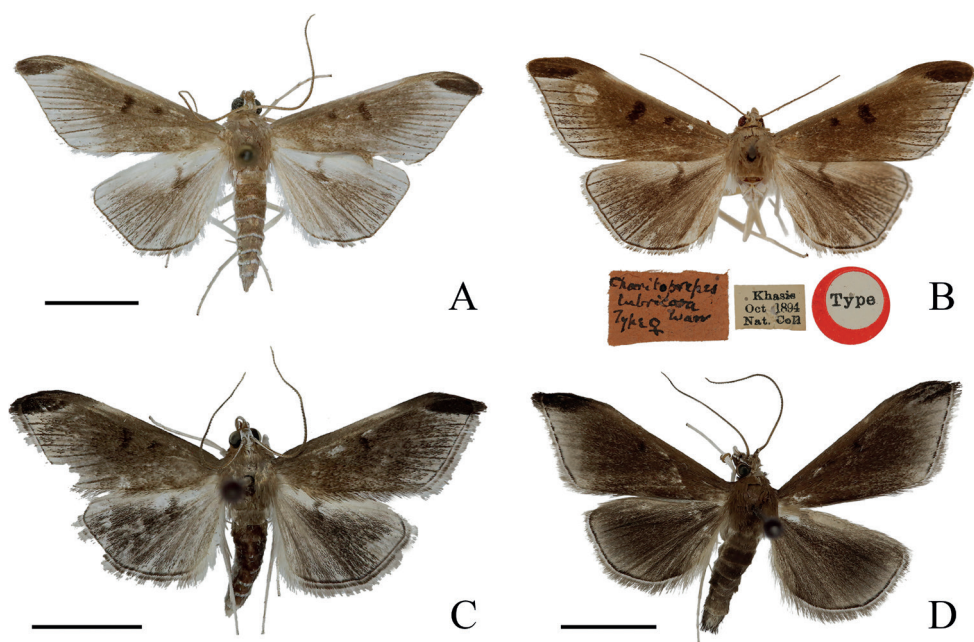


**Figure 3.** Adults of *Charitoprepes* spp. **A** *C. lubricosa*, male **B** *C. lubricosa*, female, type (NHMUK) **C** *C. apicipicta*, male **D** *C. aciculata* sp. nov., male, holotype. Scale bars: 0.5 cm.

apex. Patagium, tegula and pale greyish brown. Fore and hind wings with terminal area pearly grey. Forewing greyish brown along veins, orbicular stigma and discoidal stigma conspicuous and dark brown; middle third of costa pearly grey. Hindwing with dark brown, discoidal stigma. Veins towards margin finely dark on fore and hind wings. Cilia brown, with a white basal line. Legs shiny white, epiphysis orange-yellow. Abdomen pale greyish brown, pale grey ventrally.

**Male genitalia** (Fig. 4A). Valva square, with sparse setae, narrowed at base. Fibula well developed. Saccus broad. Phallus stout, with a spicate cornutus.

**Female genitalia** (Fig. 4B). Apophyses anteriores slightly longer than apophyses posteriores. Antrum sclerotized, developed. Ductus bursae short, about half as wide as corpus bursae. Corpus bursae large, elongate elliptical, with a pair of narrow, longitudinal, band-like signa.

**Distribution.** China (Chongqing, Fujian, Guangdong, Hubei, Jiangsu, Shanghai, Sichuan, Taiwan, Yunnan, Zhejiang), India, Japan, South Korea.

**Remarks.** The female genitalia of this species are described for the first time.

### *Charitoprepes apicipicta* (Inoue, 1963)

Figs 3C, 4C, D

*Heterocnephes apicipicta* Inoue, 1963: 109. Type locality: Japan (Honshu).

*Charitoprepes apicipicta*: Mally et al. 2019: 141.

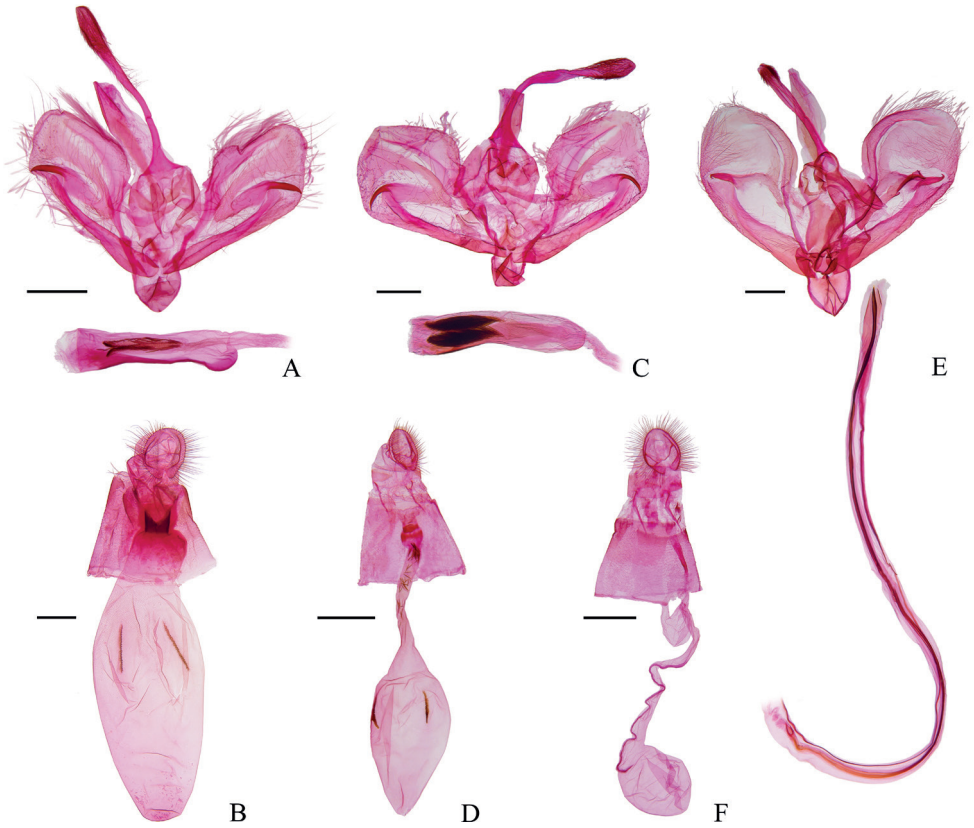


**Figure 4.** Genitalia of *Charitoprepes* spp. **A, B** *C. lubricosa* **C, D** *C. apicipicta* **E, F** *C. aciculata* sp. nov. **A** male, genitalia slide no. HSQ22166 **B** female, genitalia slide no. HSQ22163 **C** male, genitalia slide no. HSQ22161 **D** female, genitalia slide no. HSQ22167 **E** male, paratype, genitalia slide no. HSQ22164 **F** female, paratype, genitalia slide no. HSQ22168. Scale bars: 0.5 mm (**A, C, E**); 1.0 mm (**B, D, F**).

**Material examined.** CHINA, **Chongqing Municipality**, 2 ♂♂, 2 ♀♀, Wushan County, Dangyang Town, Wulipo Nature Reserve, 396 m elev., 19 April 2021, Hong Zhao & Jin-Hang Han leg., Genitalia slide no. HSQ22165 ♂; 4 ♂♂, Wuxi County, Yintiaoling Nature Reserve, Hongqihegou, 1118 m elev., 21 June 2022, Ci Tang & Xin-Lei Xue leg.; 1 ♂, Simian Mountain, 1280 m elev., 11 August 2011, Gui-Qing He & Li-Fang Song leg., Genitalia slide no. HSQ22149 ♂; **Guangdong Prov.**, 1 ♂, 1 ♀, Nanling Nature Reserve, Babao Reserve Station, 1070 m elev., 23 August 2010, Xi-Cui Du leg.; **Guangxi Zhuang Autonomous Region**, 1 ♂, 2 ♀♀, Nonggang Nature Reserve, 188 m elev., 25 July 2011, Gui-Qing He leg.; 2 ♂♂, Nonggang Nature Reserve, 170 m elev., 21 August 2020, Lin-Lin Yang leg., Genitalia slide no. HSQ22161 ♂; 1 ♀, Nonggang Nature Reserve, 170 m elev., 21 August 2020, Lin-Lin Yang leg., Genitalia slide no. HSQ22167 ♀; **Guizhou Prov.**, 3 ♂♂, Kuankuoshui Nature Reserve, 800 m elev., 11 August 2010, Xi-Cui Du leg.; **Zhejiang Prov.**, 6 ♂♂, 3 ♀♀, Jiulong Mountain, 6 August 2011, Xiao-Bing Fu leg.; 1 ♂, 3 ♀♀, Tianmu Mountain, 400 m elev., 2 August 2011, Xi-Cui Du & Xiao-Bing Fu leg.

**Diagnosis.** This species is very similar to *C. lubricosa* in appearance, but its greyish brown wings and body are darker than those of *C. lubricosa*. It also can be distinguished by the stout phallus, which has two fusiform cornuti decorated with numerous minute spines, and the ductus bursae, which is elongated and far more slender than that of *C. lubricosa*.

**Description. Male genitalia** (Fig. 4C). Valva square, with sparse setae. Saccus broad. Phallus stout, two fusiform cornuti decorated with numerous minute spines (Inoue 1963).

**Female genitalia** (Fig. 4D). Apophyses anteriores as long as apophyses posteriores. Antrum sclerotized. Ductus bursae long, membranous. Corpus bursae elliptical, taper distally, with a pair of narrow, longitudinal, band-like signa.

**Distribution.** China (Chongqing, Fujian, Guangdong, Guangxi, Guizhou, Hubei, Sichuan, Zhejiang), Japan, South Korea.

**Remarks.** There are occasionally some spines scattered in the ductus bursae of female specimens, which suggests that the cornuti in the male genitalia are deciduous (Fig. 4D).

***Charitoprepes aciculata* sp. nov.**

<https://zoobank.org/F62E09A4-F279-468A-A51C-F8ACA9149117>

Figs 1B, 3D, 4E, F

**Type material. Holotype.** ♂, pinned, with genitalia on a separate slide, CHINA, **Hainan Prov.**, Wuzhi Mountain, 18°54.60'N, 109°40.81'E, 745 m elev., 27 March 2021, Yao Shen leg., genitalia slide no. HSQ22162. **Paratypes.** CHINA, **Hainan Prov.**, 3 ♂♂, other same data as holotype, paratype genitalia slide no. HSQ22164 ♂, paratype wing slide no. HSQ22004, HSQ22005; 1 ♀, Jianfengling Nature Reserve, 963 m elev., 24 June 2020, Ruo-Nan Xu & You Zeng leg.; 4 ♀♀, Qiongzong Li and Miao Autonomous County, Shijie Reserve Station, 383 m elev., 26 March 2021, Yao Shen leg., paratype genitalia slide no. HSQ22168 ♀, HSQ22169 ♀; **Yunnan Prov.**, 1 ♂, Xishuangbanna Dai Autonomous Prefecture, 840 m elev., 23 May 2015, Man-Fei Tao leg., paratype genitalia slide no. HSQ22170.

**Diagnosis.** This species is similar to *C. lubricosa* and *C. apicipicta* in appearance, but it can be differentiated by its darker body and wings, as well as the absence of the discoidal stigma on the hindwing, which is conspicuous in *C. lubricosa* and *C. apicipicta*. The wing venation of this species is somewhat different from that of *C. lubricosa*. The forewing of the latter has the  $R_{S4}$  slightly curved and close to  $R_{S2+S3}$  at the base, while the  $R_{S4}$  is straight and distant from  $R_{S2+S3}$  in this new species (Fig. 1A, B). Furthermore, the stalk length of  $M_1$  and Rs of the hindwing in this new species is longer than that of *C. lubricosa*. It also can be distinguished by the slender and extremely elongated phallus accompanied by an elongated, bent, needle-like cornutus; the elongated ductus bursae has a sclerotized longitudinal line approximately four-fifths of its length, and the corpus bursae is much shorter than the ductus bursae and has no signa. In *C. lubricosa* and *C. apicipicta*, the phallus is stout, and the former has a spicate cornutus and the latter has two fusiform cornuti; the ductus bursae has no longitudinal

line, and the corpus bursae bears a pair of thin, band-like signa in these two species. The corpus bursae is much longer than the ductus bursae in *C. lubricosa*, and is almost as long as the ductus bursae in *C. apicipicta*.

**Description. Adult** (Fig. 3D). Body and wings dark brown, greyish. Forewing length 11.0–13.0 mm, wingspan 21.0–26.0 mm. Frons greyish brown, white laterally; vertex brown. Antenna brown, scape white ventrally. Labial palpi with first segment white, second and third segments dark brown. Maxillary palpi white, dark brown near apex. Patagium, tegula, and thorax dark brown. Fore and hind wings with terminal area pale grey. Forewing with orbicular and discoidal stigma black, sometimes indistinct; an elongated elliptical black patch at apex; a black line along terminal margin, discontinuous. Hindwing with a black line along terminal margin, discoidal stigma absent. Cilia brown, with a white basal line. Legs shiny white, epiphysis orange-yellow. Abdomen dark brown, pale grey ventrally.

**Male genitalia** (Fig. 4E). Uncus long and thin, with the distal swollen and covered with minute setae, apex obtuse rounded and slightly concaved at middle. Valva oval, with sparse setae. Fibula thick, hooked apically. Saccus broad, strongly sclerotized. Phallus slender and extremely elongated, bent, with an elongated needle-like cornutus of nearly same length.

**Female genitalia** (Fig. 4F). Apophyses anteriores ca 1.5 times as long as apophyses posteriores. Antrum weakly sclerotized. Ductus seminalis somewhat expanded near ductus bursae. Ductus bursae elongated, with a sclerotized longitudinal line approximately four-fifths of its length along one side. Corpus bursae oval, signa absent.

**Etymology.** The specific name is derived from the Latin *aciculatus* for needle, in reference to the needle-like cornutus.

**Distribution.** China (Hainan, Yunnan).

## Discussion

Kim et al. (2014) considered *Charitoprepes lubricosa* as a possible pest, but there has been no host reported for either of the two known species of the genus. The long, narrow, longitudinal signa are unusual in Spilomelinae. Besides *C. lubricosa* and *C. apicipicta*, the genus *Maruca* Walker, 1859 also have such signa, as well as a similar uncus. In *Agrioglypta* Meyrick, 1932, some species also have similar signa, but they are shorter and wider, and the other species have two rounded signa. Whether these special signa in *Charitoprepes* indicate a relationship to *Maruca* can only be made clear after a thorough phylogenetic study of the tribe Margaroniini, subfamily Spilomelinae.

## Acknowledgements

We are grateful to the other members of our laboratory for their contribution in collecting specimens and to Dr Lin-Lin Yang (Institute of Plant Protection, Henan Academy of Agricultural Sciences) for providing specimens. Cordial thanks are given to Natural

History Museum, London, United Kingdom (NHMUK) for providing access to the corresponding author for examining type specimens of *Charitoprepes*. We also give our thanks to Dr Nathalie Yonow for reviewing the language of our manuscript, and to three reviewers for their revisions and helpful suggestions for our article. This study was funded by the National Natural Sciences Foundation of China (No. 31772500) and the Natural Sciences Foundation Project of Chongqing (No. CSTB2022NSCQ-MSX1164).

## References

- Choi S-W (2010) First Report of *Heterocnephes apicipicta* (Lepidoptera: Crambidae) in Korea. Korean Journal of Systematic Zoology 26(2): 171–172. <https://doi.org/10.5635/KJSZ.2010.26.2.171>
- Hampson GF (1896) Moths.–Vol. IV. The Fauna of British India, Including Ceylon and Burma. Taylor & Francis, London, [xxviii] 594 pp. <https://doi.org/10.5962/bhl.title.100745>
- Inoue H (1963) Descriptions and records of some Pyralidae from Japan (VI) (Lepidoptera). Kontyû. Entomological Society of Japan, Tokyo 31: 107–112.
- Kim M, Park Y-M, Hyun I-H, Kang B-H, Oh S-H, Jwa J-K, Hyun Y-K, Lee H-S (2014) A newly known genus *Charitoprepes* Warren (Lepidoptera: Pyraloidea: Crambidae) in Korea, with report of *C. lubricosa* Warren. Korean Journal of Applied Entomology 53(3): 301–303. <https://doi.org/10.5656/KSAE.2014.05.0.008>
- Lederer J (1863) Beitrag zur Kenntniss der Pyralidinen. Wiener Entomologische Monatschrift 7: 243–280. [331–504, pls 2–18.]
- Li HH, Zheng ZM (1996) Methods and techniques of specimens of Microlepidoptera. Journal of Shaanxi Normal University 24(3): 63–70. [Natural Science Edition]
- Maes K (1995) A comparative morphological study of the adult Crambidae (Lepidoptera: Pyraloidea). Bulletin et Annales de la Société Royale Belge d'Entomologie 131: 383–434.
- Mally R, Hayden JE, Neinhuis C, Jordal BH, Nuss M (2019) The phylogenetic systematics of Spilomelinae and Pyraustinae (Lepidoptera: Pyraloidea: Crambidae) inferred from DNA and morphology. Senckenberg Gesellschaft für Naturforschung 77(1): 141–204. <https://doi.org/10.26049/ASP77-1-2019-07>
- Nuss M, Landry B, Mally R, Vegliante F, Tränkner A, Bauer F, Hayden J, Segerer A, Schouten R, Li H, Trofimova T, Solis MA Prins, De J, Speidel W (2023) Global Information System on Pyraloidea. <http://www.pyraloidea.org> [Accessed on: 2023-2-8]
- Wang PY (1980) Lepidoptera: Pyralidae. Economic Insect Fauna of China. Fasc. 21. Science Press, Beijing, 229 pp.
- Wang JS, Song SM, Wu YY, Chen TM (2003) Fauna of Pyralidae of Wuyishan Nature Reserve in China. China Science and Technology Press Beijing, 328 pp.
- Warren W (1896) New genera and species of Pyralidæ, Thyrididæ, and Epiplemidæ. Annals and Magazine of Natural History (Series 6) 17: 131–150. <https://doi.org/10.1080/00222939608680328>



# A new species of *Paracortina* from a Vietnamese cave, with remarkable secondary sexual characters in males (Callipodida, Paracortinidae)

Anh D. Nguyen<sup>1,2</sup>, Pavel Stoev<sup>3</sup>, Lien T. P. Nguyen<sup>1</sup>, Tam T. Vu<sup>1</sup>

**1** Institute of Ecology and Biological Resources, Vietnam Academy of Science and Technology, 18, Hoangquocviet Rd., Cau Giay District, Hanoi, Vietnam **2** Graduate University of Science and Technology, Vietnam Academy of Science and Technology, 18, Hoangquocviet Rd., Cau Giay District, Hanoi, Vietnam **3** National Museum of Natural History, Bulgarian Academy of Sciences, Tsar Osvoboditel Blvd. 1, 1000 Sofia, Bulgaria

Corresponding author: Anh D. Nguyen ([ducanh410@yahoo.com](mailto:ducanh410@yahoo.com); [ndanh@iebr.vast.vn](mailto:ndanh@iebr.vast.vn))

---

Academic editor: Nesrine Akkari | Received 6 January 2023 | Accepted 9 February 2023 | Published 23 February 2023

---

<https://zoobank.org/52FBD435-5320-4F08-8EBB-F18230DC9B62>

---

**Citation:** Nguyen AD, Stoev P, Nguyen LTP, Vu TT (2023) A new species of *Paracortina* from a Vietnamese cave, with remarkable secondary sexual characters in males (Callipodida, Paracortinidae). ZooKeys 1149: 181–195. <https://doi.org/10.3897/zookeys.1149.99651>

---

## Abstract

A new millipede species, *Paracortina kyrang* sp. nov., is described from a cave in Cao Bang Province, northern Vietnam. The new species is diagnosed by having an extraordinarily long projection on the head of males, reduced eyes, a gonocoxite with two processes, a long and slender gonotelopodite with two long, clavate prefemoroidal processes densely covered with long macrosetae apically, and with a distal, reverse, short spine on mesal side, and a rather sinuous distal part of the telopodite. This is the third species of the genus that is known from Vietnam. A brief comparison of some secondary sexual characters is made.

## Keywords

Biodiversity, cave fauna, northern Vietnam, southern China

## Introduction

The millipede order Callipodida is represented in South-east Asia by three extant families – Sinocallipodidae Zhang, 1993, Paracortinidae Wang & Zhang, 1993, and Caspiopetalidae Lohmander, 1931 (Stoev et al. 2008; Enghoff et al. 2015), as well as by the family Burmanopetalidae Stoev, Moritz & Wesener, 2019 known only from Cretaceous

amber deposits in Myanmar (Stoev et al. 2019). Of the three extant families, Paracortinidae the most widespread in South-east Asia and is also the most species rich, with 14 species known to date from China and Vietnam (Wang and Zhang 1993; Zhang 1997; Shear 2000; Stoev 2004; Stoev and Geoffroy 2004; Stoev et al. 2008; Liu and Tian 2015; Enghoff et al. 2015). The family comprises two genera, *Angulifemur* Zhang, 1997 and *Paracortina* Wang & Zhang, 1993, and the latter genus is represented by 12 species, while *Angulifemur* has only two species known from caves in Yunnan, southern China. Four out of 12 *Paracortina* species are cave-dwellers and show some cave-adaptations, although no true troglobites are known until present (Stoev and Geoffroy 2004; Liu and Tian 2015). The family will be revised in another study (Akkari et al. in prep.), in which some of species will be redescribed, together with the description of new taxa.

### **A list of the hitherto described species of *Paracortina***

1. *P. carinata* Wang & Zhang, 1993 from Shangrila (= Zhongdian) County, Yunnan, China.
2. *P. chinensis* Stoev & Geoffroy, 2004 from Zhenxiong County, Yunnan, China.
3. *P. leptoclada* Wang & Zhang, 1993 from Shangrila County, Yunnan, China.
4. *P. multisegmentata* Stoev & Geoffroy, 2004 from Ngoc-Lac and Loc Think, Thanh Hoa, Vietnam.
5. *P. serrata* Wang & Zhang, 1993 from Deqin County, Yunnan, China.
6. *P. stimula* Wang & Zhang, 1993 from Shangrila County, Yunnan, China.
7. *P. thallina* Wang & Zhang, 1993 from Batang County, Sichuan, and Shangrila County, Yunnan, China.
8. *P. viriosa* Wang & Zhang, 1993 from Shangrila County, Yunnan, and Mangkang County, Tibet, China.
9. *P. voluta* Wang & Zhang, 1993 from Yajiang County, Sichuan, China.
10. *P. warreni* (Shear, 2000) from caves at Hong Mat, Hoa Binh, Vietnam.
11. *P. zhangii* Liu & Tian, 2015 from Cave Qiaoxia Dong, Guizhou, southern China.
12. *P. yinae* Liu & Tian, 2015 from Cave in Yanchang Village, Guangxi, southern China.

Here, we describe a new species of *Paracortina* from Ky Rang Cave, Cao Bang Province, Quang Hoa District, Quoc Toan commune, in northern Vietnam. The species is highly adapted to the cave environment and exhibits several somatic characteristics of troglobionts, such as reduced eyes, elongated legs and antennae, and lack of pigmentation on parts of the body.

### **Material and methods**

All specimens were hand-collected from Ky Rang Cave, Cao Bang Province, Quang Hoa District, Quoc Toan commune, in northern Vietnam and preserved in 85–90% ethanol. All morphological characters were investigated with an Olympus SZX16 ster-

eomicroscope. Gonopods were dissected for morphological examination and photographed. Colored images were taken using a Nikon SMZ800N microscope and NIS-Element BR v. 5.20.00 and stacked using Helicon Focus v. 7.0. Images were assembled into plates using Photoshop CS6. The terminology follows Stoev and Geoffroy (2004) and Liu and Tian (2015).

Total DNA was extracted using Qiagen Dneasy Blood and Tissue Kits. A 680-bp fragment of the mitochondrial gene, cytochrome c oxidase subunit I (COI), was amplified and sequenced using a pair of universal primers, LCO1490 and HCO2198 (Folmer et al. 1994). Polymerase chain reaction (PCR) conditions for amplification of the COI gene follow those of Nguyen et al. (2019). ExoSap IT was used to successfully purify amplified PCR products, which were then sent for sequencing to the GenLab Company (Hanoi, Vietnam). COI sequences were checked and confirmed using BLASTN 2.6.0+ search (Zhang et al. 2000) and deposited in GenBank with the number accessions OQ281704, OQ281705, and OQ281706.

The holotype, paratypes, and DNA vouchers were preserved in 90% ethanol and deposited at the Institute of Ecology and Biological Resources (IEBR), Hanoi, Vietnam.

Abbreviations: **PT** pleurotergite/s.

## Results

### Taxonomy

#### Order Callipodida Pocock, 1894

#### Family Paracortinidae Wang & Zhang, 1993

#### Genus *Paracortina* Wang & Zhang, 1993

#### *Paracortina kyrang* sp. nov.

<https://zoobank.org/22146F0D-BFA6-4F91-84B5-CEB60238183D>

Figs 1–7

**Material examined. Holotype.** 1 male (**IEBR-Myr 921**) Cao Bang Province, Quang Hoa District, Quoc Toan commune, Ky Rang Cave, 2.xi.2021, leg. Anh D. Nguyen.

**Paratypes.** 1 female, 1 juvenile (**IEBR-Myr 932**), 1 female (**IEBR-Myr 935**) same locality, but 17.iii.2022, leg. Anh D. Nguyen & D.D. Nguyen.

**Non-types.** 1 male, 1 male juvenile, 1 female juvenile (**IEBR-Myr 954**), same locality, but 16.x.2018, leg. Alexandre Faille.

**Diagnosis.** The new species is well distinguished from all congeners by the strongly modified head in males bearing a unique apically bent projection. Body composed of 68–74 pleurotergites +telson, eyes reduced, composed of 19 or 20 ommatidia in two or three rows. Gonocoxa with an anterior long spiniform process (**a**), as long as ca 80% of telopodite stem, and a rather slender, much shorter, cephalad process (**b**). Process **a** with a cephalad lobe distally, process **b** about 1/3 the length of telopodite. Telopodite with two long, clavate prefemoroidal processes (**cp**), densely covered with



**Figure 1.** *Paracortina kyrang* sp. nov. **A** entrance of Ky Rang Cave **B** habitat of the species **B, C** habitus, *in situ*. Images not to scale.

long macrosetae apically. Telopodite long, slender, apically twisted laterad, with a distal, reverse, short spine. Distal part of telopodite rather sinuous, narrowed at the base, then smoothly widened at its top, to narrow sharply finally at the solenomere (**sl**) and parasolenomere (**ps**).

The new species can be keyed out into the first branch in Liu et al.'s (2015) key for identification of the species of *Paracortina*, with the clustering species having a pair of prefemoroidal clavate processes (**cp**) on the gonopods: *P. thallina*, *P. stimula*, *P. leptoclada*, *P. voluta*, *P. serrata*, *P. viriosa*, and *P. carinata* (all from southern China).

**Etymology.** The species epithet “*kyrang*” is a noun in apposition for the type locality, Ky Rang Cave.

**Description. Male holotype:** Length about 42 mm, width and height of midbody PT 2.3 mm and 2.2 mm, respectively; 68 PT+ telson.

**Colour:** living specimens greenish white (Fig. 1C, D). Ethanol preserved specimens: generally white-yellowish; posterior part of metazonites with a brown posterior margin; head, pleurotergites, antennae and telson white-yellowish; legs yellow-brownish.

**Head** (Figs 2A–C, 3A) highly modified; frons considerably elongated in large projection (**lp**), which is curved at its end; forehead and vertex concave.

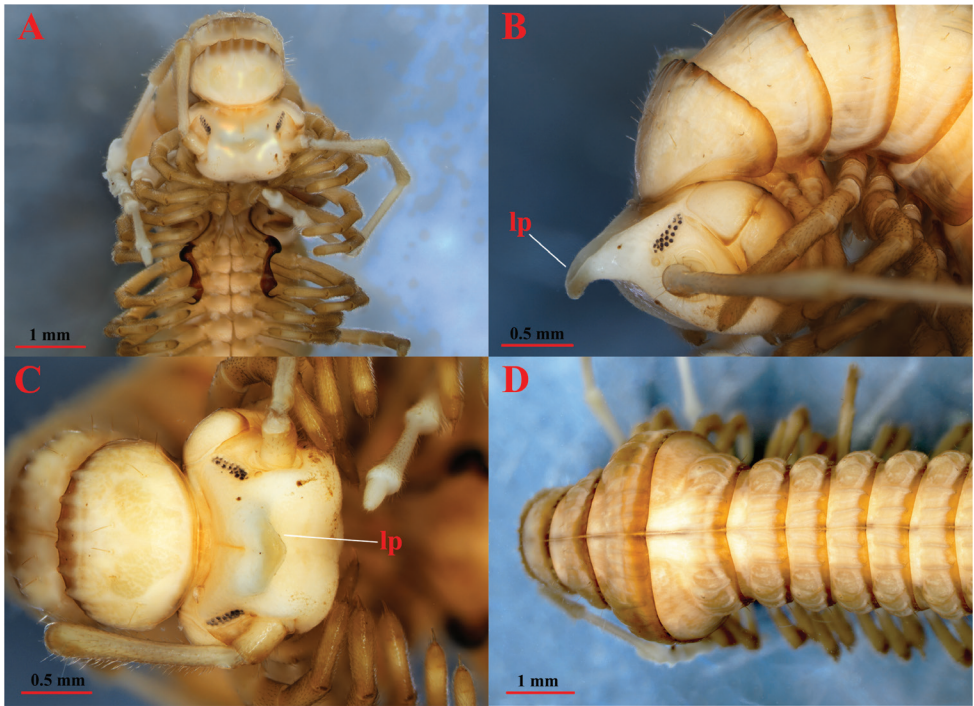


**Figure 2.** *Paracortina kyrang* sp. nov., holotype **A** anterior body in ventral view **B** anterior body in lateral view **C** head in dorsal view **D** segments 6–12 in dorsal view. Abbreviation: lp = a large projection on head.

**Antennae** (Figs 2A, 3A, 4B) extremely long, extending beyond the posterior edge of PT 9 when folded backwards; ratio antenna/body length about 1/7; all antennomeres white; length of antennomeres: 1: 0.21 mm, 2: 1.27 mm, 3: 1.26 mm, 4: 1.26 mm, 5: 1.21 mm, 6: 0.67 mm, 7: 0.23 mm; tip of antennomere 7 with four cones protruding well beyond the edge. Eyes (Fig. 2B, C) black, well delineated, composed of 19 ommatidia in three horizontal rows (9+3+7). Tömösváry's organ about three times larger than the adjacent ommatidium, placed between the eye and the base of antenna (Fig. 2B).

Width of PT: 6>7>>8–14>4>3>2>1. PT slightly broader than high; height of 10<sup>th</sup> PT: 2.19 mm, width 2.32 mm.

**Collum** (Fig. 2B, C) much narrower than head; pleurotergites 6 and 7 in males strongly enlarged (Figs 2D, 3A). Crests on collum (Fig. 2C) moderately expressed mostly in the posterior part of the segment. Complete crests series appearing from PT2 onwards. Above ozopores, midbody PT with 3+3 primary crests and with 3+3 secondary short crests between primary crests (Figs 2D, 3B); 3<sup>rd</sup> primary crest strongly enlarged, other primary crests flattened, almost equally broad along the metazonal length; only secondary crests shorter and slightly narrowed posteriorly. Ozopores lying on primary crest 3, visible from sixth to last but two PT (Figs 2D, 3B).

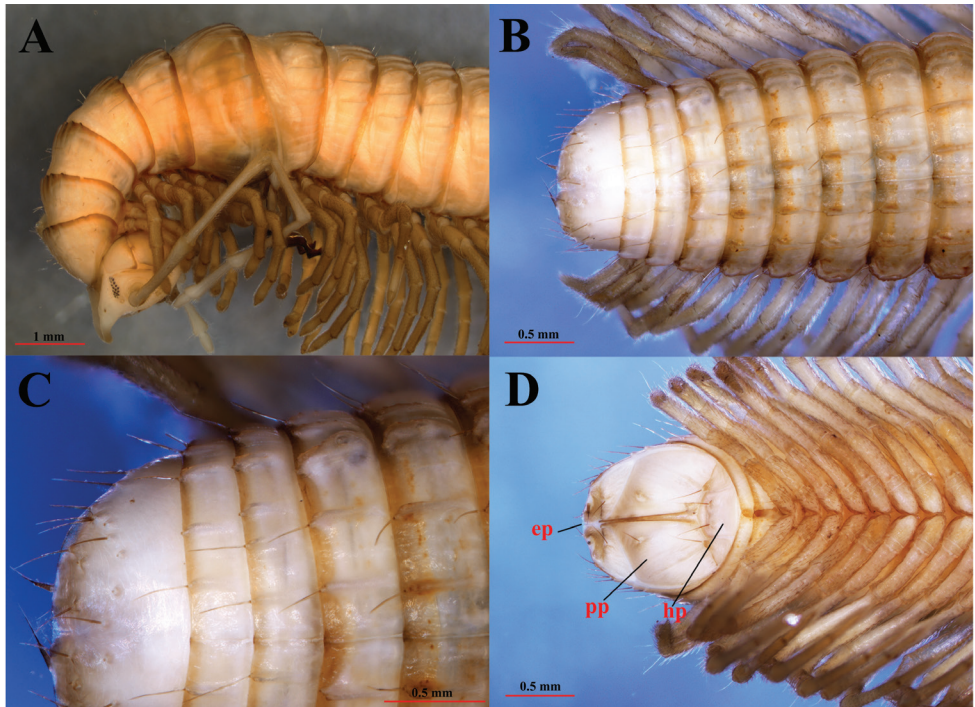


**Figure 3.** *Paracortina kyrang* sp. nov., holotype **A** anterior part of body in lateral view **B** posterior part of body in dorsal view **C** telson in dorsal view **D** hypoproct, paraproct, and epiproct in ventral view. Abbreviations: ep = epiproct; pp = paraproct; hp = hypoproct.

Below ozopores, midbody PT with 2+2 primary crests and 2+2 shorter and thinner secondary crests between primary crests, and 8–10 lower crests down to ventral pleurotergal edge (Fig. 3A).

Midbody pleurotergal setae 5+5, located at caudal edges of primary crests (Figs 2D, 3A); setal pattern as in below (Chaetotaxy). Axial line rather distinct.

**Epiproct (ep)** (Fig. 3B–D) simple, with 7+7 anterior and 4+4 posterior setiferous knobs in transverse rows. Hypoproct (**hp**) (Fig. 4D) tripartite, medial sclerite largest, subtrapeziform, bearing two paramedian macrosetae; each lateral sclerite with a single macroseta born on a large tubercle. Paraproct (**pp**) (= anal valves) (Fig. 4D) smooth, each divided into a small upper and large lower sclerites, both with a pair of macrosetae. Spinnerets long and slender, ending with a long seta each. All setae on telson brown, contrasting with the yellowish background.

Male leg-pairs 1 and 2 much shorter, with strong setae on ventral side of femorite and tibia, leg-pair 3 slightly shorter than following legs. Tarsi 1–3 1-segmented, and from tarsus 4 to ultimate pair 2-segmented; tarsal pads large until leg 26, then gradually thinner and eventually absent on subsequent legs. All legs ending with a rather slender, long, curved claw. Coxal sacs present from legs 3–26 (PT 16). Only coxae and tibia finely micropapillate ventrally (Fig. 4B).

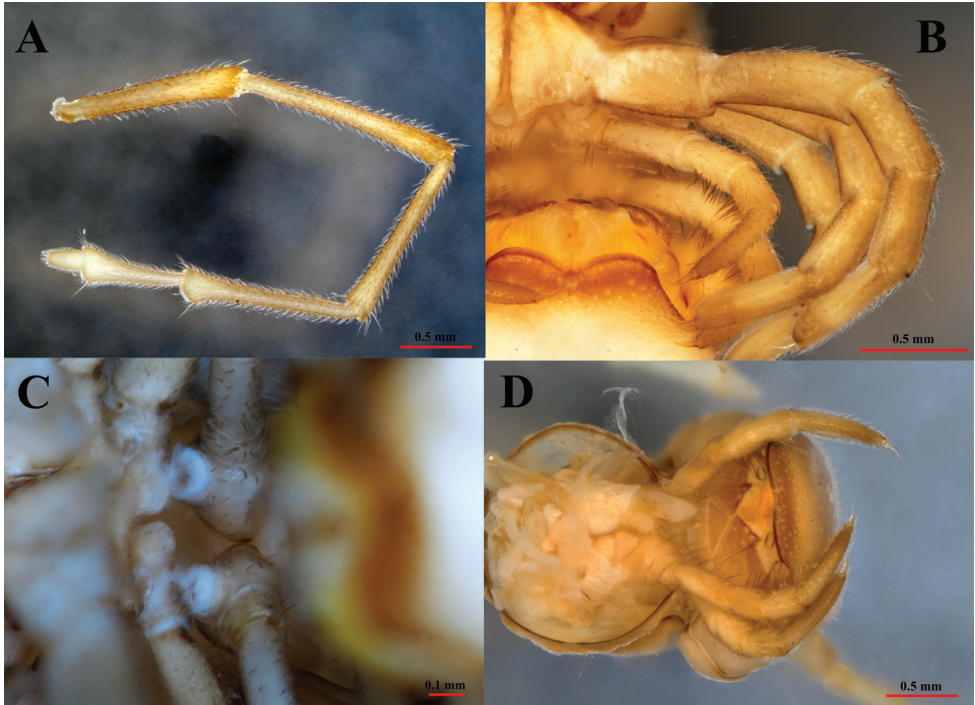


**Figure 4.** *Paracortina kyrang* sp. nov., holotype **A** right antenna **B** legs 4 and 5 in posterior view **C** gonopores in ventral view **D** female paratype (IEBR-Myr 932), cyphopods in subposterior view.

Coxa 2 with a small anterior process and a posterior gonopore, the latter placed on a small cone (Fig. 4C). Coxa 6 normal, without processes or modifications. Coxa 7 (Fig. 6A, B) with a short tubercle (**st**), and a very strong, rounded anterior process (**rap**). Coxae of the remaining legs normal.

#### Chaetotaxy:

	Anterior setae	Posterior setae
Collum	4+4	2+2
PT2	5+5	broken
PT3	5+5	broken
PT4	broken	5+5
PT5	broken	5+5
PT6-penultimate PT		5+5 (rarely 6+5)

Gonopods (Figs 6C, D, 7) yellow-brownish, some parts dark brown to black (seminal groove, solenomere, basal part of coxal process **a**). Gonopods protruding well beyond the gonocoel, stems of telopodites long, thin, subparallel, and diverging, pointing posteriad (Fig. 6C, D). Coxa with an anterior long spiniform process (**a**), and a rather slender, much shorter, posterior process (**b**) (Fig. 6C). Process **a** as long as ca 80% of telopodite stem, with a lobe distally while process **b** about 1/3 the length of telopodite. Telopodite (**te**) with two



**Figure 5.** *Paracortina kyrang* sp. nov., female paratype (IEBR-Myr 935) **A** head in ventral view **B** anterior body in lateral view **C** anterior body in subdorsal view **D** cyphopods in ventral view.

long, clavate prefemoroidal processes (**cp**), densely covered with long macrosetae apically. Telopodite long, slender, apically twisted laterad, with a distomesal, reverse, short spine (**sp**) (Figs 6C, 7A, B). Distal part of telopodite rather sinuous, narrowed at the base, then smoothly widened at its top, to narrow sharply finally at the solenomere (**sl**) and parasolenomere (**ps**) (Fig. 7D). The seminal groove (**sg**) terminating in the solenomere (Fig. 7D).

**Females.** Head unmodified (Fig. 5A–C). Length about 54.7 mm. The 10<sup>th</sup> PT ca 2.62 mm wide and 2.36 mm high; 68–74 PT + telson. Second leg-pair unmodified. Leg-pairs 1–3 with tarsal brushes. Cyphopods small, densely setose, bilobed (Figs 4D, 5A, D). Coxae 7 normal, without processes.

**DNA barcode.** The new species has a close genetic identity with *Tetracion jonesi* Hoffman, 1956 (Abacionidae) from 77.74% to 78.25%.

**Cave habitat.** Ky Rang Cave is located in close proximity to Thang Hen Lake in Cao Bang Province, northern Vietnam, at the altitude of 1,000 m a.s.l. The cave entrance is wide, but the only passage is blocked by an artificial door made by the local residents. Because of it, the semi-light part of the cave is missing, and, on entry, the cave is immediately dark (Fig. 1A). The cave is high (15–20 m), wide (15–20 m), and long (700–1,000 m). The floor is mainly wet with clay and there are some small pools (Fig. 1B). Several other millipede species were found in the cave, for example, *Hylomus srisonchaiti* Golovatch, 2019 and *Hyleoglomeris alba* Kuroda, Nguyen & Eguchi, 2022 (Golovatch 2019; Kuroda et al. 2022). The new species was found at a distance of 500 m from the entrance.

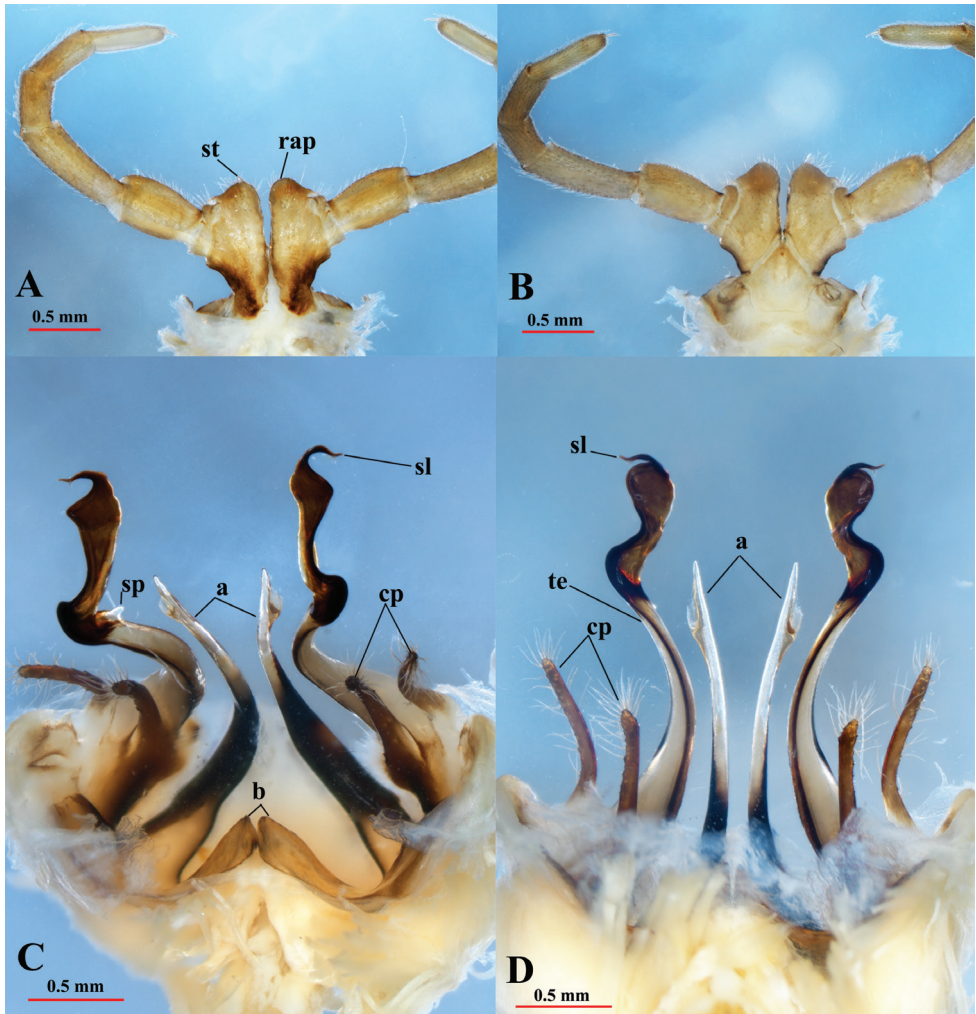


**Figure 6.** *Paracortina kyrang* sp. nov., holotype **A** leg 7 in posterior view **B** leg 7 in anterior view **C** gonopods in posterior view **D** gonopods in anterior view. Abbreviations: st = short tubercle; rap = rounded anterior process; a = coxal process a; b = coxal process b; te = telopodite; cp = clavate prefemoroidal processes; sp = distomesal spine on telopodite; sl = solenomere.

## Discussion

Currently, there are only three *Paracortina* species recorded in Vietnam: *P. warreni* Shear, 2000 from caves at Hong Mat (Hoa Binh), *P. multisegmentata* Stoev & Geoffroy, 2004 from Ngoc Lac (Thanh Hoa), and *P. kyrang* sp. nov. from Quoc Toan (Cao Bang) (Fig. 8). The first two species have been found on the west side of the Red River, in two nearby localities, while *P. kyrang* sp. nov. is currently known to occur in a single cave on the east side of Red River. This river is known to act as a natural barrier for the distribution of various animal and plant species, including some butterflies (Monastyrskii

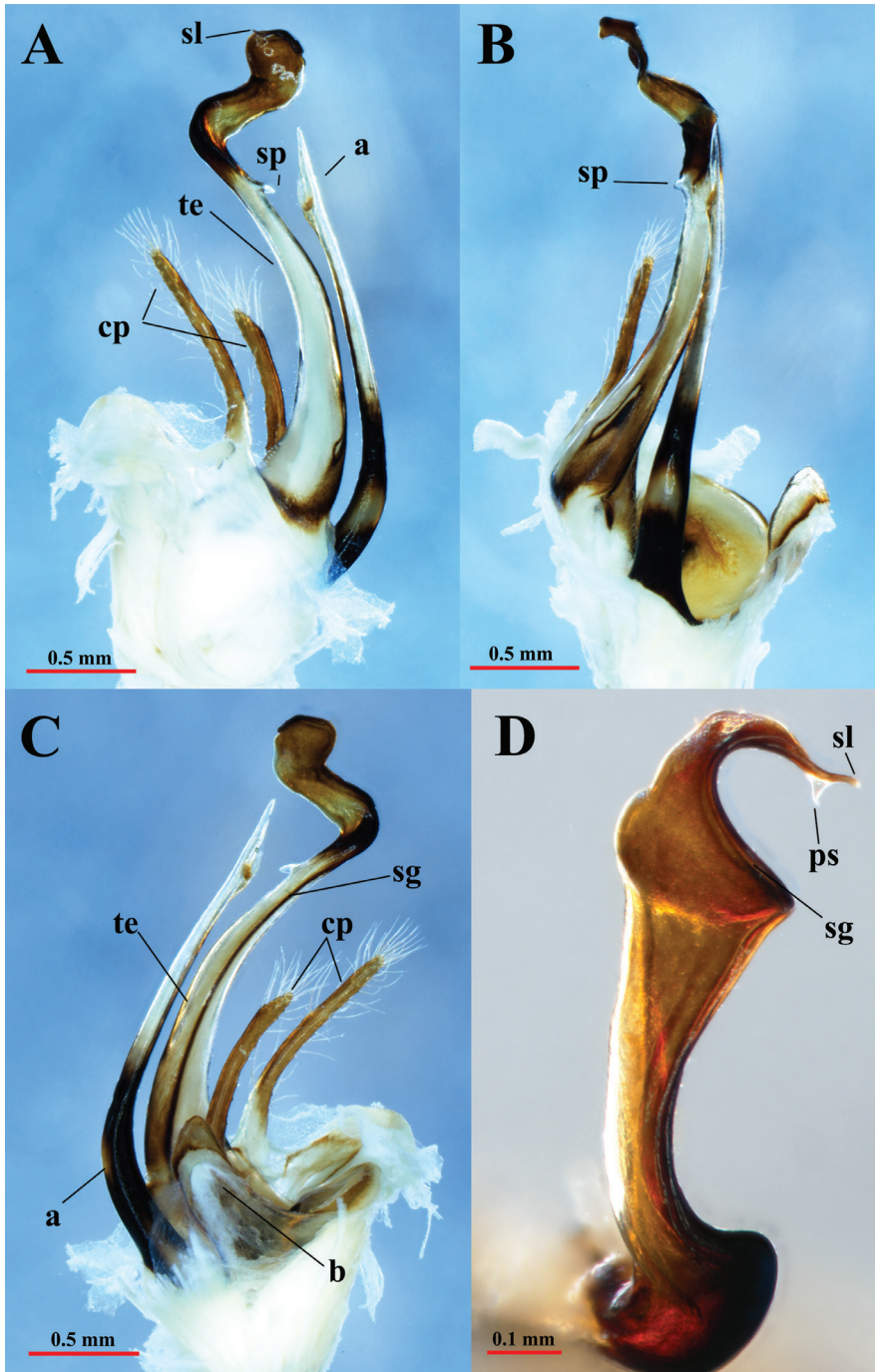


**Figure 7.** *Paracortina kyrang* sp. nov., holotype **A** right gonopod in lateral view **B** right gonopod in ventral view **C** right gonopod in mesal view **D** solenomere in ventral view. Abbreviations: a = coxal process; te = telopodite; cp = clavate prefemoroidal processes; sp = distomesal spine on telopodite; sg = seminal groove; sl = solenomere; ps = parasolenomere.

and Holloway 2013), the spider genus *Nesticella* Lehtinen & Saaristo, 1980 (Ballarin and Li 2018), the frog genus *Microhyla* Tschudi, 1838 (Yuan et al. 2016), gibbons (Hylobatidae) (Geissmann et al. 2000; Thinh et al. 2010), and the plant genus *Cycas* Linnaeus, 1753 (Zheng et al. 2016). Geologically, the northwestern and northeastern Vietnam belong to two different tectonic blocks separated by the Red River. While the northwestern part belongs to the Indochina block, the northeastern part is in the southern boundary of the South China block (Ngo et al. 2014).

Cao Bang Province is located in a karst region of northern Vietnam and supports hundreds of caves varying in size and environmental parameters (Sterling et al. 2006). Recently, several new species have been discovered from caves of Cao Bang Province, including the millipedes *Tylopus nguyeni* Golovatch, 2019, *Parasundanina faillei* Golovatch, 2019, *Hylomus srisonchaii* Golovatch, 2019, *Hyleoglomeris halang* Kuroda, Eguchi & Nguyen, 2022, and *Hyleoglomeris alba* Kuroda, Nguyen & Eguchi, 2022 (Golovatch 2019; Kuroda et al. 2022), but more new species are expected with more intensive studies and surveys.

Most callipodids live in caves and rock crevices (Enghoff et al. 2015). Completely blind representatives of the order have not yet been found, although some species have reduced eyes, for example, *Sinocallipus jaegeri* Stoev & Enghoff, 2011 from a cave in Laos and *Sinocallipus simplipodicus* Zhang, 1993 from a cave in Yunnan, China (Stoev and Enghoff 2011). Among the members of the family Paracortinidae, *P. warreni* also shows eye reduction, and the species described here also has troglomorphic features.

### Sexual dimorphic characters in Callipodida

Head shape is often dimorphic in order Callipodida (Ilić et al. 2017). Several species of the families Schizopetalidae, Caspiopetalidae, and Paracortinidae possess modified heads in males, while others, members of Abacionidae, Callipodidae, and Sinocallipodidae, have the conventional convex forehead in both sexes. The head modification can vary from a simple invagination in the forehead area (e.g., representatives of the genera *Acanthopetalum* and *Eurygyrus*), which can sometimes be very pronounced, to triangular protrusions in the middle of the head, such as are observed in most representatives of the genus *Bollmania* (Caspiopetalidae) (Stoev and Enghoff 2005; Enghoff et al. 2015). At least some of the species of Paracortinidae have a bulge on the head (e.g. *P. zhangii* and *P. yinae*; Liu and Tian 2015), but by no means does *Paracortina kyrang* sp. nov. demonstrate the most extreme case of a projection of the head. The role of these head modifications are not understood but is probably associated with reproduction.

Some callipodidans have the size of the anterior pleurotergites in females and males differing, which allows for observer to determine the sex, even with the naked eye. Usually, in females, the second and third pleurotergites are enlarged, while in males this occurs in the sixth and seventh pleurotergites, where the gonopods are located. The enlargement of pleurotergites in both sexes corresponds to the maturation, when vulvae and gonopods become fully developed. This dimorphic character is observed also in the genus *Paracortina*. The PT 6 and sometimes PT 7 are strongly enlarged in males,

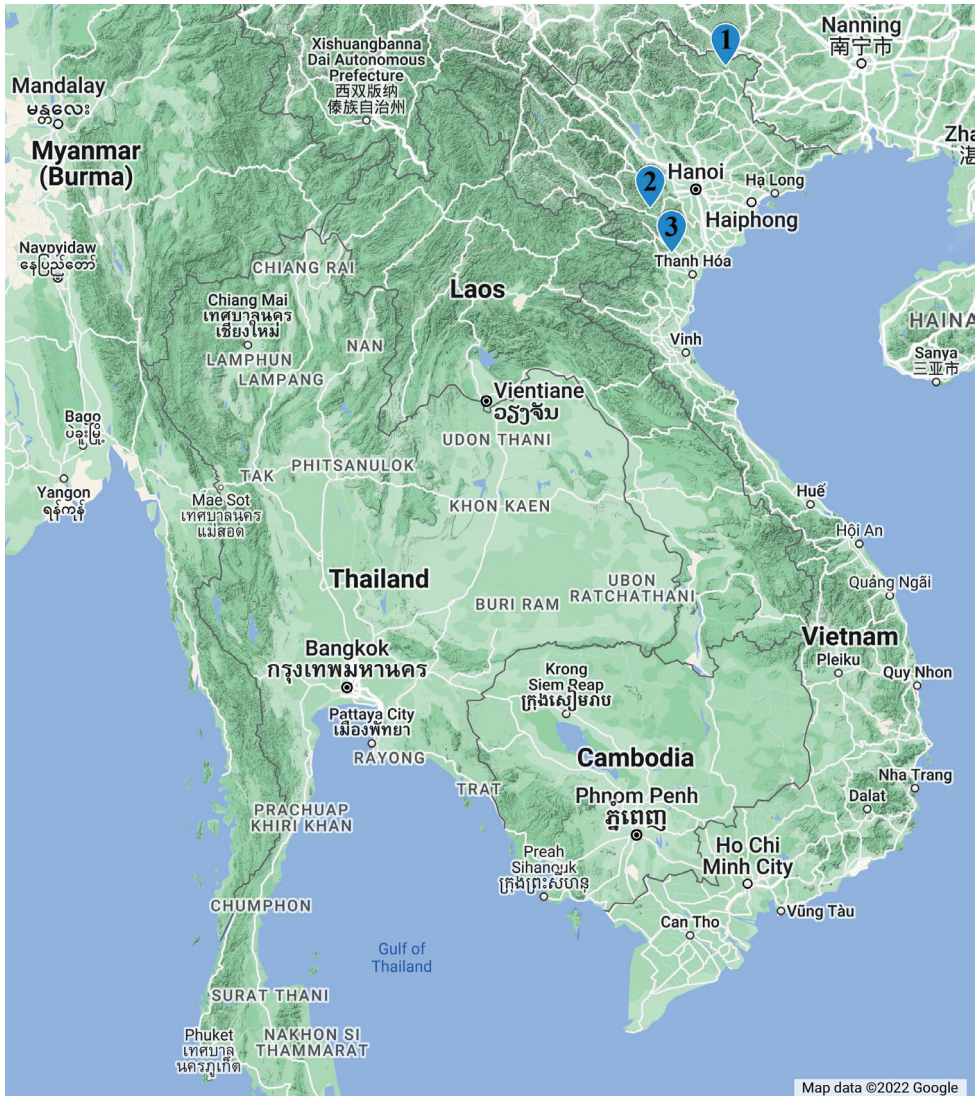


**Figure 8.** Records of *Paracortina* species in Vietnam **1** *Paracortina kyrang* sp. nov. **2** *Paracortina warreni* (Shear, 2000) **3** *Paracortina multisegmentata* Stoev & Geoffroy, 2004.

but not in females – see *P. chinensis*, *P. multisegmentata* (Stoev and Geoffroy 2004), and *P. kyrang* sp. nov. – and only PT 6 is enlarged in *P. zhangii* and *P. yinae* (Liu and Tian 2015). The enlargement of PT 6 and PT 7 in *P. kyrang* sp. nov. is remarkable, and is not present in other members of the family to the best of our knowledge. In addition, some other characters also differ between males and females: for instance, leg-pairs 1–3 bear tarsal pads in males but tarsal brushes in females; coxa 7 has modified processes in males but is unmodified in females.

## Acknowledgements

The work is supported by the Vietnam Academy of Science and Technology under the project NCXS01.04/23-25. We acknowledge Mai Van Thai, Dang Van Dong, and Nguyen Duc Hiep, all from IEBR, for their help in fieldwork. Alexandre Faille is sincerely thanked for kindly providing his specimens. Two reviewers, Dr William Shear (USA) and Dr Henrik Enghoff (Denmark), and the editor, Dr Nesrine Akkari (Austria), are acknowledged for their invaluable comments to improve the manuscript.

## References

- Ballarin F, Li S-Q (2018) Diversification in tropics and subtropics following the mid-Miocene climate change: A case study of the spider genus *Nesticella*. *Global Change Biology* 24(2): e577–e591. <https://doi.org/10.1111/gcb.13958>
- Enghoff H, Golovatch S, Short M, Stoev P, Wesener T (2015) Diplopoda – taxonomic overview. In: Minelli A (Ed.) *Treatise on Zoology – Anatomy, Taxonomy, Biology. The Myriapoda*, 2. Brill, Leiden, 363–453. <https://doi.org/10.1163/9789004188273>
- Folmer O, Black M, Hoeh W, Lutz R, Vrijenhoek R (1994) DNA primers for amplification of mitochondrial cytochrome oxidase subunit I from diverse metazoan invertebrates. *Molecular Marine Biology and Biotechnology* 3: 294–299.
- Geissmann T, Nguyen XD, Lormee N, Momberg F (2000) Vietnam Primate Conservation Status Review 2000. Part 1: Gibbons. *Fauna and Flora International*, Hanoi, 130 pp.
- Golovatch SI (2019) On several new or poorly-known Oriental Paradoxosomatidae (Diplopoda: Polydesmida), XXVII. *Arthropoda Selecta* 28(4): 459–478. <https://doi.org/10.15298/arthscl.28.4.01>
- Ilić BS, Mitić BM, Makarov SE (2017) Sexual dimorphism in *Apfelbeckia insculpta* (L. Koch, 1867) (Myriapoda: Diplopoda: Callipodida). *Archives of Biological Sciences* 69(1): 23–33. <https://doi.org/10.2298/ABS160229060I>
- Kuroda M, Eguchi K, Oguri E, Nguyen AD (2022) Two new cave *Hyleoglomeris* species (Glomerida, Glomeridae) from northern Vietnam. *ZooKeys* 1108: 161–174. <https://doi.org/10.3897/zookeys.1108.85423>
- Liu WX, Tian MY (2015) Two new cave-dwelling species of the millipede genus *Paracortina* Wang & Zhang, 1993 from southern China (Diplopoda, Callipodida, Paracortinidae). *ZooKeys* 517: 123–140. <https://doi.org/10.3897/zookeys.517.9949>
- Monastyrskii AL, Holloway JD (2013) The biogeography of the butterfly fauna of Vietnam with a focus on the endemic species (Lepidoptera). In: Silva-Opps M (Ed.) *Current Progress in Biological Research*. InTechOpen, London, 95–123. <https://www.doi.org/10.5772/55490>
- Ngo XT, Tran TH, Nguyen H, Vu QL, Kwon S, Itaya S, Santosh M (2014) Backarc mafic–ultramafic magmatism in northeastern Vietnam and its regional tectonic significance. *Journal of Asian Earth Sciences* 90: 45–60. <https://doi.org/10.1016/j.jseaes.2014.04.001>

- Nguyen AD, Eguchi K, Hwang UW (2019) Two new pill millipedes (Diplopoda: Glomerida: Glomeridae) from high mountains of Vietnam. *Journal of Natural History* 53(21–22): 1369–1384. <https://doi.org/10.1080/00222933.2019.1646338>
- Shear WA (2000) A new genus and species of callipodidan millipede from Vietnam (Callipodida, Schizopetalidae). *Myriapodologica* 6(11): 95–100. [Link]
- Sterling EJ, Hurley MM, Le DM (2006) *Vietnam: A Natural History*. Yale University Press, New Haven, 423 pp. <https://doi.org/10.12987/9780300128215>
- Stoev P (2004) The first troglomorphic species of the millipede genus *Paracortina* Wang & Zhang, 1993 from south Yunnan, China (Diplopoda: Callipodida: Paracortinidae). *Zootaxa* 441(1): 1–8. <https://doi.org/10.11646/zootaxa.441.1.1>
- Stoev P, Enghoff H (2005) A new cave-dwelling millipede of the genus *Bollmania* Silvestri, 1896 from Yunnan, China, with remarks on the reduction of the second female leg-pair (Diplopoda: Callipodida: Caspiopetalidae). *Journal of Natural History* 39(21): 1875–1891. <https://doi.org/10.1080/00222930400025896>
- Stoev P, Enghoff H (2011) A review of the millipede genus *Sinocallipus* Zhang, 1993 (Diplopoda, Callipodida, Sinocallipodidae), with notes on gonopods monotomy vs. peripheral diversity in millipedes. *ZooKeys* 90: 13–34. <https://doi.org/10.3897/zookeys.90.1291>
- Stoev P, Geoffroy JJ (2004) Review of the millipede family Paracortinidae Wang & Zhang 1993 (Diplopoda: Callipodida). *Acta Arachnologica* 53(2): 93–103. <https://doi.org/10.2476/asjaa.53.93>
- Stoev P, Sierwald P, Billey A (2008) An annotated world catalogue of the millipede order Callipodida (Arthropoda: Diplopoda). *Zootaxa* 1706(1): 1–50. <https://www.doi.org/10.11646/zootaxa.1706.1.1>
- Stoev P, Moritz L, Wesener T (2019) Dwarfs under dinosaur legs: A new millipede of the order Callipodida (Diplopoda) from Cretaceous amber of Burma. *ZooKeys* 841: 79–96. <https://doi.org/10.3897/zookeys.841.34991>
- Think VN, Mootnick AR, Geissmann T, Li M, Ziegler T, Agil M, Moisson P, Nadler T, Walter L, Roos C (2010) Mitochondrial evidence for multiple radiations in the evolutionary history of small apes. *BMC Evolutionary Biology* 10(74): 4–13. <https://doi.org/10.1186/1471-2148-10-74>
- Wang DQ, Zhang CZ (1993) A new family of millipedes (Diplopoda: Callipodida) from southwestern China. *Peking Natural History Museum* 53: 395–390.
- Yuan Z-Y, Suwannapoom C, Yan F, Poyarkov Jr NA, Nguyen SN, Chen H-M, Chomdej S, Murphy RW, Che J (2016) Red River barrier and Pleistocene climatic fluctuations shaped the genetic structure of *Microhyla fissipes* complex (Anura: Microhylidae) in southern China and Indochina. *Current Zoology* 62(6): 531–543. <https://doi.org/10.1093/cz/zow042>
- Zhang CZ (1997) Diplopoda from Yunnan Caves III. A new genus *Angulifemur*, including two new species of the cave-dwelling callipodid millipedes (Diplopoda, Callipodida, Paracortinidae). *Thesis Compilation of Tianjin Natural History Museum* 14: 1–5.
- Zhang Z, Schwartz S, Wagner L, Miller W (2000) A greedy algorithm for aligning DNA sequences. *Journal of Computational Biology* 7(1–2): 203–214. <https://doi.org/10.1089/10665270050081478>
- Zheng Y, Liu J, Gong X (2016) Tectonic and climatic impacts on the biota within the Red River Fault, evidence from phylogeography of *Cycas dolichophylla* (Cycadaceae). *Scientific Reports* 6(1): 33540. <https://doi.org/10.1038/srep33540>

## **Supplementary material I**

### **COI sequences of the new species**

Authors: Anh D. Nguyen, Pavel Stoev, Lien T.P. Nguyen, Tam T. Vu

Data type: FAS file

Copyright notice: This dataset is made available under the Open Database License (<http://opendatacommons.org/licenses/odbl/1.0/>). The Open Database License (ODbL) is a license agreement intended to allow users to freely share, modify, and use this Dataset while maintaining this same freedom for others, provided that the original source and author(s) are credited.

Link: <https://doi.org/10.3897/zookeys.1149.99651.suppl1>

